UNIVERSITÀ DEGLI STUDI DI TORINO

DIPARTIMENTO DI PSICOLOGIA

DOTTORATO DI RICERCA IN NEUROSCIENZE

CICLO XXXI

TITOLO DELLA TESI:

Distribution Patterns of Morphometric Neuropathological Alterations and Their Relationship with Brain Connectivity

TESI PRESENTATA DA: Andrea Nani

TUTOR: Prof. Franco Cauda

COORDINATORE DEL DOTTORATO: Prof. Marco Sassoè

ANNI ACCADEMICI:

1 Ottobre 2015 – 30 Settembre 2019

Index

Abstract

The pathological brain is typically characterized by network-like morphological coalterations of gray matter. These coalteration patterns can be identified by analyses of voxel-based morphometry (VBM), a technique capable of detecting values of increased or decreased gray or white matter. In a first study, a large transdiagnostic sample of VBM experiments, obtained from the BrainMap database, was analyzed with an innovative methodology, so as to construct a map of the pattern formed by co-altered cerebral areas across the brain. This coalteration pattern has been compared to three corresponding maps of connectivity profiles: functional, structural, and genetic. This comparison provided a transdiagnostical evidence of how the three different types of connectivity can influence the distribution of neuronal alterations. The analysis showed that all the three types of connectivity explain and predict with good statistical accuracy the distribution and temporal progression of the coalterations. Among these three types of brain connectivity, the functional gives the better account, followed by the structural and the genetic. In a second study, the insular cortex was taken as a target region with the aim to investigate what distribution pattern of alterations is associated with this area and whether this pattern correlates with its functional meta-analytic connectivity. The analysis revealed that the coalteration and functional maps largely overlap each other. This finding suggests that neuropathological alterations are likely to develop according to the constraints of brain connectivity, and that brain hubs are at the center of the distribution patterns of coaltered areas.

1. Background

1.1. Windows into the brain

Connectomics is a broad term that has been used in several ways since its first appearance. As it was originally defined, connectomics is "a comprehensive structural description of the network of elements and connections forming the human brain" (Sporns et al., 2005). This new approach – which can be developed either at the macroscale of cerebral areas and pathways or at the microscale of single neurons and synapses – has led to a picture of cerebral functioning in terms of networks and has emphasized the great need for an overarching mapping of the whole organization of connections that shapes the human brain (i.e., the so-called *connectome*).

This change of paradigm in neuroscience was radical, given that, before the advent of the neuroimaging techniques that made it possible, the brain was considered as an organ of different segregated modules capable of implementing different specialized cognitive functions. Apparently, it was thought that each mental faculty had its own dedicated brain area, which could operate largely in isolation with respect to the others. This idea received in the last century theoretical support by the philosopher Jerry Fodor (1983) and still to date is considered to be a milestone of cognitive neuroscience (Sternberg, 2011). This view has been also supported by the association of the clinical observation of specific deficits in neurological patients with the impairment of certain brain areas that appeared clearly damaged in the autoptic examination. But, although post-mortem investigations could provide important insights into the anatomy and structure of the brain – see for instance the ground-breaking investigations of

Paul Broca (Damasio and Geschwind, 1984) –, these inquiries were utterly silent about the functional side. After the development of brain imaging procedures, everything changed. In fact, for the first time it was possible to study the brain *in vivo*, in the very moment of its activity.

The first technique that proved itself to be effective was the computerized tomography (CT), developed around the 1970s by the independent research of the engineer Godfrey Hounsfield and physicist Allan Cormack, who in 1979 were awarded the Nobel Prize for medicine. The CT is still used nowadays in both clinical and research contexts; however, it can offer only structural images.

Other brain imaging techniques capable of providing functional patterns of brain activity were the positron emission tomography (PET), the single position emission computerized tomography (SPECT), the magnetoencephalography (MEG), and the functional magnetic resonance imaging (fMRI). All these procedures can inspect the dynamics of activation of different brain sites. Almost in real time it became possible to study the physiology of the brain in both normal and pathological conditions.

With these functional techniques, neuroscience was able to literally open windows into the brain and glimpse the dynamics of the mind. As a result, the idea of segregation at the basis of human cognition appeared to be just one side of the coin. Neuroscientists realized that in addition to functional differentiation (due to segregated brain modules), cognitive tasks also needed the integration of cerebral areas able to form widespread functional networks (Buchel and Friston 2001; Bullmore and Sporns 2009; Friston 1994; McIntosh and Gonzalez-Lima 1994). Studies provided evidence that specialized modular assemblies of neurons did not work in isolation but, rather, exchanged information and created functional networks in which this information could be integrated. Functional processes were therefore based on the interplay between segregation and integration. The new research field of brain network analysis had emerged and to date it has been one of the most dynamic and fruitful branches of neuroscience.

1.2. The brain functional connectivity

Brain connectivity can be studied at the functional, anatomical, and genetic level. This paragraph will be dedicated to a brief overview of the neuroscientific approach to the study of functional connectivity.

Although it is still a moot point whether the neural correlate of a mental process can be necessary *and* sufficient or necessary *but not* sufficient for the mental process to occur, there is sound evidence suggesting that functional changes in one's brain are always associated with changes in one's state of mind. In light of this, the standard neuroscientific view presupposes that mental processes are supported by brain processes (Shulman, 2001). Still, functional brain imaging techniques do not measure cerebral activity directly, but they detect a signal obtained from physiological parameters of energy consumption (i.e., glucose oxidation and consumption, and blood flow changes).

The average adult human brain, which is about 2% of the body weight, requires to function an amount of energy that is about 20% of an individual's resting metabolic rate (McKenna et al., 2006). The metabolism of the brain is quite constant over time, despite variation in cognitive as well as motor performances. This can be accounted for by the fact that the resting state typically needs substantial energy for the maintenance of the membrane potentials. Around 75% of energy consumed by brain is related to signaling, while the remaining 25% of energy is used to support the necessary non-signaling cellular activity, including nucleotide turnover, synthesis and degradation of proteins, mitochondrial proton leak and axoplasmic transport (Attwell and Laughlin, 2001).

Since a high metabolism rate characterizes the brain both when we are engaged in cognitive tasks and when we are behaviorally passive (resting state), it is reasonable to ask what type of brain activity are we considering in the context of neuroimaging techniques such as PET and fMRI. A possible solution requires to clarify what is meant by the term 'activation' when we refer to the transient changes in brain activity (Raichle and Gusnard, 2002). Neuronal

activations differ from the normal metabolic activity of the brain in terms of how the blood flow and oxygen consumption are related to each other. In a healthy brain the balance between oxygen delivery (i.e., blood flow) and oxygen consumption changes to an appreciable degree when neuronal activations occur during the performance of specific tasks (Raichle and Mintun, 2006). Notably, the changes in blood flow are greater than the corresponding changes in oxygen consumption. As a consequence, the oxygen supply increases more than the oxygen demand. However, while oxygen consumption increases less than blood flow, glucose utilization increases in proportion to changes in blood flow, as a portion of the metabolic increase is related to glycolysis (Fox et al., 1988). Since both blood flow and glucose utilization increase more than oxygen consumption, neuronal activations can be differentiated from the normal metabolic activity of the brain.

Furthermore, deoxyhemoglobin (i.e., hemoglobin with no oxygen) and oxyhemoglobin (i.e., hemoglobin with oxygen) have different magnetic properties. The former is paramagnetic, that is, more influenced by a magnetic field, while the latter is diamagnetic, that is, less influenced by a magnetic field. As a consequence, the fraction of oxyhemoglobin and deoxyhemoglobin produces changes in the magnetic response of the blood, so that the blood oxygenation level dependent (BOLD) effect can be used to detect indirectly brain activations.

These methodological grounds allow the design of functional imaging experimental protocols in order to detect differences in the brain signal between two behavioral conditions. In one condition (i.e., the control task) the individual is at rest, while in the other condition he or she is engaged in performing a specific task. Then, the activation patterns obtained at rest are subtracted from those obtained during task, so as to identify statistically significant changes in the brain signal. The images resulted from subtraction are supposed to show the brain areas that mainly correlate with a specific mental process.

It is important to highlight that the same cerebral region could be involved in more than one cognitive process. This phenomenon is well known and has been called ‘neuronal context’ (McIntosh, 1998) or ‘functional context’ (Bressler and Kelso, 2001). Furthermore, single-cell studies have shown that patterns of neuronal firing largely depend on many co-factors rather than on single stimulus or one response parameter. Therefore, the creation of effective connections is thought to be context-sensitive (Buchel and Friston, 1997), so that the contribution of a certain neuronal assembly or single cell to a specific cognitive process is significantly related and influenced by the state of other anatomically connected elements. This is why the same level of activity in a certain brain region may be involved in diverse mental processes depending on what other areas are momentarily co-active (McIntosh 1999). The neuronal or functional context has important consequences for the understanding of brain activation patterns, especially with regard to the study of higher-order psychological functions, in which we expect to find a great overlap of activation patterns for many different cognitive operations (McIntosh et al., 2001).

It is now well established that brain areas consistently found to be active together are supposed to be functionally connected. They form typical functional networks and, to date, brain imaging studies have identified several of them (Beckmann et al., 2005; Fransson, 2005; Salvador et al., 2005; van de Ven, et al. 2004; van den Heuvel et al., 2008). Among the most studied we can include the visual network, the motor network, a salience network composed of bilateral temporal insular and anterior cingulate cortex regions, the dorsal and ventral attention networks, and the default mode network (Buckner and Vincent, 2007; Fox and Raichle, 2007; Fox et al., 2005; Raichle and Snyder, 2007; Sporns, 2010).

These networks constitute the functional architecture of the human brain. Within them, however, brain areas play different roles: if damaged, some areas can be replaced by others, so that the network can continue to support its function. In contrast, other areas, in virtue of their centrality and elevated number

of connections, are essential for the normal function of the network. These pivotal centers are called brain hubs and are the fundamental nodes of the functional organization of the brain. Their damage leads to the inevitable disruption of the network and to the emergence of pathological functional patterns (Fornito et al., 2015).

In sum, the brain network analysis has provided a new theoretical approach for neuroscience as well as the potential to help us understand how brain functional processes produce behavior, cognition and, when impaired, mental illness (Yuste, 2015).

1.3. The brain anatomical connectivity

A second type of brain connectivity takes into consideration the fibers of white matter that link neurons to neurons. All the brain cells in the nervous system form vast webs by means of local and long-range structural connections. Axonal projections can link neurons that are near and contiguous or neurons that are far away and in different districts of the brain. The length of projections depends on the type of neuron and on the type of function that the cell supports. The patterns of anatomical connectivity are elegantly shaped by the principles of segregation and integration on the one hand, and experience on the other.

As we have seen, segregation refers to the division of the brain into regions dedicated to specific functional tasks. This makes possible for the brain to elaborate different types of information in parallel and simultaneously. Segregation implies that distinct assemblies of neurons, specialized in a specific function, can be anatomically localized, with an organization that is quite stable across individuals and species (Zamora-López et al., 2011). In turn, integration is the capacity of a system to gather information of different types and process it to combine and create new and useful information. For instance, visual sensory data need the binding of different features related to the receptive field, such as color, orientation, and position of an object (Zamora-López et al., 2011). So, if neuronal assemblies follow predominantly the segregation principle, then they will tend to

form and be part of small-world networks, in which the neighboring areas (or in the jargon of brain network analysis, the *nodes*) of any given area are likely to be neighboring nodes of each other, and most nodes can be reached from every other node by a small number of steps along the routes or axonal paths that connect them. This type of small-world networks is largely present in the primary sensory cortices, in which specialized modules interact to process specific chunks of information. As a result, these networks show unique topological properties, as they are highly clustered with a locally efficient information transfer (Telesford et al., 2011).

On the other hand, if neuronal assemblies follow predominantly the integration principle, then they will tend to form and be part of large-scale networks, in which brain areas and small networks can be organized in hierarchical arrangements. This structural organization is mainly related to associative cortices and may enhance both the brain's functional stability and information processing capabilities, as its topological aspects appear significant for implementing dynamic patterns of integration between different features of reality in order to generate global percepts (Hilgetag and Goulas, 2016). These large-scale networks are characterized by rich club properties, in which some areas play the role of central hubs in virtue of their high density of connections not only with other areas within networks but also with hubs of different networks. For instance, the insular cortex is thought to be an important brain hub. It has a central position within the salience network and some of its neurons (Von Economo's neurons, VENs) are characterized by long-range projections. VENs are large spindle-shaped cells that are supposed to be involved in higher-order processes regarding the monitoring of the state of the body, such as interoception and proprioception (Allman et al., 2005; Cauda et al., 2013, 2014; Medford and Critchley, 2010; Seeley et al., 2007).

The other fundamental factor capable of shaping the patterns of brain anatomical connectivity is experience. In neuroscience this mechanism is known as the Hebbian rule, according to which neurons that fire together wire together

(Löwel and Singer, 1992). In the words of Donald Hebb: "…the persistence or repetition of a reverberatory activity (or 'trace') tends to induce lasting cellular changes that add to its stability. [...] When an axon of cell A is near enough to excite a cell B and repeatedly or persistently takes part in firing it, some growth process or metabolic change takes place in one or both cells such that A's efficiency, as one of the cells firing B, is increased" (Hebb, 1949). This mechanism is supposed to be at the root of the formation of new synapses and, therefore, of synaptic plasticity. In turn, the creation of new anatomical connections between neurons is thought to be at the basis of the unsupervised learning process.

Techniques of diffusion MRI permit to perform fiber tracking analyses in order to obtain images of axonal bundles connecting different brain regions. Among them there are the diffusion-weighted imaging (DWI), diffusion tensor imaging (DTI), and diffusion spectrum imaging (DSI). All these methods use the detection of differences in the movement or speed of the water molecules in a medium. In fact, at a microscopic scale, in an isotropic medium water molecules move freely in all directions in a jittery and erratic manner. But in an anisotropic medium, such as the brain, water molecules move differently according to the type of cerebral tissue. Specifically, they move faster along than across structural constraints (Le Bihan et al., 2001; Mori and Zhang, 2006; Tuch et al., 2003).

These analyses allow the description of the properties of white matter with regard to a diffusion gradient, its axis and radiofrequency impulses (Hagmann et al., 2006). Data obtained with DWI, DTI and DSI can be used for the fiber tracking analysis in order to construct anatomical connectivity maps of the routes followed by white matter bundles connecting different brain regions with regard to healthy and pathological conditions.

1.4. The brain genetic connectivity

The last type of brain connectivity that we are going to discuss is based on different genetic profiles that brain areas can express. The link between gene

expression of cerebral areas and their neural connectivity patterns is one of the fundamental questions in neuroscience. Genes play an essential role in the formation and development of the nervous system, as well as in the maintenance of its functions. They store information for specifying neuronal cell types, destining neurons into specific networks and for determining their connectivity pathways (Hobert, 2003; Kania et al., 2000). In particular, neuronal wiring is supposed to take place in virtue of the selective attachment guided by certain molecular identifiers, and a number of studies have described different families of genes that play a role in axonal guidance and in defining their specific targets (Araujo and Tear, 2003; Chilton, 2006; Huber et al., 2003; Markus et al., 2002; Tessier and Goodman, 1996). The synaptic function needs the coordinated expression of genes guiding the synthesis of neurotransmitters in the presynaptic cell and of receptors in the post-synaptic cell (Polleux et al., 2007). Gene expressions are therefore deeply involved in the organization of the brain, both with regard of its functional and structural aspects.

Therefore, the understanding of gene functions, of their mutual interaction as well as of the relationship between genes expression and the brain connectome is of fundamental importance for explaining the other two brain connectivity profiles that have been discussed so far: the functional and the anatomical. During the last years, researchers have been investigating gene co-expressions patterns of the human genome in the brain. But unravelling the function of the genome will require comprehending how all of its parts co-operate in forming a complex system composed of different gene expression patterns, which is a fascinating but also a big challenge.

Thus far, the exploration and analysis of gene expression data have used genome-wide microarrays, which are tools that can identify gene co-expression patterns and detect sets of co-transcribed genes. In this way it is possible to map the expression patterns that distinguish brain regions from each other. Within this picture, brain areas expressing the same set of genes can be considered to be genetically connected. The aim of this line of research is to construct a landscape

of the human brain constituted by different patterns of gene expression associated with cerebral areas. To decipher this landscape will be a great advancement in the comprehension of the complex interplay between the genome and brain connectivity.

The study of genetic co-expression patterns can in fact shed light on the mechanisms of human cognition, emotion and personality. Furthermore, many genes have been recognized to be involved in the development of brain disorders, whose etiopathogenesis is thought to be associated, in part, with aberrant connectivity patterns (Heck et al., 2014). Explaining the role of genes in brain diseases will help achieve a better predictive diagnostic power with regard to the classification of symptoms and their development, so as to improve medical care and treatment.

1.5. Network analysis and the pathological brain

The pathoconnectivity network analysis is an intriguing subfield of connectomics, and can be defined as the 'description of networks formed by co-altered brain areas'. Studies in this recent neuroscientific discipline show that brain disorders do not typically produce alterations on a single cerebral region; in contrast, they frequently affect several different regions. Furthermore, a growing body of evidence suggests that morphological alterations of gray matter (GM) do not occur randomly but, rather, form characteristic patterns of distribution (Cauda et al., 2017; Crossley et al., 2014; Fornito et al., 2015; Menon et al., 2011). For instance, with regard to mental illness it has been proposed that alterations in a certain set of cerebral regions might be commonly related to a broad spectrum of psychiatric conditions (Crossley et al., 2015; Goodkind et al., 2015). And another meta-analysis has shown overlapping patterns of GM alterations in three neuropsychiatric disorders – i.e., autism spectrum disorder, schizophrenia, and obsessive spectrum disorder (Cauda et al., 2017).

These studies provide a transdiagnostic model for mental illness suggesting that risk factors may generate alterations in the functioning of cerebral circuits,

which in turn may induce vulnerability to psychopathologic processes in such a way that specific cognitive domains result to be affected. This view emphasizes the connection between common symptom variance and common genetic variance and considers it to be a consequence of a shared genetic liability, which might contribute to the disruption of brain networks underlying different cognitive domains (Buckholtz and Meyer-Lindenberg, 2012). Brain alterations and dysfunction would not be strictly associated with typical clinical symptoms but, rather, to endophenotypes; in other words, they may be associated with specific domains and neuropsychological functions, together with epigenetic and environmental factors that could interact with the endophenotypes to generate a complex set of symptoms and, eventually, a phenotypical syndrome. These genetic and environmental risk factors are supposed to impact on systems-level circuits for the main dimensions of cognition. Thus, the disruption of these important circuits might cause a transdiagnostic symptomatology and a sort of susceptibility to a variety of psychopathological conditions rather than to clear-cut categorical diseases (Buckholtz and Meyer-Lindenberg, 2012).

Distribution of GM alterations in network-like patterns have been found not only in neurodegenerative and psychiatric diseases, but also in other neuropathological conditions such as chronic pain (Tatu et al., 2018). In particular, Tatu et al. (2018) have showed that GM alterations are characterized by symptom-related patterns of morphometric co-alterations, which strongly reflect the patterns of brain functional connectivity. Furthermore, within the network formed by co-altered areas it is possible to identify a set of highly connected nodes. Specifically, regions exhibiting GM increases appear to be more locally distributed, while regions exhibiting GM decreases appear to produce a more densely distributed network, with long-range, intra- and inter-hemispheric connections (Tatu et al., 2018).

In another meta-analytic study, dedicated to the construction of the pathoconnectivity profile of Alzheimer's disease (AD), Manuello et al. (2018) have proposed to call the distribution patterns of neuronal alterations

“morphometric co-alteration networks”. These co-alteration networks, which seem to develop according to brain connectivity constraints (Raj et al., 2012; Zhou et al., 2012), can be considered as a form of pathologic anatomical covariance (Evans, 2013; Mechelli et al., 2005). The pathoconnectivity analysis of this study provided further evidence that GM alterations are distributed across the brain in network-like patterns. Moreover, the meta-analysis showed that certain areas of the co-alteration network, in virtue of their network centrality and high values of node degree, may be considered as pathoconnectivity hubs capable of influencing the development of morphological abnormalities (Manuello et al, 2018).

In sum, these innovative methodologies of pathoconnectivity analysis (which so far have been based almost exclusively on transdiagnostic maps, i.e, neuroimaging maps that meta-analytically merge different results related to various pathologies) are proving themselves to be important tools for opening novel perspectives on brain disorders, as their application to both neurological and psychiatric diseases provides valuable insights capable of improving our understanding of the pathological brain. Furthermore, this transdiagnostic outlook aims at cutting across existing categorical diagnoses in order to construct an improved classification system for brain diseases.

On these grounds, two studies are going to be discussed in the following chapters. One that investigates how three different types of brain connectivity can influence the distribution of GM alterations, and another that focuses on analyzing the distribution pattern of GM alterations associated with one of the most frequently pathologically affected areas of the brain, the insular cortex.

2. Study 1

2.1. Introduction

As we have seen in the preceding paragraphs, brain disorders (be they neurological or psychiatric) are characterized by distributed GM alterations. With regard to neurodegenerative diseases, in particular, GM alterations have been reported to propagate from one brain area to another in distinctive network-like patterns (Yates, 2012; Pandya et al., 2017). These distribution patterns of pathological co-alterations seem to propagate along pathways that are influenced by the constraints of brain connectivity (Cauda et al., 2018a; Iturria-Medina and Evans, 2015; Manuello et al., 2018; Oxtoby et al., 2017; Raj et al., 2012; Tatu et al., 2018; Yuan et al., 2017; Zhou et al., 2012). As a matter of fact, distribution patterns of neuronal atrophy generated by neurodegenerative processes resemble the patterns of neural connections (Warren et al., 2013). What is more, brain disorders tend to selectively target specific subpopulations of neurons, which frequently are at the center of important functional networks (Saxena and Caroni, 2011). In virtue of their significant central position, these areas can be considered as brain hubs and, thereby, more likely to be vulnerable to pathological processes (Crossley et al., 2014; Cope et al., 2018).

In light of the aforementioned studies, brain connectivity profiles are supposed to influence the spread of GM alterations across different cerebral regions; therefore, they can be significantly involved in the development of brain diseases. What remains as yet unclear is why pathological alterations propagate along such networks, how much different connectivity patterns can influence and guide the spread of alterations, and whether the strength of network connectivity may predict the severity of disease. A connectomic approach to the pathological brain is fundamental to address these issues, as it is uniquely entitled to answer the following questions. Are there some pathways that are prevalently followed

by alterations? Are there connectivity patterns that can influence more significantly the distribution as well as the spread of alterations? And, finally, is it possible to predict the development of GM alterations on the basis of connectivity constraints?

2.1.1. Mechanisms at the basis of the alterations' spread

To date, at least four underlying mechanisms (which are not necessarily mutually exclusive) have been proposed to account for the propagation of brain alterations: i) transneuronal spread, ii) nodal stress, iii) shared vulnerability, and iv) trophic failure (Fornito et al., 2015; Zhou et al., 2012).

The hypothesis of the transneuronal spread considers the involvement of toxic agents moving along axonal connections (Clavaguera et al., 2014; Goedert et al., 2010; Jucker and Walker, 2013; Korth, 2012; Kraus et al., 2013; Soto and Estrada, 2008; Walker et al., 2013). Converging findings suggest that misfolded proteins might propagate in a prion-like manner along axonal pathways, diffusing a corruptive templating that in turn might cause a cascade phenomenon of misfolded protein spread (Hardy and Revesz, 2012; Jucker and Walker, 2011; Warren et al., 2013). Within the brain, in fact, axonal projections and synaptic contacts may serve as conduits for the spread of pathological processes. In other words, misfolded proteins would diffuse GM alterations across brain areas that are anatomically connected (Chevalier-Larsen and Holzbaur, 2006; Fornito et al., 2015; Goedert et al., 2010; Iturria-Medina et al., 2014; Zhou et al., 2012). Disruption could therefore spread easily between the connected elements of a network, the dysfunction of which might eventually impact on a large-scale system. The transneuronal spread of toxic agents would produce over time a transneuronal degeneration, that is, a structural deterioration of areas connected to the ones affected by pathology. When the pathology progresses, the transneuronal deterioration often affects areas that are remote from the site of inception. This type of degeneration can be either anterograde or retrograde (Fornito et al., 2015). The former refers to the damage of one neuron that causes

deterioration to postsynaptic sites; the latter refers to the deterioration of a presynaptic neuron as a consequence of the damage of its postsynaptic target. The degeneration can have different manifestations, including reductions in dendrite and synapse number, neuronal shrinkage, alterations of axonal myelin content and fiber number, and finally the brain cell death (Cowan, 1970).

Resembling the mechanism identified in prion disease (Aguzzi et al., 2007), the transneuronal spread has been suggested to play e role in the development of neurodegenerative conditions, such as Parkinson's disease, AD, Huntington's disease, hereditary motor neuropathy, hereditary spastic paraplegia, tauopathies, amyotrophic lateral sclerosis, and Charcot-Marie-Tooth disease (Bartzokis, 2011; Bourdenx et al., 2017; Clavaguera et al., 2013; Hirokawa et al., 2010; Perlson et al., 2010). However, despite these interesting findings, it should be observed that the prion-like hypothesis at the root of neurodegenerative diseases is still an open field of research (Guest et al., 2011).

The hypothesis of the nodal stress claims that the most active brain areas (i.e., network hubs) might also be the most functionally stressed (Crossley et al., 2014). In fact, in virtue of their intense activity, these cerebral regions are supposed to be more susceptible to be structurally altered (Buckner et al., 2005; Saxena and Caroni, 2011). In the long run this intense activity might disrupt the brain cell metabolism, leading to hyperexcitability and increased vulnerability of functionally interconnected hubs (Saxena and Caroni, 2011; Zhou et al., 2012). The phenomenon of the nodal stress has been reported in humans by using brain imaging techniques and voxel-based meta-analyses (Crossley et al., 2014). It strongly suggests that not all brain areas are equal; on the contrary, some are more fundamental for the functional maintenance of the network which they contribute to, so much so that the pathological impact of network disruption depends on the centrality and connection topology of the affected areas (Alstott et al., 2009; Honey and Sporns, 2008). The centrality of a node (i.e., brain area) measures the topological importance of a network node. It is commonly quantified on the basis of the node degree, which is the number of connections or

edges linked to the node (Borgatti, 2005). Functional brain networks are characterized by various degree distributions, that is to say, they are composed of many nodes with low degree and a small amount of nodes with high degree. These are the hubs of the network and a damage to them would result in the failure of a disproportionate number of connections, leading to the network fragmentation and disruption (Albert et al., 2000). This is so because topologically central hubs are highly interconnected; they form, as we have already said, a rich club capable of favoring communications between different cerebral regions (van den Heuvel and Sporns, 2011). Of note, these brain hubs are more distributed in integration and association cortices; primary sensory cortices, on the other hand, appear to present lower degrees of topological centrality (Harriger et al., 2012; Zamora-López, 2010). It is not surprising, therefore, that a damage to these highly connected areas and/or to the connections between them has significant effect on brain network organization and function than the damage affecting topologically peripheral nodes or connections (Alstott et al., 2009; Honey and Sporns, 2008; van den Heuvel and Sporns, 2011). Furthermore, there are distinctions among hubs, since some of them are more "provincial" than others. The provincial hubs are characterized by a strong inter-modular connectivity, that is, they connect prevalently with other nodes within the same module, and for this reason they play a pivotal role in functional specialization. In contrast, other hubs, which can be called "connector hubs", exhibit a more widespread effect on network dynamics, linking different modules within a network, and, thereby, play an essential role in functional integration (Fornito et al., 2012; Guimera and Nunes Amaral, 2005; Power et al., 2013). In other words, these regions serve as "convergence zones" allowing the integration of specialized processes between different neural structures (McIntosh, 2004).

In line with this theoretical considerations and with the nodal stress hypothesis, computational models show that, when impaired, connector hubs disrupt more profoundly the network system, resulting in more pervasive

dysfunction (Honey and Sporns, 2008). Instead, impairment to provincial hubs produce specific deficits. These conclusions are also supported, for instance, by clinical evidence of patients whose dorsomedial prefrontal cortex and anterior insular cortex have been impaired. It is known that these brain areas are functionally connected to many different regions; in accord with the nodal stress hypothesis, patients with damage to these areas exhibit a pervasive clinical profile of neuropsychological deficits within several cognitive domains (Warren et al., 2014). Furthermore, on the basis of the transneuronal spread hypothesis, altered brain hubs might enhance the diffusion and progression of GM alterations (Kitsak et al, 2010). Support to this mechanism of spread is given by evidence that brain areas which are more susceptible to transneuronal degeneration are those that are connected or topologically close to the sites already altered by pathological processes (Klupp et al., 2014; Myers et al., 2014; Verstraete et al., 2013; Zhou et al., 2012). But it is also true the other way round, since a large number of shortest paths between cerebral areas pass through network hubs, which is indicative that these connected nodes can be easily reached by transneuronal degeneration processes (van den Heuvel et al., 2012). Finally, the intense baseline activity and metabolic needs of brain hubs (Liang et al., 2013; Tomasi et al., 2013) could make their neuronal structures specifically exposed to metabolic stress or activity-dependent deterioration, especially if levels of activity increase well beyond the baseline, when these areas are employed for compensation purposes (Bullmore and Sporns, 2012; de Haan et al., 2012; Saxena and Caroni, 2011).

The third hypothesis proposes that certain regions with shared gene or protein expressions may exhibit common vulnerability to brain disorders (Zhou et al., 2012). This phenomenon might be mediated in part by the relationship between patterns of brain connectivity and expression of certain genes (Cioli et al., 2014; French and Pavlidis, 2011; Wolf et al., 2011). The idea that gene expression is associated with brain connectivity should not be surprising. For instance, the expression of a neurotransmitter must be associated with the

expression of proper receptors in the postsynaptic target. Furthermore, the regulation of neurite development, plasticity mechanisms, as well as cell adhesion molecules need appropriate gene expressions in connected neurons (Gascon et al., 2007; Kiryushko et al., 2004).

Although inquiries into this field of research are very complex to conduct *in vivo*, studies on humans show that functionally connected areas share genetic characteristics, which particularly regard the regulation of axon guidance (Cioli et al., 2014; Prieto et al., 2008). Many genes that are involved in brain connectivity result to be very active during the early stages of brain development. There is evidence that these genes are not only active in the developing brain but also in the adult, when they might continue to be effective in the maintenance or tuning of neural connectivity (Murray et al., 2007; Zapala et al., 2005). Of note, some of these genes that are crucial in the growth and maintenance of cerebral structures are supposed to play a role in neuropathological processes (French and Pavlidis, 2011). If so, neuropsychiatric developmental disorders, such as autism spectrum disorder (ASD), which has been associated with connectivity abnormalities (Belmonte et al., 2004; Geschwind and Levitt, 2007), may be due in part to dysfunction in the expression patterns of genes. Given the risk of heritability of many such neurodevelopmental disorders, it is expected that future research will find the relationship between gene expression and connectivity to be strict. Investigations are paving the way for the integration between genetics and connectomics (Lichtman and Sanes, 2008). The study of the relationship between the genome and brain connectivity might be very relevant to the understanding of behavior in these disorders and potentially open new avenues for their treatment.

The fourth hypothesis of GM alterations' spread presupposes a failure in the mechanism of trophic factors' production, which can cause the pathological degeneration of neural wiring (Fornito et al., 2015; Zhou et al., 2012). The dysfunction of trophic factors, which are indispensable ingredients for the development and maintenance of axons and dendrites, could bring about

alterations in specific areas as well as in the connecting pathways. Given that genes play a fundamental role in the growth and conservation of neural routes, the disruption of these factors is also probably related to pathological gene expression patterns (Appel, 1981; Fornito et al., 2015; Salehi et al., 2006; Zhou et al., 2012).

2.1.2. A core set of co-altered areas

Pathoconnectivity studies investigating the networks composed of brain areas that occur to be co-altered are providing interesting insights into the pathological brain; these insights suggest the validity of a neurobiological and transdiagnostic approach for a better understanding of neurological and psychiatric disorders (Buckholtz and Meyer-Lindenberg, 2012; Cauda et al., 2018a; Fornito et al., 2015; Goodkind et al., 2015; Iturria-Medina and Evans, 2015; McTeague et al., 2016; Raj et al., 2012; Sprooten et al., 2017; Zhou et al., 2012). This approach may be counterintuitive, as we tend to think that brain disorders have typical etiological and pathogenetic bases, which, in turn, can cause specific patterns of GM alterations. Nonetheless, converging evidence shows that, except for some pathology-specific abnormalities, a "core set" of co-altered regions is often involved in the larger part of brain disorders (Baker et al., 2014; Cauda et al., 2018a; Douaud et al., 2014; Ellison-Wright and Bullmore, 2010; Etkin and Wager, 2007; Goodkind et al., 2015; Hamilton et al., 2012; Jagust, 2013; Menon, 2013; Saxena and Caroni, 2011). Furthermore, interesting findings obtained from animal models suggest that neurodegenerative conditions mostly affect the brain network hubs that are more susceptible to dysfunction due to the nodal stress caused by their intense activity (Crossley et al., 2014; Raj et al., 2012; Seeley et al., 2009).

As we have seen, these core areas are likely to be brain hubs, which are supposed to be more vulnerable to alterations and more responsible for their propagation. In particular, in humans this "core set" is usually constituted by regions, such as the insular and anterior cingulate cortices, which are involved in

important associative and cognitive functions. These areas are key parts of the cognitive control system, which is thought to monitor a variety of higher-order functions (Cauda et al., 2012b). In particular, the cognitive control exerted through executive functions refers to those brain processes related to the efficient and flexible employment of cognitive resources for dealing with changing contingencies. It is activated in multiple demands involving tasks that range from performance monitoring to focusing attention, allocating information in working memory, inhibiting irrelevant inputs and assessing for selection competing task-relevant responses (Fedorenko et al., 2013; Müller et al., 2015). Consequently, cognitive control is essential for self-regulation as well as for the dynamic response to the requests of the environment (Diamond, 2013). Thus, a prolonged distress favored by brain disorders is likely to enhance the recruitment of cognitive control circuits and areas (such as dorsolateral prefrontal and posterior parietal cortices, anterior cingulate cortex, anterior insula, and anterior prefrontal cortex) in order to cope with symptoms and emotions (Kohn et al., 2014).

In virtue of both its functional and topological features, a large number of brain disorders could impact on the cognitive control system (McTeague et al., 2016). Therefore, perturbations in this important system are likely to be present in a variety of brain diseases (i.e., transdiagnostically). This phenomenon would make it more difficult to distinguish neuropathological conditions that are uniquely based on functional or structural abnormalities regarding the regions of this system (Sprooten et al., 2017). In such cases, an in-depth pathoconnectivity analysis might be of great use to better discriminate between different diseases.

2.1.3. The research hypotheses of this study and the introduction of a new method to test them

As we have seen when we discussed the studies within the field of pathoconnectivity, it is supposed that the spread of GM alterations across the brain might form recognizable networks that in part may be guided by the organization of brain connectivity (Yates, 2012; Raj et al., 2012; Zhou et al.,

2012). Furthermore, a number of studies suggest that these co-alterations networks are associated with both neurodegenerative and psychiatric disorders. In support of this view, genetic studies regarding neurodegenerative dementias indicate how brain alterations antedate the beginning of symptoms by many years (Chhatwal et al., 2018; Rohrer et al., 2015; Quiroz et al., 2015), a finding that implies a less clear-cut boundary between degenerative and neurodevelopmental diseases (Lahiri and Maloney, 2010; Warren et al., 2013; Zawia and Basha, 2005). Eventually, a growing body of investigations about structural and functional changes in psychiatric conditions will increasingly bridge psychiatry and neurology together (Douaud et al., 2014; Du et al., 2017; Gupta et al., 2015).

The absence of direct correspondence between the development of brain disorders and the manifestation of GM alterations suggests an overlap of symptoms depending on the impairment of large-scale networks. Furthermore, transdiagnostic symptomatology is frequently caused by environmental and genetic factors affecting brain circuits at system-level for several domains of cognitive functions. The disruption of these circuits produces susceptibility to different psychopathological conditions rather than specific diseases (Buckholtz and Meyer-Lindenberg, 2012).

In light of the fact that the diffusion of GM alterations appears to be non-random in both neurological and psychiatric conditions (Cauda et al., 2018a; Tatu et al., 2018), a crucial and still unanswered question is whether there is a prevalence of one or more mechanisms of spread at the basis of the development of different brain diseases. One study (Cope et al., 2018) tried to estimate using *in vivo* techniques, such as PET and fMRI, which mechanism of spread is mainly related to the distribution patterns of AD and progressive supranuclear palsy. This study, however, was limited to these two neurodegenerative conditions. As a matter of fact, if GM alterations are guided by the constraints of brain connectivity, it should in theory be possible to predict the distribution of GM alterations on the basis on certain connectivity profiles (Iturria-Medina et al.,

2014; Raj et al., 2012; Robinson, 2012; Zhou et al., 2012). In other words, it should be possible to simulate the temporal development of GM alterations and deduce which of the different connectivity patterns (i.e., functional, anatomical, and genetic) can better account for the distribution of a specific structural co-alteration pattern. Furthermore, we can reason that the different contributions of the mechanisms of spread might cause typical patterns of structural co-alterations. Thus, the presence of a distribution pattern of GM alterations prevalently constituted by anatomically connected regions is supposed to be better accounted for by the hypothesis of the transneuronal spread, which, as we have seen, entails a diffusion of GM alterations to contiguous and directly connected areas. On the other hand, the presence of a distribution pattern of GM alterations prevalently constituted by functionally connected areas is supposed to be better explained by the hypothesis of the nodal stress, which implies a distribution of alterations to functionally associated areas (Biswal, 2012; Buckner et al., 2013). Finally, the presence of a distribution pattern of GM alterations prevalently constituted by similar gene co-expression profiles is supposed to be better accounted for by the hypothesis of the shared vulnerability, which, as we have seen, suggests that structurally co-altered regions are those sharing specific gene expressions (Stuart et al., 2003).

As already said, these four mechanisms should not be considered as mutually exclusive. Conversely, it is very likely that different pathological processes might occur simultaneously and cause the complex picture of increasing dysfunction of brain networks. Furthermore, the distribution of GM abnormalities could result in different patterns, depending on which mechanisms are predominant in a specific disease. Therefore, identifying what patterns are associated with the alteration of different brain regions is the first important step to achieve an in-depth comprehension of how brain disorders affect the connectome. If certain brain areas – typically those having a pivotal role in the cerebral functional organization (i.e., brain hubs) – are supposed to be generally affected in brain degeneration (Crossley et al., 2014, 2016), then it can be hypothesized that these

altered hubs might form typical co-alteration patterns with other altered brain regions.

This co-alteration network analysis would allow to better understand how GM alterations are distributed within the brain, and provide clues to assess the aforementioned different hypotheses of brain alterations' spread (Cauda et al., 2015). To test the hypotheses of the present study and achieve this pathoconnectivity analysis, an innovative methodology has been applied, which is capable of estimating how each type of brain connectivity profile can predict the distribution patterns produced by GM co-alterations (Cauda et al., 2018a, 2018b). This method has been employed transdiagnostically in order to analyze a large number of meta-analytical data and demonstrate that, in principle, the methodological procedure is applicable for the analysis of GM alterations produced by any brain disorder.

The voxel-based morphometry (VBM, for a detailed description of this technique, see the Materials and Methods section) database of BrainMap (Fox et al., 2005; Fox and Lancaster, 2002; Laird et al., 2005b; see the Materials and Methods section for an illustration of the BrainMap initiative) was examined in order to create a transdiagnostic map of GM alterations. GM alterations identified by VBM were used as a proxy for morphological abnormalities. Then, co-occurrences of alteration between different brain areas were established. In other words, given an altered brain regions A, it was calculated whether other brain regions resulted to be altered with A (Cauda et al., 2018a; Manuello et al., 2018; Tatu et al., 2018).

The result of this procedure was the construction of undirected co-alteration graphs illustrating the brain regions constituting the structural co-alteration network. Subsequently, to evaluate which of the three different connectivity profiles (anatomical, functional, and genetic) could explain better the patterns of structural co-alterations, connectivity networks associated with the three profiles were calculated using anatomical, resting state functional, and genetic (i.e., the correlated gene expression patterns) data, on the basis of the most altered regions

as starting points (nodes). The obtained different network matrices were eventually compared with the structural co-alteration matrix. This allowed to discover the contribution of each connectivity profile to the co-alteration network derived from the VBM database. With the help of simulation techniques, the spatial and temporal progressions of the distribution patterns of co-alterations were estimated; this allowed to assess whether the distribution of structural co-alterations could be predictable in terms of anatomical, functional, and genetic connectivity.

It was therefore possible to address the following issues. 1) What are the distribution patterns of structural co-alterations across the pathological brain? 2) Given that GM alterations tend to propagate from one brain area to another, is the propagation influenced by the constraints of brain connectivity? 3) What type of connectivity (anatomical, functional, or genetic) can mainly account for the distributions patterns of GM alterations? 4) And what type of connectivity is able to better predict the development of these co-alterations?

2.2. Materials and methods

2.2.1. The voxel-based morphometry

Among the structural techniques of brain imaging, the most used is probably the voxel-based morphometry (VBM), originally proposed by Wright et al. (1995). Today most neuroimaging software can do this type of analysis. The VBM is a computational approach that measures differences in local concentration of brain tissue. It is an essential tool for studying the conformation of the brain and is mainly employed to examine and compare the anatomical characteristics of specific populations (Ashburner and Friston, 2000).

Before VBM, this type of studies required the manual individuation of brain areas on MR images throughout a long and painstaking process. But the anatomical details were coarse. In contrast, the automatic approach of VBM allowed a higher resolution, faster times of elaboration and more accuracy in the detection of anatomical structures (Filippi, 2009). VBM is generally used in cortical and subcortical analyses of GM, but morphometric studies of white matter (WM) are also possible.

The 3-D neuroimaging unit is the voxel, which can have a cubic form, if isometric, or be a parallelepiped. Each voxel conveys the information associated with the brain tissue represented in the image; different levels of intensity indicate different concentration of tissues. In case of GM measures, therefore, decreases are values of GM density below the average, while increases are values of GM density above the average. In order to compare subjects and population of subjects, it is necessary to standardize the data through a spatial normalization. This process brings the individual anatomical coordinates into a common stereotactic space (Ashburner and Friston, 2000). There are different reference templates but the most used are certainly the Talairach and MNI atlases. The former was realized in 1967 by the neurosurgeon Jean Talairach and is based on the post-mortem dissection of a single brain; the latter, instead, was realized by the Montreal Neurological Institute and is based on a wider sample of brains.

After the spatial normalization, each voxel is assigned to one of three classes (GM, WM, and liquor). Algorithms implement a probabilistic calculus and take primarily into consideration values of luminous intensity of every voxel as well as its spatial position (Ashburner and Friston, 2000). The degree of reliability of this procedure is higher for wider and more uniform regions, lower for regions that are less uniform or because they are adjacent to different brain tissues. At this point it is possible to compare different subjects or different populations, evaluating the values of couples of voxels having the same position in the standardized space. The VBM analysis is therefore voxel-wise, as each voxel is always taken into consideration.

To date, limitations of this technique are related to difficulties in the physiological interpretation of results. Despite the best available resolution, the biological processes at the basis of changes in brain structure are still unobservable with MR images. Furthermore, it is as yet not possible to precisely define the histological nature of the tissue within a specific voxel.

For instance, with regard to neurodegenerative diseases such as AD, quantification of atrophy progression need straightforward methods. Historically, a region of interest such as the hippocampus could be manually delineated on a baseline scan, then a volume was calculated, and the same process was repeated on a follow-up scan, so that the difference in volumes represented the measure of change over the interval between scans. Such methodology, applied in many studies, was transparent, but frequently lacked power. Measurement errors in manual outlining are in fact aroud the order of 5%. Furthermore, trials aiming to show disease impact using atrophy as a sign of alteration are typically powered for a 25% reduction in rate of loss, i.e. to include enough subjects for a significant difference between those on placebo declining at 4% per year and those on treatment declining at 3% per year. It is not surprising that the difficulty of detecting such small changes has led to costly trials involving many hundreds of patients. Therefore, the development of automated techniques capable of more precise and robust measures with increased power to detect change has been

warmly welcomed. On the other hand, this new procedures have caused the emergence of other potential methodological biases. For instance, the possible bias arising from asymmetric image registration has been a concern pointed out by many authors, including Smith et al. (2002), Reuter et al. (2010) and Yushkevich et al. (2010). These problems can be addressed by using different metrics to compare measurements as well as by defining the sample size, which is the number of subjects needed per study, whose construction is driven by two key components: the amount of change in the measure over time (in case of atrophy the mean "pathological" atrophy rate), and the variability (variance) of that measure in the population under study.

Another problem for atrophy quantification, as well as for several areas in the field of neuroimaging is the lack of "ground truth". Unlike many biochemical tests, there is not a gold standard according to which we can evaluate image quantification, in particular in the case of heterogeneous and complex neurodegenerative diseases. In fact imaging reports of atrophy patterns are hardly to be confirmed, as the brain is rarely available for direct examination, and never serially. In order to address this problem, an approach proposes to simulate atrophy (Camara et al., 2006) and to assess the precision and accuracy by which a methodology can quantify the simulated change (Camara et al., 2008). Yet, the complex interplay between the human brain and its response to disease implies that simulations are always partial. Furthermore, highly sophisticated simulations may be susceptible to biases of their own.

Facing this situation, Fox et al. (2011) have put forward the following suggestions in order to improve methodologies designed to quantify atrophy from serial scans: 1) using simulations of atrophy; 2) assessing the commutative symmetry of measures; 3) assessing the transitivity of measures: if three sequential scans are available, does the sum of measures for A→B and B→C reproduce the outcome of directly measuring A→C?; 4) if possible, comparing automated imaging results with low-bias (but high-variability) manual measurements; 5) comparing results of different techniques on the same data set;

6) assessing the “reproducibility” of results after short interval scans; 7) when possible, comparing imaging results with the known disease biology and pathological studies.

VBM have been largely used to evaluate the pathology of various neurodegenerative disorders, following the assumption that there is a close relationship between specific alteration patterns of cerebral atrophy and the symptomatic cognitive disturbances. But although focusing the analyses on similar disease states, many studies have varied significantly with respect to the steps employed in the sequence of image processing, and this may produce difficulties in the comparison of results between studies. Thus, in the absence of a precise quantitative procedure for comparing VBM implementations, a useful approach is to qualitatively compare results of each methodology against well-known concepts about the anatomic distribution of a neurodegenerative disease, as well as the application of different VBM pipelines and the subsequent comparison of the obtained results.

An evaluation of different VBM implementations was carried out by Senjem et al. (2005), who compared five VBM methods. Authors observed that changes in the image processing chain of VBM can significantly influence the results of inter-group morphometric comparisons. It is therefore suggested to be careful in the interpretation of results, so as not to mistake differences due to implementation details for real biological differences. Conclusions of the authors were the following. Optimized VBM provides different results than those obtained with standard VBM. The use of custom template and prior images improves the plausibility of inter-group comparisons, probably because of the improved segmentation and spatial normalization. Instead, the use of manually edited brain masks in the segmentation and normalization processes does not significantly affect group comparison results. But the additional step of Method 5, which uses previous estimates to initialize the normalization and segmentation routines can give more plausible results. Table 1 illustrates the general features of each of the five VBM methods examined by Senjem at al. (2005).

Table 1. Comparison of different voxel-based morphometry (VBM) procedures.

Description	**Pipeline steps**
Method 1: Standard VBM with the Montreal Neurological Istitute (MNI) template	(i) performing a 12 degrees of freedom (DOF) affine registration between each subject's MRI image and the MNI template; (ii) performing of a non-linear normalization of the affine registered subject image to the MNI template; (iii) segmenting the normalized image using the MNI priors; (iv) applying Jacobian modulation to the segmented GM image; (v) applying a 12-mm full width at half maximum (FWHM) spatial smoothing to the modulated GM image; (vi) statistical comparison between patient and control populations using a two-sided t test.
Method 2: Optimized VBM with the MNI template and priors	(i) performing a 12 DOF affine registration between each subject's MRI image and the MNI template; (ii) segmenting the affine-registered image using the MNI priors; (iii) performing a non-linear normalization of the segmented GM image to the MNI GM prior, applying the parameters obtained to the original whole head image; (iv) segmenting the normalized whole head image using the MNI priors; (v) applying Jacobian modulation to the segmented GM image; (vi) applying the 12 mm FWHM spatial smoothing to the modulated GM image, and proceed to the statistics stage.
Method 3: Optimized VBM with a custom template and priors	(i) performing a 12 DOF affine registration between each subject's MRI image and the custom template; (ii) segmenting the affine-registered image using the custom priors; (iii) performing a non-linear normalization of the segmented GM image to the custom GM prior, applying the parameters obtained to the original whole head image; (iv) segmenting the normalized whole head image using the custom priors; (v) applying Jacobian modulation to the segmented GM image; (vi) applying 12 mm FWHM spatial smoothing to the modulated GM image, and proceed to the statistics stage.
Method 4: Optimized VBM with a custom template plus manually edited brain masks for each patient	Steps are identical to Method 3, except that the hand edited brain mask are used as a weighting image during both segmentation steps.
Method 5: Optimized VBM with a custom template plus a re-initialization routine	This Method follows the same algorithm as Method 3, except for the re-initialization routines: when creating the custom template and priors, the original images are normalized to the MNI template, and then segmented using the MNI priors.

As we have seen, VBM has been widely applied both in group studies (Focke et al., 2008a; Keller and Roberts, 2008) and in comparing single subjects against a group (Focke et al., 2008b; 2009; Woermann et al., 1999). It is important to highlight that within the preprocessing of VBM data, correction of image bias is a key step, which is iteratively improved together with the segmentation technique, e.g. in FAST4 (Zhang et al., 2001) or in the unified segmentation algorithm of the SPM packages (Ashburner and Friston, 2005). Given the differences in VBM procedures, especially in the segmentation techniques, some authors have investigated whether or not data coming from different scanners could be combined together in order to be meta-analytically examined. Stonnington et al. (2008) concluded that "data can be pooled from different scanners without corroding the integrity of results is reassuring for largemulti-site studies". However, another study considering three different sites (2×1.5 T, 1 x 3T, all with transmit-receive head coils) have reported stronger scanner specific than disease specific (childhood absence epilepsy) differences, exceeding a $p < 0.05$ (FWE corrected) threshold (Pardoe et al., 2008). Finally, a study by Focke et al. (2011) showed severe scanner differncences and concluded that the applied version of the SPM8 segmentation algorithm seems to be more robust than the FSL4.1/FAST4 method. A lowered bias cutoff in the unified segmentation of SPM8 reduced cortical differences but resulted in higher coeffD values in basal ganglia regions (putamen/pallidum). This study, however, was carried out on healthy controls only and could not, therefore, compare volumetric differences to changes due to a disease condition.

For all these considerations, results of Study 1 are to be interpreted with caution, as clearly stated in the limitation section.

2.2.2. Selection of studies

The VBM BrainMap database (Fox and Lancaster, 2002; Fox et al., 2005; Laird et al., 2005b; Vanasse et al., 2018) was queried in December 2017 with the following search criteria:

(i) decreases: Experiments Context is Disease AND Experiment Contrast is Gray Matter AND Experiments Observed Changes is Controls > Patients;

(ii) increases: Experiments Context is Disease AND Experiment Contrast is Gray Matter AND Experiments Observed Changes is Patients > Controls.

The retrieved experiments were 912 for the first query and 350 for the second query. All the experiments having a sample size smaller than 8 subjects were removed. This threshold is in line with Scarpazza et al. (2015), who provided evidence that VBM experiments based on groups of equal size should not be biased by a high false positive rate.

Furthermore, all the experiments that did not clearly compare pathological population with healthy controls were removed. The remaining experiments were coded on the basis of the ICD-10 system. All the experiments not coded with the labels 'F' (i.e., mental, behavioral and neurodevelopmental disorders) or 'G' (i.e., diseases of the nervous system) were excluded. Finally, all the experiments that were associated with codes not regarding primary brain disorders were removed (i.e., F10: Alcohol related disorders; F15: Other stimulant related disorders; F28: Other psychotic disorder not due to a substance or known physiological condition; F91: Conduct disorders; G11: Hereditary ataxia; G43: Migraine; G44: Other headache syndromes; G47: Sleep disorders; G50: Disorders of trigeminal nerve; and G71: Primary disorders of muscles).

At the end of this selection, experiments fed to the analyses for the first query were 642 (for a total of 15820 subjects and 7704 foci) and 204 (for a total of 4966 subjects, and 2244 foci) for the second query.

With regard to the first query, the majority of VBM studies investigated F20: Schizophrenia (17.9%); F32-F33: Major depressive disorder, single

episode/recurrent (9.8%); G40: Epilepsy and recurrent seizures (8.7%); G30: Alzheimer's disease (8.3%) and G31: Other degenerative diseases of the nervous system (8.1%).

With regard to the second query, the majority of VBM studies investigated F20: Schizophrenia (16.2%); G40: Epilepsy and recurrent seizures (12.7%); F84: Pervasive developmental disorders (11.3%); F31: Bipolar disorder (9.8%) and F32-F33: Major depressive disorder, single episode/recurrent (9.3%). The entire overview of the pathologies considered in this study is reported in Table 2.

Table 2. Synopsis of pathologies of the database used for analyses.

Exp (n) = number of experiments; Exp (%) = percentage of the total of the experiments; Subj (n) = number of subjects.

	ICD-10 code	Exp (n)	Exp (%)	Subj (n)
First query	F20: Schizophrenia	115	17.9	3807
	F28: Other psychotic disorder not due to a substance or known physiological condition	3	0.5	68
	F31: Bipolar Disorder	45	7.0	1191
	F32-F33: Major depressive disorder, single episode/recurrent	63	9.8	1919
	F41: Other Anxiety Disorders	13	2.0	306
	F42: Obsessive Compulsive Disorder	12	1.9	377
	F43: Reaction to Severe Stress and Adjustment Disorders	24	3.7	367
	F50: Eating Disorders	12	1.9	148
	F60: Specific Personality Disorders	10	1.6	222
	F65: Paraphilias	1	0.2	18
	F80: Specific Developmental Disorders of Speech and Language	2	0.3	22
	F84: Pervasive Developmental Disorders	29	4.5	696
	F90: Attention Deficit/Hyperactivity Disorder	9	1.4	139
	F95: Tic Disorder	2	0.3	33
	G10: Huntington's Disease	12	1.9	258
	G12: Spinal Muscular Atrophy and Related Syndromes	14	2.2	211
	G20: Parkinson’s Disease	28	4.4	501
	G23: Other degenerative diseases of basal ganglia	13	2.0	212
	G24: Dystonia	6	0.9	89
	G25: Other extrapyramidal and movement disorders	7	1.1	135
	G30: Alzheimer's Disease	53	8.3	1194
	G31: Other Degenerative Diseases of Nervous System	52	8.1	838
	G35: Multiple Sclerosis	45	7.0	1422
	G40: Epilepsy and Recurrent Seizures	56	8.7	1426
	G90: Disorders Autonomic Nervous System	13	2.0	181
	G93: Other disorders of brain	3	0.5	40

Second query	F20: Schizophrenia	33	16.2	1175
	F28: Other psychotic disorder not due to a substance or known physiological condition	3	1.5	75
	F31: Bipolar Disorder	20	9.8	545
	F32-F33: Major depressive disorder, single episode/recurrent	19	9.3	453
	F41: Other Anxiety Disorders	4	2.0	51
	F42: Obsessive Compulsive Disorder	10	4.9	287
	F43: Reaction to Severe Stress and Adjustment Disorders	2	1.0	48
	F50: Eating Disorders	4	2.0	54
	F80: Specific Developmental Disorders of Speech and Language	3	1.5	48
	F84: Pervasive Developmental Disorders	23	11.3	515
	F90: Attention Deficit/Hyperactivity Disorder	2	1.0	27
	F95: Tic Disorder	2	1.0	45
	G10: Huntington's Disease	1	0.5	21
	G12: Spinal Muscular Atrophy and Related Syndromes	1	0.5	22
	G20: Parkinson's Disease	9	4.4	139
	G24: Dystonia	8	3.9	133
	G25: Other extrapyramidal and movement disorders	7	3.4	125
	G30: Alzheimer's Disease	7	3.4	114
	G31: Other Degenerative Diseases of Nervous System	10	4.9	123
	G35: Multiple Sclerosis	10	4.9	253
	G40: Epilepsy and Recurrent Seizures	26	12.7	713

The outline of the search strategy in order to select the studies is illustrated in the flow chart of Figure 1, which reports the key steps implemented to get the final data set, elaborate data and obtain different levels of results. Tables 3 and 4 reports the full list of the selected studies (432 for the first query and 135 for the second query, respectively).

Figure 1. Flow chart of key steps implemented to get the final data set, elaborate data and obtain different levels of results.

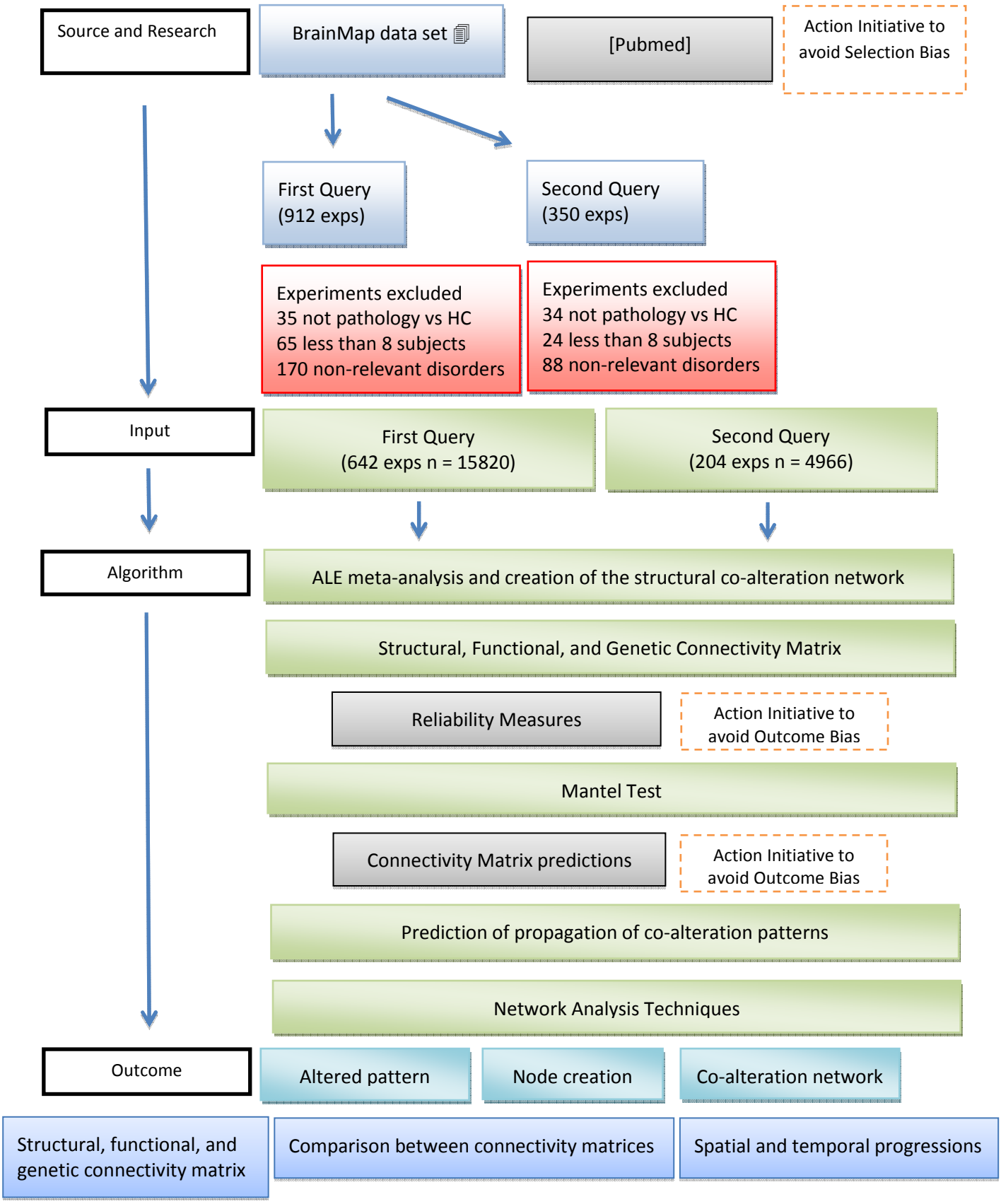

Table 3. List of experiments obtained and selected from the first query.

	Year	1st Author	Journal	Medline	ICD-10 Code
1	2010	Abe O	Psychiatry Res	-	F32-F33: Major depressive disorder. single episode/recurrent
2	1999	Abell F	NeuroReport	10501551	F84: Pervasive Developmental Disorders
3	2012	Adleman N E	J Child Psycho Psychiatry	3472043	F31: Bipolar Disorder
4	2005	Adler C M	Biol Psychiatry	15922309	F31: Bipolar Disorder
5	2007	Agosta F	Hum Brain Mapp	17370339	G12: Spinal Muscular Atrophy and Related Syndromes
6	2010	Agosta F	Eur J Neurosci	20597976	G23: Other degenerative diseases of basal ganglia
7	2011	Agosta F	Radiology	21177393	G30: Alzheimer's Disease
8	2011	Agosta F	Radiology	21177393	G31: Other Degenerative Diseases of Nervous System
9	2012	Ahmed F	Neuropsychobiology	22948482	F43: Reaction to Severe Stress and Adjustment Disorders
10	2011	Ahrendts J	World J Biol Psychiatry	20879808	F90: Attention Deficit/Hyperactivity Disorder
11	2013	Alemany S	J affect disord	-	F32-F33: Major depressive disorder. single episode/recurrent
12	2009	Almeida J R C	Psychiatry Res NeuroImaging	19101126	F31: Bipolar Disorder
13	2016	Alonso_Lana S	PLoS One	4957815	F31: Bipolar Disorder
14	2013	Ambrosi E	J Affect Disord	-	F31: Bipolar Disorder
15	2002	Ananth H	Am J Psychiatry	12202269	F20: Schizophrenia
16	2005	Antonova E	Biol Psychiatry	16039619	F20: Schizophrenia
17	2009	Arnone D	Eur Neuropsychopharmacol	-	F32-F33: Major depressive disorder. single episode/recurrent
18	2013	Arnone D	Mol Psychiatry	23128153	F32-F33: Major depressive disorder. single episode/recurrent
19	2009	Asami T	Psychiatry Res	19560907	F41: Other Anxiety Disorders
20	2011	Ash S	Brain Lang	21689852	G31: Other Degenerative Diseases of Nervous System
21	2004	Audoin B	J magn reson imaging	15503338	G35: Multiple Sclerosis
22	2006	Audoin B	J Neurol	17093899	G35: Multiple Sclerosis
23	2010	Audoin B	J Neurol Neurosurg Psychiatr	20392976	G35: Multiple Sclerosis
24	2007	Audoin B	Mult Scler	17463071	G35: Multiple Sclerosis
25	2008	Barbeau E	Neuropsychologia	18191160	G31: Other Degenerative Diseases of Nervous System
26	2001	Baron J C	NeuroImage	11467904	G30: Alzheimer’s Disease
27	2007	Bassitt D P	Eur Arch Psychiatry Clin Neurosci	16960651	F20: Schizophrenia
28	2006	Baxter L C	J Alzheimers Dis	16914835	G30: Alzheimer’s Disease
29	2005	Bell-McGinty S	Arch Neurol	16157746	G31: Other Degenerative Diseases of Nervous System
30	2011	Bergè	Acta Psychiatr Scand	21054282	F20: Schizophrenia

31	2009	Bergouignan L	NeuroImage	19071222	F32-F33: Major depressive disorder. single episode/recurrent
32	2008	Berlingeri M	Behav Neurosci	18413913	G30: Alzheimer's Disease
33	2004	Bernasconi N	NeuroImage	15488421	G40: Epilepsy and Recurrent Seizures
34	2013	Bertsch K	Eur Arch Psychiatry Clin Neurosci	23381548	F60: Specific Personality Disorders
35	2008	Beste C	Hum Brain Mapp	17497629	G10: Huntington's Disease
36	2007	Beyer M K	J Neurol Neurosurg Psychiatr	17028119	G20: Parkinson's Disease
37	2011	Biundo R	J Neurol Sci	21862438	G20: Parkinson's Disease
38	2005	Boccardi M	Neurobiol Aging	15585344	G31: Other Degenerative Diseases of Nervous System
39	2009	Bodini B	Hum Brain Mapp	19172648	G35: Multiple Sclerosis
40	2011	Boghi A	Psychiatry Res	21546219	F50: Eating Disorders
41	2011	Bonavita S	Mult Scler	21239414	G35: Multiple Sclerosis
42	2008	Bonilha L	Schizophr Res	18164594	F20: Schizophrenia
43	2004	Bonilha L	Arch Neurol	15364683	G40: Epilepsy and Recurrent Seizures
44	2010	Borgwardt S J	Biol Psychiatry	20006324	F20: Schizophrenia
45	2008	Borroni B	Arch Neurol	18541800	G31: Other Degenerative Diseases of Nervous System
46	2009	Bose S K	Schizophr Res	19450953	F20: Schizophrenia
47	2008	Bouilleret V	Neurology	18195263	G40: Epilepsy and Recurrent Seizures
48	2006	Boxer A L	Arch Neurol	16401739	G23: Other degenerative diseases of basal ganglia
49	2003	Boxer A L	Arch Neurol	12873851	G30: Alzheimer's Disease
50	2003	Boxer A L	Arch Neurol	12873851	G31: Other Degenerative Diseases of Nervous System
51	2006	Boxer A L	Arch Neurol	16401739	G31: Other Degenerative Diseases of Nervous System
52	2006	Bozzali M	Neurology	16894107	G30: Alzheimer's Disease
53	2006	Bozzali M	Neurology	16894107	G31: Other Degenerative Diseases of Nervous System
54	2009	Brambati S M	Neurobiol Aging	17604879	G31: Other Degenerative Diseases of Nervous System
55	2009	Brazdil M	Hum Brain Mapp	18609565	G40: Epilepsy and Recurrent Seizures
56	2004	Brenneis C	J Neurol Neurosurg Psychiatr	14742598	G23: Other degenerative diseases of basal ganglia
57	2004	Brenneis C	NeuroReport	15257132	G30: Alzheimer's Disease
58	2004	Brenneis C	NeuroReport	15257132	G31: Other Degenerative Diseases of Nervous System
59	2003	Brenneis C	J Mov Disord	14534916	G90: Disorders Autonomic Nervous System
60	2006	Brenneis C	J Mov Disord	16161039	G90: Disorders Autonomic Nervous System
61	2007	Brieber S	J Child Psychol Psychiatry	-	F84: Pervasive Developmental Disorders
62	2007	Brieber S	J Child Psychol Psychiatry	-	F90: Attention Deficit/Hyperactivity Disorder

63	2010	Brunner R	NeuroImage	19660555	F60: Specific Personality Disorders
64	2004	Burton E J	Brain	14749292	G20: Parkinson's Disease
65	2002	Burton E J	NeuroImage	12377138	G31: Other Degenerative Diseases of Nervous System
66	2015	Cai Y	Neurosci Bull	25502401	F31: Bipolar Disorder
67	2015	Cai Y	Neurosci Bull	25502401	F32-F33: Major depressive disorder. single episode/recurrent
68	2009	Camicioli R	Parkinsonism Relat Disord	18573676	G20: Parkinson's Disease
69	2010	Canu E	Neurobiol Aging	21074899	G30: Alzheimer's Disease
70	2005	Carmona S	Neurosci Lett	16129560	F90: Attention Deficit/Hyperactivity Disorder
71	2007	Caroli A	J Neurol	17990057	G30: Alzheimer's Disease
72	2010	Cascella N	Schizophr Res	20452187	F20: Schizophrenia
73	2009	Castro-Fornieles J	J Psychiatr Res	18486147	F50: Eating Disorders
74	2011	Castro-Manglano P D	Bipolar Disord	22017223	F20: Schizophrenia
75	2009	Ceccarelli A	Hum Brain Mapp	19172642	G35: Multiple Sclerosis
76	2008	Ceccarelli A	NeuroImage	18501636	G35: Multiple Sclerosis
77	2010	Celle S	J Neurol	19768657	G25: Other extrapyramidal and movement disorders
78	2013	Cerasa A	J Neurol	23271221	G35: Multiple Sclerosis
79	2006	Chan C H	Epilepsia	16499767	G40: Epilepsy and Recurrent Seizures
80	2014	Chaney A	J Psychiatry Neurosci	23900024	F32-F33: Major depressive disorder. single episode/recurrent
81	2009	Chang C C	European J Neurol	19486137	G90: Disorders Autonomic Nervous System
82	2005	Chang J L	Neurology	16009889	G12: Spinal Muscular Atrophy and Related Syndromes
83	2012	Chao L L	NeuroReport	22453299	F43: Reaction to Severe Stress and Adjustment Disorders
84	2009	Chen S	BMC Psychiatry	19538748	F43: Reaction to Severe Stress and Adjustment Disorders
85	2006	Chen S	Psychiatry Res	16371250	F43: Reaction to Severe Stress and Adjustment Disorders
86	2007	Chen X	Aust N Z J Psychiatry	17464719	F31: Bipolar Disorder
87	2012	Chen Y	PLoS One	23155380	F43: Reaction to Severe Stress and Adjustment Disorders
88	2015	Cheng B	Front Behav Neurosci	26347628	F43: Reaction to Severe Stress and Adjustment Disorders
89	2010	Cheng Y	Neurosci Lett	20594947	F32-F33: Major depressive disorder. single episode/recurrent
90	2011	Cheng Y	PLoS One	21541322	F84: Pervasive Developmental Disorders
91	2002	Chetelat G	NeuroReport	12395096	G30: Alzheimer's Disease
92	2002	Chetelat G	NeuroReport	12395096	G31: Other Degenerative Diseases of Nervous System
93	2011	Chow E W	Am J Psychiatry	21362743	F20: Schizophrenia
94	2007	Chua S E	Schizophr Res	17098398	F20: Schizophrenia
95	2012	Compta Y	Parkinsonism Relat Disord	22595621	G20: Parkinson's Disease

96	2008	Cooke M A	Schizophr Res	18539438	F20: Schizophrenia
97	2005	Corbo V	Biol Psychiatry	16038682	F43: Reaction to Severe Stress and Adjustment Disorders
98	2005	Cordato N J	Brain	15843423	G20: Parkinson's Disease
99	2005	Cordato N J	Brain	15843423	G23: Other degenerative diseases of basal ganglia
100	2005	Cormack F	NeuroImage	16006149	G93: Other disorders of brain
101	2012	Cosottini M	Exp Neurol	22226599	G12: Spinal Muscular Atrophy and Related Syndromes
102	2007	Craig M C	Br J Psychiatry	17766762	F84: Pervasive Developmental Disorders
103	2003	Critchley H D	NeuroImage	12725766	G90: Disorders Autonomic Nervous System
104	2011	Cui L	Neurosci Lett	21138758	F20: Schizophrenia
105	2011	Cui L	Neurosci Lett	21138758	F31: Bipolar Disorder
106	2009	de Araujo-Filho G M	Epilepsy Behav	19303459	G40: Epilepsy and Recurrent Seizures
107	2008	de Oliveira-Souza R	NeuroImage	18289882	F60: Specific Personality Disorders
108	2007	Delmaire C	Neurology	17646630	G24: Dystonia
109	2009	Deng M Y	Psychopharmacology	19641900	F20: Schizophrenia
110	2007	Di Paola M	J Neurol	17404777	G30: Alzheimer's Disease
111	2005	Dickstein D P	Arch Gen Psych	15997014	F31: Bipolar Disorder
112	2004	Doris A	Psychiatry Res NeuroImaging	15033185	F31: Bipolar Disorder
113	2007	Douaud G	J Neurol	17698497	F20: Schizophrenia
114	2003	Draganski B	Neurology	14610125	G24: Dystonia
115	2010	Ebdrup B H	J Psychiatry Neurosci	20184807	F20: Schizophrenia
116	2011	Eckart C	J Psychiatry Neurosci	21118656	F43: Reaction to Severe Stress and Adjustment Disorders
117	2012	Ecker C	Arch Gen Psych	22310506	F84: Pervasive Developmental Disorders
118	2010	Ecker C	NeuroImage	19683584	F84: Pervasive Developmental Disorders
119	2008	Egger K	Psychiatry Res	19013058	F32-F33: Major depressive disorder. single episode/recurrent
120	2001	Ellis C M	Neurology	11706094	G12: Spinal Muscular Atrophy and Related Syndromes
121	2014	Eshaghi A	NeuroImage	3898881	G35: Multiple Sclerosis
122	2005	Etgen T	NeuroImage	15670702	G25: Other extrapyramidal and movement disorders
123	2009	Euler M	Schizophr Res	19775870	F20: Schizophrenia
124	2005	Farrow T F D	Biol Psychiatry	15993858	F31: Bipolar Disorder
125	2011	Focke N K	Hum Brain Mapp	21246668	G20: Parkinson's Disease
126	2001	Foong J	Brain	11335691	F20: Schizophrenia
127	2012	Friedrich H C	NeuroImage	21967727	F50: Eating Disorders
128	2002	Frisoni G B	J Neurol Neurosurg Psychiatr	12438466	G30: Alzheimer's Disease
129	2008	Frodl T	Arch Gen Psych	18838632	F32-F33: Major depressive disorder. single episode/recurrent
130	2013	Gao W	J Affect Disord	-	F31: Bipolar Disorder

131	2008	Garcia-Marti G	Neuropsychopharmacol Psychiatry	17716795	F20: Schizophrenia
132	2011	Gaudio S	Psychiatry Res NeuroImaging	21081268	F50: Eating Disorders
133	2007	Gavazzi C	J Comput Assist Tomogr	17882035	G10: Huntington's Disease
134	2012	Ghosh B C	Brain	22637582	G23: Other degenerative diseases of basal ganglia
135	2008	Gilbert A R	J Affect Disord	18342953	F42: Obsessive Compulsive Disorder
136	2013	Giordano A	Parkinsonism Relat Disord	23477861	G23: Other degenerative diseases of basal ganglia
137	2005	Giuliani N R	Schizophr Res	15721994	F20: Schizophrenia
138	2014	Gobbi C	Acad Radiol	23812284	G35: Multiple Sclerosis
139	2010	Gold B T	Hum Brain Mapp	20063353	G31: Other Degenerative Diseases of Nervous System
140	2011	Gong Q	NeuroImage	21134472	F32-F33: Major depressive disorder. single episode/recurrent
141	2011	Granert O	J Neurol Neurosurg Psychiatr	21705464	G24: Dystonia
142	2012	Gregory S	Arch Gen Psych	22566562	F60: Specific Personality Disorders
143	2013	Grieve S M	NeuroImage	24273717	F32-F33: Major depressive disorder. single episode/recurrent
144	2010	Gross RG	Cogn Behav Neurol	20299856	G31: Other Degenerative Diseases of Nervous System
145	2006	Grosskreutz J	BMC Neurol	16638121	G12: Spinal Muscular Atrophy and Related Syndromes
146	2009	Guedj E	Eur J Nucl Med	19224210	G31: Other Degenerative Diseases of Nervous System
147	2014	Guo W	Neuropsychopharmacol Psychiatry	24863419	F32-F33: Major depressive disorder. single episode/recurrent
148	2010	Guo X	Neurosci Lett	19879920	G30: Alzheimer's Disease
149	2004	Ha T H	Psychiatry Res	15664796	F20: Schizophrenia
150	2010	Ha T H	Neurosci Lett	19429131	F31: Bipolar Disorder
151	2007	Hakamata Y	Neuroscience Research	17923164	F43: Reaction to Severe Stress and Adjustment Disorders
152	2008	Haldane M	J Psychopharmacol	18308812	F31: Bipolar Disorder
153	2008	Hall A M	Alzheimers Dement	18631978	G30: Alzheimer's Disease
154	2011	Haller S	J Psychiatry Neurosci	21284917	F31: Bipolar Disorder
155	2007	Hamalainen A	Neurobiol Aging	16997428	G30: Alzheimer's Disease
156	2007	Hamalainen A	Neurobiol Aging	16997428	G31: Other Degenerative Diseases of Nervous System
157	2009	Henley S M	J Neurol	19266143	G10: Huntington's Disease
158	2009	Herold R	Acta Psychiatr Scand	19016669	F20: Schizophrenia
159	2012	Herringa R	Psychiatry Res	23021615	F43: Reaction to Severe Stress and Adjustment Disorders
160	2008	Hirao K	Schizophr Res	18774263	F20: Schizophrenia
161	2006	Hirao K	Nucl Med Commun	16404228	G30: Alzheimer's Disease
162	2008	Honea R A	Biol Psychiatry	17689500	F20: Schizophrenia
163	2009	Honea R A	Alzheimer Dis Assoc Disord	19812458	G30: Alzheimer's Disease
164	2009	Horn H	Br J Psychiatry	19182174	F20: Schizophrenia

165	2010	Horn H	Psychiatry Res NeuroImaging	20418073	F20: Schizophrenia
166	2009	Huey E D	Arch Neurol	19822784	G31: Other Degenerative Diseases of Nervous System
167	2001	Hulshoff Pol H E	Arch Gen Psych	11735840	F20: Schizophrenia
168	2004	Hulshoff Pol H E	NeuroImage	14741639	F20: Schizophrenia
169	2006	Hulshoff Pol H E	NeuroImage	16497519	F20: Schizophrenia
170	2010	Hwang J	J Geriatr Psychiatry Neurol	-	F32-F33: Major depressive disorder. single episode/recurrent
171	2010	Hyde K L	Hum Brain Mapp	19790171	F84: Pervasive Developmental Disorders
172	2011	Ille R	J Psychiatry Neurosci	21406159	G10: Huntington's Disease
173	2011	Inkster B	J Neuroimaging	20977527	F32-F33: Major depressive disorder. single episode/recurrent
174	2005	Ishii K	Eur J Nucl Med	15800784	G30: Alzheimer's Disease
175	2008	Janssen J	J Am Acad Child Adolesc Psychiatry	18827723	F20: Schizophrenia
176	2008	Janssen J	J Am Acad Child Adolesc Psychiatry	18827723	F28: Other psychotic disorder not due to a substance or known physiological condition
177	2008	Janssen J	J Am Acad Child Adolesc Psychiatry	18827723	F31: Bipolar Disorder
178	2005	Jayakumar P N	Neuropsychopharmacol Psychiatry	15866362	F20: Schizophrenia
179	2010	Joos A	Psychiatry Res NeuroImaging	20400273	F50: Eating Disorders
180	2008	Kanda T	Eur J Nucl Med	18661129	G30: Alzheimer's Disease
181	2008	Kanda T	Eur J Nucl Med	18661129	G31: Other Degenerative Diseases of Nervous System
182	2008	Kasai K	Biol Psychiatry	17825801	F43: Reaction to Severe Stress and Adjustment Disorders
183	2010	Kasparek T	Hum Brain Mapp	19777553	F20: Schizophrenia
184	2007	Kasparek T	Neuropsychopharmacol Psychiatry	17011096	F20: Schizophrenia
185	2009	Kasparek T	Neuropsychopharmacol Psychiatry	19647777	F20: Schizophrenia
186	2005	Kassubek J	Cereb Cortex	15459079	G10: Huntington's Disease
187	2004	Kassubek J	J Neurol Neurosurg Psychiatr	14742591	G10: Huntington's Disease
188	2007	Kassubek J	J Neurol Neurosurg Psychiatr	17332050	G12: Spinal Muscular Atrophy and Related Syndromes
189	2012	Kato S	J Neurol	21850388	G20: Parkinson's Disease
190	2006	Kawachi T	Eur J Nucl Med	16550383	G30: Alzheimer's Disease
191	2009	Kawada R	Neuropsychopharmacol Psychiatry	19625009	F20: Schizophrenia
192	2004	Kawasaki Y	Eur Arch Psychiatry Clin Neurosci	15538599	F20: Schizophrenia
193	2007	Kawasaki Y	NeuroImage	17045492	F20: Schizophrenia
194	2008	Ke X	NeuroReport	18520994	F84: Pervasive Developmental Disorders
195	2007	Keller S S	Epilepsy Res	17412561	G40: Epilepsy and Recurrent Seizures

196	2002	Keller S S	J Neurol Neurosurg Psychiatr	12438464	G40: Epilepsy and Recurrent Seizures
197	2007	Khaleeli Z	NeuroImage	17566765	G35: Multiple Sclerosis
198	2013	Kim D	J Affect Disord	23769608	F31: Bipolar Disorder
199	2007	Kim E J	J Neurol Neurosurg Psychiatr	17615169	G31: Other Degenerative Diseases of Nervous System
200	2007	Kim J H	NeuroImage	17689105	G40: Epilepsy and Recurrent Seizures
201	2008	Kim M J	Psychiatry Res	18930633	F32-F33: Major depressive disorder. single episode/recurrent
202	2011	Kim S	J Clin Neurosci	21570296	G30: Alzheimer's Disease
203	2010	Kobel M	Psychiatry Res NeuroImaging	20702071	F90: Attention Deficit/Hyperactivity Disorder
204	2009	Koprivova J	Neurosci Lett	19666084	F42: Obsessive Compulsive Disorder
205	2010	Kosaka H	NeuroImage	20123027	F84: Pervasive Developmental Disorders
206	2009	Koskenkorva P	Neurology	19704079	G40: Epilepsy and Recurrent Seizures
207	2008	Koutsouleris N	NeuroImage	18054834	F20: Schizophrenia
208	2002	Kubicki M	NeuroImage	12498745	F20: Schizophrenia
209	2002	Kubicki M	NeuroImage	12498745	F28: Other psychotic disorder not due to a substance or known physiological condition
210	2011	Kurth F	Biol Psychiatry	21531390	F84: Pervasive Developmental Disorders
211	2004	Kwon H	Dev Med Child Neurol	15540637	F84: Pervasive Developmental Disorders
212	2010	Labate A	Epilepsia	19780790	G40: Epilepsy and Recurrent Seizures
213	2008	Ladoucer C D	J Am Acad Child Adolesc Psychiatry	18356765	F31: Bipolar Disorder
214	2013	Lagarde J	PLoS One	24278277	G23: Other degenerative diseases of basal ganglia
215	2013	Lagarde J	PLoS One	24278277	G31: Other Degenerative Diseases of Nervous System
216	2015	Lai C H	J Affect Disord	-	F32-F33: Major depressive disorder. single episode/recurrent
217	2015	Lai C H	J Affect Disord	-	F41: Other Anxiety Disorders
218	2012	Lai C H	J Affect Disord	22386047	F41: Other Anxiety Disorders
219	2011	Lee H Y	J Affect Disord	21546094	F32-F33: Major depressive disorder. single episode/recurrent
220	2009	Leung K K	Psychol Med	18945378	F32-F33: Major depressive disorder. single episode/recurrent
221	2010	Li C T	NeuroImage	19931620	F32-F33: Major depressive disorder. single episode/recurrent
222	2006	Li L	Can J Psychiatry	16838824	F43: Reaction to Severe Stress and Adjustment Disorders
223	2011	Li M	Psychiatry Res NeuroImaging	21236649	F31: Bipolar Disorder
224	2009	Libon D J	Neurology	19687454	G31: Other Degenerative Diseases of Nervous System
225	2013	Lin A	Neural Regen Res	25206504	G35: Multiple Sclerosis
226	2013	Lin C H	Front Hum Neurosci	23785322	G20: Parkinson's Disease

227	2013	Lin C H	Front Hum Neurosci	23785322	G25: Other extrapyramidal and movement disorders
228	2009	Lin K	Epilepsy Res	19570650	G40: Epilepsy and Recurrent Seizures
229	2014	Liu C H	Neuroscience	24406440	F32-F33: Major depressive disorder. single episode/recurrent
230	2011	Liu M	Epilepsia	22092238	G40: Epilepsy and Recurrent Seizures
231	2010	Lu C	Cortex	19375076	F80: Specific Developmental Disorders of Speech and Language
232	2006	Ludolph A G	Br J Psychiatry	16648537	F95: Tic Disorder
233	2009	Lui S	Am J Psychiatry	18981063	F20: Schizophrenia
234	2004	Lyoo I K	Biol Psychiatry	15013835	F31: Bipolar Disorder
235	2012	Mainz V	Psychosom Med	22511729	F50: Eating Disorders
236	2009	Mak A K	Neuropsychopharmacol Psychiatry	19596037	F32-F33: Major depressive disorder. single episode/recurrent
237	2013	Mak E	J Neurol Neurosurg Psychiatr	24133286	G20: Parkinson's Disease
238	2003	Marcelis M	Psychiatry Res	12694890	F28: Other psychotic disorder not due to a substance or known physiological condition
239	2007	Marti-Bonmati L	Radiology	17641373	F20: Schizophrenia
240	2003	Massana G	Am J Psychiatry	12611840	F41: Other Anxiety Disorders
241	2002	Matsuda H	Eur J Nucl Med Mol Imaging	11884488	G30: Alzheimer's Disease
242	2010	Matsumoto R	Psychiatry Clin Neurosci	20923432	F42: Obsessive Compulsive Disorder
243	2007	Matsunari I	Eur J Nucl Med Mol Imaging	18006622	G30: Alzheimer's Disease
244	2008	Mazere J	NeuroImage	18191587	G30: Alzheimer's Disease
245	2005	McAlonan G M	Brain	15548557	F84: Pervasive Developmental Disorders
246	2002	McAlonan G M	Brain	12077008	F84: Pervasive Developmental Disorders
247	2008	McAlonan G M	J Child Psychol Psychiatry	18673405	F84: Pervasive Developmental Disorders
248	2007	McAlonan G M	Psychiatry Res	17291727	F90: Attention Deficit/Hyperactivity Disorder
249	2004	McIntosh A M	Biol Psychiatry	15476683	F20: Schizophrenia
250	2004	McIntosh A M	Biol Psychiatry	15476683	F31: Bipolar Disorder
251	2004	McMillan A B	NeuroImage	15325363	G40: Epilepsy and Recurrent Seizures
252	2008	Meda S A	Schizophr Res	18378428	F20: Schizophrenia
253	2008	Meisenzahl E M	Schizophr Res	18378428	F20: Schizophrenia
254	2011	Mengotti P	Brain Res Bull	21146593	F84: Pervasive Developmental Disorders
255	2011	Meppelink A M	J Mov Disord	20922809	G20: Parkinson's Disease
256	2008	Mesaros S	Neurology	18272867	G35: Multiple Sclerosis
257	2007	Mezzapesa D M	Am J Neuroradiol	17296989	G12: Spinal Muscular Atrophy and Related Syndromes
258	2011	Miettinen P S	Eur J Neurosci	21692882	G30: Alzheimer's Disease

259	2011	Miettinen P S	Eur J Neurosci	21692882	G31: Other Degenerative Diseases of Nervous System
260	2005	Milham M P	Biol Psychiatry	15860335	F41: Other Anxiety Disorders
261	2007	Minnerop M	NeuroImage	17512219	G90: Disorders Autonomic Nervous System
262	2011	Molina V	Eur Arch Psychiatry Clin Neurosci	21188405	F20: Schizophrenia
263	2010	Molina V	Psychiatry Res NeuroImaging	20153145	F20: Schizophrenia
264	2011	Molina V	Eur Arch Psychiatry Clin Neurosci	21188405	F31: Bipolar Disorder
265	2005	Moorhead T W	NeuroImage	16085427	F20: Schizophrenia
266	2006	Morgen K	NeuroImage	16360321	G35: Multiple Sclerosis
267	2006	Mueller S G	Epilepsia	16686655	G40: Epilepsy and Recurrent Seizures
268	2007	Muhlau M	J Neural Transm	17024326	G10: Huntington's Disease
269	2013	Muhlau M	Mult Scler	23462349	G35: Multiple Sclerosis
270	2009	Muller-Vahl K R	BMC Neuroscience	19435502	F95: Tic Disorder
271	2013	Na K S	Prog Neuropsychopharmacol Biol Psychiatry	-	F41: Other Anxiety Disorders
272	2005	Nagano-Saito A	Neurology	15668417	G20: Parkinson's Disease
273	2013	Nardo D	Acta Psychiatr Scand	23113800	F43: Reaction to Severe Stress and Adjustment Disorders
274	2011	Narita K	Neuropsychopharmacol Psychiatry	21115089	F31: Bipolar Disorder
275	2006	Neckelmann G	Int J Neurosci	-	F20: Schizophrenia
276	2003	Nestor P J	Brain	12902311	G31: Other Degenerative Diseases of Nervous System
277	2013	Niedtfeldl I	PLoS One	23776553	F60: Specific Personality Disorders
278	2010	Nishio Y	European J Neurol	20298422	G20: Parkinson's Disease
279	2006	Nugent A C	NeuroImage	16256376	F31: Bipolar Disorder
280	2007	O'Daly O	Psychiatry Res	17720459	F20: Schizophrenia
281	2011	O'Muircheartaigh J	Neurology	21205693	G40: Epilepsy and Recurrent Seizures
282	2007	Obermann M	J Mov Disord	17443700	G24: Dystonia
283	2006	Ohnishi T	Brain	16330500	F20: Schizophrenia
284	2001	Ohnishi T	Am J Neuroradiol	11673161	G30: Alzheimer's Disease
285	2011	Ortiz-Gil J	Br J Psychiatry	21727234	F20: Schizophrenia
286	2001	Overmeyer S	Psychol Med	11722157	F90: Attention Deficit/Hyperactivity Disorder
287	2006	Padovani A	J Neurol Neurosurg Psychiatr	16306152	G23: Other degenerative diseases of basal ganglia
288	2010	Pail M	Epilepsia	19817822	G40: Epilepsy and Recurrent Seizures
289	2001	Paillere-Martinot M L	Schizophr Res	11378311	F20: Schizophrenia
290	2011	Pantano P	Am J Neuroradiol	20947646	G24: Dystonia
291	2009	Pardini M	Arch Neurol	19139305	G31: Other Degenerative Diseases of Nervous System
292	2014	Parisi L	J neurol	24952616	G35: Multiple Sclerosis

293	2005	Peinemann A	J Neurol Sci	16185716	G10: Huntington's Disease
294	2008	Pell G S	NeuroImage	18042496	G40: Epilepsy and Recurrent Seizures
295	2010	Peng J	Eur J Radiol	20466498	F32-F33: Major depressive disorder. single episode/recurrent
296	2005	Pennanen C	J Neurol Neurosurg Psychiatr	15607988	G31: Other Degenerative Diseases of Nervous System
297	2009	Pereira J B	NeuroReport	19349926	G20: Parkinson's Disease
298	2009	Pereira J M	Neurology	19433738	G31: Other Degenerative Diseases of Nervous System
299	2010	Pomarol-Clotet E	Mol Psychiatry	20065955	F20: Schizophrenia
300	2010	Prakash R S	Brain Res	19560443	G35: Multiple Sclerosis
301	2016	Preziosa P	Hum Brain Mapp	26833969	G35: Multiple Sclerosis
302	2010	Price G	NeuroImage	19632338	F20: Schizophrenia
303	2004	Pujol J	Arch Gen Psych	15237084	F42: Obsessive Compulsive Disorder
304	2011	Qiu L	PLoS One	21991357	F20: Schizophrenia
305	2008	Quattrone A	Am J Neuroradiol	18653686	G25: Other extrapyramidal and movement disorders
306	2007	Rabinovici G D	Am J Alzheimers Dis Other Demen	18166607	G30: Alzheimer's Disease
307	2007	Rabinovici G D	Am J Alzheimers Dis Other Demen	18166607	G31: Other Degenerative Diseases of Nervous System
308	2009	Rami L	Int J Geriatr Psychiatry	19259976	G30: Alzheimer's Disease
309	2009	Rami L	Int J Geriatr Psychiatry	19259976	G31: Other Degenerative Diseases of Nervous System
310	2007	Ramirez-Ruiz B	European J Neurol	17594330	G20: Parkinson's Disease
311	2015	Ranjeva J P	Am J Neuroradiol	15661713	G35: Multiple Sclerosis
312	2014	Redlich R	Arch Gen Psych	25188810	F31: Bipolar Disorder
313	2014	Redlich R	Arch Gen Psych	25188810	F32-F33: Major depressive disorder. single episode/recurrent
314	2005	Remy F	NeuroImage	15734360	G30: Alzheimer's Disease
315	2012	Riccitelli G	Mult Scler	22422807	G35: Multiple Sclerosis
316	2008	Riederer F	Neurology	18678824	G40: Epilepsy and Recurrent Seizures
317	2009	Ries M L	Brain Imaging Behav	19701486	F32-F33: Major depressive disorder. single episode/recurrent
318	2011	Riva D	Am J Neuroradiol	21700792	F84: Pervasive Developmental Disorders
319	2014	Rocca M A	Radiology	24927473	G35: Multiple Sclerosis
320	2012	Rocha-Rego V	PLoS One	22952599	F43: Reaction to Severe Stress and Adjustment Disorders
321	2012	Rossi R	Psychiatry Res NeuroImaging	23146251	F31: Bipolar Disorder
322	2012	Rossi R	Psychiatry Res NeuroImaging	23146251	F60: Specific Personality Disorders
323	2004	Rusch N	J Neuropsychiatry Clin Neurosci	15260365	G40: Epilepsy and Recurrent Seizures
324	2003	Salgado-Pineda P	NeuroImage	12814586	F20: Schizophrenia
325	2004	Salgado-Pineda P	NeuroImage	15006650	F20: Schizophrenia
326	2011	Salgado-Pineda P	Schizophr Res	21095105	F20: Schizophrenia

327	2007	Salmond C H	Cortex	17710821	F84: Pervasive Developmental Disorders
328	2011	Salvadore G	NeuroImage	21073959	F32-F33: Major depressive disorder. single episode/recurrent
329	2016	Sanchis-Segura C	Neuroscience Letters	27436479	G35: Multiple Sclerosis
330	2010	Santana M	Epilepsy Res	20223639	G40: Epilepsy and Recurrent Seizures
331	2015	Saricicek A	J Affect Disord	26233321	F31: Bipolar Disorder
332	2010	Sasayama D	Psychiatry Clin Neurosci	20546170	F90: Attention Deficit/Hyperactivity Disorder
333	2006	Saykin A J	Neurology	16966547	G31: Other Degenerative Diseases of Nervous System
334	2010	Scheuerecker J	J Psychiatry Neurosci	20569645	F32-F33: Major depressive disorder. single episode/recurrent
335	2013	Schiffer B	Schizophr Bull	23015687	F20: Schizophrenia
336	2007	Schiffer B	J Psychiatr Res	16876824	F65: Paraphilias
337	2009	Schmidt-Wilcke T	NeuroImage	19442751	G31: Other Degenerative Diseases of Nervous System
338	2012	Schuster C	Schizophr Bull	21205677	F20: Schizophrenia
339	2008	Seeley W W	Arch Neurol	18268196	G31: Other Degenerative Diseases of Nervous System
340	2011	Senda J	Amyotroph Lateral Scler	21271792	G12: Spinal Muscular Atrophy and Related Syndromes
341	2006	Sepulcre J	Arch Neurol	16908748	G35: Multiple Sclerosis
342	2013	Serra-Blasco M	Br J Psychiatry	23620451	F32-F33: Major depressive disorder. single episode/recurrent
343	2012	Shad M U	J Child Adolesc Psychopharmacol	22537357	F32-F33: Major depressive disorder. single episode/recurrent
344	1998	Shah P J	Br J Psychiatry	9828995	F32-F33: Major depressive disorder. single episode/recurrent
345	2002	Shapleske J	Cereb Cortex	12427683	F20: Schizophrenia
346	2006	Shiino A	NeuroImage	16904912	G30: Alzheimer's Disease
347	2006	Shiino A	NeuroImage	16904912	G31: Other Degenerative Diseases of Nervous System
348	2012	Shin S	J Neurol Neurosurg Psychiatr	22933812	G20: Parkinson's Disease
349	2001	Sigmundsson T	Am J Psychiatry	11156806	F20: Schizophrenia
350	2012	Singh M K	Bipolar Disord	22938166	F31: Bipolar Disorder
351	2010	Smesny S	NeuroImage	20478385	F20: Schizophrenia
352	2010	Sobanski T	Psychol Med	20056020	F41: Other Anxiety Disorders
353	2011	Soriano-Mas C	Biol Psychiatry	20875637	F32-F33: Major depressive disorder. single episode/recurrent
354	2010	Spanò B	Mult Scler	20007429	G35: Multiple Sclerosis
355	2003	Specht K	Arch Neurol	14568814	G90: Disorders Autonomic Nervous System
356	2005	Specht K	NeuroImage	15734363	G90: Disorders Autonomic Nervous System
357	2006	Spencer M D	NeuroImage	16996749	F84: Pervasive Developmental Disorders
358	2009	Stanfield A C	Bipolar Disord	19267696	F31: Bipolar Disorder
359	2014	Stratmann M	PLoS One	25051163	F32-F33: Major depressive disorder. single episode/recurrent

360	2010	Suchan B	Behav Brain Res	19729041	F50: Eating Disorders
361	2010	Sui S G	Acta Neuropsychiatr	-	F43: Reaction to Severe Stress and Adjustment Disorders
362	2005	Summerfield C	Arch Neurol	15710857	G20: Parkinson's Disease
363	2002	Suzuki M	Schizophr Res	11955962	F20: Schizophrenia
364	2008	Szeszko P R	Am J Psychiatry	18413702	F42: Obsessive Compulsive Disorder
365	2006	Tae W S	Korean J Radiol	16969045	G40: Epilepsy and Recurrent Seizures
366	2010	Tae W S	Korean J Radiol	20046492	G40: Epilepsy and Recurrent Seizures
367	2011	Takahashi R	Dement Geriatr Cogn Disord	22187545	G23: Other degenerative diseases of basal ganglia
368	2010	Takahashi R	Am J Neuroradiol	20634303	G30: Alzheimer's Disease
369	2010	Takahashi R	Am J Neuroradiol	20634303	G31: Other Degenerative Diseases of Nervous System
370	2005	Taki Y	J Affect Disord	16150493	F32-F33: Major depressive disorder. single episode/recurrent
371	2014	Tang L R	Psychiatry Res NeuroImaging	25218414	F31: Bipolar Disorder
372	2012	Tavanti M	Neurol Sci	21710131	F43: Reaction to Severe Stress and Adjustment Disorders
373	2012	Tavazzi E	Neurol Sci	25228014	G12: Spinal Muscular Atrophy and Related Syndromes
374	2012	Tessitore A	Am J Neuroradiol	22538070	G20: Parkinson's Disease
375	2007	Theberge J	Br J Psychiatry	17906243	F20: Schizophrenia
376	2007	Thivard L	J Neurol Neurosurg Psychiatr	17635981	G12: Spinal Muscular Atrophy and Related Syndromes
377	2010	Thomaes K	J Clinic Psychiatry	20673548	F43: Reaction to Severe Stress and Adjustment Disorders
378	2011	Tian L	PLoS One	22174900	F20: Schizophrenia
379	2008	Tiihonen J	Psychiatry Res	18662866	F60: Specific Personality Disorders
380	2009	Tir M	J Mov Disord	19194988	G20: Parkinson's Disease
381	2009	Tir M	J Mov Disord	19194988	G90: Disorders Autonomic Nervous System
382	2010	Toal F	Psychol Med	19891805	F84: Pervasive Developmental Disorders
383	2010	Togao O	Psychiatry Res	20833001	F42: Obsessive Compulsive Disorder
384	2009	Tomelleri L	Eur Neuropsychopharmacol	19717283	F20: Schizophrenia
385	2010	Tost H	J Affect Disord	19419772	F31: Bipolar Disorder
386	2007	Tregellas J R	Schizophr Res	17890058	F20: Schizophrenia
387	2010	Tzarouchi L C	J Neuroimaging	19187475	G90: Disorders Autonomic Nervous System
388	2008	Uchida R R	Psychiatry Res	18417322	F41: Other Anxiety Disorders
389	2005	Valente A A Jr	Biol Psychiatry	15978549	F42: Obsessive Compulsive Disorder
390	2015	van de Pavert S H	J Neurol Neurosurg Psychiatry	25926483	G35: Multiple Sclerosis
391	2009	van den Heuvel O A	Brain	18952675	F42: Obsessive Compulsive Disorder
392	2013	van Eijndhoven P	Am J Psychiatry	23929204	F32-F33: Major depressive disorder. single episode/recurrent

393	2010	van Tol M J	Arch Gen Psych	20921116	F32-F33: Major depressive disorder. single episode/recurrent
394	2013	van Tol M J	Psychol Med	24176247	F32-F33: Major depressive disorder. single episode/recurrent
395	2010	van Tol M J	Arch Gen Psych	20921116	F41: Other Anxiety Disorders
396	2008	Venkatasubramanian G	Psychiatry Res NeuroImaging	19019637	F20: Schizophrenia
397	2008	Voets N L	NeuroImage	18793730	F20: Schizophrenia
398	2008	Wagner G	J Psychiatry Neurosci	18592043	F32-F33: Major depressive disorder. single episode/recurrent
399	2011	Wagner G	NeuroImage	20832482	F32-F33: Major depressive disorder. single episode/recurrent
400	2011	Wang F	Brain	21666263	F31: Bipolar Disorder
401	2007	Wang J	Am J Neuroradiol	17353333	F90: Attention Deficit/Hyperactivity Disorder
402	2009	Waragai M	J Neurol Sci	19552926	G30: Alzheimer's Disease
403	2002	Watkins K E	Brain	11872605	F80: Specific Developmental Disorders of Speech and Language
404	2012	Watson D R	Behav Brain Res	22056751	F20: Schizophrenia
405	2012	Watson D R	Behav Brain Res	22056751	F31: Bipolar Disorder
406	2016	Wei W	Medicine	26962820	G40: Epilepsy and Recurrent Seizures
407	2006	Whitford T J	NeuroImage	16677830	F20: Schizophrenia
408	2013	Whitwell J L	European J Neurol	23078273	G23: Other degenerative diseases of basal ganglia
409	2007	Whitwell J L	Neurobiol Aging	16797786	G30: Alzheimer's Disease
410	2005	Whitwell J L	Arch Neurol	16157747	G31: Other Degenerative Diseases of Nervous System
411	2007	Whitwell J L	Neurobiol Aging	16797786	G31: Other Degenerative Diseases of Nervous System
412	2007	Whitwell J L	NeuroImage	17240166	G31: Other Degenerative Diseases of Nervous System
413	2001	Wilke M	NeuroImage	11304078	F20: Schizophrenia
414	2010	Wilson S M	Brain	20542982	G31: Other Degenerative Diseases of Nervous System
415	2000	Woermann F G	J Neurol Neurosurg Psychiatr	10644781	G40: Epilepsy and Recurrent Seizures
416	2008	Wolf R C	Eur Psychiatry	18434103	F20: Schizophrenia
417	2009	Wolf R C	Hum Brain Mapp	18172852	G10: Huntington's Disease
418	2006	Xie S	Neurology	16801648	G30: Alzheimer's Disease
419	2009	Xu L	Hum Brain Mapp	18266214	F20: Schizophrenia
420	2007	Yamada M	NeuroImage	17240165	F20: Schizophrenia
421	2010	Yasuda C L	Neurology	20350980	G40: Epilepsy and Recurrent Seizures
422	2003	Yoneyama E	Acta Psychiatr Scand	14531753	F60: Specific Personality Disorders
423	2005	Yoo H K	Eur J Neurosci	16262646	F41: Other Anxiety Disorders
424	2008	Yoo S Y	J Korean Med Sci	18303194	F42: Obsessive Compulsive Disorder
425	2008	Yoshihara Y	Arch Gen Psych	19102744	F20: Schizophrenia
426	2005	Zahn R	Psychiatry Res NeuroImaging	16253483	G30: Alzheimer's Disease

427	2008	Zamboni G	Neurology	18765649	G31: Other Degenerative Diseases of Nervous System
428	2011	Zhang J	Psychiatry Res	21498053	F43: Reaction to Severe Stress and Adjustment Disorders
429	2009	Zhang T	J Affect Disord	19211150	F32-F33: Major depressive disorder. single episode/recurrent
430	2012	Zhang X	J Affect Disord	22129771	F32-F33: Major depressive disorder. single episode/recurrent
431	2016	Zhang X	Int J Mol Sci	28035997	G35: Multiple Sclerosis
432	2010	Zou K	Biol Psychiatry	19897176	F32-F33: Major depressive disorder. single episode/recurrent

Table 4. List of experiments obtained and selected from the second query.

	Year	1st Author	Journal	Medline	ICD-10 Code
1	1999	Abell F	NeuroReport	10501551	F84: Pervasive Developmental Disorders
2	2005	Adler C M	Biol Psychiatry	15922309	F31: Bipolar Disorder
3	2007	Adler C M	Biol Psychiatry	17027928	F31: Bipolar Disorder
4	2011	Amico F	J Psychiatry Neurosci	20964952	F32-F33: Major depressive disorder. single episode/recurrent
5	2004	Antonini G	J Neurol Neurosurg Psychiatr	15489397	G12: Spinal Muscular Atrophy and Related Syndromes
6	2005	Antonova E	Biol Psychiatry	16039619	F20: Schizophrenia
7	2009	Arnone D	Eur Neuropsychopharmacol	-	F32-F33: Major depressive disorder. single episode/recurrent
8	2013	Arnone D	Mol Psychiatry	23128153	F32-F33: Major depressive disorder. single episode/recurrent
9	2009	Asami T	Psychiatry Res	19560907	F41: Other Anxiety Disorders
10	2007	Bassitt D P	Eur Arch Psychiatry Clin Neurosci	16960651	F20: Schizophrenia
11	2006	Baxter L C	J Alzheimers Dis	16914835	G30: Alzheimer's Disease
12	2007	Beal D S	NeuroReport	17632278	F80: Specific Developmental Disorders of Speech and Language
13	2006	Betting L E	NeuroImage	16702001	G40: Epilepsy and Recurrent Seizures
14	2015	Biederman S V	Magn Reson Med	25809140	F32-F33: Major depressive disorder. single episode/recurrent
15	2004	Bonilha L	Arch Neurol	15364683	G40: Epilepsy and Recurrent Seizures
16	2008	Bonilha L	Brain Dev	18362056	F84: Pervasive Developmental Disorders
17	2007	Bonilha L	J Neurol Neurosurg Psychiatr	17012334	G40: Epilepsy and Recurrent Seizures
18	2007	Brieber S	J Child Psychol Psychiatry	-	F84: Pervasive Developmental Disorders
19	2007	Brieber S	J Child Psychol Psychiatry	-	F90: Attention Deficit/Hyperactivity Disorder
20	2011	Brown G G	Psychiatry Res	21924872	F20: Schizophrenia
21	2011	Brown G G	Psychiatry Res	21924872	F31: Bipolar Disorder
22	2009	Butler C R	Brain	19073652	G40: Epilepsy and Recurrent Seizures
23	2012	Calderoni S	NeuroImage	21896334	F84: Pervasive Developmental Disorders
24	2006	Calhoun V D	Hum Brain Mapp	16108017	F20: Schizophrenia
25	2009	Carrion V G	Psychiatry Res NeuroImaging	19349151	F43: Reaction to Severe Stress and Adjustment Disorders
26	2009	Castro-Fornieles J	J Psychiatr Res	18486147	F50: Eating Disorders

27	2010	Celle S	J Neurol	19768657	G25: Other extrapyramidal and movement disorders
28	2006	Chan C H	Epilepsia	16499767	G40: Epilepsy and Recurrent Seizures
29	2014	Chaney A	J Psychiatry Neurosci	23900024	F32-F33: Major depressive disorder. single episode/recurrent
30	2007	Chen X	Aust N Z J Psychiatry	17464719	F31: Bipolar Disorder
31	2012	Chen Z	Neuropsychopharmacol Psychiatry	22119745	F31: Bipolar Disorder
32	2011	Cheng Y	PLoS One	21541322	F84: Pervasive Developmental Disorders
33	2008	Christian C J	Psychiatry Res NeuroImaging	18938065	F42: Obsessive Compulsive Disorder
34	2011	Cui L	Neurosci Lett	21138758	F20: Schizophrenia
35	2011	Cui L	Neurosci Lett	21138758	F31: Bipolar Disorder
36	2009	de Araujo-Filho G M	Epilepsy Behav	19303459	G40: Epilepsy and Recurrent Seizures
37	2011	de Castro-Manglano P	Psychiatry Res	21316203	F28: Other psychotic disorder not due to a substance or known physiological condition
38	2009	Deng M Y	Psychopharmacology	19641900	F20: Schizophrenia
39	2012	Ecker C	Arch Gen Psych	22310506	F84: Pervasive Developmental Disorders
40	2010	Ecker C	NeuroImage	19683584	F84: Pervasive Developmental Disorders
41	2007	Egger K	J Mov Disord	17588241	G24: Dystonia
42	2005	Etgen T	NeuroImage	15670702	G25: Other extrapyramidal and movement disorders
43	2012	Frangou S	Front Hum Neurosci	3277296	F31: Bipolar Disorder
44	2006	Garraux G	Ann Neurol	16437578	F95: Tic Disorder
45	2004	Garraux G	Ann Neurol	15122716	G24: Dystonia
46	2003	Gee J	Acad Radiol	14697007	G30: Alzheimer's Disease
47	2008	Gilbert A R	J Affect Disord	18342953	F42: Obsessive Compulsive Disorder
48	2005	Giuliani N R	Schizophr Res	15721994	F20: Schizophrenia
49	2011	Gong Q	NeuroImage	21134472	F32-F33: Major depressive disorder. single episode/recurrent
50	2011	Granert O	J Neurol Neurosurg Psychiatr	21705464	G24: Dystonia
51	2013	Grieve S M	NeuroImage	24273717	F32-F33: Major depressive disorder. single episode/recurrent
52	2004	Grossman M	Brain	14761903	G30: Alzheimer's Disease
53	2004	Grossman M	Brain	14761903	G31: Other Degenerative Diseases of Nervous System
54	2010	Ha T H	Neurosci Lett	19429131	F31: Bipolar Disorder
55	2004	Ha T H	Psychiatry Res	15664796	F20: Schizophrenia
56	2008	Haldane M	J Psychopharmacol	18308812	F31: Bipolar Disorder
57	2007	Hamalainen A	NeuroImage	17683950	G31: Other Degenerative Diseases

58	2006	Hendry J	NeuroImage	16214373	F84: Pervasive Developmental Disorders
59	2009	Henley S M	J Neurol	19266143	G10: Huntington's Disease
60	2008	Honea R A	Biol Psychiatry	17689500	F20: Schizophrenia
61	2007	Hornyak M	J Sleep Med	17512782	G25: Other extrapyramidal and movement disorders
62	2001	Hulshoff Pol H E	Arch Gen Psych	11735840	F20: Schizophrenia
63	2010	Hwang J	J Geriatr Psychiatry Neurol	-	F32-F33: Major depressive disorder. single episode/recurrent
64	2010	Hyde K L	Hum Brain Mapp	19790171	F84: Pervasive Developmental Disorders
65	2008	Hyde T M	Brain	18669483	F20: Schizophrenia
66	2010	Kasparek T	Hum Brain Mapp	19777553	F20: Schizophrenia
67	2004	Kawasaki Y	Eur Arch Psychiatry Clin Neurosci	15538599	F20: Schizophrenia
68	2008	Ke X	NeuroReport	18520994	F84: Pervasive Developmental Disorders
69	2007	Keller S S	Epilepsy Res	17412561	G40: Epilepsy and Recurrent Seizures
70	2002	Keller S S	J Neurol Neurosurg Psychiatr	12438464	G40: Epilepsy and Recurrent Seizures
71	2009	Kempton M J	J Neurosci	19726644	F31: Bipolar Disorder
72	2007	Kim J H	NeuroImage	17689105	G40: Epilepsy and Recurrent Seizures
73	2001	Kim J J	Br J Psychiatry	11581113	F42: Obsessive Compulsive Disorder
74	2010	Kostic V S	Neurology	20686125	G20: Parkinson's Disease
75	2013	Kozicky J M	Bipolar Disord	23919287	F31: Bipolar Disorder
76	2008	Ladoucer C D	J Am Acad Child Adolesc Psychiatry	18356765	F31: Bipolar Disorder
77	2013	Lee S H	Acta Radiologica	23474765	G20: Parkinson's Disease
78	2009	Leung K K	Psychol Med	18945378	F32-F33: Major depressive disorder. single episode/recurrent
79	2013	Lin C H	Front Hum Neurosci	23785322	G20: Parkinson's Disease
80	2013	Lin C H	Front Hum Neurosci	23785322	G25: Other extrapyramidal and movement disorders
81	2009	Lin K	Epilepsy Res	19570650	G40: Epilepsy and Recurrent Seizures
82	2010	Lu C	Cortex	19375076	F80: Specific Developmental Disorders of Speech and Language
83	2006	Ludolph A G	Br J Psychiatry	16648537	F95: Tic Disorder
84	2015	Mallik S	Mult Scler	4390521	G35: Multiple Sclerosis
85	2003	Marcelis M	Psychiatry Res	12694890	F28: Other psychotic disorder not due to a substance or known physiological condition
86	2005	McDonald C	Br J Psychiatry	15863740	F20: Schizophrenia
87	2011	Mengotti P	Brain Res Bull	21146593	F84: Pervasive Developmental Dis

88	2011	Molina V	Eur Arch Psychiatry Clin Neurosci	21188405	F20: Schizophrenia
89	2010	Moriya J	Schizophr Res	19854618	F20: Schizophrenia
90	2007	O'Daly O	Psychiatry Res	17720459	F20: Schizophrenia
91	2007	Obermann M	J Mov Disord	17443700	G24: Dystonia
92	2011	Perico C A M	Bipolar Disord	21320250	F31: Bipolar Disorder
93	2011	Perico C A M	Bipolar Disord	21320250	F32-F33: Major depressive disorder. single episode/recurrent
94	2013	Prell T	BMC Neuroscience	24131497	G24: Dystonia
95	2010	Price G	NeuroImage	19632338	F20: Schizophrenia
96	2004	Pujol J	Arch Gen Psych	15237084	F42: Obsessive Compulsive Disorder
97	2014	Qiu L	Transl Psychiatry	24713859	F32-F33: Major depressive disorder. single episode/recurrent
98	2009	Raji C A	Neurology	19846828	G30: Alzheimer's Disease
99	2007	Ramirez-Ruiz B	European J Neurol	17594330	G20: Parkinson's Disease
100	2008	Riederer F	Neurology	18678824	G40: Epilepsy and Recurrent Seizures
101	2015	Rocca M A	Radiology	26348234	G35: Multiple Sclerosis
102	2002	Rosen H J	Neurology	11805245	G31: Other Degenerative Diseases of Nervous System
103	2004	Rusch N	J Neurol Neurosurg Psychiatr	15260365	G40: Epilepsy and Recurrent Seizures
104	2003	Salgado-Pineda P	NeuroImage	12814586	F20: Schizophrenia
105	2007	Salmond C H	Cortex	17710821	F84: Pervasive Developmental Disorders
106	2015	Saricicek A	J Affect Disord	26233321	F31: Bipolar Disorder
107	2010	Schafer A	NeuroImage	20035881	F50: Eating Disorders
108	2010	Scheuerecker J	J Psychiatry Neurosci	20569645	F32-F33: Major depressive disorder. single episode/recurrent
109	2013	Schiffer B	Schizophr Bull	23015687	F20: Schizophrenia
110	2006	Schmitz N	Biol Psychiatry	16140278	F84: Pervasive Developmental Disorders
111	2002	Shapleske J	Cereb Cortex	12427683	F20: Schizophrenia
112	2010	Smesny S	NeuroImage	20478385	F20: Schizophrenia
113	2002	Suzuki M	Schizophr Res	11955962	F20: Schizophrenia
114	2008	Szeszko P R	Am J Psychiatry	18413702	F42: Obsessive Compulsive Disorder
115	2014	Tang L R	Psychiatry Res NeuroImaging	25218414	F31: Bipolar Disorder
116	2010	Tanskanen P	Schizophr Bull	19015212	F20: Schizophrenia
117	2012	Tavazzi E	Neurological Sciences	25228014	G35: Multiple Sclerosis
118	2007	Theberge J	Br J Psychiatry	17906243	F20: Schizophrenia
119	2010	Toal F	Psychol Med	19891805	F84: Pervasive Developmental Disorders
120	2013	Truong W	Psychiatry Res	24099630	F32-F33: Major depressive disorder. single episode/recurrent

121	2008	Uchida R R	Psychiatry Res	18417322	F41: Other Anxiety Disorders
122	2005	Valente A A Jr	Biol Psychiatry	15978549	F42: Obsessive Compulsive Disorder
123	2013	van Eijndhoven P	Am J Psychiatry	23929204	F32-F33: Major depressive disorder. single episode/recurrent
124	2004	Waiter G D	NeuroImage	15193590	F84: Pervasive Developmental Disorders
125	2007	Wang J	Am J Neuroradiol	1735333	F90: Attention Deficit/Hyperactivity Disorder
126	2002	Watkins K E	Brain	11872605	F80: Specific Developmental Disorders of Speech and Language
127	2012	Watson D R	Behav Brain Res	22056751	F20: Schizophrenia
128	2012	Watson D R	Behav Brain Res	22056751	F31: Bipolar Disorder
129	2009	Wattendorf E	J Neurosci	20007465	G20: Parkinson's Disease
130	2006	Whitford T J	NeuroImage	16677830	F20: Schizophrenia
131	2004	Whitwell J L	Neurodegener Dis	16908994	G31: Other Degenerative Diseases of Nervous System
132	2001	Wilke M	NeuroImage	11304078	F20: Schizophrenia
133	1999	Woermann F G	Brain	10545395	G40: Epilepsy and Recurrent Seizures
134	2010	Yasuda C L	Neurology	20350980	G40: Epilepsy and Recurrent Seizures
135	2008	Yoo S Y	J Korean Med Sci	18303194	F42: Obsessive Compulsive Disorder

2.2.3. *Anatomical likelihood estimation and creation of a modeled alteration map*

An anatomical likelihood estimation (ALE) (Eickhoff et al., 2009, 2012; Turkeltaub et al., 2012) was carried out to summarize the results of the selected experiments by means of an in-house developed MATLAB script according to the algorithms implemented in Gingerale 2.3.6 and the advices of Eickhoff et al. (2017). Results were clustered at a level of $p < 0.05$, family-wise error (FWE)-corrected for multiple comparisons, with a threshold for cluster-forming of $p < 0.001$ (Eickhoff et al., 2016).

The ALE is a method of voxel-based meta-analysis capable of providing information about the anatomical reliability of results by comparing them to a sample of reference studies from the existing literature (Laird et al., 2005a). An ALE meta-analysis considers the foci of each experiment as distributions of Gaussian probability, with the following formula:

$$p(d) = \frac{1}{\sigma^3\sqrt{(2\pi)^3}}\, e^{-\frac{d^2}{2\sigma^2}}$$

where d refers to the Euclidean distance between the voxels and the considered focus, and σ refers to the standard deviation of the distribution. The standard deviation can be calculated by means of the full-width half-maximum (FWHM), as follows:

$$\sigma = \frac{FWHM}{\sqrt{8\ln 2}}$$

The combination of these Gaussian distributions produced a modeled activation (MA) map for each experiment. The final ALE map was eventually generated by merging the MA maps. The significance of alteration values in the

ALE map was determined by means of a permutation test: the same number of foci was redistributed across the brain and an ALE map was redetermined. The score histogram so obtained was employed to attribute a threshold p value.

2.2.4. Construction of nodes

The construction of nodes was derived from the ALE map by using a peak detection algorithm that was able to detect the local maxima. The ALE value of a voxel that is a local peak is higher than the values of the adjacent voxels. Voxels exhibiting a peak value above a given threshold (the 75th percentile of the peak values distribution). Subsequently, a distance matrix was created calculating the Euclidean distance between peaks. In order to avoid that regions of interest overlap each other, all the peaks in a distance of 10 mm from the others were removed. A 10 mm^2 region of interest was delineated around each surviving peak (see Fig. 2 for an illustration of the node construction pipeline, and Tables 5 and 6 for the nodes' coordinates).

These choices were taken on the basis of the following three rationales (Cauda et al., 2018a). (1) The nodes' dimension was established according to Eickhoff et al. (2009), who examined meta-analytical imaging data estimating the spatial uncertainty regarding the reported coordinates. Since their study showed an uncertainty in spatial location with a mean of 10.2 mm and a standard deviation of 0.4 mm, a radius of 10 mm was consequently chosen for the nodes. (2) The 75 percentile was chosen because, as shown by Kotz et al. (2000), independently of the type of the probability distribution, the amount of the observation falling within k standard deviations of the population mean is at least $1 - \frac{1}{k^2}$, which, with $k = 2$, corresponds to the 75 percentile. (3) As shown by Zalesky et al. (2010), despite an arbitrary definition of nodes, it is possible to compare the networks if the node parcellation has been constructed at the same spatial scale. This is why all the analyses were carried out at a comparable spatial scale.

Table 5. Synopsis of the nodes related to GM decreases.

Record number	*X*	*Y*	*Z*	*Side*	*Label (Talairach Client)*	*BA*
1	-4	-4	12	L	Thal	/
2	6	-16	14	R	VLN	/
3	-8	-12	20	L	Thal	/
4	14	-40	-6	R	Culm	/
5	-52	38	-2	L	IFG	BA 10
6	-24	-4	-34	L	Uncus	BA 36
7	-34	-10	-34	L	Uncus	BA 20
8	40	52	0	R	IFG	/
9	46	14	38	R	MFG	BA 9
10	54	-2	12	R	PrecG	BA 6
11	40	4	0	R	Ins	BA 13
12	-46	18	34	L	MFG	BA 9
13	-54	-4	-30	L	ITG	BA 20
14	-50	10	-28	L	MTG	BA 21
15	-60	-32	-2	L	MTG	BA 39
16	26	-82	-34	R	Pyr	/
17	-30	-34	-14	L	PHG	BA 36
18	50	-30	18	R	Ins	BA 13
19	-44	2	-22	L	MTG	BA 21
20	30	-42	-10	R	PHG	BA 37
21	-28	48	28	L	SFG	BA 9
22	-8	54	28	L	SFG	BA 9
23	54	-8	32	R	PrecG	BA 6
24	-40	46	-14	L	MFG	BA 11
25	42	-4	-4	R	Ins	BA 13
26	42	-30	50	R	PostcG	BA 40
27	-52	-8	34	L	PrecG	BA 6
28	46	4	34	R	PrecG	BA 6
29	-42	10	-4	L	Ins	BA 13
30	58	-14	42	R	PrecG	BA 6
31	8	2	6	R	Cau Body	/
32	-52	2	36	L	PrecG	BA 6
33	-38	18	6	L	Ins	BA 13
34	52	-48	24	R	SMG	BA 40
35	54	8	-20	R	MTG	BA 21
36	-58	-50	-10	L	MTG	BA 37
37	-10	8	10	L	Cau Body	/

38	38	16	6	R	Ins	BA 13
39	42	-6	6	R	Ins	BA 13
40	42	-14	12	R	Ins	BA 13
41	-48	-52	28	L	SMG	BA 40
42	50	-24	6	R	STG	BA 41
43	-48	-30	10	L	STG	BA 41
44	44	-12	0	R	Ins	BA 13
45	-42	-10	12	L	Ins	BA 13
46	-12	-58	8	L	PCC	BA 30
47	6	24	20	R	ACC	BA 24
48	0	-34	44	L	PCun	BA 7
49	10	10	12	R	Cau Body	/
50	-4	26	20	L	ACC	BA 24
51	-42	-4	4	L	Ins	BA 13
52	-56	-4	-20	L	MTG	BA 21
53	-38	6	6	L	Ins	BA 13
54	6	24	-24	R	RG	BA 11
55	40	12	-34	R	STG	BA 38
56	-40	16	-28	L	STG	BA 38
57	32	14	-24	R	STG	BA 38
58	-10	0	16	L	Cau Body	/
59	-2	14	26	L	Cing	BA 24
60	38	4	10	R	Ins	BA 13
61	-10	-22	36	L	Cing	BA 31
62	10	-22	40	R	Cing	BA 31
63	0	-18	34	L	Cing	BA 24
64	-8	-12	38	L	Cing	BA 24
65	50	12	6	R	PrecG	BA 44
66	-2	10	50	L	SFG	BA 6
67	16	6	64	R	SFG	BA 6
68	56	-16	12	R	TTG	BA 41
69	40	8	-22	R	STG	BA 38
70	0	40	38	L	MedFG	BA 8
71	-40	0	14	L	Ins	BA 13
72	-12	-28	44	L	Cing	BA 31
73	36	-24	-22	R	PHG	BA 36
74	-34	10	-22	L	STG	BA 38
75	40	16	-16	R	IFG	BA 47
76	-40	8	-14	L	STG	BA 38
77	-46	10	38	L	MFG	BA 8
78	38	22	12	R	Ins	BA 13

79	-38	12	14	L	Ins	BA 13
80	-6	28	-20	L	RG	BA 11
81	14	-72	32	R	Cun	BA 7
82	4	-70	32	R	Cun	BA 7
83	-2	-50	32	L	PCun	BA 31
84	38	-10	16	R	Ins	BA 13
85	-8	-2	36	L	Cing	BA 24
86	-48	-20	14	L	TTG	BA 41
87	-12	-74	38	L	PCun	BA 7
88	42	4	-12	R	STG	BA 38
89	-62	-32	12	L	STG	BA 22
90	46	12	-6	R	STG	BA 38
91	-10	-52	38	L	PCun	BA 7
92	-62	-22	-14	L	MTG	BA 21
93	24	-8	-14	R	PHG	/
94	-58	-54	14	L	STG	BA 22
95	-8	20	-4	L	Cau Head	/
96	-6	66	-4	L	MedFG	BA 10
97	-4	58	2	L	MedFG	BA 10
98	-48	-36	20	L	Ins	BA 13
99	10	-30	46	R	PCL	BA 31
100	-20	-64	14	L	PCC	BA 31
101	18	-60	16	R	PCC	BA 31
102	4	0	46	R	Cing	BA 24
103	-28	28	40	L	MFG	BA 8
104	0	0	-6	L	ACC	BA 25
105	34	-36	-18	R	FFG	BA 20
106	10	20	-6	R	Cau Head	/
107	52	-22	-14	R	MTG	BA 21
108	24	-72	24	R	PCun	BA 31
109	-26	18	46	L	MFG	BA 8
110	-46	-8	-16	L	ITG	BA 20
111	-26	6	-30	L	Uncus	BA 28
112	-52	-14	14	L	PostcG	/
113	-46	-76	10	L	MTG	BA 39
114	62	-6	16	R	PostcG	BA 43
115	-6	10	0	L	Cau Head	/
116	0	40	6	L	ACC	BA 32
117	44	-18	22	R	Ins	BA 13
118	-22	-4	-12	L	PHG	/
119	2	-48	42	R	Cing	BA 31

120	56	-4	-12	R	MTG	BA 21
121	0	-14	8	L	MDN	/
122	-52	0	-12	L	MTG	BA 21
123	-6	50	10	L	MedFG	BA 10
124	-42	0	-8	L	Ins	BA 13
125	-48	14	10	L	IFG	BA 44
126	-48	6	16	L	IFG	BA 44
127	-8	-20	14	L	Thal	/
128	14	-34	10	R	Pulv	/
129	12	-24	10	R	Pulv	/
130	58	-12	-10	R	MTG	BA 21
131	-54	-64	-4	L	MOG	BA 19
132	-30	-86	18	L	MOG	BA 19
133	-22	2	-20	L	Uncus	BA 34
134	38	-84	18	R	MOG	BA 19
135	-30	-42	-8	L	PHG	BA 37
136	0	26	-12	L	MedFG	BA 11
137	-48	-62	28	L	MTG	BA 39
138	-56	-18	42	L	PostcG	BA 4
139	-8	22	6	L	Cau Body	/
140	12	20	4	R	Cau Head	/
141	28	-16	-20	R	PhG	BA 28
142	52	-30	-6	R	MTG	BA 21
143	-60	-18	-6	L	MTG	BA 21
144	-60	-46	-4	L	MTG	BA 21
145	4	48	12	R	MedFG	BA 10
146	-8	60	14	L	MedFG	BA 10
147	0	36	-8	L	ACC	BA 32
148	-60	-10	24	L	PostcG	BA 3
149	-50	-10	44	L	PrecG	BA 4
150	-28	-12	-16	L	PHG	/
151	-62	-52	4	L	MTG	BA 21
152	-22	10	-8	L	LentN	/
153	44	44	-6	R	MFG	BA 10
154	2	32	12	R	ACC	BA 24
155	2	34	46	R	SFG	BA 8
156	-50	30	18	L	MFG	BA 46
157	34	-28	-12	R	Hip	/
158	-24	2	-2	L	Put	/
159	-28	-74	40	L	PCun	BA 19
160	-4	2	4	L	Cau Head	/

161	0	4	-16	L	SubcallG	BA 25
162	-34	-24	48	L	PrecG	BA 4
163	-34	-26	-8	L	Hip	/
164	-20	8	6	L	Put	/
165	-26	26	-20	L	IFG	BA 11
166	52	-34	6	R	MTG	BA 22
167	-30	50	-4	L	MFG	BA 10
168	-30	56	4	L	MFG	BA 10
169	60	-24	44	R	PostcG	BA 2
170	58	-20	-22	R	FFG	BA 20
171	2	16	-12	R	SubcallG	BA 25
172	4	-26	-6	R	RedN	/
173	-24	-20	-8	L	PHG	BA 28
174	32	-34	-4	R	Hip	/
175	4	-16	-6	R	RedN	/
176	-18	-34	-16	L	Culm	/
177	-46	-38	-24	L	Culm	/
178	-60	-38	6	L	MTG	BA 22
179	-40	28	-12	L	IFG	BA 47
180	50	-20	-4	R	STG	BA 22
181	42	-4	-18	R	Fus	BA 20
182	12	-32	0	R	PHG	BA 27
183	-14	-34	0	L	PHG	BA 27
184	48	32	24	R	MFG	BA 46
185	-28	-34	-2	L	Hip	/
186	-16	-42	-8	L	Culm	/
187	-26	-30	-24	L	Culm	/
188	50	6	22	R	IFG	BA 44
189	8	-40	-20	R	Culm	/
190	-58	-4	-4	L	MTG	BA 21
191	8	-6	14	R	Thal	/
192	-6	44	-4	L	ACC	BA 32
193	52	20	24	R	IFG	BA 9
194	-38	22	-20	L	IFG	BA 47
195	-62	-24	6	L	STG	BA 22
196	56	8	14	R	IFG	BA 44
197	-26	56	20	L	MFG	BA 10
198	38	42	22	R	MFG	BA 10
199	38	-6	-38	R	ITG	BA 20
200	28	-4	-32	R	Unc	BA 36
201	-42	54	2	L	IFG	BA 10

202	-2	42	16	L	MedFG	BA 9
203	-52	4	26	L	IFG	BA 9
204	-54	-60	-14	L	Fus	BA 37
205	-46	-20	8	L	STG	BA 13
206	50	20	12	R	IFG	BA 45
207	-48	24	10	L	IFG	BA 45
208	54	-10	6	R	STG	BA 22
209	4	-32	-14	R	Culm	/
210	-52	-20	-32	L	ITG	BA 20
211	6	52	-8	R	MedFG	BA 10
212	-2	34	26	L	Cing	BA 32
213	24	-14	-30	R	Unc	BA 28
214	6	20	30	R	Cing	BA 32
215	52	28	18	R	MFG	BA 46
216	-8	10	36	L	Cing	BA 32
217	58	6	28	R	IFG	BA 9
218	-2	-4	-14	L	HypoThal	/
219	34	28	-12	R	IFG	BA 47
220	42	-16	-32	R	ITG	BA 20
221	-46	46	-4	L	IFG	BA 10
222	-30	60	-6	L	SFG	BA 10
223	-54	-10	-28	L	ITG	BA 20
224	58	-10	-20	R	ITG	BA 20
225	58	-52	-14	R	ITG	BA 20
226	30	58	-4	R	SFG	BA 10
227	-56	-46	36	L	IPL	BA 40
228	4	24	42	R	Cing	BA 32
229	26	58	6	R	SFG	BA 10
230	-24	4	-12	L	SubcallG	BA 34
231	26	6	-30	R	Unc	BA 28
232	-24	-8	-28	L	Unc	BA 28
233	-50	24	26	L	MFG	BA 46
234	-2	52	20	L	MedFG	BA 9
235	26	-16	-8	R	LentN	/
236	28	50	14	R	SFG	BA 10
237	12	16	-22	R	RG	BA 11
238	-50	16	20	L	IFG	BA 9
239	-40	18	-10	L	IFG	BA 47
240	4	30	34	R	MedFG	BA 6
241	-26	46	18	L	SFG	BA 10
242	-48	36	-10	L	IFG	BA 47

243	-34	36	-8	L	MFG	BA 11
244	38	20	-6	R	IFG	BA 47
245	26	4	-20	R	Unc	BA 28
246	-56	-32	-12	L	ITG	BA 20
247	-36	24	-2	L	IFG	BA 47
248	16	30	-24	R	OrbG	BA 47
249	28	38	-20	R	MFG	BA 11
250	-10	-10	48	L	MedFG	BA 6
251	-2	38	-18	L	MedFG	BA 11
252	6	46	-16	R	MedFG	BA 11
253	26	2	-10	R	SubcallG	BA 34
254	22	-6	-24	R	PhG	BA 35
255	56	-20	24	R	IPL	BA 40
256	4	-14	52	R	MedFG	BA 6
257	-4	48	-14	L	MedFG	BA 11
258	48	38	2	R	IFG	BA 46
259	-50	24	0	L	IFG	BA 47
260	-28	-22	-18	L	PhG	BA 35
261	-42	6	48	L	MFG	BA 6
262	-54	-4	8	L	PrecG	BA 6
263	-32	34	-18	L	MFG	BA 11
264	38	24	0	R	IFG	BA 47
265	44	14	28	R	MFG	BA 9
266	-40	-54	44	L	IPL	BA 40
267	-50	36	10	L	IFG	BA 46
268	-58	-16	32	L	PostcG	BA 3
269	44	38	-14	R	MFG	BA 11
270	18	36	28	R	MedFG	BA 9
271	44	32	-6	R	MFG	BA 47
272	-18	-28	-8	L	PHG	BA 28
273	-28	-18	-28	L	PhG	BA 36
274	48	38	12	R	IFG	BA 46
275	-2	44	28	L	MedFG	BA 9
276	-46	42	18	L	MFG	BA 46
277	-44	10	28	L	IFG	BA 9

Table 6. Synopsis of the nodes related to GM increases.

Record Number	*X*	*Y*	*Z*	*Side*	*Label (Talairach Client)*	*BA*
1	34	-44	-40	R	CerTons	/
2	-22	-70	-40	L	Inf_Semi-lunar_Lob	/
3	14	-68	-40	R	Inf_Semi-lunar_Lob	/
4	-52	-12	-38	L	ITG	BA 20
5	-34	-16	-38	L	Uncus	BA 20
6	46	-44	-34	R	CerTons	/
7	-42	0	-30	L	MTG	BA 21
8	-24	-2	-30	L	Uncus	BA 36
9	38	2	-30	R	MTG	BA 21
10	-48	-16	-28	L	ITG	BA 20
11	-30	-10	-30	L	Uncus	BA 28
12	28	-22	-26	R	PHG	BA 36
13	24	-8	-26	R	Uncus	BA 28
14	22	2	-26	R	Uncus	BA 28
15	2	-36	-24	R	Culm	/
16	-46	-34	-24	L	FFG	BA 20
17	-30	-30	-24	L	Culm	/
18	-52	-26	-24	L	FFG	BA 20
19	34	-14	-24	R	Uncus	BA 20
20	-24	-12	-22	L	PHG	/
21	-24	4	-22	L	Uncus	BA 28
22	34	-38	-22	R	Culm	/
23	-16	-24	-22	L	Culm	/
24	-30	-18	-20	L	PHG	/
25	38	-4	-22	R	MTG	BA 21
26	24	10	-20	R	IFG	BA 47
27	8	28	-20	R	RG	BA 11
28	8	38	-20	R	RG	BA 11
29	18	40	-20	R	MFG	BA 11
30	-8	20	-18	L	RG	BA 11
31	24	28	-18	R	IFG	BA 11
32	-20	42	-18	L	SFG	BA 11
33	36	-80	-16	R	Declive	/
34	34	-46	-16	R	Culm	/
35	6	-30	-16	R	Culm	/
36	32	-28	-18	R	PHG	BA 36
37	28	-14	-16	R	PHG	/

38	20	-6	-16	R	Amyg	/
39	-16	4	-16	L	PHG	BA 34
40	38	16	-16	R	IFG	BA 47
41	-22	28	-20	L	IFG	BA 11
42	34	32	-18	R	IFG	BA 47
43	36	-70	-14	R	FFG	BA 19
44	-36	-66	-16	L	Declive	/
45	-26	-38	-14	L	Culm	/
46	-34	-28	-14	L	PHG	BA 36
47	-64	-22	-14	L	MTG	BA 21
48	-52	-22	-14	L	MTG	BA 21
49	40	4	-14	R	STG	BA 38
50	10	20	-14	R	MedFG	BA 25
51	-36	-86	-12	L	IOG	BA 18
52	50	-56	-12	R	FFG	BA 37
53	-12	-18	-12	L	SN	/
54	-26	-12	-12	L	PHG	/
55	-48	-4	-14	L	MTG	BA 21
56	20	4	-12	R	SubcallG	BA 34
57	-18	12	-10	L	LentN	/
58	-42	12	-12	L	STG	BA 38
59	-6	30	-14	L	MedFG	BA 11
60	-12	40	-12	L	MedFG	BA 10
61	56	-48	-10	R	ITG	BA 20
62	28	-38	-10	R	PHG	BA 36
63	-6	-28	-6	L	Thal	/
64	-20	-26	-12	L	PHG	BA 35
65	50	-22	-10	R	STG	BA 22
66	-4	-8	-12	L	MammB	/
67	22	16	-12	R	SubcallG	BA 47
68	34	24	-10	R	IFG	BA 47
69	6	30	-10	R	ACC	BA 32
70	-28	34	-10	L	MFG	BA 11
71	26	-92	-10	R	FFG	BA 18
72	-14	-48	-10	L	Culm	/
73	-54	-44	-8	L	MTG	BA 20
74	-28	-46	-6	L	PHG	BA 19
75	26	-8	-8	R	Amyg	/
76	-42	2	-8	L	Ins	BA 13
77	-10	18	-8	L	Cau Head	/
78	-20	22	-6	L	LentN	/

79	-36	40	-8	L	MFG	BA 11
80	34	48	-10	R	MFG	BA 11
81	40	-78	-6	R	IOG	BA 19
82	40	-64	-6	R	FFG	BA 19
83	-44	-62	-10	L	FFG	BA 37
84	12	-38	-6	R	Culm	/
85	28	-26	-8	R	Hip	/
86	40	-12	-6	R	Ins	BA 13
87	-30	-4	-6	L	Put	/
88	-18	-4	-6	L	LGP	/
89	8	-2	-8	R	HypoThal	/
90	36	10	-6	R	Ins	BA 13
91	-36	20	-8	L	IFG	BA 47
92	-10	48	-4	L	MedFG	BA 10
93	30	62	-6	R	SFG	BA 10
94	38	-90	-4	R	IOG	BA 18
95	16	-48	-6	R	Culm	/
96	-26	-32	-6	L	PHG	Hip
97	10	8	-4	R	Cau Head	/
98	48	-56	0	R	ITG	BA 19
99	-14	-40	-4	L	PHG	BA 30
100	12	-24	-2	R	MGB	/
101	-28	-16	0	L	LentN	/
102	52	-14	-4	R	STG	BA 22
103	12	-12	-2	R	SN	/
104	48	-4	-4	R	STG	BA 22
105	-18	6	-2	L	LentN	/
106	22	6	-2	R	Put	/
107	-40	10	-2	L	Ins	BA 13
108	-8	24	0	L	Cau Head	/
109	10	36	0	R	ACC	/
110	-40	58	-4	L	MFG	BA 10
111	20	-92	-2	R	LG	BA 17
112	58	-36	-2	R	MTG	BA 21
113	-40	-24	-2	L	Ins	BA 13
114	40	-24	-2	R	Ins	BA 13
115	-8	-10	0	L	VLN	/
116	-40	-4	0	L	Ins	BA 13
117	-10	8	0	L	Cau Head	/
118	-10	40	4	L	ACC	BA 32
119	6	-56	2	R	Culm	/

120	-48	-36	2	L	STG	BA 22
121	-16	-32	2	L	Pulv	/
122	2	-14	0	R	Thal	/
123	28	-8	2	R	Put	/
124	40	-2	2	R	Ins	BA 13
125	42	18	2	R	Ins	/
126	-44	22	2	L	IFG	BA 47
127	10	46	0	R	ACC	BA 32
128	26	52	2	R	SFG	BA 10
129	14	-36	4	R	PHG	BA 30
130	-18	-18	4	L	VPLN	/
131	-28	-8	4	L	Put	/
132	-20	-2	4	L	Put	/
133	10	12	4	R	Cau Head	/
134	-46	32	4	L	IFG	BA 47
135	-32	56	2	L	MFG	BA 10
136	-8	-56	6	L	PCC	BA 30
137	-64	-30	4	L	MTG	BA 22
138	12	-18	6	R	Pulv	/
139	44	-16	4	R	Ins	BA 13
140	-42	4	6	L	PrecG	BA 44
141	44	8	4	R	Ins	BA 13
142	-24	12	6	L	Put	/
143	-6	18	8	L	Cau Body	/
144	24	0	12	R	LentN	/
145	28	46	10	R	MFG	BA 10
146	20	60	6	R	SFG	BA 10
147	24	-90	8	R	MOG	BA 18
148	10	6	8	R	Cau Body	/
149	32	30	8	R	IFG	BA 45
150	-36	40	10	L	MFG	BA 10
151	32	58	10	R	MFG	BA 10
152	-32	-92	12	L	MOG	BA 18
153	36	-78	12	R	MOG	BA 19
154	-10	-50	12	L	PCC	BA 30
155	-46	-40	12	L	STG	BA 41
156	-16	-30	12	L	Pulv	/
157	16	-22	14	R	LPN	/
158	30	-14	12	R	Put	/
159	6	-10	12	R	MDN	/
160	38	-8	10	R	Ins	BA 13

161	-22	4	12	rePut	Put	/
162	-48	10	12	L	PrecG	BA 44
163	52	12	10	R	IFG	BA 44
164	-4	28	10	L	ACC	BA 24
165	40	38	10	R	MFG	BA 10
166	-32	50	10	L	MFG	BA 10
167	-26	-10	14	L	Put	/
168	38	2	12	R	Ins	BA 13
169	46	20	12	R	IFG	BA 45
170	12	28	14	R	ACC	BA 24
171	-44	34	14	L	MFG	BA 46
172	20	54	14	R	SFG	BA 10
173	-36	-82	16	L	MOG	BA 19
174	-56	-30	16	L	STG	BA 42
175	-8	48	16	L	MedFG	BA 10
176	34	-86	18	R	MOG	BA 19
177	44	-34	18	R	Ins	BA 13
178	56	-26	18	R	PostcG	BA 40
179	12	-18	18	R	LDN	/
180	18	-6	18	R	Cau Body	/
181	20	64	16	R	SFG	BA 10
182	22	-90	20	R	Cun	BA 18
183	-10	-42	18	L	PCC	BA 29
184	-50	-22	20	L	Ins	BA 13
185	56	-6	18	R	PrecG	BA 4
186	-18	-8	20	L	Cau Body	/
187	-52	4	20	L	IFG	BA 44
188	-46	16	20	L	IFG	BA 9
189	-52	34	16	L	MFG	BA 46
190	-38	-72	18	L	MTG	BA 39
191	-8	24	20	L	ACC	BA 32
192	12	-48	24	R	PCC	BA 31
193	-48	-32	24	L	IPL	BA 40
194	48	-60	26	R	STG	BA 39
195	-12	-56	26	L	Pcun	BA 31
196	48	-40	26	R	IPL	BA 40
197	56	-20	24	R	IPL	BA 40
198	54	14	26	R	IFG	BA 9
199	-44	-78	26	L	SOG	BA 19
200	-38	-58	28	L	STG	BA 39
201	56	-30	28	R	IPL	BA 40

202	-4	-28	28	L	Cing	BA 23
203	-52	-16	28	L	PostcG	BA 4
204	-44	-2	26	L	IFG	BA 9
205	-46	12	28	L	IFG	BA 9
206	-2	14	26	L	ACC	BA 24
207	-48	24	26	L	MFG	BA 46
208	12	-90	28	R	Cun	BA 19
209	8	-56	28	R	PCC	BA 31
210	-60	-56	30	L	SMG	BA 40
211	-8	-38	28	L	PCC	BA 31
212	-56	2	32	L	PrecG	BA 6
213	-12	56	32	L	SFG	BA 9
214	40	-62	34	R	AngG	BA 39
215	-48	-26	32	L	PostcG	BA 2
216	32	-80	34	R	Pcun	BA 19
217	-10	-62	34	L	Pcun	BA 7
218	-36	-50	34	L	IPL	BA 40
219	8	-36	32	R	PCC	BA 31
220	52	-8	34	R	PrecG	BA 6
221	-52	-68	36	L	AngG	BA 39
222	-34	-66	36	L	PCun	BA 19
223	38	-42	36	R	SMG	BA 40
224	58	-26	34	R	IPL	BA 40
225	6	-12	36	R	ACC	BA 24
226	50	4	38	R	MFG	BA 6
227	-44	6	36	L	PrecG	BA 9
228	-46	16	34	L	MFG	BA 9
229	22	46	34	R	SFG	BA 9
230	48	-70	38	R	AG	BA 39
231	-34	-42	40	L	IPL	BA 40
232	-50	-18	38	L	PostcG	BA 3
233	-52	-8	38	L	PrecG	BA 6
234	-8	-54	40	L	Pcun	BA 7
235	-8	48	38	L	SFG	BA 8
236	-32	-58	42	L	IPL	BA 7
237	-48	-30	40	L	IPL	BA 40
238	58	-18	40	R	PrecG	BA 4
239	32	18	42	R	MFG	BA 8
240	12	-46	46	R	PCun	BA 7
241	-44	12	44	L	MFG	BA 8
242	-44	-44	44	L	IPL	BA 40

243	-22	20	46	L	MFG	BA 8
244	-2	-42	46	L	PCun	BA 7
245	44	-40	46	R	IPL	BA 40
246	-32	-36	48	L	PostcG	BA 3
247	-46	-26	50	L	PostcG	BA 2
248	48	-26	46	R	PostcG	BA 2
249	-38	-20	46	L	PostcG	BA 3
250	-52	-16	48	L	PostcG	BA 1
251	-52	-6	48	L	PrecG	BA 4
252	8	6	44	R	ACC	BA 24
253	32	24	50	R	SFG	BA 8
254	22	-26	48	R	PostcG	BA 3
255	16	-4	50	R	ACC	BA 24
256	30	10	50	R	MFG	BA 6
257	-34	-52	52	L	SPL	BA 40
258	20	12	50	R	SFG	BA 6
259	4	-50	52	R	PCun	BA 7
260	46	-18	52	R	PostcG	BA 3
261	0	-68	54	L	PCun	BA 7
262	-30	-30	56	L	PrecG	BA 4
263	-20	-50	56	L	PCun	BA 7
264	-12	-42	56	L	PCun	BA 7
265	2	-40	56	R	ParacLob	BA 5
266	12	-54	58	R	PCun	BA 7
267	10	-32	62	R	PostcG	BA 3
268	-6	-48	66	L	PostcG	BA 7
269	-18	-44	64	L	PostcG	BA 5
270	6	6	66	R	SFG	BA 6
271	16	-48	66	R	PostcG	BA 7

Figure 2. Left panel: Pipeline used for detecting the regions of interest (i.e., nodes). Right panel: Nodes obtained for the decrease (top) and increase (bottom) conditions.

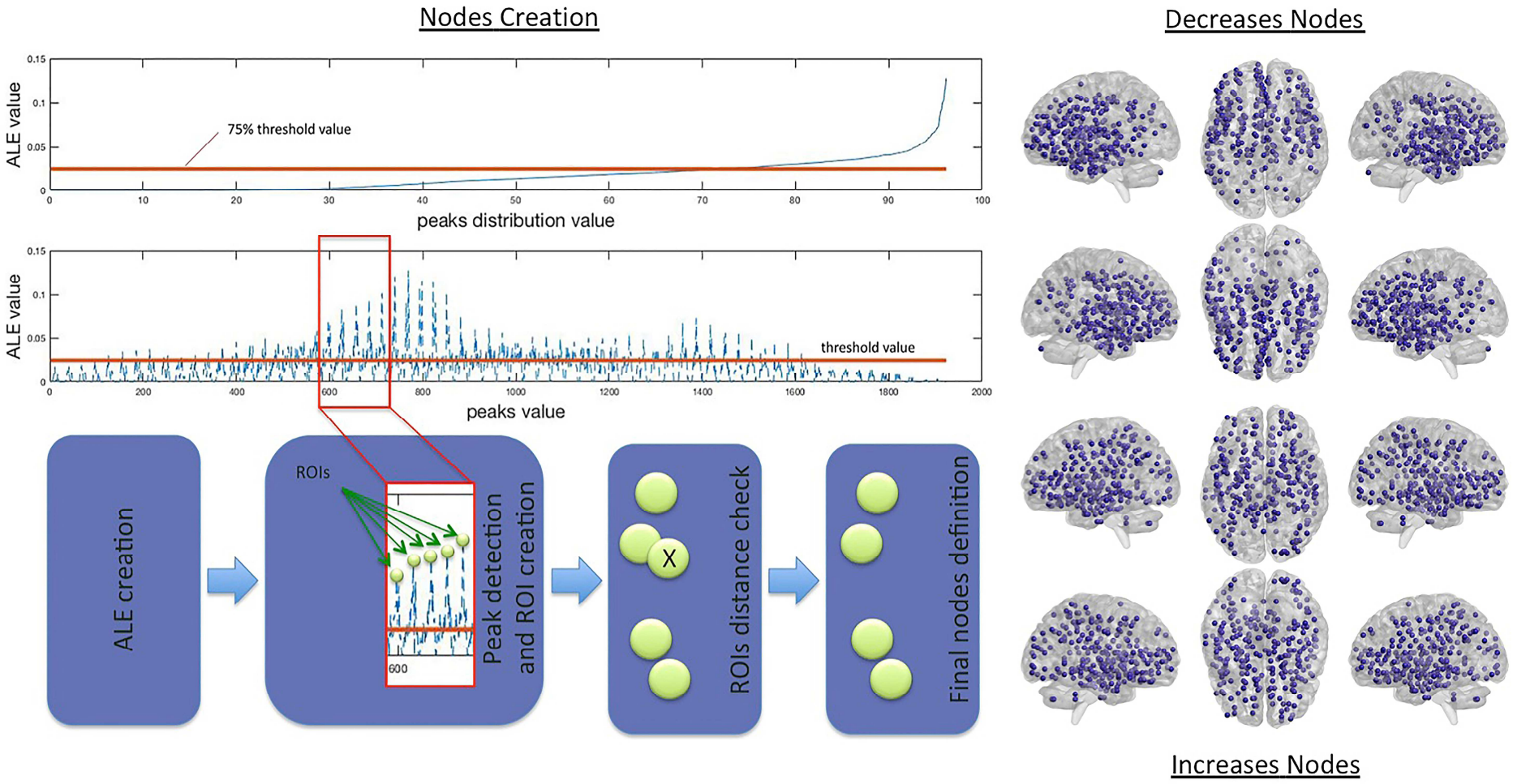

2.2.5. Construction of the structural co-alteration network

In order to map the distribution of GM alterations, a method capable of identifying the structural co-alterations associated with brain disorders was applied (Cauda et al., 2018a; Manuello et al., 2018; Tatu et al., 2018). This methodology can find whether the alteration of a certain area statistically co-occurs with the alteration of one or more other cerebral areas. In particular, a co-alteration matrix was built on the basis of the previously defined set of nodes. In the matrix of NxM dimension, N rows stand for experiments and the M columns for the network nodes. For each couple of nodes of this matrix, it is possible to get the strength of their co-alteration applying the Jaccard index, which is the ratio between the number of experiments (rows) activating both nodes and the union of the experiments activating the two nodes independently. The Jaccard matrix was then thresholded at $p < 0.01$, with the method of Toro et al. (2008). More specifically, given A and B (two nodes), the null hypothesis affirms that the probability that B is altered does not depend on the probability that A, too, is altered; on the contrary, the alternative hypothesis affirms that there is a relationship of dependence between the occurrences of A and B, which can be expressed formally as follows:

$$p_0 = Prob(B = 1|A = 0)$$

$$p_1 = Prob(B = 1|A = 1)$$

$$H_0: p_0 = p_1 = p$$

$$H_1: p_0 \neq p_1$$

From VBM data, an estimate $\hat{p}$ can be obtained under the null hypothesis that $\hat{p} = m/N$, where m is the number of experiments in which node B is altered and N is the total number of experiments. In a similar way, the estimated probabilities

under the alternative hypothesis that there is dependency in the alteration of nodes can be obtained as follows:

$$\hat{p}_0 = \frac{(m-k)}{(N-n)}$$

and

$$\hat{p}_1 = \frac{k}{n}$$

where n is the number of experiments in which node A is altered and k the number of experiments in which both A and B result to be altered. The following formula determines the likelihood-ratio test:

$$\lambda = \frac{L(H_1)}{L(H_0)}$$

This formula evaluates the alternative hypothesis H_1 with respect to the null hypothesis H_0. The probability of the null hypothesis is expressed as follows:

$$L(H_0) = B(k; n, p)B(m-k; N-n, p)$$

where B stands for the binomial distribution in which n is the number of contrasts altering the second node; m is the number of contrasts altering the first node; N is the total number of contrasts; and $p = m/N$ and k are the numbers of contrasts altering both nodes. The probability of the alternative hypothesis is expressed as follows:

$$L(H_1) = B(k; n, p_1)B(m-k; N-n, p_0)$$

The λ distribution is modelled by a χ^2 function with one degree of freedom. Connection at $p < 0.01$ corrected for false discovery rate (FDR) was retained, or else discarded.

2.2.6. Construction of the functional connectivity matrix

The functional connectivity matrix was built for the same set of nodes of the previous analysis using resting state data (minimally pre-processed and ICA-FIX denoised) from 200 healthy adult subjects within the 22–35 age range, obtained from the Human Connectome Project (2015 Q4, 900-subject release). For details regarding the pre-processing of these data see Van Essen et al. (2012) and Glasser et al. (2013).

The matrix was built on the basis of previously determined ROIs, which were used with the dual regression approach (Beckmann et al., 2009) to produce a spatial map and subject-specific associated time series of the functional data. The spatial map of every subject was regressed into the subject's 4D space-time data set, so that a set of subject-specific time series was created. The output of the dual regression was a set of 200 matrices, one for every subject, in which columns were the time series of the corresponding ROIs. From these matrices the partial correlation between nodes was determined for each subject and then mediated so as to obtain a final partial correlation matrix of the subjects' group. This final connectivity matrix was then thresholded ($\alpha < 0.05$) with one sample permutation test (5000 permutation) by means of the FSL randomise program (Smith and Nichols, 2009; Winkler et al., 2014).

2.2.7. Construction of the anatomical connectivity matrix

The anatomical connectivity matrix was built using diffusion tensor imaging (DTI) data of 842 subjects within the 22–35 age range. These data were obtained from the Human Connectome Project (2015 Q4, 900-subject release) (Van Essen et al., 2013). The DTI images were obtained with a multishell diffusion scheme. The b-values were 1000, 2000 and 3000 s/mm2. The numbers

of the diffusion sampling directions were 90, 90 and 90. The in-plane resolution was 1.25 mm, and the slice thickness 1.25 mm. The DTI data were reconstructed in the MNI space applying the q-space diffeomorphic reconstruction (Yeh and Tseng, 2011) so as to have the spin distribution function (Yeh et al., 2010). A diffusion sampling length ratio of 1.25 was used; its output resolution was 1 mm. The atlas was built by averaging the spike density functions of the 842 subjects.

A deterministic fiber tracking algorithm (Yeh et al., 2013) was employed in order to reveal the anatomical pathways. The parameters were the following: whole-brain seeding region method; angular threshold of 60°; step size of 0.5 mm; the anisotropy threshold was determined automatically by DSI Studio (Yeh et al., 2016). Paths with a length less than 30 mm were discarded. A total of 5000 seeds were located in the brain. The previously defined set of nodes was used to determine the connectivity matrix by considering the numbers of tracts passing between two nodes normalized by the median length of the connecting tracks.

2.2.8. Construction of the genetic co-expression matrix

The "gene expression network" developed by Richiardi et al. (2015) is a type of genetic connectivity that can quantify anatomical region to anatomical region (i.e., region of interest to region of interest) across genes. This network was constructed on the basis of the complete microarray data sets of six brains from the Human Brian Atlas Project (Hawrylycz et al., 2012). The data sets are constituted by values of gene expression that are normalized across all the six brains – for details see the Allen Human Brain Atlas (2013).

To address the idiosyncrasies of the Allen Brain Atlas (for instance, only two brains have bi-hemispheric samples and the variability among cerebral areas samples is high, as they were obtained with different stereotactic coordinates), a method based on the Voronoi tessellation was employed (Cauda et al., 2012a). The tessellation of Voronoi (Voronoi, 1907) is a particular metric division of space based on a finite set of points. In a 3D space, a given set of points S, the tessellation is a division that relates a volume V(p) to every point $p \in S$, in such

a way that all the surface points of V(p) are closer to p than to any other point in S. With this procedure a parcellation of each of the six brains was created, based on the position of their samples, which were treated as the barycentres of the polygons of Voronoi. In this way, the gene expression value of the sample situated in the barycenter of a particular polygon was attributed to all the voxels included in that polygon.

Six parcellations were then created, and in each of them every voxel was associated with a gene expression vector related to its nearest sample. As to the four subjects with samples constituted by one hemisphere, just half brain was parcellated. Subsequently, the gene expressions of the six individuals were averaged voxel-wise. Gene expressions that were reported to be non-statistically significant in the Allen database were removed from the averaging process. This procedure was able to reduce the variance between the gene expression values of the six subjects, which minimized the idiosyncrasies of the Allen database.

The final result was a single brain tessellation in which every Voronoi polygon had the six subjects' mean gene expression (Cauda et al., 2012a). This information was used to construct the genetic co-expression matrix based on the set of nodes as previously defined. The gene expression of the Voronoi polygon related to a node was attributed to that node. The rows of the matrix were the gene expressions and its columns the nodes. From this matrix the full and partial correlation of the mean gene expression between the nodes was determined, so that a partial correlation matrix was obtained. This final matrix was thresholded ($\alpha < 0.05$) with a permutation test (5000 permutations).

2.2.9. Assessing the reliability of measures

To evaluate the reliability of the calculations, the Spearman-Brown's prediction formula was used (Stanley, 1971; Allen and Yen, 2001). Each data set (meta-analytic, functional, and genetic) was divided into even and odd groups. For every group, the connectivity matrices were determined. Subsequently, the

correlation between these matrices were calculated employing the Spearman-Brown's correction (Allen and Yen, 2001), with the following formula:

$$\rho = 2r/(1 + r)$$

where r is the Spearman's correlation.

As DTI data were obtained from the Human Connectome Project as mean connectivity matrices, a different approach to evaluate the reliability of the anatomical connectivity measures was used. Specifically, another mean DTI connectivity matrix was constructed using a replication data set. This data set led to a different anatomical connectivity matrix based on 842 subjects' diffusion MRI data, within the 22–35 age range, obtained from the Human Connectome Project (2015 Q4, 900-subject release) (Van Essen et al., 2013). In the end, the correlation between the anatomical connectivity matrix of the primary data set and the matrix of the replication data set was determined.

2.2.10. Comparison of connectivity matrices

The co-alteration, anatomical, functional, and genetic matrices were compared using the Mantel test (Mantel, 1967). In this test the correlation is calculated with a permutation test (5000 permutations). In other words, the correlation between the matrices was determined by randomly permutating rows and columns. Then, the distribution of the correlations was obtained and the p-value was calculated.

2.2.11. Construction of the diffusion connectivity matrix

To evaluate the progression of the different types of connectivity patterns, a diffusion model was created. The spread of GM alterations was thought of as a diffusion process by using a brain network-based model G = {N,E}, where nodes $n_i \in N$ and N stands for the cortical and subcortical structures obtained in this meta-analysis, while edges $e_{ij} \in E$ and E stands for the connection strength

connecting node i and node j. Three types of connection strength were considered, one for the anatomical matrix, one for the functional matrix, and another one for the genetic matrix.

The diffusion process was modeled with the heat equation following Abdelnour et al. (2014) and Kondor and Lafferty (2002), as follows:

$$\frac{d\mathrm{x}(t)}{dt} = -\beta\mathcal{L}\mathrm{x(t)}$$

in which $\mathcal{L}$ is the Laplacian matrix:

$$\mathcal{L} = I - \Delta^{-1/2} E \Delta^{1/2}$$

where Δ is the diagonal matrix having $\delta_i = \sum_j e_{ij}$ as the ith diagonal element.

The heat equation can be expressed as follows:

$$\mathrm{x}(t) = \exp(-\beta\mathcal{L}t)\,\mathrm{x}_0$$

This formula describes the progression of the initial phase x_0. An initial phase in which the neuropathological process was uniform in all nodes was postulated, thus leading to the following equation:

$$\mathrm{Cov}(t) = \exp(-\beta\mathcal{L}\mathrm{t})$$

As the diffusion factor β and the time t are free parameters, the formula can describe the covariance of the system at each time of its progression.

In this case, the covariance matrix (obtained from meta-analytic data) and the Laplacian matrices (obtained from the resting state data, the anatomical data and genetic data) were considered. The diffusion factor β was estimated and, thereby, the progression of the diffusion for the functional, anatomical and genetic data was obtained. The estimate of β and the progression of the diffusion

were determined with a grid search on the parameter β, ranging between 0 and 1 with a step of 0.1. For every β value, the matrix of this simulation was correlated with the meta-analytic covariance matrix. With a Mantel test the significance of this correlation was evaluated and the β value maximizing the correlation was selected.

2.2.12. Contribution of the connectivity profiles to the co-alteration matrix

A model D (i.e., co-alteration matrix) to study the contribution of the different types of connectivity profiles to the co-alteration network was developed as follows:

$$D = \alpha M_{funct} + \beta M_{anat} + \gamma M_{genet}$$

in which D stands for the co-alteration matrix, M_{funct} for the functional connectivity matrix, M_{anat} for the anatomical connectivity matrix, and M_{genet} for the genetic connectivity matrix.

By applying an unconstrained nonlinear optimization, the minimum of the scalar function of the variables was found. The employed algorithm was the search method proposed by Lagarias et al. (1998):

$$\min_{\alpha,\beta,\gamma} ||(D - \alpha M_{funct} - \beta M_{anat} - \gamma M_{genet})^2 ||$$

This formula allows to find the coefficients minimizing the square difference norm between the co-alteration matrix and the other matrices. The algorithm was run 1000 times with different initial conditions, every time to assess the stability of the obtained minimum (see Fig. 3).

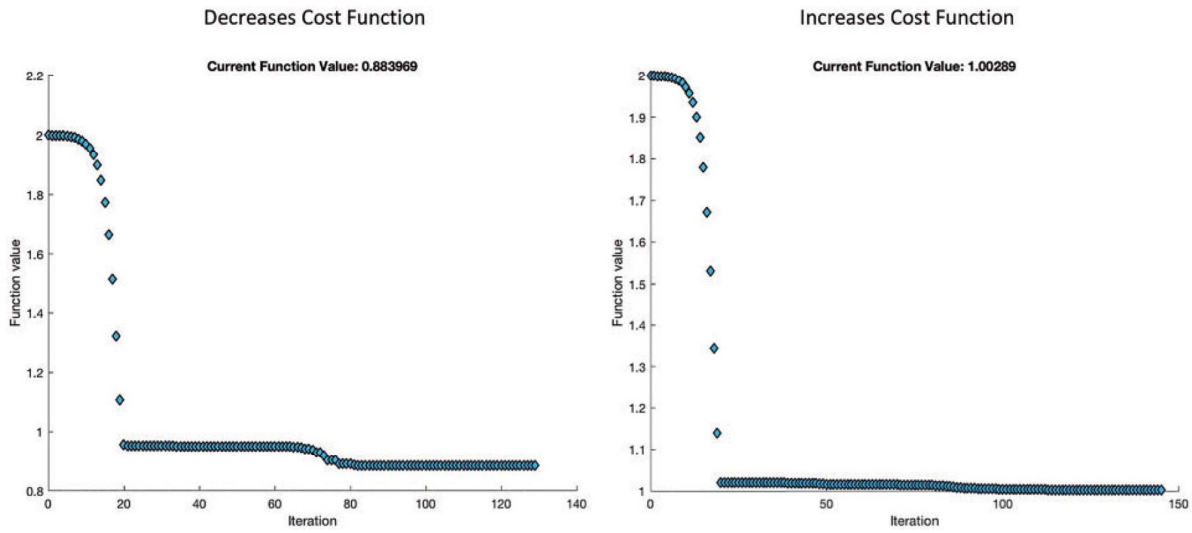

Figure 3. This schema shows the progression of the cost function of the minimization algorithm that predicts the distribution of the structural GM co-alterations.

2.2.13. Techniques of network analysis

The co-alteration network was investigated by applying a network-based analysis technique.

The node degree is defined as the number of links that connect the node with the other nodes. The degree distribution, which is the fraction of nodes with degree k, was used to compare the node degree of different networks' nodes. In this way it was possible to compare the co-alteration network with the other networks. The degree distribution is expressed as follows:

$$P(k) = \frac{n_k}{n}$$

The average path length is considered as the average number of steps along the shortest paths for all couples of nodes of a network. Thus, for an unweighted graph G with n vertices, the average path length is expressed as follows:

$$l_G = \frac{1}{n(n-1)} \sum_{i \neq j} d(v_i, v_j)$$

in which *d* represents the shortest distance between node v_i and node v_j (with *d* = 0 if it is not possible to reach v_j starting from v_i).

This measure is one of the most robust in network topology and is inversely associated with efficiency, which measures the capacity of a network to exchange information between its elements. Specifically, the local efficiency measures the network resistance in case of specific nodes' failure.

2.3. Results

2.3.1. The most frequently altered areas of the brain

Figure 4 illustrates the cerebral areas that are mostly altered in the VBM studies of this meta-analysis. These areas can be considered to be a "core set" that is frequently affected by brain diseases. Regions exhibiting significant statistical decreases are the insulae, anterior cingulate cortices, superior and middle temporal gyri, superior, middle and inferior frontal, pre- and postcentral gyri. Regions exhibiting significant statistical increases are the right anterior and posterior insula, left middle insula, right pre- and postcentral gyri, right superior frontal gyrus, right superior temporal gyrus, left inferior temporal and inferior frontal gyri (see also Tables 7 and 8).

Figure 4. Results of the ALE for decreased (left) and increased foci (right). Results of the ALE are clustered at $p < 0.05$ and family-wise error-corrected for multiple comparisons, with a cluster-forming threshold of $p < 0.001$.

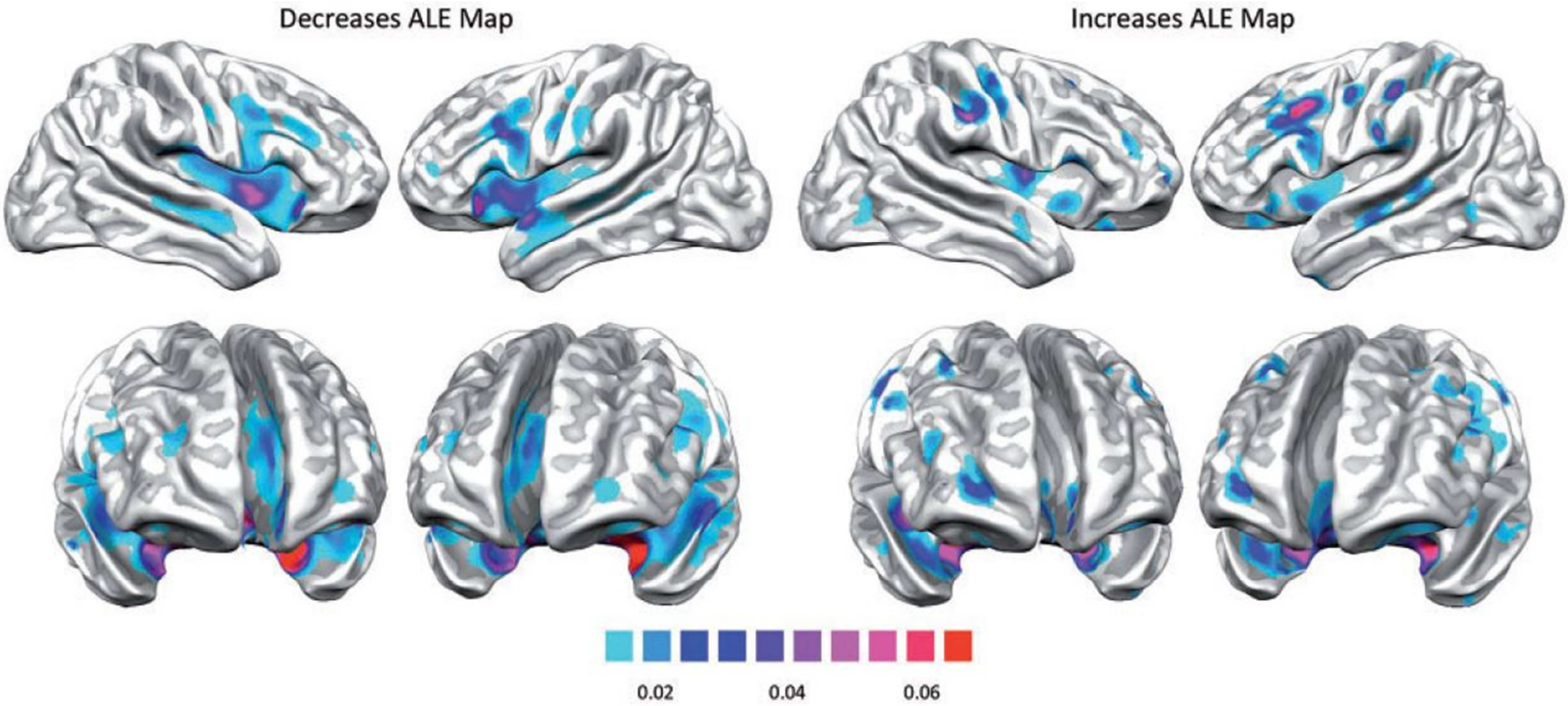

Table 7. Clusters of gray matter decreases.

Cluster #	Volume (mm^3)	x	y	z	Side	Label (Talairach Client)	BA
1	112080	-22	-6	-18	L	Parahippocampal Gyrus. Amygdala	
		-28	-14	-16	L	Parahippocampal Gyrus. Hippocampus	
		-4	-16	8	L	Thalamus. (Medial Dorsal Nucleus)	
		2	-16	6	R	Thalamus	
		-36	20	0	L	Insula	13
		-8	12	6	L	Caudate (Caudate Body)	
		22	-6	-18	R	Parahippocampal Gyrus. Amygdala	
		-28	-36	-4	L	Parahippocampal Gyrus. Hippocampus	
		10	12	8	R	Caudate (Caudate Body)	
		38	20	2	R	Insula	13
		34	-26	-12	R	Temporal Lobe. Sub-Gyral. Hippocampus	
		30	-36	-4	R	Temporal Lobe. Sub-Gyral. Hippocampus	
		-4	8	-6	L	Caudate (Caudate Head)	
		40	0	6	R	Insula	13
		38	10	0	R	Insula	13
		44	12	0	R	Insula	13
		2	6	-6	R	Anterior Cingulate	25
		-54	4	-6	L	Superior Temporal Gyrus	38
		-42	-6	0	L	Insula	13
		-38	4	6	L	Insula	13
		-44	14	30	L	Middle Frontal Gyrus	9
		12	-32	2	R	Thalamus (Pulvinar)	
		-22	8	2	L	Lentiform Nucleus. Putamen	
		-36	-14	-38	L	Inferior Temporal Gyrus	20
		58	-8	-12	R	Inferior Temporal Gyrus	21
		-50	10	20	L	Inferior Frontal Gyrus	44
		44	-16	12	R	Insula	13
		-48	-20	14	L	Transverse Temporal Gyrus	41
		-14	-32	2	L	Thalamus (Pulvinar)	
		34	30	-12	R	Inferior Frontal Gyrus	47
		50	-20	-4	R	Superior Temporal Gyrus	22
		54	-18	14	R	Transverse Temporal Gyrus	41
2	8048	-2	36	24	L	Anterior Cingulate	32
		6	24	32	R	Cingulate Gyrus	32
3	4920	-4	56	2	L	Medial Frontal Gyrus	10
		0	38	-12	L	Medial Frontal Gyrus	11
		4	38	-24	R	Rectal Gyrus	11
		6	50	-4	R	Medial Frontal Gyrus	10
4	688	-52	-16	-22	L	Fusiform Gyrus	20
5	464	44	10	34	R	Middle Frontal Gyrus	9
6	432	-30	56	-2	L	Superior Frontal Gyrus	10

7	288	44	38	-8	R	Middle Frontal Gyrus	47
8	216	-58	-8	30	L	Precentral Gyrus	4
		-52	-8	34	L	Precentral Gyrus	6

Table 8. Clusters of gray matter increases.

Cluster #	Volume (mm^3)	x	y	z	Side	Label (Talairach Client)	BA
1	5016	10	4	0	R	Caudate (Caudate Head)	
		26	-12	-16	R	Parahippocampal Gyrus. Hippocampus	
		30	-22	-20	R	Parahippocampal Gyrus	36
		22	2	-20	R	Uncus	34
		22	-14	-26	R	Parahippocampal Gyrus	35
2	3752	-18	4	-6	L	Lentiform Nucleus. Putamen	
		-8	18	0	L	Caudate (Caudate Head)	
		-20	4	4	L	Lentiform Nucleus. Putamen	
		-24	-2	12	L	Lentiform Nucleus. Putamen	
		-20	16	-6	L	Lentiform Nucleus.Putamen	
		-8	18	-10	L	Anterior Cingulate	32
3	2096	-26	-14	-16	L	Parahippocampal Gyrus. Hippocampus	
		-30	-10	-4	L	Lentiform Nucleus. Putamen	
		-32	-24	-18	L	Parahippocampal Gyrus	35
		-22	-4	-22	L	Uncus. Amygdala	
4	1960	26	-32	-2	R	Parahippocampal Gyrus	27
		16	-22	10	R	Thalamus (Lateral Posterior Nucleus)	
5	1208	40	-16	-4	R	Insula	13
6	1208	-44	8	38	L	Middle Frontal Gyrus	9
7	1080	-18	-22	8	L	Thalamus (Ventral Posterior Medial Nucleus)	
8	640	-38	16	-6	L	Inferior Frontal Gyrus	47
9	568	-50	-22	26	L	Postcentral Gyrus	2
10	424	-28	-36	-4	L	Parahippocampal Gyrus. Hippocampus	
11	352	32	-40	-18	R	Fusiform Gyrus	20
12	344	-10	42	-6	L	Anterior Cingulate	32
13	328	-40	4	2	L	Insula	13
14	280	4	-44	56	R	Paracentral Lobule	5
15	224	58	-24	32	R	Inferior Parietal Lobule	40

2.3.2. Creation of nodes and the structural co-alteration network

From the sets of GM decreases and GM increases, 277 and 271 nodes were obtained, respectively. These nodes are shown in Fig. 2 (right panel) – see also Tables 5 and 6. On the basis of these nodes, the structural co-alteration networks were constructed for both GM decreases and GM increases. These networks are illustrated by Figure 3 (top panel).

Notably, the two co-alteration networks are topologically different (Fig. 5, bottom). The one constituted by GM decreases is more compact and mainly involves the insulae and the anterior cingulate cortices. These areas have the nodes with the highest values of degree. In turn, the network constituted by GM increases is more widespread and less anatomically defined, though it involves parts of the insulae and appears to be somewhat prevalent in subcortical areas.

2.3.3. Anatomical, functional and genetic connectivity

For the same sets of nodes, the resting state functional, anatomical and genetic networks were constructed. These networks are visualized in Figures 6 and 7. In accordance with previous research (Gong et al., 2014; Huang and Ding, 2016), anatomical and functional connectivity profiles appear to be correlated (decreased nodes $r = 0.14$, $p < 0.00002383$; increased nodes $r = 0.12$, $p < 0.00002421$). Interestingly, genetic connectivity appears to correlate with both anatomical (decreased nodes $r = 0.21$, $p < 0.00002195$; increased nodes $r = 0.18$, $p < 0.00003028$) and functional connectivity (decreased nodes $r = 0.18$, $p < 0.00003021$; increased nodes $r = 0.14$, $p < 0.00002359$).

Figure 5. Top: The GM decreases (left) and GM increases (right) co-alterations networks. For the sake of visualization, matrices were thresholded at the 95th percentile. Colors from blue to red show lower to higher correlation values. Bottom: Topological analysis of the co-alteration networks, applying a force directed spring embedded layout. Smaller nodes represent lower average shortest path length. Colors from green to red show lower to greater degree values.

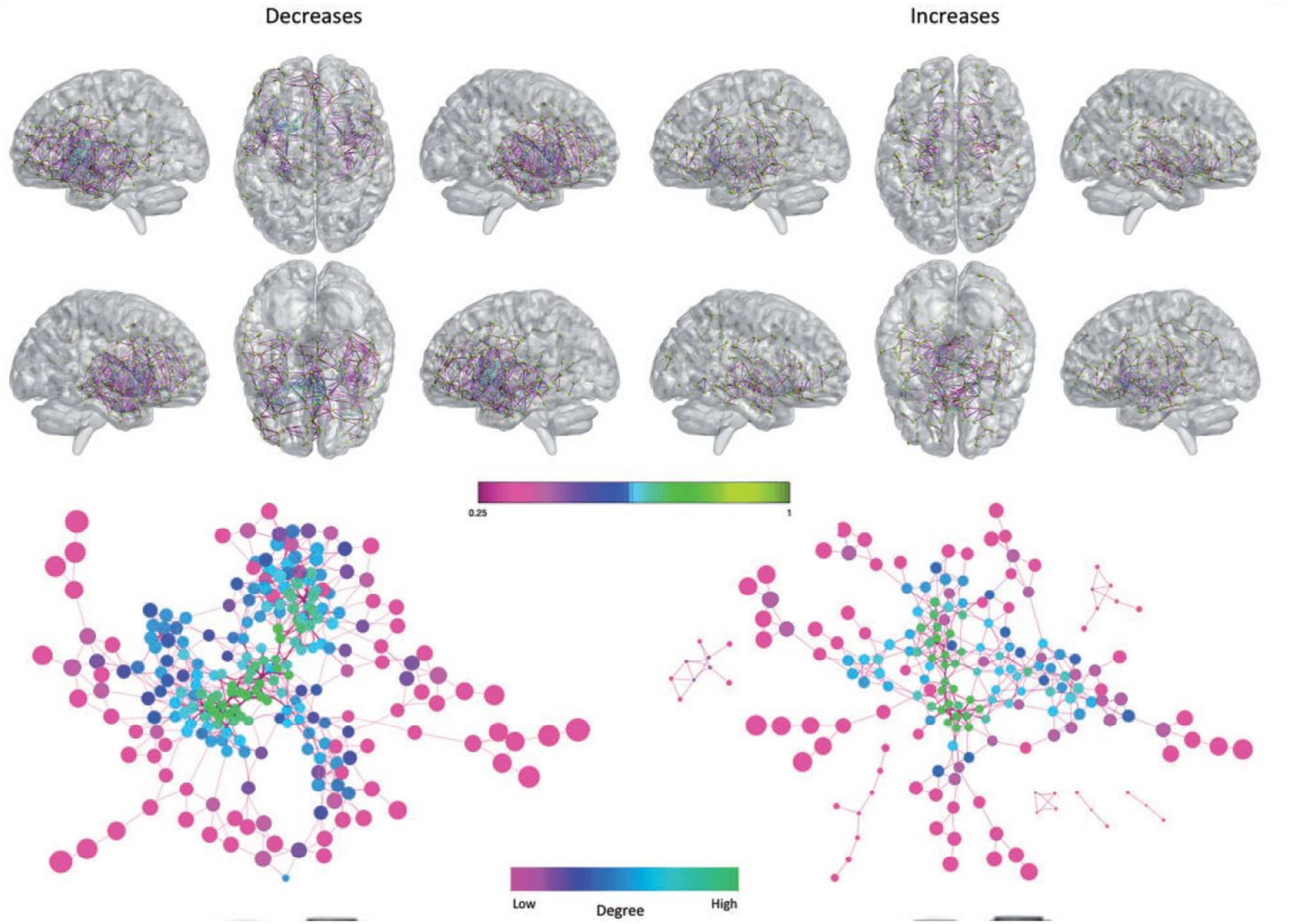

2.3.4. Reliability of connectivity matrices

The connectivity matrices have a good reliability (Spearman-Brown split half test). The obtained mean values are 0.80, 0.72, 0.80, and 0.75 for structural co-alteration, functional, gene co-expression and anatomical connectivity matrices, respectively. These values suggest a good internal consistency of measures. Specifically, the Spearman-Brown formula is associated with the Cronbach's alpha (Carlson et al., 2009; Nunnally and Bernstein, 1994); both formulas quantify the ratio of the true-score and total-score variances. As pointed out by Nunnally and Bernstein (1994), the rule of thumb for that measure generally regards figures > 0.7 as consistent values.

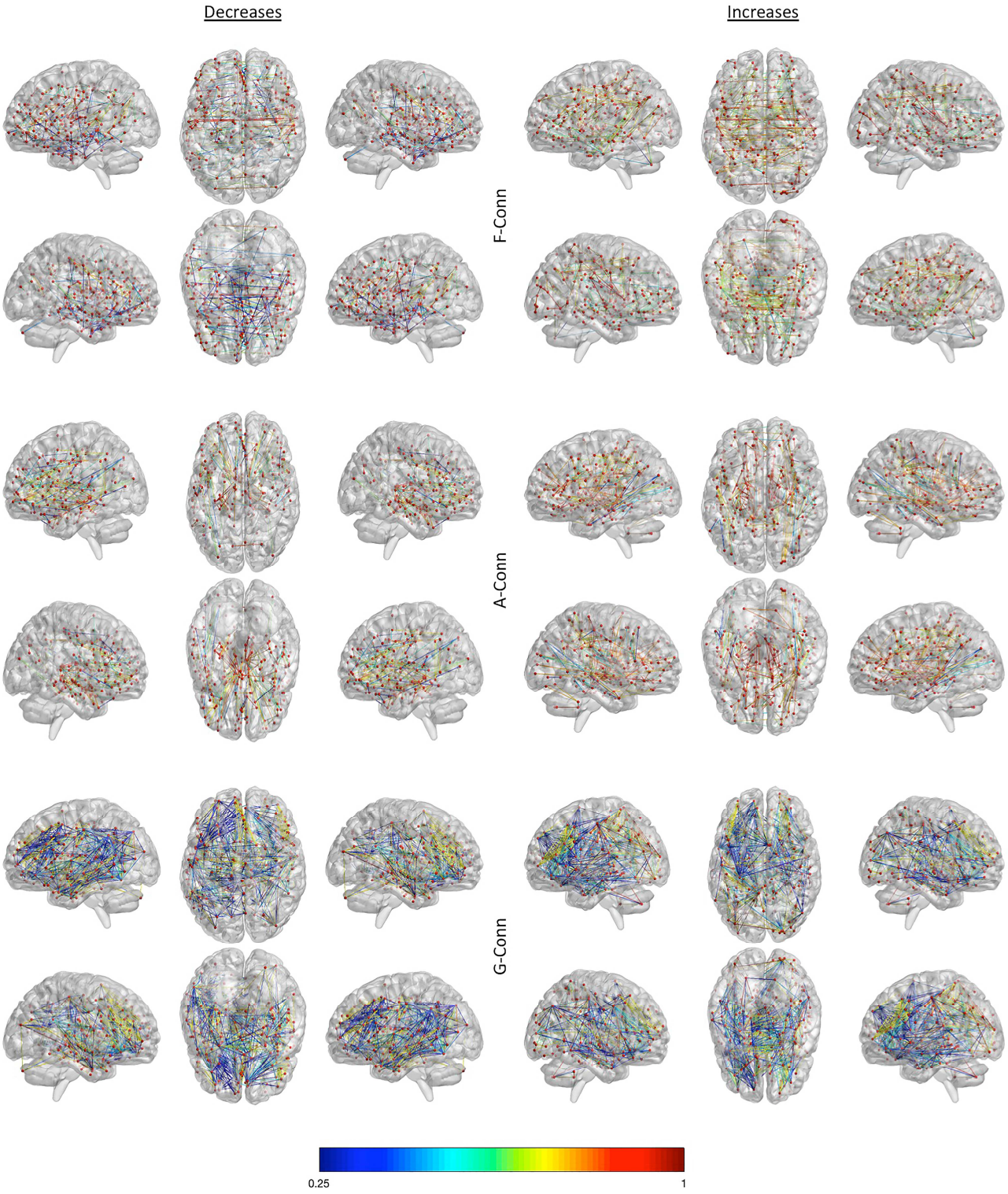

Figure 6. *Top*: functional connectivity (F-Conn) network. *Middle*: anatomical connectivity (A-Conn) network. *Bottom*: genetic connectivity (G-Conn) network. For visualization purposes, matrices were thresholded at the 95th percentile. Colors from blue to red indicate lower to higher correlation values. For anatomical connectivity, colors from blue to red indicate lower to higher fiber density values.

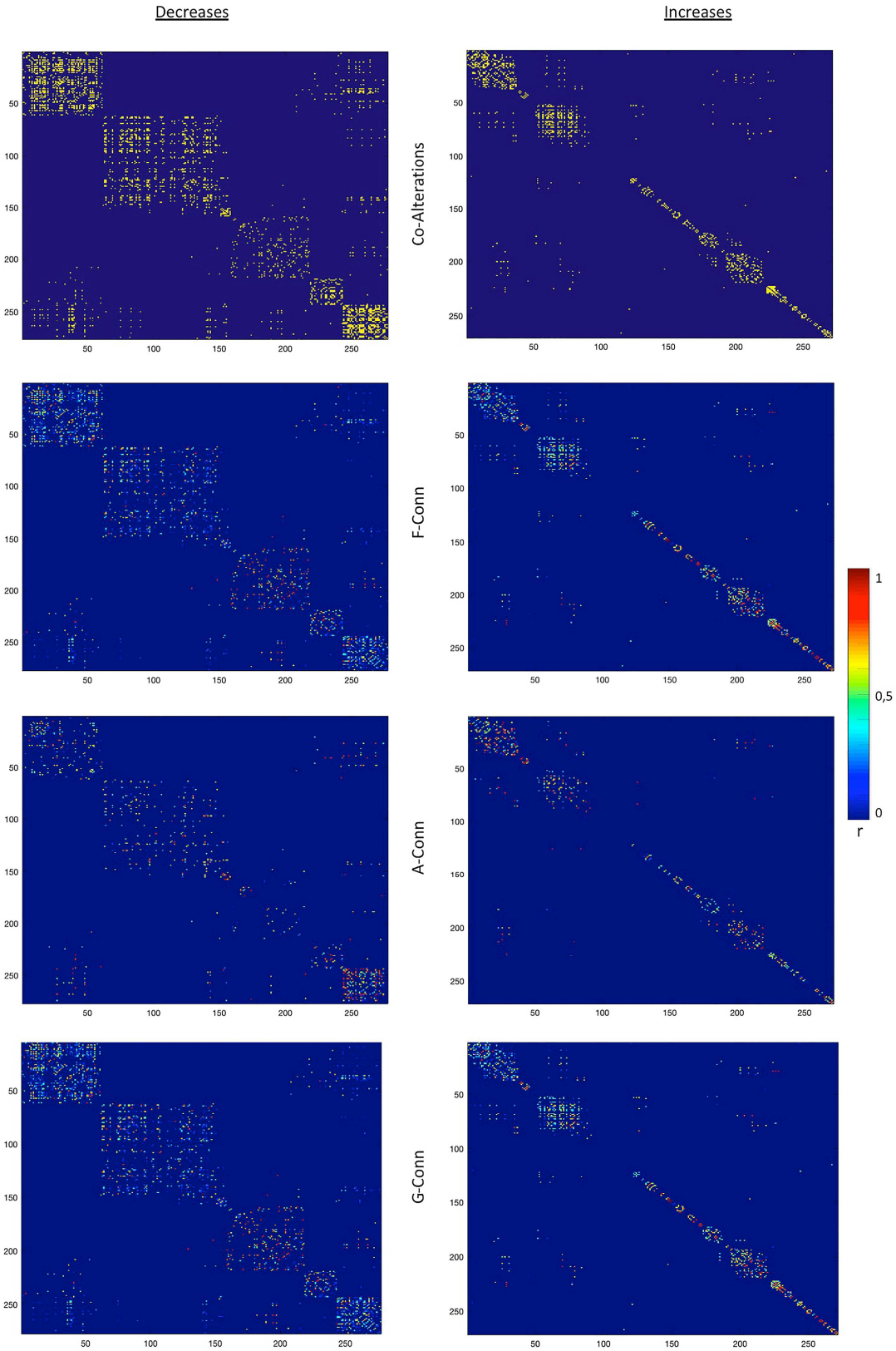

Figure 7. Distance matrices of the structural co-alteration, functional, anatomical and genetic connectivity. Colors from blue to red represent lower to higher correlation values.

2.3.5. Correlational analyses

As the experimental question of this study was to investigate whether and how morphometric neuropathological co-alterations networks (formed by GM decreases or GM increases) are influenced by different types of normal brain connectivity profiles (i.e., functional, anatomical, and genetic connectivity), these co-alterations networks were compared with normal brain connectivity patterns obtained from healthy individuals.

Statistical comparisons between structural co-alteration matrix and the other matrices (functional, anatomical, and genetic) show that each connectivity profile is statistically correlated with the co-alteration patterns associated with both GM decreases and GM increases; in other words, each connectivity profile can account for a statistically substantial portion of those co-alteration patterns.

The left top panel of Figure 8 shows the full correlation between the structural co-alteration matrix and the other three connectivity matrices. The structural co-alteration network of GM decreases is better explained by functional connectivity ($r = 0.28$), then by anatomical ($r = 0.19$), and finally by genetic connectivity ($r = 0.18$); while the structural co-alteration network of GM increases is better explained by functional connectivity ($r = 0.26$), then by genetic ($r = 0.23$), and finally by anatomical connectivity ($r = 0.22$).

As these three types of connectivity profiles are known to be correlated with each other and have a shared variance, the partial correlation between them and the structural co-alteration matrix was determined, so as to observe how each type of connectivity profile correlates with the structural co-alteration network with the exclusion of the shared variance. The right top panel of Figure 8 shows the results of this analysis, providing further evidence that the structural co-alteration of GM decreases correlates more with functional ($r = 0.24$), then with anatomical ($r = 0.14$), and finally with genetic connectivity ($r = 0.11$). In turn, the structural co-alteration of GM increases appears to correlate similarly with the three types of connectivity profiles, even though it is slightly better explained by functional ($r = 0.22$), then by genetic ($r = 0.17$), and finally by anatomical

connectivity (r = 0.16). Notably, all results of partial and full correlations are statistically significant: p values < 2×10^{-7} for partial correlation, and p values < 3×10^{-4} for full correlation, respectively. Overall, this suggests that all the three types of brain connectivity profiles can in part account for the GM decreases and GM increases structural co-alterations networks.

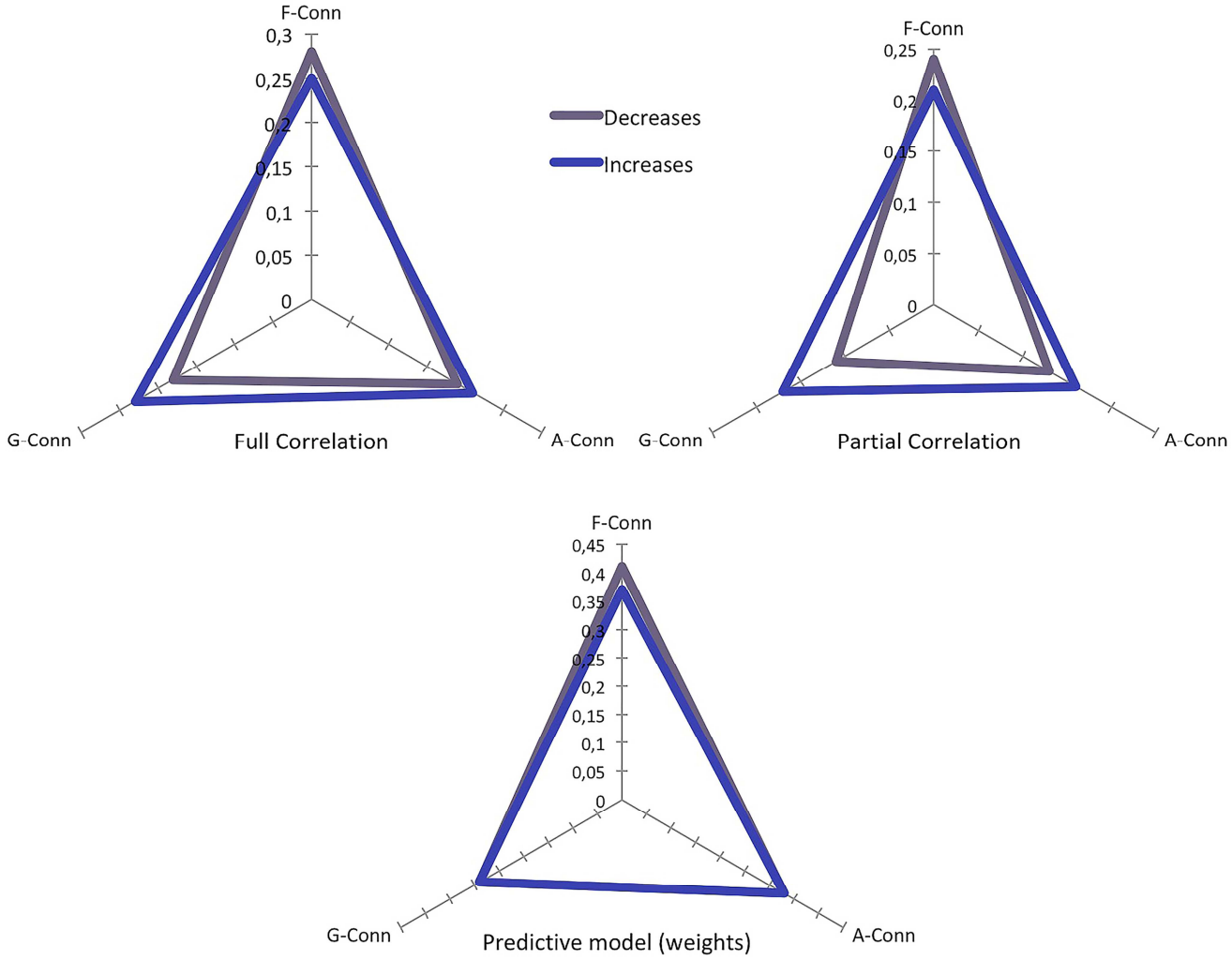

Figure 8. Results of the correlational and predictive tests. The top panel illustrates the results of correlational analyses (left part regards the full correlation, right part regards the partial correlation). The bottom panel illustrates the predictive results.

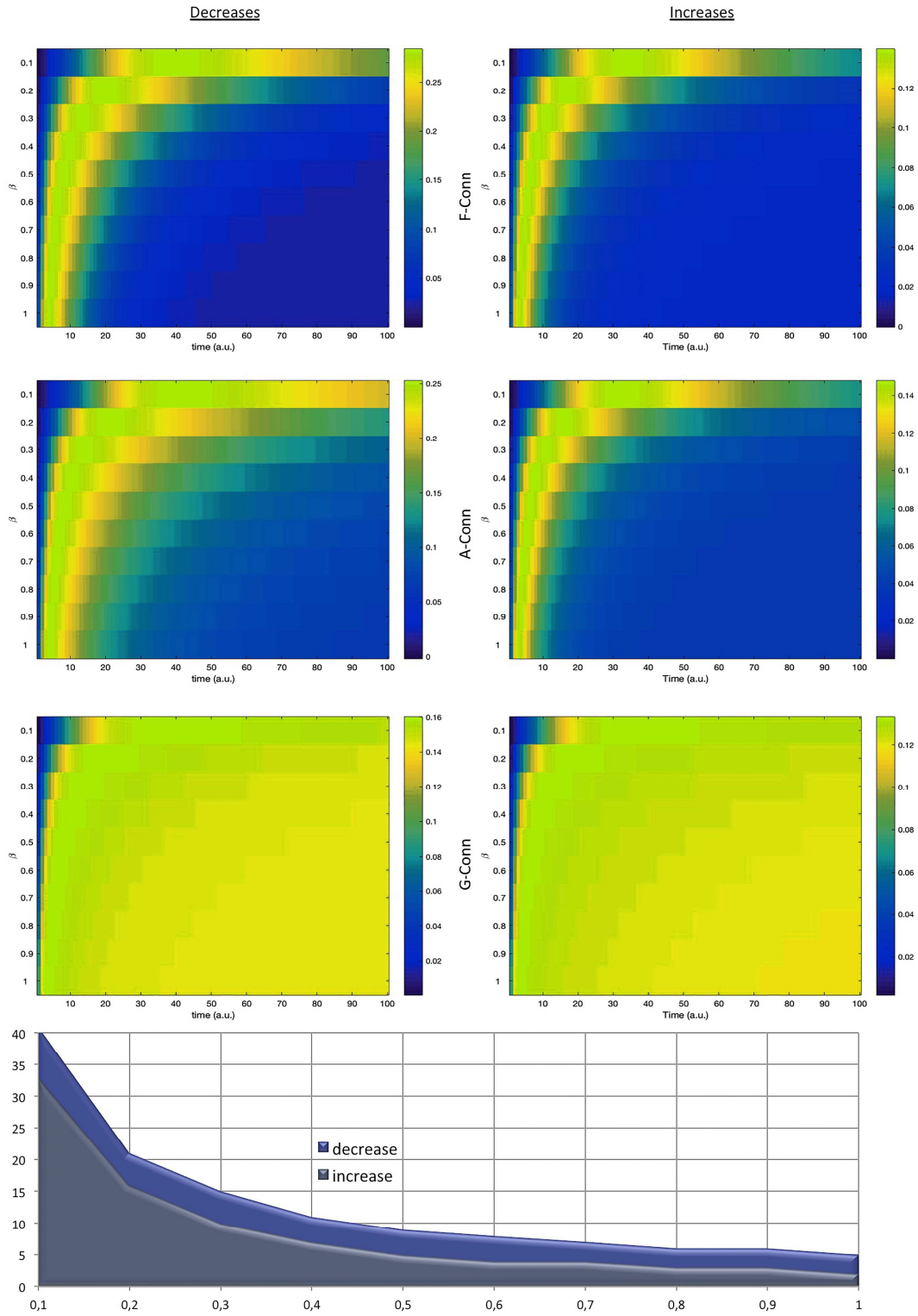

Figure 9. *Top*: Maps illustrating the correlations of the functional, anatomical and genetic matrices with the structural co-alteration matrix for different β values as a function of time (arbitrary units). Colors from blue to red indicate lower to higher correlation values. *Bottom*: Chart showing the time in which the diffusion of alterations reaches the steady state as a function of the β rate for the decrease and increase conditions.

2.3.6. Progressions along the spatial and temporal dimensions

The predictive model was able to describe the distribution of neuronal alterations' patterns with good statistical confidence (all predictions survived the conservative statistic threshold of $p < 0.00001$). Figure 9 shows the temporal progression of the GM co-alteration patterns (expressed in arbitrary units) as predicted by the model's β values. For every β value the temporal progression of the alteration process was calculated, and for every time step the diffusion matrix obtained from the distribution patterns of co-alterations was correlated with the co-alteration matrix derived from the meta-analysis. Around 30 time steps all the three types of connectivity profiles can predict the complete distribution of GM alterations. Yet, within the initial steps, only genetic connectivity is able to predict how structural co-alterations are going to diffuse. This result supports the idea that genetic connectivity makes it possible to predict a significant portion of the distribution pattern of neuropathological alterations in a range of brain disorders just on the basis of its initial phases. The chart at the bottom of Figure 9 shows how the average temporal progression of co-alterations obtained from the model based on GM increases presents a faster development in comparison with the one obtained from the model based on GM decreases.

The model of the distribution patterns of the structural co-alteration ($D = \alpha M_{F-Conn} + \beta M_{A-Conn} + \gamma M_{G-Conn}$) indicates that it is possible to describe the meta-analytic GM co-alteration matrix as a weighted sum of the functional, anatomical and genetic connectivity matrices. The D matrix was correlated with the co-alteration matrix derived from the meta-analytical data: the found variance for the GM decreases was $R^2 = 0.77$ ($p < 0.0012$), and for the GM increases was $R^2 = 0.72$ ($p < 0.0025$). All the three matrices contribute substantially to the description of the meta-analytic structural co-alteration matrix (see Table 9 and the bottom panel of Figure 8). With regard to both GM decreases and increases, the major contribution is given by functional, then by anatomic, and finally by genetic connectivity matrix.

	F-Conn R^2	A-Conn R^2	G-Conn R^2	Total R^2
Decrease	0.41	0.34	0.25	0.77
Increase	0.38	0.33	0.29	0.72

Table 9. Correlation values between the three connectivity matrices and the meta-analytic structural co-alteration matrix obtained with either GM increase or decrease data. The total R^2 value was the result of the correlation between the diffusion matrix derived from the diffusion model and the co-alteration matrix derived from the meta-analytic data. In this way the contribution of every connectivity profile to the variance explained was calculated, determining the R^2 of each network with the diffusion matrix of the predictive model.

F-Conn = functional connectivity matrix; A-Conn = anatomical connectivity matrix; G-Conn = genetic connectivity matrix.

2.4. Discussion

Results of this study have provided support for the following points: 1) cerebral regions affected by neuropathological processes tend to constitute typical patterns of structural co-alterations; 2) the development of these coalteration patterns is not random but is likely to follow the pathways of brain connectivity; 3) anatomical, functional and genetic connectivity profiles are differently involved in the development of structural co-alterations; 4) finally, on the basis of different types of brain connectivity, it is possible to describe and predict with relatively high accuracy the development of the coalteration patterns and, consequently, estimate the progression of how GM co-alterations are distributed across the brain.

Analyses provide evidence that the distribution of brain morphological alterations manifests a specific development: alterations are distributed across cerebral regions in such a way as to create a network of pathological nodes. These co-alteration patterns have a topological definite architecture, which includes some areas (i.e., insular and anterior cingulate cortices) that are considered to be essential brain functional hubs.

Interestingly, on the basis of brain connectivity, the predictive model has been able to account for the 77% and the 72% of the variance in the co-alteration patterns associated with GM decreases and GM increases, respectively. This result supports the hypothesis that the network-like distribution of these two structural co-alteration patterns, along with their temporal development (Cauda et al., 2018a, 2018b), are strictly influenced by brain connectivity constraints. In particular, the predictive model has showed that, on the basis of functional and anatomical connectivity profiles, more time steps are required to wholly describe and predict the progression of GM co-alterations. However, the predictive model based on genetic connectivity has been able to describe and predict the progression much more early, that is, just within the first stages of the neuropathological co-alteration process.

This finding allows to appraise the plausibility of three (i.e., transneuronal spread, nodal stress, and shared vulnerability) among the four mechanisms so far hypothesized for explaining the spread of brain alterations (Saxena and Caroni, 2011; Zhou et al., 2012; Fornito et al., 2015), since each of them should lead to a specific progression (see the "Background" section for an in-depth discussion of this point).

With regard to both GM decreases and GM increases, the functional connectivity profile seems to be the best predictor of the co-alteration patterns. Yet, it should be observed that also the other two types of connectivity profiles are important factors in the distribution of GM co-alterations; their contribution, nonetheless, is characterized by different timings. This finding is in line with the fact that analyses were carried out on a cross-diagnostic data set (Goodkind et al., 2015), which included a variety of brain disorders. And as shown by Cope et al. (2018), specific mechanisms can be more or less involved in brain disorders.

2.4.1. The distribution of gray matter alterations

Results, especially those about GM decreases, show that a core set of brain regions often appears to be altered in a wide range of neuropathological conditions – discussions of the advantages of the transdiagnostic approach applied in the present study are provided by Buckholtz and Meyer-Lindenberg (2012), and McTeague et al. (2016). This finding gives a further confirmation of what found by other meta-analyses, which nonetheless were limited to three (Cauda et al., 2017) and six psychiatric conditions (Goodkind et al., 2015). Of note, this typical pattern largely includes brain regions that have been proposed to be part of the cognitive control network (Cauda et al., 2012b, 2017: McTeague et al., 2016). It should be observed, however, that the finding of a common alteration pattern in a number of brain disorders does exclude that each disorder may exhibit its own typical distribution of GM alterations (Crossley et al., 2015).

Several studies (Braak and Braak, 1991; Braak et al., 2011; Brooks, 1991; Cauda et al., 2014; Fornito et al., 2015; Iturria-Medina and Evans, 2015; Iturria-

Medina et al., 2014; Pearson et al., 1985; Raj et al., 2012; Ravits, 2014; Saper et al., 1987; Weintraub and Mesulam, 1996) have suggested that the distribution of GM pathological alterations is not random but associated with typical network-like patterns. These suggestions have already been supported (Seeley et al., 2006; Seeley et al., 2009; Zhou et al., 2012) and now this investigation provides for them further evidence: GM alterations are distributed in patterns forming a "neurodegenerative networking" (Yates, 2012) or, as it has been called, a "morphometric co-alteration network" (Cauda et al., 2018a). This last expression seems to be preferable, as it has the advantage to refer to all types of disorders causing GM alterations (both increases and decreases), with no commitment to just neurodegenerative factors.

GM decreased regions are mostly parts of the cognitive control network (Goodkind et al., 2015; McTeague et al., 2016) and include the insulae, anterior cingulate cortices, superior and middle temporal gyri, superior, middle and inferior frontal, pre- and postcentral gyri. Instead, GM increased regions include the right anterior and posterior insula, left middle insula, right pre- and postcentral gyri, right superior frontal gyrus, right superior temporal gyrus, left inferior temporal and inferior frontal gyri. The minor contribution of the precuneus in the co-alterations patterns could be considered as counterintuitive, as this region, being a fundamental hub of the default mode network, is extremely connected. Most likely, given the transdiagnostic approach of this study and though in some brain disorders the precuneus is undoubtedly altered, the frequency of this alteration is not sufficient for reaching statistical relevance. Furthermore, it should be observed that the fact that many alterations affect a certain brain regions does not necessarily entail for this area to be always co-altered with other ones. With regard to this point a study by Manuello et al. (2018) has showed that in the co-alteration patterns of Alzheimer's disease the precuneus contributes only for a significant node. So, even in the case of AD, the precuneus' degree of alteration seems to be less substantial than previously thought.

If we compare the structural co-alteration networks of GM decreases and GM increases, we see that they differ significantly. With regard to GM decreases, insular, cingulate and prefrontal cortices (areas of the cognitive control/salience network), appear to be more involved (Seeley et al., 2007; Cauda et al., 2011, 2012a, 2013); in contrast, with regard to GM increases, alterations appear to be more uniformly distributed, though with a little prevalence in subcortical areas (Figure 5, top panel). This differentiation is probably due to the different factors underlying the development of GM increases and GM decreases. As a matter of fact, GM decreases are commonly related to neurodegenerative processes, while GM increases are commonly related to compensatory mechanisms (Lin et al., 2013; Premi et al., 2014, 2016), which are thought to occur at the initial stages of brain degeneration. This interpretation is in line with the results of the progression analysis, according to which patterns of GM increased values exhibit a faster temporal development than patterns of GM decreased values (Figure 9, bottom panel). It is also worth noting that decreases are equidistributed between neurodevelopmental and degenerative diseases (if one considers schizophrenia a neurodevelopmental deficit), while increases are more frequently reported in studies about neurodevelopmental deficits. Compensatory processes might therefore be considered as more likely to occur during the reorganization that the brain undergoes in neurodevelopmental conditions. In these conditions the ability of recruiting new cognitive strategies may produce different functional patterns (Berlingeri et al., 2010). And in order to face tasks demands the recruitment would be “atypical” (for instance, the recruitment of the homologue areas of the undamaged contralateral hemisphere).

On the basis of the topological analysis, when altered, brain regions exhibiting a higher node degree and/or less average shortest path length are likely to play a pivotal role in the development of GM alterations’ patterns. Their large number of connections and intense activity might favor the mechanisms hypothesized to be at the root of alterations’ development, in particular the nodal stress and the transneuronal spread mechanisms. As it is shown by the predictive

model, these two mechanisms are thought to contribute more in the development of the GM structural co-alterations, which appear to be more influenced by both functional and anatomical connectivity profiles. Nonetheless, as the hypothesized causal mechanisms are not mutually exclusive, they all are probably involved in the formation of GM structural co-alterations, albeit each with its own characteristic temporal pace.

2.4.2. The relationship between the distribution of GM alterations and brain connectivity

All the three profiles of connectivity considered in this meta-analysis (functional, anatomical, and genetic) explain a significant part of the variance of the distribution of GM co-alterations. Specifically, functional connectivity can account for a greater part of the GM co-alteration patterns than the other connectivity profiles (followed by anatomic and genetic connectivity, respectively). A similar result has also been found by calculating the partial correlation between the GM co-alteration matrix and each connectivity matrix, with the removal of the contribution of the other connectivity matrices. This procedure was needed because, as we have already said, both functional and anatomical connectivity patterns are known to be partially correlated (Honey et al., 2009; Misic et al., 2016; Skudlarski et al., 2008; van den Heuvel et al., 2009), and because both these types of connectivity have been related to the patterns of genetic co-expression (Cioli et al., 2014; French and Pavlidis, 2011; French et al., 2011; Goel et al., 2014; Lichtman and Sanes, 2008; Richiardi et al., 2015; Wolf et al., 2011).

The progression of the alterations' diffusion described by the predictive model, based on functional and anatomical connectivity profiles, requires many steps (between 30 and 40 arbitrary units) before reaching completion. In contrast, the prediction based on genetic connectivity needs a shorter time: between 10 and 20 units. This is an interesting finding that is in line with the shared vulnerability hypothesis, according to which the GM alterations' diffusion

caused by the disruption of the co-expression of specific genes is thought to require a shorter accretion time than when other diffusion mechanisms are involved. In other words, it is likely that at the early stages of brain disorders, several regions with similar genetic patterns can be affected by pathology. Furthermore, since the genetic risk is pleiotropic, it can involve wide and transdiagnostic symptomatically-related domains (Buckholtz and Meyer-Lindenberg, 2012; Gejman et al., 2011), thus causing disruption in brain connectivity patterns of networks related to important cognitive functions (Cauda et al., 2012b).

The results of the predictive model may be indicative that a chain of pathological factors is probably involved in a wide range of brain disorders in which types of connectivity play different roles. In fact, dysfunctional genetic co-expressions might produce a neuronal shared vulnerability, which, in turn, might cause the alteration of brain networks, with the subsequent development of abnormal functional and anatomical connectivity patterns. As suggested by Buckholtz and Meyer-Lindenberg (2012), "genetic factors shape connectivity in networks linked to symptom domains, and imply that connectivity changes observed in mental disorders reflect a cause, rather than a consequence, of being ill". The same authors remark that "the latent structure of psychopathology may reflect, in part, a genetically determined latent structure of brain connectivity".

The finding that functional and anatomical connectivity profiles seem to explain better the distribution patterns of GM co-alterations in a longer run than the genetic connectivity profile is in accordance with the consideration that both nodal stress and transneuronal spread mechanisms require time to exert their effects. The nodal stress causes a progressive intensification of excitotoxicity factors, while the transneuronal spread entails the transport of pathological elements via axons or the extracellular liquid.

The results suggest that the three mechanisms of alterations' diffusion considered in the present study (transneuronal spread, nodal stress and shared vulnerability) might play a synergistic role in the etiology of neurodegenerative

disorders and of psychiatric and neurodevelopmental conditions. Even though psychiatric and neurodevelopmental conditions are not directly associated with a specific proteinopathy, their structural and functional alterations tend to develop morphometric co-atrophy patterns that seem to be shaped by connectivity constraints (Cauda et al., 2018a). It has also been suggested that schizophrenia might be more appropriately conceived as a failure of communication between critical nodes of large brain networks rather than a dysfunction of isolated regions (Kaspárek et al., 2010; Northoff and Duncan, 2016).

In brain disorders different factors (such as misfolded proteins, molecular nexopathies, and genetic/environmental interactions) might be at play. Overall, all these pathological factors can "stress" cerebral circuits and "shape" the distribution of GM alterations in network-like patterns. As suggested for neurodegenerative proteinopathies (Warren et al., 2013), in other diseases (like psychiatric conditions) the complex interplay between neurodevelopmental abnormalities and environmental/genetic factors might trigger brain deterioration (both functional and structural), even if a proteinopathy is not clearly detected, but with a similar impact on brain functioning.

Given that the transneuronal mechanism (Zhou et al., 2012; Fornito et al., 2015) implies a sort of spread along anatomical (axonal) routes, that the nodal stress mechanism implies a sort of intense functional activity between altered regions, and that the shared vulnerability mechanism implies shared gene expressions between brain areas, it is possible to hypothesize that, on the grounds of the results of this study, the distribution patterns of the GM decreases and increases might be more influenced, in sequence, by nodal stress, transneuronal spread, and shared vulnerability mechanisms. As we have already said, these mechanisms are not supposed to be mutually exclusive; in other words, the presence of one mechanism does not rule out the presence of the others. In different degrees, therefore, all of them might play a role in neuropathological processes according to the constraints of brain connectivity.

2.4.3. Brain connectivity can account for the distribution patterns of gray matter alterations

The three matrices related to the types of brain connectivity can account well for the distribution patterns of structural co-alterations. This finding is important in order to better understand how the pathological brain responds to neuropathology, as it allows to link the progression of GM alterations to a neurobiological substrate. What is more, the results of this study confirms that brain connectivity can influence the development of neuropathological processes (Iturria-Medina and Evans, 2015). Some suggestions about this view have already been explored. For example, in patients suffering from Alzheimer's disease functional disruption and GM decreases in different brain districts reflect covariance patterns of the default mode network, which may indicate that these atrophic areas are not altered independently. On the contrary, the main alteration in one of these areas might bring about a secondary alteration in other connected areas (Wang et al., 2013; Wang et al., 2015). The cognitive deterioration would therefore develop through sequential increases in connectivity, thus causing a functional overload. Increased connectivity in frontal areas (in particular those related to the salience network) are supposed to have a compensatory role. This complex pattern of functional disruption appears to mostly mirror the pattern that can be recognized in frontotemporal dementia, which involves largely frontal areas and the salience network (Zhou et al., 2010).

Two important clarifications need to be addressed. First, even though brain connectivity appears to influence the development of GM co-alterations, this does not mean that every type of neuropathology is expected to exhibit similar structural co-alterations. In fact, with regard to each brain disease and to the patients involved, different network nodes can be affected. Furthermore, even if the final set of altered nodes results to be similar, the foci from which GM alterations started to propagate might have been different and, consequently, different progressions might have occurred.

The second clarification regards the relationship between the co-alteration network analysis carried out in this study and the anatomical covariance investigations (Mechelli et al., 2005). Anatomical covariances are described as "the covariance of morphological metrics derived from morphological MRI" (Evans, 2013). Apparently, the morphological neuropathological co-alterations investigated here may be conceived as a type of anatomical covariance. Yet, anatomical covariance is always obtained from single-subject data, while the meta-analytic data used here originated from a statistical comparison between pathological and healthy individuals. Thus, from the methodological perspective, the two approaches, though similar, are different and should not be equated with each other (Cauda et al., 2018a).

2.4.4. Limitations and future directions

The distribution patterns of morphometric neuropathological alterations have been investigated by analyzing meta-analytic data, which, compared to their original quality, are known to be characterized in part by deterioration. This loss of quality can increase the spatial uncertainty and influence the identification of alterations by decreasing the probability of statistical co-occurrences between nodes. Future studies may use native data, ideally derived from the same group of individuals.

Although VBM analyses are extensively used and based on a well validated technique, there are methodological features that could influence the results of VBM experiments (e.g., field strength of the scanner, software used for analysis, smoothing amount). Yet, it is unlikely that these parameters can bias results in a systematic way, as different combinations of them occurred in the experiments considered in this meta-analysis. Furthermore, it has been proposed that possible false positives in VBM tend to be randomly distributed throughout the brain rather than accumulate in certain points, and this should avoid the inclusion of spurious nodes of alteration in the co-alteration network. Nonetheless, the possibility of some inclusion cannot be ruled out with certainty.

To solve the problem of heterogeneity due to experiments with a low sample size, a lower bound of 8 subjects for sample size was set, so that all the experiments with a sample size smaller than 8 subjects were removed from analyses. As already said, this lower bound is in accordance with Scarpazza et al. (2015), which have found that using a balanced small samples in the VBM studies of just 8 subjects does not influence the false positive rate. Furthermore, as the methodology used here identifies the co-occurrences between alterations across studies, experiments of small samples showing different results from others are supposed to cause a sort of "noise" that likely increases the false negative rather than the false positive rate. So, although the potential bias due to studies with a limited sample size cannot be completely excluded, it is more likely that real co-alterations were missed rather than false ones were detected. Yet, future research on larger and more controlled samples are needed as soon as they will be available.

The ALE technique is one of the most used methods in the field of coordinate based meta-analysis. One of the limitations of this approach is that results can be driven by one, or a few, experiments, thus representing a specific case rather that an overall effect. Nonetheless, the ALE technique has been tested for its reliability and power specifically for what concerns sample size and number of experiments. In fact, a number of 20 experiments is usually thought to be the minimum sufficient amount to solve this bias. Therefore, analyses based on bigger data sets, as the one carried out here, should avoid the problem. However, other factors that could bias the results, such as the uncontrolled selection of a variety of different tasks or experimental conditions, had never been tested.

Also the genetic matrix can present idiosyncrasies. First, the sample used in this study is made of just six human brains. Therefore, results can hardly be generalized to the whole population. Second, some of the six brains were not completely sampled. Third, samples had different stereotactic coordinates and were not evenly spaced. Although these issues were addressed methodologically,

results of the genetic analysis should be interpreted with caution and need the support of further evidence. Nonetheless, at present the complex procedure and the high costs for obtaining gene expressions data do not allow a more accurate analysis.

Spatial and temporal errors related to fMRI and DTI procedures may affect both functional and anatomical connectivity patterns. However, such errors should increase more the amount of false negatives than the amount of false positives, thus diminishing the correlation values between matrices. Instead, given the good significance of the statistical models, results are likely to describe real phenomena than spurious factors. In support of the findings of this study the reliability values of the connectivity matrices are very good. This suggests that the possible errors related to the neuroimaging procedures are not likely to bias the conclusions of this study. Yet, future investigations using different statistical techniques are needed to be carried out on wider and better samples.

With regard to possible confounding variables, such as the heterogeneity of ICD-10 categories, it should be observed that images' categorization for meta-analytical purposes are performed exclusively on the basis of key words; other variables are not taken into account. The aim of meta-analyses is in fact to provide a general picture of a phenomenon in which the possible influence of confounding variables is moderated by considering them as noise. The effectiveness of this approach is proven by the fact that a software like Neurosynth, which is based on automatic categorizations of certain words that are used in the scientific articles, is able to give meaningful maps with a robust statistics by comparing meta-analytic results in a specific domain with known experimental data. The same principle applies to the transdiagnostic approach of this meta-analysis, in which all the ICD-10 categories converge together.

This meta-analysis focused on transdiagnostic data, coming from a range of brain disorders as well as from heterogeneous patients studied in different stages of their symptomatology. The aim was to study globally how GM alterations are distributed across the brain and, to do so, the widest retrievable sample was

needed to get a good statistical significance. Therefore, the obtained distribution patterns of GM alterations are not precisely associated with one or another brain disorder. Future inquiries can explore more specific patterns of GM co-alterations with regard to specific diseases. It would be particularly interesting to compare the co-alteration patterns detected in this meta-analysis with both those obtained from native single subject data stored in publicly available MRI data sets (e.g., ADNI, UK Biobank) and with those obtained from longitudinal studies. An intriguing line of research concerns the difference of GM alterations' patterns within patients with fast or slow cognitive decline. Finally, a significant scientific advance will be to comprehend how exactly each connectivity profile (functional, anatomical, and genetic) contributes in influencing the development of structural co-alterations associated with different brain disorders.

2.5. Conclusion

This meta-analytical study has successfully addressed the four issues raised in the introduction. It has highlighted that 1) GM co-alterations across the pathological brain are not randomly distributed but present recognizable network-like patterns. It has also investigated the relationship between these distribution patterns of morphometric neuropathological alterations and brain connectivity, providing evidence that 2) the development of GM co-alterations is influenced by the constraints of brain connectivity. Specifically, the focus of the study has been on whether or not three types of connectivity profiles may shape and account for the development of structural GM co-alterations. The prediction model based on these connectivity profiles has showed that 3) all the three types of connectivity are involved and can statistically explain a good portion of the pattern variance of structural GM co-alterations (72% for GM increases and 77% for GM decreases, respectively). However, 4) the roles played by three types of brain connectivity require different timings in predicting the development of the GM co-alteration networks.

These findings provide valuable insights into the mechanisms underlying neuropathological processes. In particular, analyses carried out in this study show that three (i.e., nodal stress, shared vulnerability, and transneuronal spread) of the four hypotheses suggested so far for the diffusion of GM alterations (Saxena and Caroni, 2011; Zhou et al., 2012; Fornito et al., 2015) are likely to have a role with different timings in the formation and development of structural co-alteration patterns. Functional connectivity seems to give the better account of the distribution patterns of structural co-alterations, followed by anatomic and, finally, by genetic connectivity. However, even though one connectivity profile can be predominant, it is worth noting the all these three types are significantly involved in the progression of GM alterations, which is to be expected, given the cross-diagnostic nature of the data used in this study.

In sum, the three brain connectivity profiles appear to be strictly entwined with the distribution patterns of morphometric neuropathological alterations. This is an exciting finding that is a further step in the quest for a better understanding of the pathological brain.

3. Study 2

3.1. Introduction

After gathering evidence from study 1 that different types of connectivity patterns can influence the distribution of GM alteration across the brain, study 2 aimed to explore whether or not traces of this influence can be identified in the co-alteration network related to a specific brain area, specifically, the insular cortex. The insula was chosen because of its distinctive characteristics of being both an important brain hub and a preferential target for neuropathological processes.

Among the brain hubs, the insula has vast and extensive connections to many regions of the cortex and limbic system (Cauda et al., 2011, 2013; Cauda and Vercelli, 2013; Chang et al., 2013; Kelly et al., 2012; Stephani et al., 2011; Uddin, 2015; Vercelli et al., 2016). The insular cortex has been associated with a variety of important functions, ranging from pain perception and speech production to social emotions (Cauda et al., 2012b), including the conscious monitoring of the body's condition via the integration of different unconscious stimuli (both external and internal) with emotional processes, as well as the conscious detection of error (Cauda et al., 2011, 2012a; Klein et al., 2013; Nieuwenhuys, 2012; Vercelli et al., 2016; Wylie and Tregellas, 2010). The integration of external sensory stimuli with inputs coming from the limbic system has led to think that the insula may play a fundamental role in the generation and maintenance of a state of awareness related to the body's condition (Cauda et al., 2011; Manuello et al., 2018). These relevant roles put the insula at the interface between the inner and the external worlds, thus making it a pivotal center within the brain functional architecture (Ahmed et al., 2016; Douaud et al., 2014; Fjell et al., 2015; Jagust, 2013; Jones et al., 2016; Klein et al., 2013; Voytek and Knight, 2015).

Furthermore, Cauda et al. (2019) have highlighted that the insula is among the areas most frequently affected by brain disorders. This suggests that the insular cortex may have as yet an unknown role in the development of alterations caused by brain disorders. In light of this, study 2 aimed to investigate: 1) what pattern of neuronal alterations' distribution is associated with different portions of the insula; 2) whether or not this pattern correlates with the insula meta-analytic functional connectivity; and 3) the behavioral profile associated with the areas of the insular co-alteration networks.

To do so, the VBM experiments stored in the BrainMap database were retrieved. As VBM can be applied transdiagnostically (Cauda et al., 2019; McTeague et al., 2016), data about all brain disorders that were present in the BrainMap VBM repository were used, with the aim to achieve the most overarching analysis of how pathological processes affect the insular cortex.

3.2. Materials and methods

3.2.1. The parcellation of the insular cortex

It is well known that the insular cortex exhibits a marked heterogeneity both in functional and cytoarchitectonical aspects (Cauda et al., 2011, 2012a). For this reason, this brain area can be better described by adopting some kind of parcellation. However, no consensus has been reached on the number of parcels to be used (Cauda and Vercelli, 2013). As it is based on multimodal convergence criterion and non-hierarchical clustering, the solution proposed by Kelly et al. (2012) was chosen for the parcellation of the insula. Among the various dimensionality options (i.e., from 2 to 15 clusters), those showing the best cross-model agreement for both the hemispheres were selected (i.e., 2, 3 and 9 clusters), as highlighted by Cauda and Vercelli (2013). Since a number of clusters over 3 was not sufficient to guarantee reliable amount of data for statistical results, the bipartite (K2) and tripartite (K3) solutions were preferred.

The related regions of interest (ROIs) were downloaded from http://fcon_1000.projects.nitrc.org.

3.2.2. Selection of studies

An extensive meta-analytic search was conducted using the software Sleuth to query the VBM database of BrainMap (Fox, Laird, et al., 2005; Fox and Lancaster, 2002; Laird et al., 2005b). At the moment of the search (February 2018), the BrainMap VBM database contained 994 articles, for a total of 3151 experiments, 75727 subjects, and 21827 locations.

In order to assess the impact of brain disorders on the insular cortex, a first search was performed with the following query:

[Experiments Contrast is Gray Matter] AND [Experiment Context is Disease Effects] AND [Observed Changes is Controls > Patients] AND [Locations TD Label is Gyrus Insula].

The study focused on decreased values only as these effects were reported by all VBM studies retrieved in the search. This allowed to achieve a better statistical significance. Furthermore, from a theoretical point of view, there is general agreement in the neuroscientific literature that decreased values can be seen as density reduction or atrophy of GM.

In order to describe the co-alteration of the insula subsections (i.e., K2 and K3), an additional search was performed using the following criteria:

[Experiments Contrast is Gray Matter] AND [Experiment Context is Disease Effects] AND [Observed Changes is Controls > Patients] AND [Locations MNI image is *]

where the MNI images represent each of the parcels selected from the work of Kelly et al. (2012). In order to improve the statistical power and the reliability

of analyses, as well as to avoid performing ALE on small sets of experiments, the left and right homologous clusters were merged in a same ROI. Hence, the query was repeated twice to retrieve the data related to the K=2 segmentation and 3 times for what concerns the K=3 segmentation.

3.2.3. Anatomical likelihood estimation and comparison between functional connectivity and alteration patterns

The VBM data retrieved were statistically elaborated with the method of the ALE (Eickhoff et al., 2012; Eickhoff et al., 2009; Turkeltaub et al., 2012), so as to obtain modelled anatomical effect maps representing the overall distribution of gray matter co-alterations within the target seed area (Insulae).

ALE maps showed the brain areas in which multiple studies reported statistically significant alteration peaks (i.e., foci of interest). The ALE map derived from the analysis of the whole insula was thresholded at a voxel-level (FWE $p < 0.05$) (Eickhoff et al., 2016, 2017), while the remaining maps were thresholded at a cluster-level (FWE $p < 0.01$). Since locations with morphologic alterations (and not functional activations) were analyzed, ALE maps revealed the brain regions that were likely to be altered together (Cauda et al., 2018a; Manuello et al., 2018; Tatu et al., 2018).

Finally, a meta-analytic connectivity modeling (MACM) was performed on data derived from the BrainMap functional repository, so as to construct the meta-analytic functional connectivity pattern of each of the five bilateral parcels of the insula (Robinson et al., 2010). According to MACM, brain areas exhibiting common activation patterns are considered to be connected. Then the co-alteration patterns and the functional connectivity patterns were compared to inspect their similarity. To do so, Pearson's r was used to calculate the degree of correlation between ALE values of both the insula MACM maps and the co-alteration patterns.

3.2.4. Behavioral profile analysis

To associate specific psychological functions with the areas forming the co-alteration networks related to the five bilateral parcels, an analysis of behavioral profile was carried out using the behavioral analysis plug-in for the software Mango (Lancaster et al., 2012). This tool is based on the BrainMap functional database and provides a quantitative association between a user defined ROI (i.e., each on the ALE maps) and 51 behavioral sub-domains, organized in 5 classes: action, cognition, emotion, interoception, and perception. In accordance with Lancaster et al. (2012), only sub-domains with a z-score ≥ 3 were maintained. An average value was obtained for each of the 5 classes by computing the mean of the related sub-domains with above threshold z-score.

3.2.5. Construction of the morphometric co-alteration networks

The anatomical co-alteration networks of the bilateral insulae were constructed in order to describe in detail the statistical relationship between the insula and the co-altered regions. This type of analysis (Cauda et al., 2018; Manuello et al., 2018) can determine whether or not the alteration of a specific area (in this case, the insula) is statistically related to the alteration of other brain areas. In the produced output the nodes represent altered regions, while edges link couples of nodes which are more likely to be altered together than one independently from the other. This particular dependency was computed using the Patel's k index (Patel et al., 2006).

From this complete network one sub-network was extracted for each of the selected unilateral parcels. This was achieved with a three-steps procedure. First, the nodes anatomically located inside the given parcel of interest were identified and considered as roots. Second, only the first neighbors of the root nodes (i.e., nodes directly linked with at least one node located in the parcel) were preserved. Third, all the edges between non-roots nodes were eliminated. For each of the obtained sub-networks, the total number of nodes and edges was calculated. In order to describe the spatial pattern of co-alterations of each parcel at macro-

level, the location of the non-root nodes were divided in 7 groups: frontal lobe, parietal lobe, temporal lobe, occipital lobe, midbrain, subcortical areas, and insula. Of note, non-root nodes located in the insulae were counted separately from the other lobes, in order to highlight the co-alteration between them. The repartition of the nodes was based on the Talairach Client tool (Lancaster et al., 2000). To estimate the strength of co-alteration of each cluster with every lobe, the values of the edges connecting a given cluster with a given node were summed, and then divided for the sum of all the edges of the cluster. This measure was expressed as the percentage of the strength of the co-alteration of each lobe with a given cluster.

3.3. Results

3.3.1. Results from the queries

The first search retrieved a total of 207 papers, 277 experiments, 4213 foci, for a total of 14916 subjects (see Figure 10 and Table 10). Experiments were distributed as follows: schizophrenia (46), multiple sclerosis (24), Alzheimer's disease (19), epilepsy (14), depression (12), Huntington's disease (9), frontotemporal lobe degeneration (8), multiple system atrophy (7), post-traumatic stress disorder (7), migraine (7), psychosis (7), bipolar disorder (7), frontotemporal dementia (6), supranuclear palsy (6), mild cognitive impairment (6), Parkinson's disease (4), obsessive-compulsive disorder (3), Lewy body dementia (3), autism spectrum disorder (3), olfactory disorders (3), alcohol (3), spinocerebellar ataxia (2), panic/anxiety disorder (2), narcolepsy (2), corticobasal degeneration system (2), at-risk mental state (2), and amyotrophic lateral sclerosis (2). Other papers (61) were classified as "Others" if they investigated more than one brain disorder or if the study was the only one retrieved in the data set on a certain neuropathology (Fig. 11).

Figure 10. PRISMA flow diagram illustrating the selection of experiments.

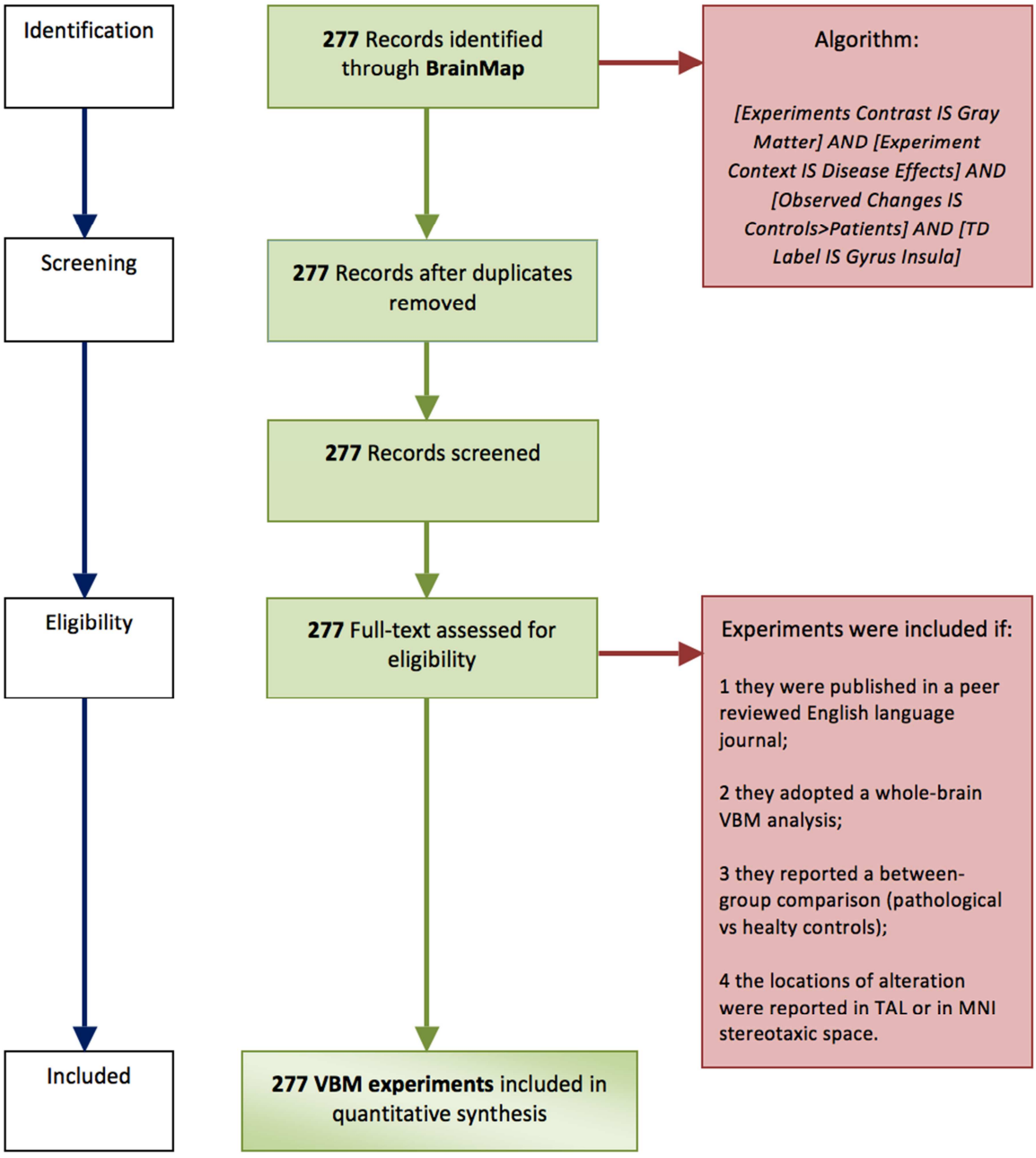

Table 10. List of studies selected from the first query.

	1st Author	Year	Journal	Medline	Number of experiments
1	Adleman N E	2012	Journal of Child Psychology and Psychiatry	22650379	1
2	Agosta F	2010	European Journal of Neuroscience	20597976	2
3	Agosta F	2011	Radiology	21177393	1
4	Alcauter S	2011	NeuroImage	21147232	1
5	Antonova E	2005	Biological Psychiatry	16039619	1
6	Arnone D	2009	European Neuropsychopharmacology	-	1
7	Asami T	2009	Psychiatry Research	19560907	1
8	Ash S	2011	Brain and Language	21689852	1
9	Ash S	2009	Journal of Neurolinguistics	22180700	2
10	Aubert-Broche B	2011	NeuroImage	21414412	1
11	Audoin B	2007	Multiple Sclerosis	17463071	1
12	Barbeau E	2008	Neuropsychologia	18191160	1
13	Baron J C	2001	NeuroImage	11467904	4
14	Bassitt D P	2007	European Archives of Psychiatry and Clinical Neuroscience	16960651	1
15	Baxter L C	2006	Journal of Alzheimer's Disease	16914835	1
16	Bell-McGinty S	2005	Archives of Neurology	16157746	2
17	Bendfeldt K	2009	NeuroImage	19013533	1
18	Bernasconi N	2004	NeuroImage	15488421	1
19	Bertsch K	2013	European Archives of Psychiatry and Clinical Neuroscience	23381548	2
20	Bitter T	2010	Brain Research	20553879	2
21	Bitter T	2011	Neuroscience	21241781	1
22	Boccardi M	2005	Neurobiology of Aging	15585344	1
23	Boddaert N	2004	NeuroImage	15325384	1
24	Bodini B	2009	Human Brain Mapping	19172648	1
25	Boghi A	2011	Psychiatry Research	21546219	1
26	Bonavita S	2011	Multiple Sclerosis	21239414	1
27	Bonilha L	2004	Archives of Neurology	15364683	1
28	Borgwardt S J	2007	Biological Psychiatry	17098213	1

29	Borgwardt S J	2007	British Journal of Psychiatry	18055941	1
30	Borgwardt S J	2010	Biological Psychiatry	20006324	1
31	Borroni B	2008	Archives of Neurology	18541800	1
32	Boxer A L	2006	Archives of Neurology	16401739	1
33	Bozzali M	2006	Neurology	16894107	3
34	Brambati S M	2004	Neurology	15326259	1
35	Brambati S M	2009	Neurobiology of Aging	17604879	3
36	Brenneis C	2004	Journal of Neurology, Neurosurgery, and Psychiatry	14742598	1
37	Brenneis C	2007	Journal of Neurology	17334661	1
38	Brenneis C	2003	Movement Disorders	14534916	1
39	Brenneis C	2006	Movement Disorders	16161039	2
40	Brenneis C	2003	NeuroReport	14534423	1
41	Brenneis C	2004	NeuroReport	15257132	2
42	Brys M	2009	Journal of Alzheimer's Disease	19221425	1
43	Burton E J	2002	NeuroImage	12377138	1
44	Burton E J	2004	Brain	14749292	2
45	Cascella N	2010	Schizophrenia Research	20452187	2
46	de Castro-Manglano P	2011	Bipolar Disorders	21316203	2
47	Ceccarelli A	2009	Human Brain Mapping	19172642	1
48	Chang C C	2009	European Journal of Neurology	19486137	2
49	Chanraud S	2007	Neuropsychopharmacology	17047671	1
50	Chen S	2006	Psychiatry Research	16371250	2
51	Chen S	2009	BMC Psychiatry	19538748	1
52	Chua S E	2007	Schizophrenia Research	17098398	1
53	Cordato N J	2005	Brain	15843423	1
54	Critchley H D	2003	NeuroImage	12725766	1
55	de Araujo-Filho G M	2009	Epilepsy & Behavior	19303459	1
56	de Oliveira-Souza R	2008	NeuroImage	18289882	1
57	Di Paola M	2007	Journal of Neurology	17404777	1
58	Douaud G	2007	Journal of Neurology	17698497	1
59	Farrow T F D	2005	Biological Psychiatry	15993858	2

60	Feldmann A	2008	Psychiatry Research	18945600	1
61	Frisoni G B	2002	Journal of Neurology, Neurosurgery, and Psychiatry	12438466	1
62	Fusar-Poli P	2011	Journal of Psychiatric Research	20580022	1
63	Gale S D	2005	Journal of Neurology, Neurosurgery, and Psychiatry	15965207	2
64	Garcia-Marti G	2008	Progress In Neuro-Psychopharmacology & Biological Psychiatry	17716795	1
65	Garrido L	2009	Brain	19887506	1
66	Gavazzi C	2007	Journal of Computer Assisted Tomography	17882035	1
67	Ghosh B C	2012	Brain	22637582	1
68	Giuliani N R	2005	Schizophrenia Research	15721994	1
69	Gobbi C	2014	Academic Radiology	23812284	5
70	Gong Q	2011	NeuroImage	21134472	1
71	Gregory S	2012	Archives of General Psychiatry	22566562	1
72	Grieve S M	2013	NeuroImage	24273717	1
73	Guo X	2010	Neuroscience Letters	19879920	1
74	Ha T H	2010	Neuroscience Letters	19429131	1
75	Ha T H	2004	Psychiatry Research	15664796	1
76	Han X	2017	Neural Regeneration Research	28616036	1
77	Henley S M	2009	Journal of Neurology	19266143	1
78	Herringa R	2012	Psychiatry Research	23021615	1
79	Hoeft F	2008	Archives of General Psychiatry	18762595	1
80	Hoeft F	2007	Proceedings of the National Academy of Sciences	17360506	1
81	Honea R A	2008	Biol Psychiatry	17689500	1
82	Honea R A	2009	Alzheimer's Disease and Related Disorders	19812458	1
83	Horn H	2009	British Journal of Psychiatry	19182174	1
84	Huang W	2011	Journal of Neuroradiology	22200974	1
85	Huey E D	2009	Archives of Neurology	19822784	1
86	Hulshoff Pol H E	2001	Archives of General Psychiatry	11735840	1
87	Hulshoff Pol H E	2004	NeuroImage	14741639	1
88	Ille R	2011	Journal of Psychiatry and Neuroscience	21406159	1
89	Ivo R	2013	European Spine Journal	23392554	1
90	Jang D P	2007	Neuroscience Letters	17951002	1

91	Janssen J	2008	Journal of the American Academy of Child and Adolescent Psychiatry	18827723	1
92	Jayakumar P N	2005	Progress In Neuro-Psychopharmacology & Biological Psychiatry	15866362	1
93	Kasai K	2008	Biol Psychiatry	17825801	1
94	Kasparek T	2010	Human Brain Mapping	19777553	1
95	Kassubek J	2004	Journal of Neurology, Neurosurgery, and Psychiatry	14742591	1
96	Kassubek J	2007	Journal of Neurology, Neurosurgery, and Psychiatry	17332050	1
97	Kaufmann C	2002	Neurology	12084891	1
98	Kawachi T	2006	European Journal of Nuclear Medicine and Molecular Imaging	16550383	1
99	Kawada R	2009	Progress In Neuro-Psychopharmacology & Biological Psychiatry	19625009	1
100	Kawasaki Y	2007	NeuroImage	17045492	1
101	Kawasaki Y	2004	European Archives of Psychiatry and Clinical Neuroscience	15538599	2
102	Kesler S R	2008	The Journal of Pediatrics	18346506	2
103	Kim J H	2008	Cephalalgia	17689105	1
104	Kim S	2011	Journal of Clinical Neuroscience	21570296	1
105	Kim S J	2009	Acta Neurologica Scandinavica	18624787	1
106	Koprivova J	2009	Neuroscience Letters	19666084	1
107	Kosaka H	2010	NeuroImage	20123027	1
108	Koutsouleris N	2008	NeuroImage	18054834	4
109	Kubicki M	2002	NeuroImage	12498745	2
110	Kuchinad A	2007	Journal of Neuroscience	17428976	1
111	Lai C H	2015	Journal of Affective Disorders	-	1
112	Lee J E	2013	Journal of Neurology, Neurosurgery, and Psychiatry	23828835	2
113	Leung K K	2009	Psychological Medicine	18945378	1
114	Libon D J	2009	Neurology	19687454	2
115	Lin C H	2013	Frontiers in Human Neuroscience	23785322	2
116	Lin K	2009	Epilepsy Research	19570650	2
117	Lochhead R A	2004	Biological Psychiatry	15184034	1
118	Lui S	2009	Psychiatry Research	18981063	2
119	Lyoo I K	2004	Biological Psychiatry	15013835	1

120	Maneru C	2003	Journal of Neuroimaging	12593134	1
121	Marcelis M	2003	Psychiatry Research	12694890	2
122	Marti-Bonmati L	2007	Radiology	17641373	1
123	Matsuda H	2002	Journal of Nuclear Medicine	11884488	1
124	McAlonan G M	2008	Journal of Child Psychology and Psychiatry	18673405	2
125	McIntosh A M	2004	Biological Psychiatry	15476683	1
126	Meda S A	2008	Schizophrenia Research	18378428	3
127	Meisenzahl E M	2008	Schizophrenia Research	18378428	4
128	Mesaros S	2008	Archives of Neurology	18272867	1
129	Mezzapesa D M	2007	American Journal of Neuroradiology	17296989	1
130	Milham M P	2005	Biological Psychiatry	15860335	1
131	Minnerop M	2007	NeuroImage	17512219	1
132	Molina V	2011	European Archives of Psychiatry and Clinical Neuroscience	21188405	1
133	Moorhead T W	2005	NeuroImage	16085427	1
134	Morgen K	2006	NeuroImage	16360321	1
135	Muhlau M	2007	Journal of Neural Transmission	17024326	1
136	Muhlau M	2013	Multiple Sclerosis	23462349	1
137	Nardo D	2010	Journal of Psychiatric Research	23113800	2
138	Narita K	2011	Progress In Neuro-Psychopharmacology & Biological Psychiatry	21115089	1
139	Neckelmann G	2006	International Journal of Neuroscience	-	1
140	Nestor P J	2003	Brain	12902311	1
141	O'Daly O	2007	Psychiatry Research	17720459	1
142	Obermann M	2013	NeuroImage	23485849	2
143	Padovani A	2006	Journal of Neurology, Neurosurgery, and Psychiatry	16306152	1
144	Paillere-Martinot M	2001	Schizophrenia Research	11378311	1
145	Peinemann A	2005	Journal of the Neurological Sciences	16185716	3
146	Pell G S	2008	NeuroImage	18042496	1
147	Peng J	2010	European Journal of Radiology	20466498	1
148	Pereira J B	2009	Movement Disorders	19349926	1
149	Pereira J M	2009	Neurology	19433738	5
150	Petrie E C	2014	Journal of Neurotrauma	24102309	1

151	Preziosa P	2016	Human Brain Mapping	26833969	1
152	Price G	2010	NeuroImage	19632338	1
153	Prinster A	2006	NeuroImage	16203159	1
154	Prinster A	2010	Multiple Sclerosis	20028706	1
155	Pujol J	2004	Archives of General Psychiatry	15237084	1
156	Quarantelli M	2006	NeuroImage	16806975	1
157	Rabinovici G D	2007	American Journal of Alzheimer's Disease and Other Dementias	18166607	1
158	Riccitelli G	2012	Multiple Sclerosis	22422807	4
159	Riederer F	2008	Neurology	18678824	1
160	Riederer F	2012	The World Journal of Biological Psychiatry	22746999	1
161	Riva D	2011	American Journal of Neuroradiology	21700792	1
162	Rocca M A	2006	Stroke	16728687	3
163	Rossi R	2006	Journal of Neurology	16502217	1
164	Rossi R	2012	Psychiatry Research NeuroImaging	23146251	2
165	Rowan A	2007	NeuroImage	17462915	1
166	Salmond C H	2007	Cortex	17710821	1
167	Santana M	2010	Epilepsy Research	20223639	3
168	Saykin A J	2006	Neurology	16966547	1
169	Scheuerecker J	2010	Journal of Psychiatry and Neuroscience	20569645	1
170	Schiffer B	2013	Schizophrenia Bullettin	23015687	3
171	Schmidt-Wilcke T	2010	Headache	20236343	1
172	Schmidt-Wilcke T	2008	Cephalalgia	17986275	1
173	Schmidt-Wilcke T	2005	Neurology	16275843	1
174	Schwartz D L	2010	NeuroImage	20096794	1
175	Seeley W W	2008	Archives of Neurology	18268196	3
176	Senda J	2011	Amyotropic Lateral Sclerosis	21271792	1
177	Serra-Blasco M	2013	British Journal of Psychiatry	23620451	2
178	Shad M U	2012	Journal of Child and Adolescent Psychopharmacology	22537357	1
179	Shapleske J	2002	Cerebral Cortex	12427683	2
180	Shiino A	2006	NeuroImage	16904912	1
181	Shin S	2012	Journal of Neurology, Neurosurgery, and Psychiatry	22933812	1

182	Sowell E R	2001	NeuroReport	11234756	1
183	Spanò B	2010	Multiple Sclerosis	20007429	1
184	Stratmann M	2014	PLoS One	25051163	2
185	Sydykova D	2007	Cerebral Cortex	17164468	1
186	Takahashi R	2011	Dementia and Geriatric Cognitive Disorders	22187545	2
187	Tang L R	2014	Psychiatry Research NeuroImaging	25218414	1
188	Tiihonen J	2008	Psychiatry Research	18662866	1
189	Tir M	2009	Movement Disorders	19194988	1
190	Tregellas J R	2007	Schizophrenia Research	17890058	1
191	Tzarouchi L C	2010	Journal of Neuroimaging	19187475	1
192	Wang F	2011	Brain	21666263	1
193	Wei W	2016	Medicine	26962820	1
194	Whitwell J L	2005	Archives of Neurology	16157747	1
195	Whitwell J L	2013	European Journal of Neurology	23078273	1
196	Wolf R C	2008	European Psychiatry	18434103	1
197	Wolf R C	2009	Human Brain Mapping	18172852	1
198	Xie S	2006	Neurology	16801648	1
199	Xu L	2009	Human Brain Mapping	18266214	1
200	Yamada M	2007	NeuroImage	17240165	1
201	Yang F C	2013	Pain	23582154	1
202	Yasuda C L	2010	NeuroImage	19683060	2
203	Yasuda C L	2010	Neurology	20350980	1
204	Yoo S Y	2008	Journal of Korean Medical Science	18303194	1
205	Zamboni G	2008	Neurology	18765649	1
206	Zhang T	2009	Journal of Affective Disorders	19211150	1
207	Zhang X	2016	International Journal of Molecular Sciences	28035997	1

Figure 11. Repartition of the 277 experiments across disorders.

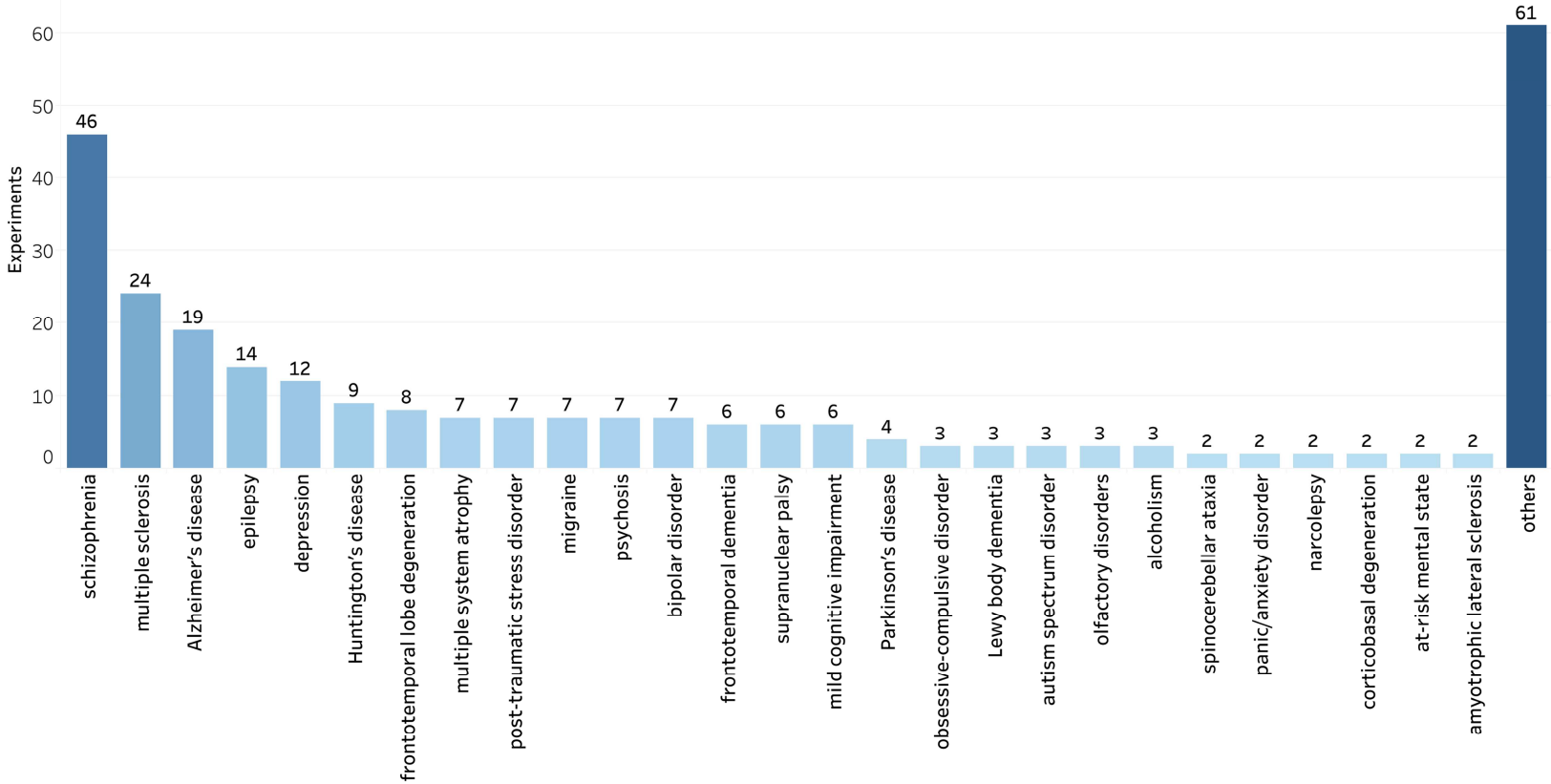

3.3.2. The co-alteration pattern of the insula

K2-anterior

The related search retrieved 122 experiments and 2080 foci. The density of alteration in this parcel was the 207% of the density of the whole brain. Along with the insula, alterations were mainly localized in the superior and inferior frontal gyri, anterior cingulate gyrus, superior temporal gyrus, caudate, thalamus, and claustrum (Fig. 12).

K2-posterior

The related search retrieved 80 experiments and 1330 foci. The density of alteration in this parcel was the 209% of the density of the whole brain. Along with the insula, alterations were mainly localized in the precentral and postcentral gyri, inferior frontal gyrus, anterior cingulate gyrus, left hippocampus, caudate, and thalamus (Fig. 12).

K3-anterior

The related search retrieved 76 experiments and 1433 foci. The density of alteration in this parcel was the 242% of the density of the whole brain. Along with the insula, alterations were mainly localized in the medial frontal gyrus, anterior cingulate gyrus, right central opercular cortex, right precuneus, left hippocampus, claustrum, amygdala, thalamus, and caudate (Fig. 13).

K3-middle

The related search retrieved 87 experiments and 1317 foci. The density of alteration in this parcel was the 178% of the density of the whole brain. Along with the insula, alterations were mainly localized in the left middle and inferior frontal gyri, right hippocampus, right claustrum, left amygdala, thalamus, and caudate (Fig. 13).

K3-posterior

The related search retrieved 40 experiments and 664 foci. The density of alteration in this parcel was the 206% of the density of the whole brain. Along with the insula, alterations were mainly localized in the left inferior frontal gyrus, right middle frontal gyrus, left anterior cingulate cortex, thalamus, and caudate (Fig. 13).

3.3.3. Comparison between co-alteration pattern and functional connectivity of the insula

K2-anterior

The degree of correlation between the co-alteration pattern and the MACM of the insula was r = 0.5611, which suggests a relevant overlap between the two patterns. Brain areas with peaks of high degree of overlap were the right paracentral lobule, right superior, middle, and inferior frontal gyri, left inferior and medial frontal gyri, right anterior cingulate gyrus, right medial dorsal nucleus of the thalamus, and left fusiform gyrus (Fig. 14).

K2-posterior

The degree of correlation between the co-alteration pattern and the MACM of the insula was r = 0.6062, which suggests a relevant overlap between the two patterns. Brain areas with peaks of high degree of overlap were the left precentral and postcentral gyri, left medial and middle frontal gyri, right superior and inferior frontal gyri, right middle cingulate gyrus, right precentral gyrus, left parahippocampal gyrus, and left amygdala (Fig. 14).

K3-anterior

The degree of correlation between the co-alteration pattern and the MACM of the insula was r = 0.5347, which suggests a relevant overlap between the two

patterns. Brain areas with peaks of high degree of overlap were the right superior frontal gyrus, left precentral gyrus, bilateral inferior parietal lobule, bilateral anterior cingulate gyrus, bilateral inferior frontal gyrus, right middle frontal gyrus, bilateral precuneus, bilateral caudate, right medial dorsal nucleus of the thalamus, left putamen, right inferior occipital gyrus, and left fusiform gyrus (Fig. 14).

K3-middle

The degree of correlation between the co-alteration pattern and the MACM of the insula was r = 0.6220, which suggests a relevant overlap between the two patterns. Brain areas with peaks of high degree of overlap were the right anterior cingulate gyrus, bilateral paracingulate gyrus, bilateral precentral gyrus, bilateral parietal and central operculum cortex, bilateral thalamus, right pallidum, left inferior temporal gyrus, bilateral amygdala (Fig. 14).

K3-posterior

The degree of correlation between the co-alteration pattern and the MACM of the insula was r = 0.5577, which suggests a relevant overlap between the two patterns. Brain areas with peaks of high degree of overlap were the bilateral medial frontal gyrus, left inferior frontal gyrus, right precentral and postcentral gyri, left precentral gyrus, bilateral anterior cingulate gyrus, bilateral middle frontal gyrus, bilateral superior temporal gyrus, left inferior temporal gyrus, right caudate, right red nucleus, left thalamus, right culmen, bilateral hippocampus, and left fusiform gyrus (Fig. 14).

Figure 12. The co-alteration networks of the anterior and posterior parcels of the K2 solution.

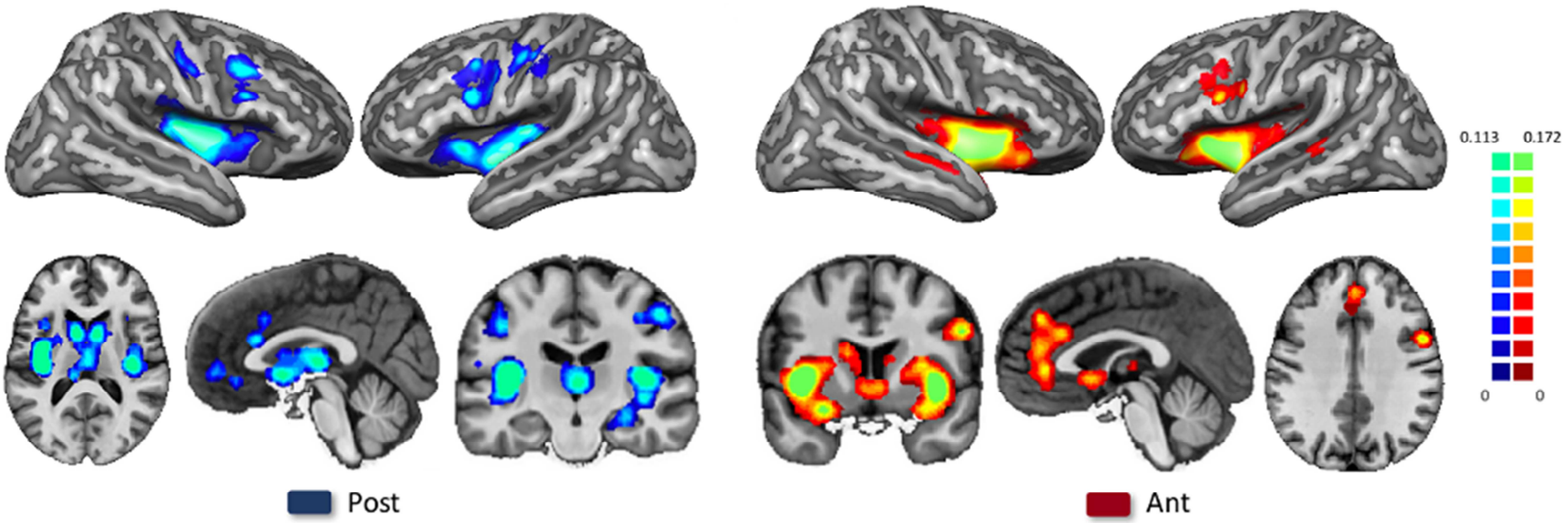

Figure 13. The co-alteration networks of the anterior, middle, and posterior parcels of the K3 solution.

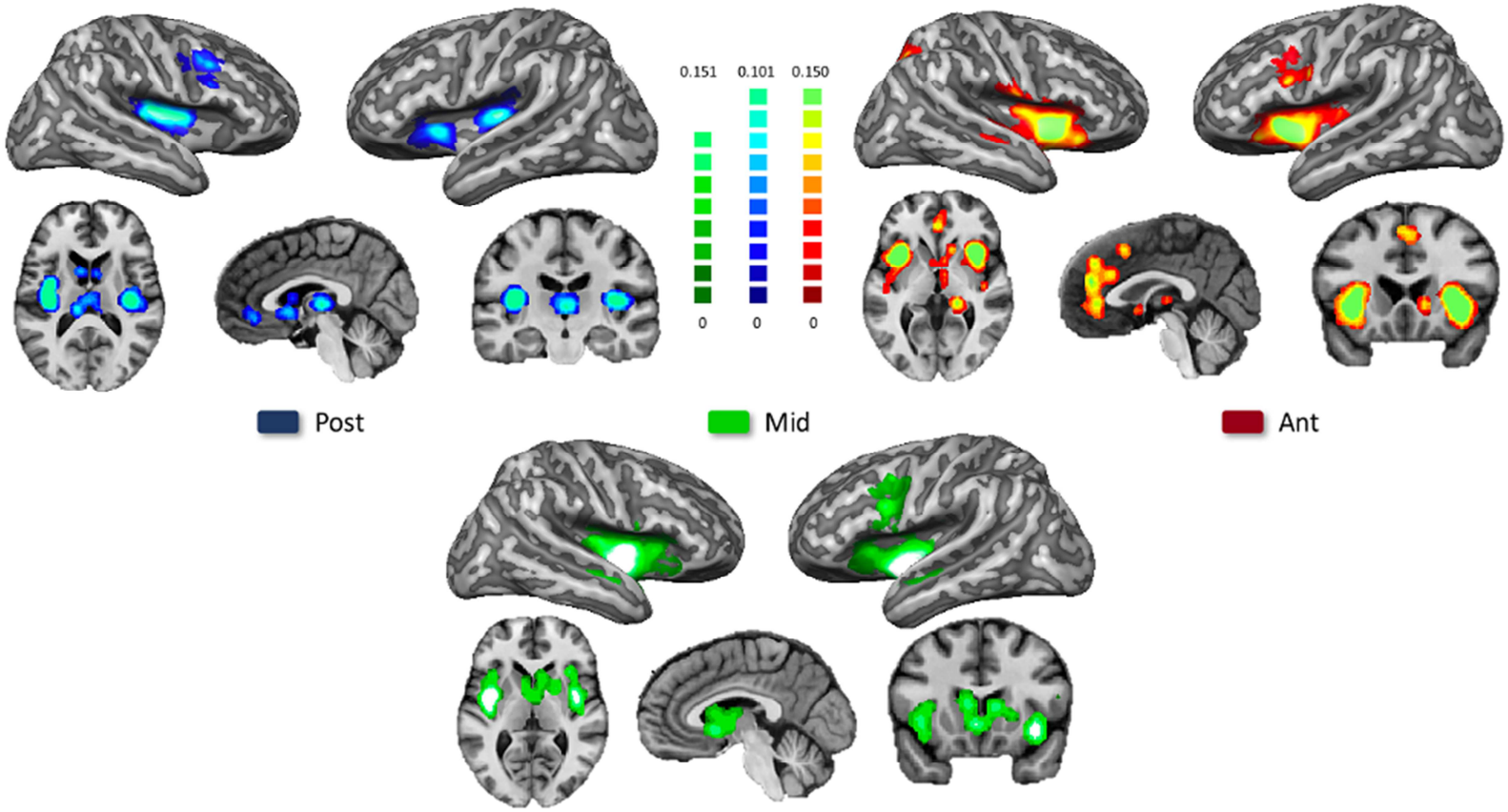

Figure 14. Overlap between the patterns of co-atrophy (red) and of functional MACM (blue).

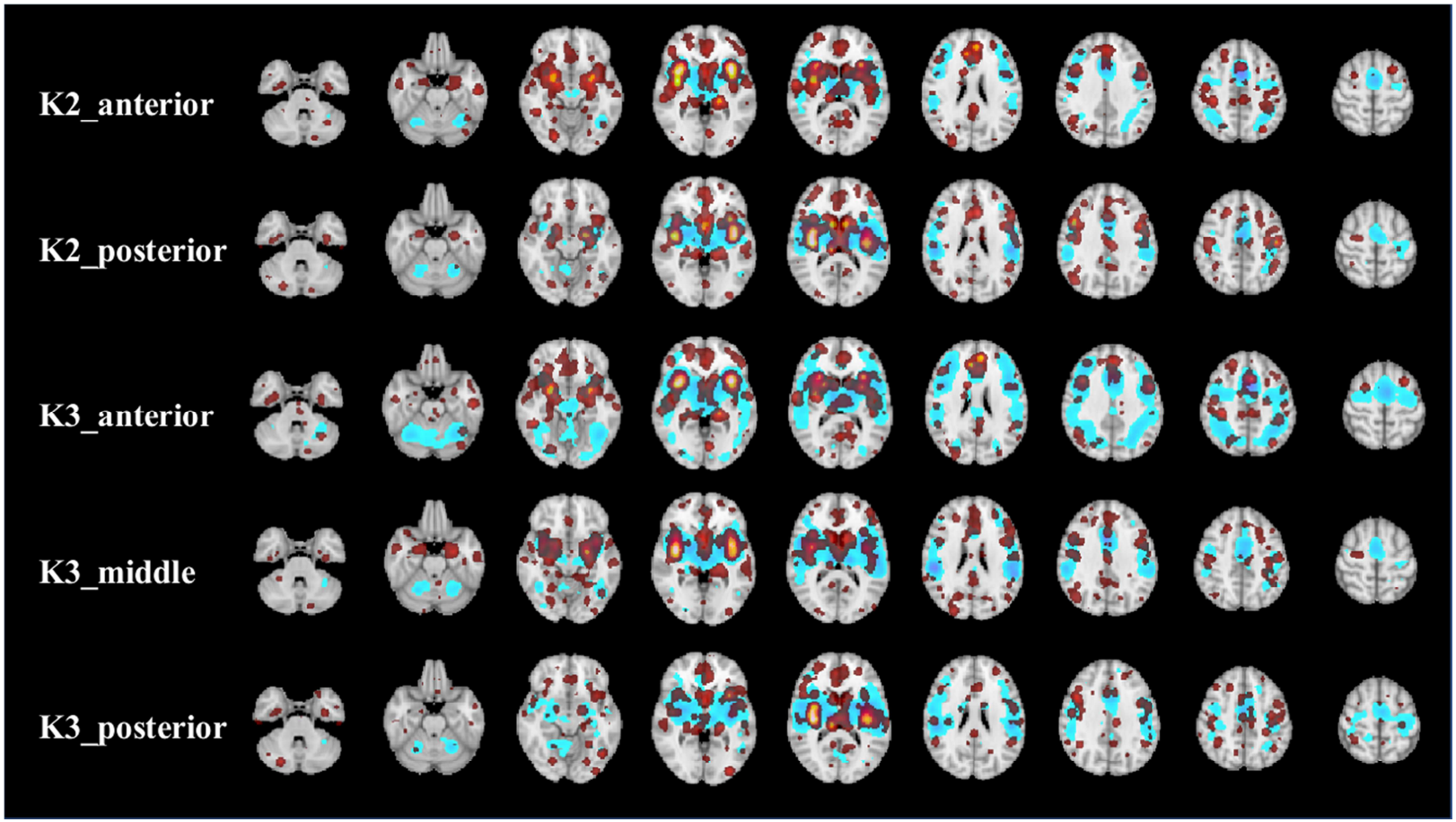

3.3.4. Behavioral profile analysis

K2

The behavioral profile of the co-alteration pattern related to the anterior parcel produced a score of 7.1 for "Emotion", 7 for both "Interoception" and "Perception", 6.6 for "Cognition", and 4.7 for "Action". In turn, the co-alteration pattern related to the posterior parcel scored 8 for "Emotion", 6.9 for "Cognition", 5.9 for "Perception", 4.9 for "Action", and 4.5 for "Interception" (Fig. 15).

K3

The behavioral profile of the co-alteration pattern related to the anterior parcel produced a score of 6.5 for "Cognition", 6.4 for "Emotion", 5.6 for "Action", 5.5 for "Perception", and 5.2 for "Interoception". Scores of the co-alteration pattern related to the middle parcel were 6.2 for "Emotion", 5.9 for "Perception", 5.7 for "Interoception", 5.3 for "Cognition", and 4.2 for "Action". Finally, the behavioral decoding of the co-alteration pattern related to the posterior parcel scored 7.7 for "Emotion", 4.9 for "Perception", 4.7 for "Cognition", 3.8 for "Action", and 3.3 for "Interoception" (Fig. 15).

3.3.5. The co-alteration network of the insula

The complete bilateral network counts 14 nodes in the right insula and 6 in the left insula, for a total of 20 nodes. Of note, none of the nodes was localized in the middle parcel of left insula when using the tripartite subdivision. Therefore, it was not possible to create the K3_mid_L network. Coherently, K2_ant_L and K2_post_L were identical to K3_ant_L and K3_post_L, respectively. When moving from the bipartite partition to the tripartite one, all but one of the nodes that become part of the right middle partition were previously in the posterior one (for the Talairach coordinates of the nodes as well as their membership to Kelly's parcels, see Table 11).

K2-left anterior

The network originating from the 2 root-nodes in the left anterior insula (K2_ant_L) was composed of 449 edges and 268 nodes. The Patel's k was distributed as follows: 31.96% for the 145 edges linking the insula to the frontal lobe, 23.13% for the 93 edges to the temporal lobe, 16.70% for the 98 edges to the parietal lobe, 12.80% for the 53 edges to the occipital lobe, 9.36% for the 35 edges to the subcortical regions, 5.34% for the 19 edges to the insulae, and 0.63% for the 4 edges to the midbrain (Fig. 16).

K2-left posterior

The network originating from the 4 root-nodes in the left posterior insula (K2_post_L) was composed of 871 edges and 259 nodes. The Patel's k was distributed as follows: 43.23% for the 384 edges linking the insula to the frontal lobe, 21.66% for the 192 edges to the temporal lobe, 19.43% for the 195 edges to the parietal lobe, 6.20% for the 28 edges to the occipital lobe, 5.13% for the 45 edges to the insulae, 2.93% for the 19 edges to the subcortical regions, and 0.91% for the 2 edges to the midbrain (Fig. 16).

Of note, both the K2-left anterior and K2-left posterior networks remained unchanged when moving to the 3 parcels solution. This meant that K2_ant_L was identical to K3_ant_L, and that K2_post_L was identical to K3_post_L.

K2-right anterior

The network originating from the 11 root-nodes in the right anterior insula (K2_ant_R) was composed of 2084 edges and 312 nodes. The Patel's k was distributed as follows: 33.71% for the 164 edges linking the insula to the frontal lobe, 21.65% for the 149 edges to the parietal lobe, 18.13% for the 53 edges to the temporal lobe, 12.68% for the 45 edges to the occipital lobe, 8.61% for the 21 edges to the subcortical regions, 1.63% for the 4 edges to the insulae, and 0.65% for the edge to the midbrain (Fig. 16).

K2-right posterior

The network originating from the 3 root-nodes in the right posterior insula (K2_post_R) was composed of 437 edges and 218 nodes. The Patel's k was distributed as follows: 38.98% for the 703 edges linking the insula to the frontal lobe, 33.78% for the 527 edges to the parietal lobe, 11.63% for the 343 edges to the temporal lobe, 9.41% for the 226 edges to the occipital lobe, 5.48% for the 168 edges to the subcortical regions, 0.35% for the 26 edges to the insulae, and 0.11% for the 8 edges to the midbrain (Fig. 16).

K3-right anterior

The network originating from the 6 root-nodes in the right anterior insula (K3_ant_R) was composed of 1041 edges and 235 nodes. The Patel's k was distributed as follows: 36.09% for the 369 edges linking the insula to the frontal lobe, 25.24% for the 304 edges to the parietal lobe, 14.35% for the 141 edges to the temporal lobe, 12.97% for the 123 edges to the occipital lobe, 7.35% for the 75 edges to the subcortical regions, 1.61% for the 12 edges to the insulae, and 0.64% for the 3 edges to the midbrain (Fig. 17).

K3-right middle

The network originating from the 6 root-nodes in the right middle insula (K3_mid_R) was composed of 1184 edges and 312 nodes. The Patel's k was distributed as follows: 31.22% for the 383 edges linking the insula to the frontal lobe, 22.29% for the 222 edges to the temporal lobe, 17.86% for the 262 edges to the parietal lobe, 12.13% for the 148 edges to the occipital lobe, 10.67% for the 107 edges to the subcortical regions, 3.73% for the 41 edges to the insulae, and 0.65% for the 6 edges to the midbrain (Fig. 17).

K3-right posterior

The network originating from the 2 root-nodes in the right posterior insula (K3_post_R) was composed of 296 edges and 177 nodes. The Patel's k was

distributed as follows: 40.28% for the 114 edges linking the insula to the frontal lobe, 34.60% for the 105 edges to the parietal lobe, 11.53% for the 35 edges to the occipital lobe, 10.59% for the 34 edges to the temporal lobe, and 2.68% for the 7 edges to the subcortical regions. No edge linked the insulae or the midbrain (Fig. 17).

Table 11. Talairach coordinates of the nodes and their membership to Kelly's parcels.

Node	***TAL coordinates***			***Kelly's parcels***	
(Name)	***x***	***y***	***z***	***K=2***	***K=3***
Insula_R	28	12	-20	K2_ant_R	K3_mid_R
Insula_R_1	40	2	-14	K2_ant_R	K3_mid_R
Insula_R_2	42	-6	-10	K2_ant_R	K3_mid_R
Insula_R_3	40	0	-10	K2_ant_R	K3_mid_R
Insula_R_4	48	14	-6	K2_ant_R	K3_ant_R
Insula_R_5	44	4	-4	K2_ant_R	K3_mid_R
Insula_R_6	44	14	-4	K2_ant_R	K3_ant_R
Insula_R_7	38	22	-2	K2_ant_R	K3_ant_R
Insula_R_8	38	12	2	K2_ant_R	K3_ant_R
Insula_R_9	40	14	2	K2_ant_R	K3_ant_R
Insula_R_10	42	14	2	K2_ant_R	K3_ant_R
Insula_R_11	44	-8	4	K2_post_R	K3_post_R
Insula_R_12	34	-24	10	K2_post_R	K3_post_R
Insula_R_13	42	-24	-2	K2_post_R	K3_mid_R
Insula_L	-36	16	-12	K2_ant_L	K3_ant_L
Insula_L_1	-34	16	-12	K2_ant_L	K3_ant_L
Insula_L_2	-46	-14	-10	K2_post_L	K3_post_L
Insula_L_3	-42	-14	-10	K2_post_L	K3_post_L
Insula_L_4	-32	-12	-10	K2_post_L	K3_post_L
Insula_L_5	-50	4	-4	K2_post_L	K3_post_L

Figure 15. Results of the behavioral analysis for the K2 (top), and K3 (bottom) solutions. Blue = anterior; orange = posterior; green = middle.

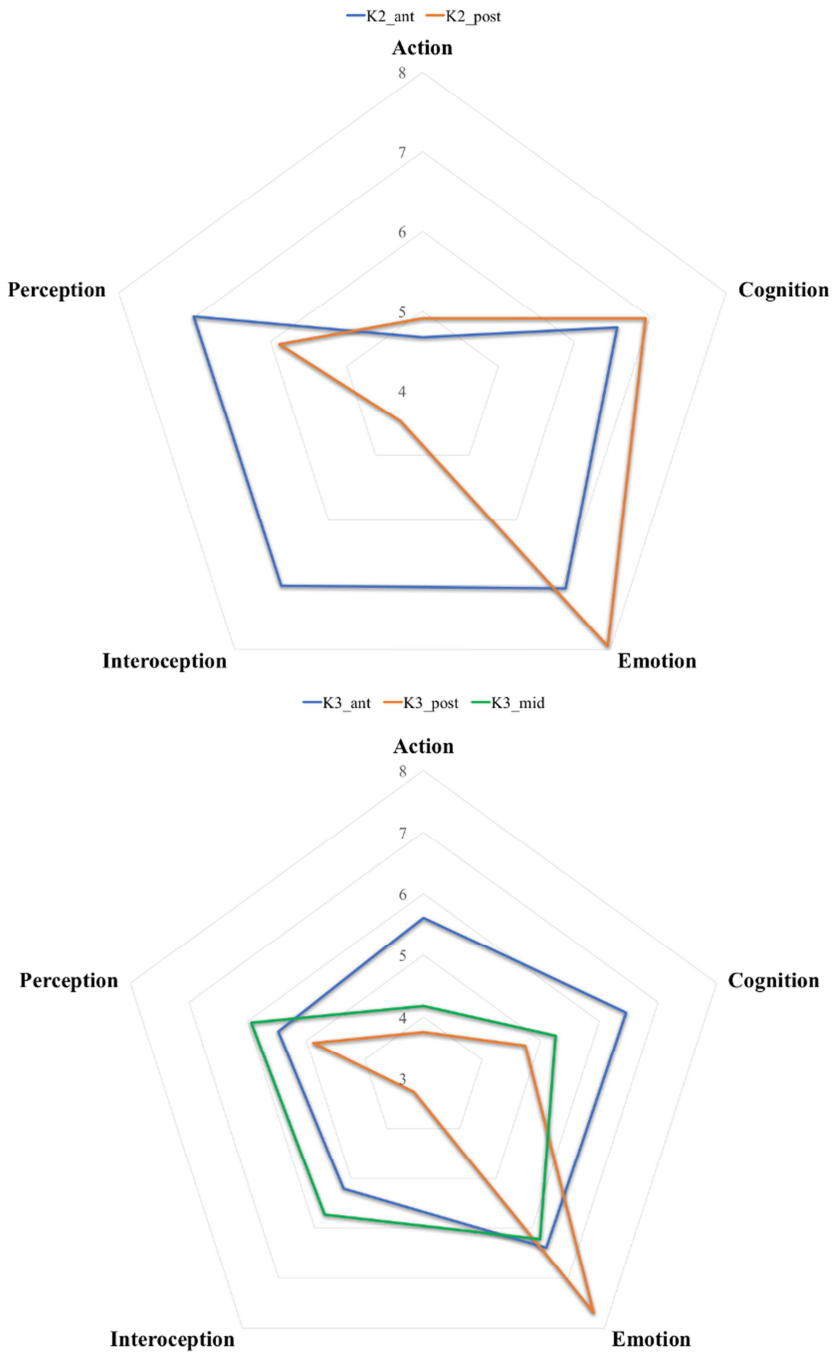

Figure 16. Distribution of the edges' values for each lobe/group, for the K2 solution. Only lobes/groups accounting at least for the 2% of the total Patel's k were visualized. Blue = frontal lobe, green = insula (non-root), red = midbrain, yellow = occipital lobe, purple = parietal lobe, pink = subcortical regions, brown = temporal lobe.

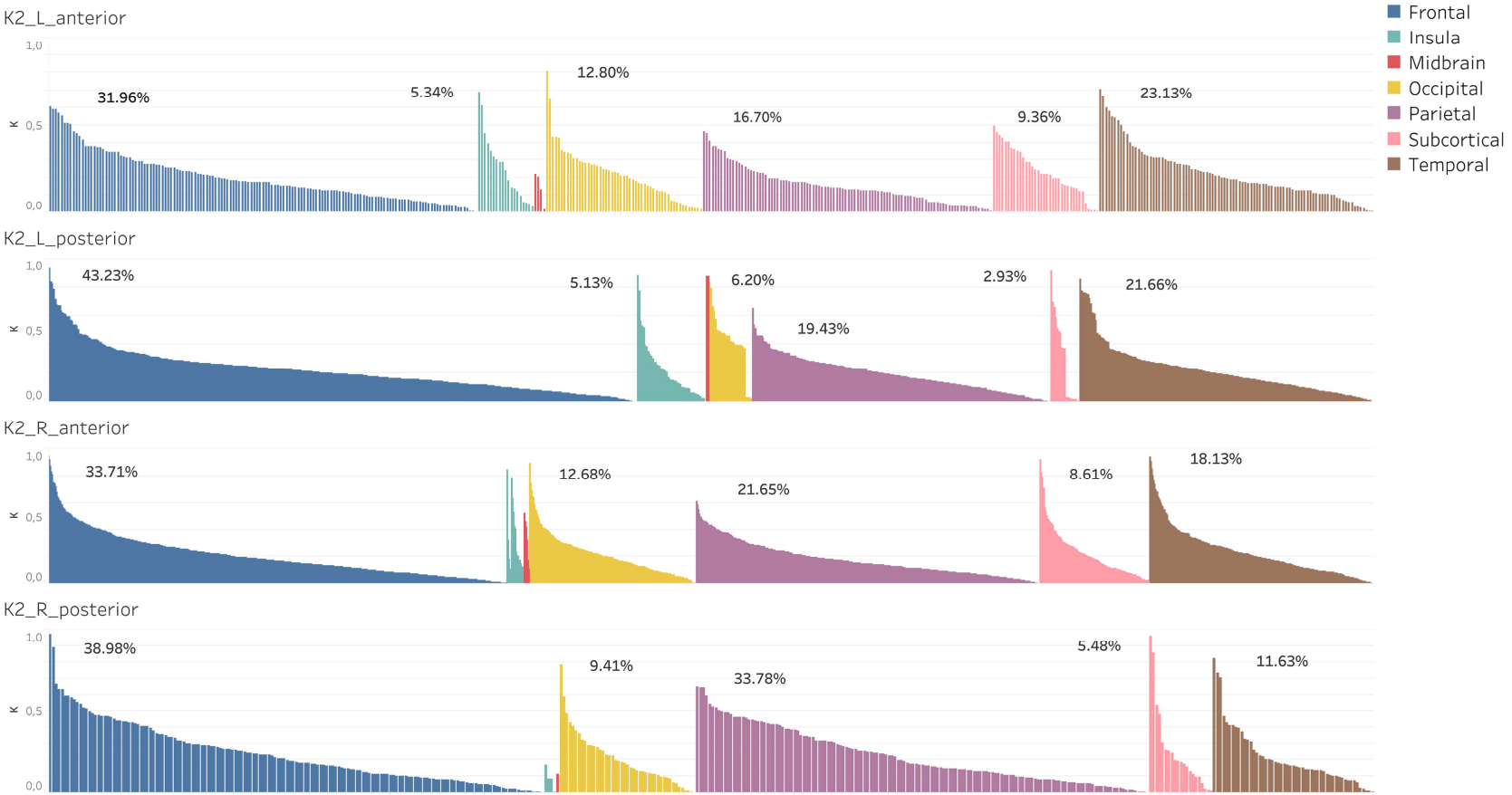

Figure 17. Distribution of the edges' values for each lobe/group, for the K3 solution. Only lobes/groups accounting at least for the 2% of the total Patel's k were visualized. Blue = frontal lobe, green = insula (non-root), red = midbrain, yellow = occipital lobe, purple = parietal lobe, pink = subcortical regions, brown = temporal lobe.

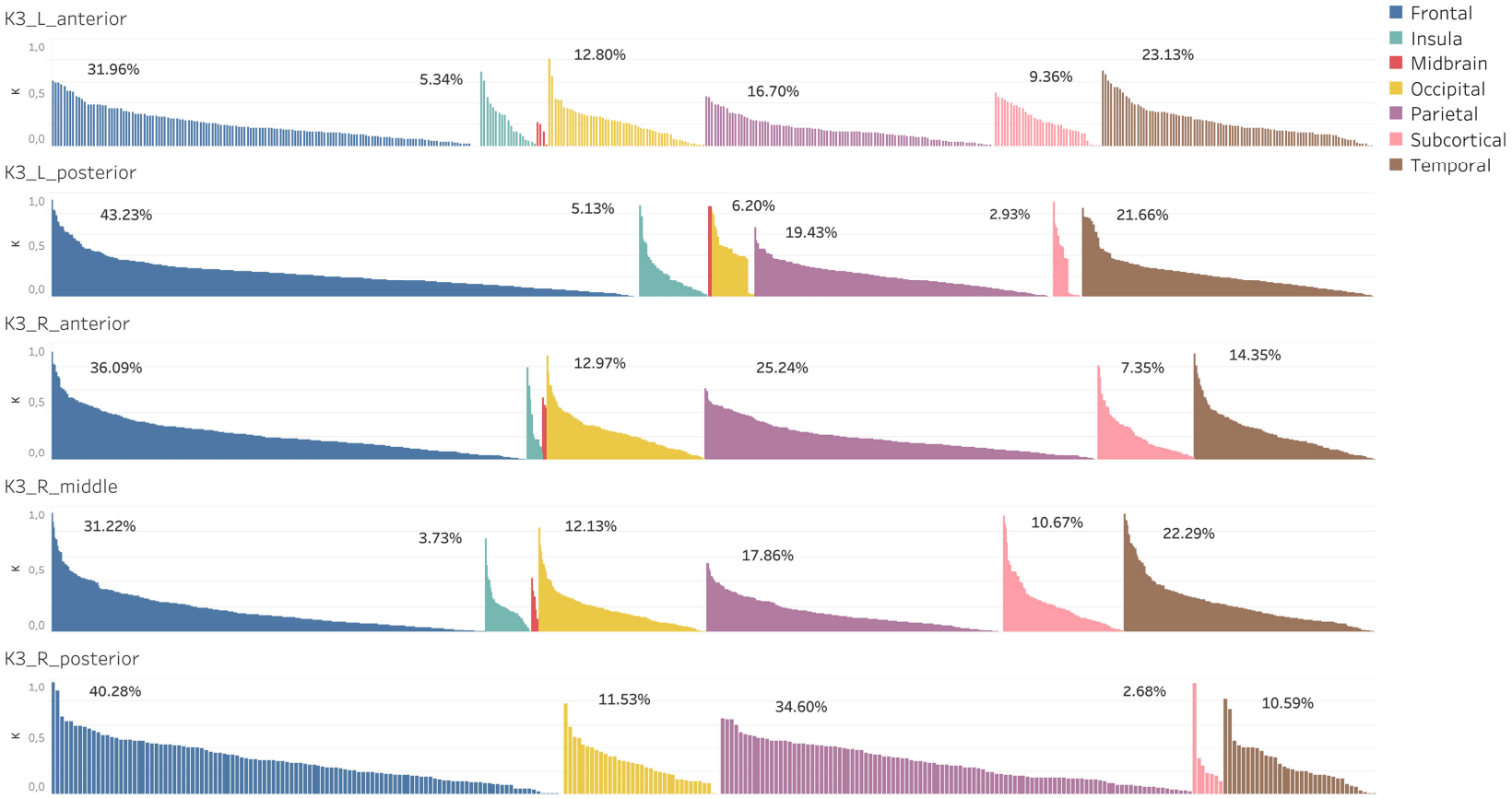

3.4. Discussion

3.4.1. The co-alteration network of the insula

The analysis provides further evidence for what has been showed by Cauda et al. (2019): the insular cortex is often and variously altered by a wide range of brain disorders. Of note, the insula, along with some subcortical nuclei, appears to be one of the most altered cerebral areas (Cauda et al., 2019). Both K2 and the K3 clusters present a density of alteration which is almost twice the alteration of the whole brain. Furthermore, the variety of diseases causing alterations in the insula is highly diversified, including both neurological and psychiatric conditions. All these types of disorders impact on the insula, albeit in different ways.

Both the insula co-alterations networks based on the K2 and K3 solutions include cortical and subcortical sites. Frontal regions (particularly the inferior frontal gyrus) are included in both K2 and K3 parcellations, as well as subcortical areas such as thalamus and caudate. Interestingly, the amygdala and parietal areas appear to be co-altered in the K3 parcellation but not in the K2 parcellation, which may imply that K3 parcellation is the solution which is more specific.

These findings reflect the widespread anatomical connections of the insula with many cerebral regions (Cauda et al., 2011, 2012a; Dosenbach et al., 2007; Mesulam and Mufson, 1982; Taylor et al., 2009; van den Heuvel et al., 2009). Portions of these connections are long-range projections, as the insular cortex has been found to be rich of Von Economo's neurons (VENs), large spindle-shaped cells that are supposed to be involved in processes regarding the monitoring of the state of the body, such as proprioception and interoception (Allman et al., 2005; Cauda et al., 2013, 2014; Medford and Critchley, 2010; Seeley et al., 2007). In particular, the anterior cingulate cortex (ACC) seems to be often co-altered with the insula. These two regions are essential parts of the salience network, a dysfunction of which might explain the deficits of salience detection

and self-monitoring that can be observed transdiagnostically in many neurological and psychiatric conditions.

3.4.2. Distribution analysis of edges

It worth noting that edges link the insula with areas tending to be not below the z coordinate of the insula node itself, with no co-alteration with the cerebellum and only few with the midbrain and subcortical areas. This may indicate that the insular cortex is co-altered by brain disorders only together with higher-order areas, especially with cortical ones. As the insula is related to functions integrating lower- and higher-order cognitive processes, evaluating sensory and limbic stimuli, monitoring the body and the environment in order to perform error detection (Ahmed et al., 2016; Cauda et al., 2011, 2012a, 2012b; Douaud et al., 2014; Fjell et al., 2015; Jagust, 2013; Jones et al., 2016; Klein et al., 2013; Nieuwenhuys, 2012; Vercelli et al., 2016; Voytek & Knight, 2015; Wylie & Tregellas, 2010), it should be surprising to find it not much co-altered with limbic and subcortical sites. As the co-activation map reveals that the insular cortex is functionally connected with several extracortical regions (for example, the cerebellum), the co-alteration patterns of every insular parcel indicate that the insula exhibits a characteristic pathoconnectivity profile. In other words, this region seems to be co-altered mainly with the cortical areas with which it is functionally connected rather than with those lower-order areas whose information is supposed to be the inputs for insular integration.

Interestingly, every cluster is extensively connected with many cortical regions, but their co-alteration edges are not equally distributed across the cortical lobes. The most co-altered lobe with every insular cluster is the frontal lobe, which indicates again that the insula tends to be altered along with higher-order and philogenetically recent areas. This finding may also be accounted for by the anatomical closeness between the frontal cortices and the insula. Accordingly, the occipital lobe, which is relatively distant from the insula and is

principally involved in sensory processes, is one of the less co-altered areas with the insula.

The edges' distribution across the lobes is also different between clusters. The left posterior cluster is the most co-altered with the frontal lobe. Within the right insula, the posterior K2 cluster is slightly more co-altered than the anterior, and the posterior K3 cluster, even though it has less edges than the others, presents a 40% of the strength of its co-alteration toward the frontal lobes. Counterintuitively, posterior clusters are less connected with the occipital lobe than the anterior ones. These results are quite unexpected, as Kelly and colleagues (2012) found that the posterior clusters are principally involved in motor and perceptual functions, while the anterior ones are principally involved in cognition. It should be noted that all the insular clusters have been found to be involved in cognition, both in this analysis and in the one carried out by Kelly and colleagues (2012). However, the findings of this study indicate that the co-alteration network of the posterior insula may be more related to brain areas which are characterized by higher-order functions.

Another interesting point is that the right insula exhibits more nodes and edges of co-alterations than the left one. This finding might suggest that the right insular cortex may be more vulnerable to pathological processes than the left one, an intriguing aspect that deserves to be further investigated and confirmed.

3.4.3. The co-alteration networks and functional connectivity of the insula

With the exception of the subcortical sites (i.e., the cerebellum), which are functionally associated but not co-altered with the insula, the insular co-alteration networks correlate well with the patterns of the MACM of this region. This result shows that the cerebral regions that are co-altered with the insula are not randomly affected; on the contrary, they tend to be altered on the basis of their functional connectivity. This result significantly corroborates the deep relationship between anatomical and functional connectivity profiles (Abdelnour et al., 2014) and is consistent with the hypothesis that brain connectivity might

play an important role in the development and distribution of GM alterations (Cauda et al., 2018; Iturria-Medina and Evans, 2015; Raj et al., 2012; Zhou et al., 2012). For instance, structural and functional connectivity patterns have been related to the spatial distribution of GM alterations caused by Alzheimer's disease, the behavioral variant of frontotemporal dementia, and amyotrophic lateral sclerosis (Buckner et al., 2009; Du et al., 2007; Ravits, 2014; Zhou et al., 2010). A relationship between neurodegenerative diseases and intrinsic connectivity network has been proposed (Seeley et al., 2009), and functional abnormal patterns of the default mode network have been related to deficits of semantic memory in patients with mild cognitive impairment (Gardini et al., 2015).

These results provide evidence for the hypothesis that large-scale functional networks might be selectively more susceptible to the assault of pathology and, consequently, might favor the development of alterations more quickly than region-specific functional circuits. Furthermore, dysfunction in functional hubs and/or pathways may contribute with neurophysiological, metabolic, and genetic factors of neuronal biology to enhance the impact of the alteration process (Iturria-Medina and Evans, 2015; Saxena and Caroni, 2011). As we have seen in study 1, functional and anatomical connectivity correlate with each other not only in the normal and healthy brain (Cauda et al., 2011; Honey et al., 2009) but also in the pathological brain (Crossley et al., 2016b; Gardini et al., 2015; Iturria-Medina and Evans, 2015; Iturria-Medina et al., 2014; Seeley et al., 2009).

The findings of this study highlight that when the insular cortex is altered the co-alteration networks likely reflect the functional connectivity patterns of this region, thus supporting the nodal stress hypothesis in the development and distribution of GM alterations (Crossley et al., 2016a; Crossley et al., 2014). An impaired insula may lead to hyperexcitability to its functionally connected areas and, consequently, produce metabolic stress and dysfunction.

If the relationship between the co-alteration networks and functional connectivity of the insula is examined in more detail, it can be observed that

peaks of correlation between the K2 network and MACM are mostly located in frontal and subcortical regions. On the other hand, peaks of correlation between the K3 network and MACM are not only largely located in frontal and subcortical regions, but also in temporal and parietal areas. This suggests that the solution based on the K3 parcellation may be more specific than the solution based on the K2 parcellation. However, the lack of correlation between functional connectivity and co-alterations with regard to subcortical and lower cortical areas points out that other factors might play a role in the distribution of co-alterations. For instance, a shared vulnerability mechanism based on genetic influences (Zhou et al., 2012) may be involved in the development of pathological alterations.

3.4.4. Behavioral profile analysis

The analysis of the behavioral profile reveals a predominance of labels associated with emotional and cognitive spheres, an aspect that is consistent with the evidence that emotional and cognitive functions are often disrupted in many neurological and psychiatric conditions. As we have seen, the insula is involved in important cognitive and interoceptive functions, such as the processing of salience, attention, emotions, and the integration of sensory and interoceptive stimuli.

Furthermore, the insula is a fundamental part of the salience network, together with the dorsal anterior cingulate cortex and other subcortical and limbic structures (Seeley et al., 2007; Uddin, 2015). This network has an essential role in processing the perception of behaviorally significant stimuli as well as in coordinating the use of brain resources (Uddin et al., 2013; Uddin et al., 2011). Being a fundamental hub of the salience network, the insula (particularly the right one) is involved in coordinating dynamically two other important brain networks, the default mode network and the central executive network (Chen et al., 2013; Goulden et al., 2014; Sridharan et al., 2008; Supekar and Menon, 2012). Independently of the nature of the stimuli (homeostatic, emotional or

cognitive), the insula appears to be involved in a variety of functions related to subjective salience (Bartra et al., 2013; Craig, 2002). Disruption of the salience network can occur in many diseases, including schizophrenia, psychosis, anxiety, bipolar disorder, depression, addiction, autism spectrum disorder, obsessive-compulsive disorder, chronic pain, and dementia (Di Martino et al., 2009; Etkin et al., 2009; Goodkind et al., 2015; Hamilton et al., 2012; Kapur, 2003; Klin et al., 2003; Li et al., 2010; Palaniyappan and Liddle, 2012; Schroeter et al., 2008; Seeley et al., 2012; Simons et al., 2014). Moreover, the insula is essential in evaluating the emotional feature of bodily states. In particular, the organized activity of the insula, prefrontal cortex and amygdala is crucial for modulating and regulating emotions, both in normal and pathological conditions (Foland et al., 2008; Lee et al., 2012).

Finally, as to the solution based on two parcels, the anterior sub-network appears to be more involved in the processing of interoception and perception, while the posterior sub-network seems to be more involved in the processing of emotions. These two sub-networks have comparable scores for the functions of cognition and action. On the other hand, as to the solution based on three parcels, the anterior sub-network seems to be more involved in the processing of cognition and action, the middle sub-network seems to be more involved in the processing of perception and interoception, and the posterior sub-network in emotional functions.

3.4.5. Limitations and future directions

A limitation of this study is that it is not possible to differentiate the impact of brain disorders on the insular cortex. Findings point out that a number of conditions affect this area but what parts of the insula are the most affected and by which disorders remain as yet unknown. This is also due to the methodology applied in this study, which carried out analyses on a variety of brain disorders stored in the BrainMap database with the aim to achieve an overarching research about the pathological processes affecting the insula. There was also the

methodological need of analyzing the most abundant sample of studies to get a better statistical outcome. In any case, a more fine-grained parcellation could not be used, since otherwise the amount of data to obtain reliable results would not be sufficient. Future studies are needed to explore the directionality (spatial and temporal) of GM alterations throughout the brain when a key hub, like the insula, is initially affected.

3.5. Conclusion

This second study carried out a pathoconnectivity network analysis of the insula, a very important hub of the brain. Findings provide evidence that the insular cortex is altered by a range of brain diseases. This result is in accordance with recent research that found the insular cortex to be among the most affected brain regions by a number of brain disorders, both neurological and psychiatric (Cauda et al., 2019). This second study provides further evidence for that finding, suggesting that the central and intense activity of the insula might make it more vulnerable to GM alterations.

The analysis of the insular pathoconnectivity network shows: 1) that the distribution pattern of GM alterations within areas that are co-altered with the insular cortex mainly extends to cortical rather than to subcortical sites; that 2) the insular co-alteration networks based on the K2 and K3 parcellations correlate well with the patterns of functional meta-analytic connectivity of this cerebral region; and that 3) these patterns of co-alterations might involve the dysfunction of cognitive (i.e., salience) and emotional processes. The fact that higher-order regions result in contributing more to the co-alteration network of the insula than lower-order areas is indicative that other mechanisms (perhaps biological ones, such as cytological and genetic factors), in association with functional connectivity constraints, might play a role in the development of co-alterations patterns.

The hypothesis of the nodal stress, therefore, receives further support, as findings indicate that the cerebral regions which are altered together with the insular cortex are not randomly affected but tend to be altered on the basis of their functional connectivity. Finally, the substantial overlaps shown by the correlation analysis between the insular co-alteration networks and the patterns of the MACM reveal that GM alterations caused by brain diseases present a distribution according to the logic of the organization of functional networks. This might be particularly the case when brain hubs are involved in the alteration

process. According to this perspective, brain hubs might be at the center of pathological networks constituted by co-altered areas. If confirmed by future investigations, this aspect will help to better understand how brain connectivity can influence the regional alteration profiles as well as the severity of symptoms both in neurological and in psychiatric conditions.

4. Epilogue

The first meta-analytical study has addressed four important issues of pathoconnectomics, providing evidence that GM co-alterations are distributed across the brain in recognizable network-like patterns. These distribution patterns of morphometric neuropathological alterations present a strong association with brain connectivity, as the development of GM co-alterations has found to be influenced by the constraints of functional, anatomic and genetic connectivity profiles. These findings help assess the contributions of different mechanisms underlying neuropathological processes, as they show that the hypotheses of the nodal stress, shared vulnerability, and transneuronal spread are all supposed to influence the diffusion of GM alterations.

In turn, the second meta-analytical study has showed that the insula, which is among the most important functional hubs of the brain, appears to be altered by a wide range of neurological and psychiatric diseases. Of note, GM co-alterations with the insula mainly affect cortical rather than subcortical areas, and the distribution patterns of these co-alterations, which particularly involve the dysfunction of cognitive (i.e., salience) and emotional processes, correlate well with the patterns of functional meta-analytic connectivity of the insula. In line with the first study, these findings provide a further evidence of the intimate relationship between brain connectivity and the development of GM co-alterations. In fact, cerebral areas that are altered together with the insula are not randomly affected but tend to be altered on the basis of functional connectivity.

These results pave the way for a new understanding of the pathological brain. A pathoconnectivity perspective is in fact able to give a picture that can have profound implications for clinical and treatment purposes. On the one hand, research in the field of pathoconnectomics can improve the diagnostic power by providing more precise and accurate descriptions of the morphological alterations patterns that are distinctive for each brain disorder. On the other hand, this type of research is able to produce models for predicting the future development of

co-alterations and for identifying the most vulnerable areas to the pathological assault. And this information is crucial for achieving a better care of the pathological brain.

Acknowledgments

I would like to deeply thank my mentor, Franco Cauda, for having accompanied me during these exciting PhD years with wisdom and encouragement. I also would like to thank my parents, for their relentless support, and the members of the FocusLab, Tommaso Costa, Sergio Duca, Donato Liloia, Lorenzo Mancuso, Jordi Manuello, Karina Tatu and Ugo Vercelli, with whom I shared a tremendous amount of scientific adventures.

Bibliography

Abdelnour, F., Voss, H.U., Raj, A. (2014). Network diffusion accurately models the relationship between structural and functional brain connectivity networks. *Neuroimage*, 90, 335-347.

Abe, O., Yamasue, H., Kasai, K., Yamada, H., et al. (2010). Voxel-based analyses of gray/white matter volume and diffusion tensor data in major depression. *Psychiatry Research*, 181, 64-70.

Abell F., Krams, M., Ashburner, J., et al. (1999). The neuroanatomy of autism: a voxel-based whole brain analysis of structural scans. *Neuroreport*, 10(8), 1647-1651.

Adleman, N.E., Fromm, S.J., Razdan, V., et al. (2012). Cross-sectional and longitudinal abnormalities in brain structure in children with severe mood dysregulation or bipolar disorder. *Journal of Child Psychology and Psychiatry*, 53, 1149-1156.

Adler, C.M., Levine, A.D., DelBello, M.P., Strakowski, S.M. (2005). Changes in Gray Matter Volume in Patients with Bipolar Disorder. *Biological Psychiatry*, 58, 151-157.

Agosta, F., Kostić, V.S., Galantucci, S., et al. (2010). The in vivo distribution of brain tissue loss in Richardson's syndrome and PSP-parkinsonism: a VBM-DARTEL study. *European Journal of Neuroscience*, 32, 640-647.

Agosta, F., Pagani, E., Rocca, M., et al. (2007). Voxel-based morphometry study of brain volumetry and diffusivity in amyotrophic lateral sclerosis patients with mild disability. *Human Brain Mapping*, 28, 1430-1438.

Agosta F., Pievani, M., Sala, S., et al. (2011). White matter damage in Alzheimer disease and its relationship to gray matter atrophy. *Radiology*, 258(3), 853-863.

Aguzzi, A., Heikenwalder, M., Polymenidou, M. (2007). Insights into prion strains and neurotoxicity. *Nature reviews. Molecular cell biology*, 8, 552-561.

Ahmed, R. M., Devenney, E. M., Irish, M., Ittner, A., Naismith, S., Ittner, L. M., et al. (2016). Neuronal network disintegration: common pathways linking neurodegenerative diseases. *Journal of Neurology, Neurosurgery and Psychiatry*, 87(11), 1234-1241.

Ahmed, F., Spottiswoode, B.S., Carey, P., et al. (2012). Relationship between Neurocognition and Regional Brain Volumes in Traumatized Adolescents with and without Posttraumatic Stress Disorder. *Neuropsychobiology*, 66, 174-184.

Ahrendts, J., Rüsch, N., Wilke, M., et al. (2011). Visual cortex abnormalities in adults with ADHD: a structural MRI study. *World Journal of Biological Psychiatry*, 12(4), 260-270.

Albert, R., Jeong, H., Barabasi, A. L. (2000). Error and attack tolerance of complex networks. *Nature*, 406, 378-382.

Alcauter, S., Barrios, F.A., Díaz, R., Fernández-Ruiz, J. (2011). Gray and white matter alterations in spinocerebellar ataxia type 7: an in vivo DTI and VBM study. *Neuroimage*, 55(1), 1-7.

Alemany, S., Mas, A., Goldberg, X., et al. (2013). Regional gray matter reductions are associated with genetic liability for anxiety and depression: an MRI twin study. *Journal of Affective Disorders*, 149, 175-181.

ALLEN Human Brain Atlas. (2013). Technical white paper: microarray data normalization, v.1. Seattle, WA: Allen Institute.

Allen, M.J., Yen, W.M. (2001). Introduction to measurement theory Long Grove, IL: Waveland Press.

Allman, J. M., Watson, K. K., Tetreault, N. A., Hakeem, A. Y. (2005). Intuition and autism: a possible role for Von Economo neurons. *Trends in Cognitive Sciences*, 9(8), 367-373.

Almeida, J.R., Akkal, D., Hassel, S., et al. (2009). Reduced gray matter volume in ventral prefrontal cortex but not amygdala in bipolar disorder: significant effects of gender and trait anxiety. *Psychiatry research*, 171(1), 54-68.

Alonso-Lana, S., Goikolea, J.M., Bonnin, C.M., et al. (2016). Structural and Functional Brain Correlates of Cognitive Impairment in Euthymic Patients with Bipolar Disorder. *PloS one*, 11(7), e0158867. doi:10.1371/journal.pone.0158867.

Alstott, J., Breakspear, M., Hagmann, P., Cammoun, L., Sporns, O. (2009). Modeling the impact of lesions in the human brain. *PLoS Computational Biology*, 5, e1000408.

Ambrosi, E., Rossi-Espagnet, M.C., Kotzalidis, G.D., et al. (2013). Structural brain alterations in bipolar disorder II: a combined voxel-based morphometry (VBM) and diffusion tensor imaging (DTI) study. *Journal of Affective Disorders*, 150(2), 610-615.

Ananth, H., Popescu, I., Critchley, H.D., et al. (2002). Cortical and subcortical gray matter abnormalities in schizophrenia determined through structural magnetic resonance imaging with optimized volumetric voxel-based morphometry. *American Journal of Psychiatry*, 159(9), 1497-1505.

Antonova, E., Kumari, V., Morris, R., et al. (2005). The relationship of structural alterations to cognitive deficits in schizophrenia: a voxel-based morphometry study. *Biological Psychiatry*, 58(6), 457-467.

Appel, S.H. (1981). A unifying hypothesis for the cause of amyotrophic lateral sclerosis, parkinsonism, and Alzheimer disease. *Annuals in Neurology*, 10, 6, 499-505.

Araujo, S.J., Tear, G. (2003). Axon guidance mechanisms and molecules: lessons from invertebrates. *Nature Reviews Neuroscience*, 4, 910-922.

Arnone, D., McKie, S., Elliott, R., et al. (2013). State-dependent changes in hippocampal grey matter in depression. *Molecular Psychiatry*, 18(12), 1265-1272.

Asami, T., Yamasue, H., Hayano, F., et al. (2009). Sexually dimorphic gray matter volume reduction in patients with panic disorder. *Psychiatry Research*, 173(2), 128-134.

Ash, S., McMillan, C., Gross, R. G., et al. (2011). The organization of narrative discourse in Lewy body spectrum disorder. *Brain and language*, 119(1), 30-41.

Ash, S., Moore, P., Vesely, L., et al. (2009). Non-Fluent Speech in Frontotemporal Lobar Degeneration. *Journal of neurolinguistics*, 22(4), 370-383.

Ashburner, J., Friston, K.J. (2000). Voxel-Based Morphometry—The Methods. *Neuroimage*, 11(6), 805-821.

Ashburner, J., Friston, K.J. (2005). Unified segmentation. *Neuroimage*, 26(3), 839-851.

Attwell, D., Laughlin, S.B. (2001). An energy budget for signaling in the grey matter of the brain. *Journal of Cerebral Blood Flow & Metabolism*, 21, 1133-1145.

Aubert-Broche, B., Fonov, V., Ghassemi R., et al. (2011). Regional brain atrophy in children with multiple sclerosis. *Neuroimage*, 58(2), 409-415.

Audoin, B., Davies, G.R., Finisku, L., et al. (2006). Localization of grey matter atrophy in early RRMS : A longitudinal study. *Journal of Neurology*, 253(11), 1495-1501.

Audoin, B., Davies, G., Rashid, W., et al. (2007). Voxel-based analysis of grey matter magnetization transfer ratio maps in early relapsing remitting multiple sclerosis. *Multiple Sclerosis*, 13(4), 483-489.

Audoin, B., Ranjeva, J.P., Duong, M.V.A., et al. (2004). Voxel-based analysis of MTR images: A method to locate gray matter abnormalities in patients at the earliest stage of multiple sclerosis. *Journal of Magnetic Resonance Imaging*, 20, 765-771.

Audoin, B., Zaaraoui, W., Reuter, F., et al. (2010). Atrophy mainly affects the limbic system and the deep grey matter at the first stage of multiple sclerosis. *Journal of Neurology, Neurosurgery and Psychiatry*, 81(6), 690-695.

Baker, J.T., Holmes. A.J., Masters, G.A., Yeo, B.T., Krienen, F., Buckner, R.L., et al. (2014). Disruption of cortical association networks in schizophrenia and psychotic bipolar disorder. *JAMA Psychiatry*, 71, 109-118.

Barbeau, E.J., Ranjeva, J.P., Didic, M., et al. (2008). Profile of memory impairment and gray matter loss in amnestic mild cognitive impairment. *Neuropsychologia*, 46(4), 1009-1019.

Baron, J.C., Chételat, G., Desgranges, B., et al. (2001). In vivo mapping of gray matter loss with voxel-based morphometry in mild Alzheimer's disease. *Neuroimage*, 14(2), 298-309.

Bartra, O., McGuire, J. T., Kable, J. W. (2013). The valuation system: a coordinate-based meta-analysis of BOLD fMRI experiments examining neural correlates of subjective value. *Neuroimage*, 76, 412-427.

Bartzokis, G. (2011). Alzheimer's disease as homeostatic responses to age-related myelin breakdown. *Neurobiology of Aging*, 32, 1341-1371.

Bassitt, D.P., Neto, M.R., de Castro, C.C., Busatto, G.F. (2007). Insight and regional brain volumes in schizophrenia. *European Archives of Psychiatry and Clinical Neuroscience*, 257(1), 58-62.

Baxter, L.C., Sparks, D.L., Johnson, S.C., et al. (2006). Relationship of cognitive measures and gray and white matter in Alzheimer's disease. *Journal of Alzheimer's Disease*, 9(3), 253-260.

Beckmann, C.F., De Luca, M., Devlin, J.T., Smith, S.M. (2005). Investigations into resting-state connectivity using independent component analysis. *Philosophical Transactions of the Royal Society of London B Biological Sciences*, 360(1457), 1001-1013.

Beckmann, C.F., Mackay, C.E., Filippini, N., Smith, S.M. (2009). Group comparison of resting-state FMRI data using multi-subject ICA and dual regression. *Neuroimage*, S39-41.

Bell-McGinty, S., Lopez, O.L., Meltzer, C.C. et al. (2005). Differential cortical atrophy in subgroups of mild cognitive impairment. *Archives of Neurology*, 62(9), 1393-1397.

Belmonte, M.K., Allen, G., Beckel-Mitchener, A., Boulanger, L.M., Carper, R.A., et al. (2004). Autism and abnormal development of brain connectivity. *Journal of Neuroscience*, 24, 9228-9231.

Bendfeldt, K., Kuster, P., Traud, S., et al. (2009). Association of regional gray matter volume loss and progression of white matter lesions in multiple sclerosis – A longitudinal voxel-based morphometry study. *Neuroimage*, 45(1), 60-67.

Bergé, D., Carmona, S., Rovira, M., et al. (2011). Gray matter volume deficits and correlation with insight and negative symptoms in first-psychotic-episode subjects. *Acta Psychiatrica Scandinavica*, 123, 431-439.

Bergouignan, L., Chupin, M., Czechowska, Y., et al. (2009). Can voxel based morphometry, manual segmentation and automated segmentation equally detect hippocampal volume differences in acute depression? *Neuroimage*, 45(1), 29-37.

Berlingeri, M., Bottini, G., Basilico, S., et al. (2008). Anatomy of the episodic buffer: a voxel-based morphometry study in patients with dementia. *Behavioural neurology*, 19, 29-34.

Berlingeri, M., Bottini, G., Danelli, L., et al. (2010). With time on our side? Task-dependent compensatory processes in graceful aging. *Experimental brain research*, 205(3), 307-324.

Bernasconi, N., Duchesne, S., Janke, A., et al. (2004). Whole-brain voxel-based statistical analysis of gray matter and white matter in temporal lobe epilepsy. *Neuroimage*, 23(2), 717-723.

Bertsch, K., Grothe, M., Prehn, K., et al. (2013). Brain volumes differ between diagnostic groups of violent criminal offenders. *European Archives of Psychiatry and Clinical Neuroscience*, 263(7), 593-606.

Beste, C., Saft, C., Konrad, C., et al. (2008). Levels of error processing in Huntington's disease: A combined study using event-related potentials and voxel-based morphometry. *Human Brain Mapping*, 29, 121-130.

Beyer, M.K., Janvin, C.C., Larsen, J.P., Aarsland, D. (2007). A magnetic resonance imaging study of patients with Parkinson's disease with mild cognitive impairment and dementia using voxel-based morphometry. *Journal of neurology, neurosurgery, and psychiatry*, 78(3), 254-259.

Biswal, B.B. (2012). Resting state fMRI: a personal history. *Neuroimage*, 62, 938-944.

Bitter, T., Brüderle, J., Gudziol, H., et al. (2010). Gray and white matter reduction in hyposmic subjects – A voxel-based morphometry study. *Brain Research*, 1347, 42-47.

Bitter, T., Siegert, F., Gudziol, H., et al. (2011). Gray matter alterations in parosmia. *Neuroscience*, 177, 177-182.

Biundo, R., Formento-Dojot, P., Facchini, S., et al. (2011). Brain volume changes in Parkinson's disease and their relationship with cognitive and behavioural abnormalities. *Journal of Neurological Sciences*, 310, 64-69.

Boccardi, M., Sabattoli, F., Laakso, M.P., et al. (2005). Frontotemporal dementia as a neural system disease. *Neurobiology of Aging*, 26(1), 37-44.

Boddaert, N., Chabane, N., Gervais, H., et al. (2004). Superior temporal sulcus anatomical abnormalities in childhood autism: a voxel-based morphometry MRI study. *Neuroimage*, 23(1), 364-369.

Bodini, B., Khaleeli, Z., Cercignani, M., et al. (2009). Exploring the relationship between white matter and gray matter damage in early primary progressive multiple sclerosis: An in vivo study with TBSS and VBM. *Human Brain Mapping*, 30, 2852-2861.

Boghi, A., Sterpone, S., Sales, S., et al. (2011). In vivo evidence of global and focal brain alterations in anorexia nervosa. *Psychiatry Research*, 192(3), 154-159.

Bonavita, S., Gallo, A., Sacco, R., et al. (2011). Distributed changes in default-mode resting-state connectivity in multiple sclerosis. *Multiple Sclerosis*, 17(4), 411-422.

Bonilha, L., Molnar, C., Horner, M. D., et al. (2008). Neurocognitive deficits and prefrontal cortical atrophy in patients with schizophrenia. *Schizophrenia research*, 101, 142-151.

Bonilha, L., Rorden, C., Castellano, G., et al. (2004). Voxel-based morphometry reveals gray matter network atrophy in refractory medial temporal lobe epilepsy. *Archives of Neurology*, 61(9), 1379-1384.

Borgatti, S. P. (2005). Centrality and network flow. *Social Networks*, 27, 55-71.

Borgwardt, S.J., McGuire, P.K., Aston, J., et al. (2007). Structural brain abnormalities in individuals with an at-risk mental state who later develop psychosis. *British Journal of Psychiatry*, 51, s69-75. doi: 10.1192/bjp.191.51.s69.

Borgwardt, S.J., Picchioni, M.M., Ettinger, U., et al. (2010). Regional gray matter volume in monozygotic twins concordant and discordant for schizophrenia. *Biological Psychiatry*, 67(10), 956-964.

Borgwardt, S.J., Riecher-Rössler, A., Dazzan, P., et al. (2007). Regional gray matter volume abnormalities in the at risk mental state. *Biological Psychiatry*, 61(10), 1148-1156.

Borroni, B., Garibotto, V., Agosti, C., et al. (2008). White matter changes in corticobasal degeneration syndrome and correlation with limb apraxia. *Archives of Neurology*, 65(6), 796-801.

Bose, S.K., Mackinnon, T., Mehta, M.A., et al. (2009). The effect of ageing on grey and white matter reductions in schizophrenia. *Schizophrenia Research*, 112, 7-13.

Bouilleret, V., Semah, F., Chassoux, F., et al. (2008). Basal ganglia involvement in temporal lobe epilepsy: a functional and morphologic study. *Neurology*, 70(3), 177-184.

Bourdenx, M., Koulakiotis, N.S., Sanoudou, D., Bezard, E., Dehay, B., Tsarbopoulos, A. (2017). Protein aggregation and neurodegeneration in prototypical neurodegenerative diseases: examples of amyloidopathies, tauopathies and synucleinopathies. *Progress in Neurobiology*, 2017; 155, 171-193.

Boxer, A.L., Geschwind, M.D., Belfor, N., et al. (2006). Patterns of brain atrophy that differentiate corticobasal degeneration syndrome from progressive supranuclear palsy. *Archives of Neurology*, 63(1), 81-86.

Boxer, A.L., Rankin, K.P., Miller, BL., et al. (2003). Cinguloparietal atrophy distinguishes Alzheimer disease from semantic dementia. *Archives of Neurology*, 60(7), 949-956.

Bozzali, M., Filippi, M., Magnani, G., et al. (2006). The contribution of voxel-based morphometry in staging patients with mild cognitive impairment. *Neurology*, 67(3), 453-460.

Braak, H., Braak, E. (1991). Neuropathological stageing of Alzheimer-related changes. *Acta Neuropathologyca*, 82, 239-59.

Braak, H., Thal, D.R., Ghebremedhin, E., Del Tredici, K. (2011). Stages of the pathologic process in Alzheimer disease: age categories from 1 to 100 years. *Journal of neuropathology and experimental neurology*, 70: 960-969.

Brambati, S. M., Rankin, K. P., Narvid, J., et al. (2009). Atrophy progression in semantic dementia with asymmetric temporal involvement: a tensor-based morphometry study. *Neurobiology of aging*, 30(1), 103-111.

Brambati, S.M., Termine, C., Ruffino, M., et al. (2004). Regional reductions of gray matter volume in familial dyslexia. *Neurology*, 63(4), 742-745.

Brázdil, M., Mareček, R., Fojtíková, D., et al. (2009). Correlation study of optimized voxel-based morphometry and 1H MRS in patients with mesial temporal lobe epilepsy and hippocampal sclerosis. *Human Brain Mapping*, 30, 1226-1235.

Brenneis, C., Boesch, S.M., Egger, K.E., et al. (2006). Cortical atrophy in the cerebellar variant of multiple system atrophy: A voxel-based morphometry study. *Movements Disorders*, 21, 159-165.

Brenneis, C., Boesch, S.M., Schocke, M., et al. (2003). Atrophy pattern in SCA2 determined by voxel-based morphometry. *Neuroreport*, 14(14), 1799-1802.

Brenneis, C., Egger, K., Scherfler, C., et al. (2007). Progression of brain atrophy in multiple system atrophy. A longitudinal VBM study. *Journal of Neurology*, 254(2), 191-196.

Brenneis, C., Seppi, K., Schocke, M., et al. (2003). Voxel-based morphometry detects cortical atrophy in the Parkinson variant of multiple system atrophy. *Movements Disorders*, 18, 1132-1138.

Brenneis, C., Seppi, K., Schocke, M., et al. (2004). Voxel based morphometry reveals a distinct pattern of frontal atrophy in progressive supranuclear palsy. *Journal of neurology, neurosurgery and psychiatry*, 75(2), 246-249.

Brenneis, C., Wenning, G.K., Egger, K.E., et al. (2004). Basal forebrain atrophy is a distinctive pattern in dementia with Lewy bodies. *Neuroreport*, 15(11),1711-1714.

Bressler, S.L., and Kelso, J.A.S. (2001). Cortical coordination dynamics and cognition. *Trends in Cognitive Sciences*, 5, 26-36.

Brieber, S., Neufang, S., Bruning, N., et al. (2007). Structural brain abnormalities in adolescents with autism spectrum disorder and patients with attention deficit/hyperactivity disorder. *Journal of Child Psychology and Psychiatry*, 48, 1251-1258.

Brooks B. (1991). The role of axonal transport in neurodegenerative disease spread: a meta-analysis of experimental and clinical poliomyelitis compares with amyotrophic lateral sclerosis. *The Canadian journal of neurological sciences*, 18 (3 Suppl), 435–438.

Brunner, R., Henze, R., Parzer P., et al. (2010). Reduced prefrontal and orbitofrontal gray matter in female adolescents with borderline personality disorder: is it disorder specific? *Neuroimage*. 49(1), 114-120.

Brys, M., Glodzik, L., Mosconi, L., et al. (2009). Magnetic resonance imaging improves cerebrospinal fluid biomarkers in the early detection of Alzheimer's disease. *Journal of Alzheimer's disease*, 16(2), 351-362.

Buchel, C., and Friston, K. (1997). Modulation of connectivity in visual pathways by attention: cortical interactions evaluated with structural equation modeling and fMRI. *Cerebral Cortex*, 7, 768-778.

Buchel, C., and Friston, K. (2001). Interactions among neuronal systems assessed with functional neuroimaging. *Revue Neurologique (Paris)*, 157, 807-15.

Buckholtz, J. W., and Meyer-Lindenberg, A. (2012). Psychopathology and the human connectome: toward a transdiagnostic model of risk for mental illness. *Neuron*, 74(6), 990-1004. doi: 10.1016/j.neuron.2012.06.002.

Buckner, R.L., Krienen, F.M., Yeo, B.T. (2013). Opportunities and limitations of intrinsic functional connectivity MRI. *Nature Neuroscience*, 16, 832-837.

Buckner, R. L., Sepulcre, J., Talukdar, T., Krienen, F. M., Liu, H., Hedden, T., et al. (2009). Cortical hubs revealed by intrinsic functional connectivity: mapping, assessment of stability, and relation to Alzheimer's disease. *Journal of Neuroscience*, 29(6), 1860-1873.

Buckner, R.L., Vincent, J.L. (2007). Unrest at rest: default activity and spontaneous network correlations. *Neuroimage*, 37(4), 1091-1096.

Bullmore, E., Sporns, O. (2009). Complex brain networks: graph theoretical analysis of structural and functional systems. *Nature Reviews Neuroscience*, 10, 186-198.

Bullmore, E., Sporns, O. (2012). The economy of brain network organization. *Nature Reviews Neuroscience*, 13, 336-349.

Burton, E.J., Karas, G., Paling, S.M., et al. (2002). Patterns of cerebral atrophy in dementia with Lewy bodies using voxel-based morphometry. *Neuroimage*, 17(2), 618-630.

Burton, E.J., McKeith, I.G., Burn, D.J., et al. (2004). Cerebral atrophy in Parkinson's disease with and without dementia: a comparison with Alzheimer's disease, dementia with Lewy bodies and controls. *Brain*, 127, 791-800.

Cai, Y., Liu, J., Zhang, L., et al. (2015). Grey matter volume abnormalities in patients with bipolar I depressive disorder and unipolar depressive disorder: a voxel-based morphometry study. *Neuroscience bulletin*, 31(1), 4-12.

Camara, O., Schnabel, J.A., Ridgway, G.R., et al. (2008). Accuracy assessment of global and local atrophy measurement techniques with realistic simulated longitudinal Alzheimer's disease images. *Neuroimage*, 42, 696-709.

Camara, O., Schweiger, M., Scahill, R., et al. (2006). Phenomenological model of diffuse global and regional atrophy using finite-element methods. *IEEE Transactions Medical Imaging*, 25, 1417-1430.

Camicioli, R., Gee, M., Bouchard, T.P., et al. (2009). Voxel-based morphometry reveals extra-nigral atrophy patterns associated with dopamine refractory cognitive and motor impairment in parkinsonism. *Parkinsonism and Related Disorders*, 15(3), 187-95.

Canu, E., Frisoni, G.B., Agosta, F., et al. (2012). Early and late onset Alzheimer's disease patients have distinct patterns of white matter damage. *Neurobiology of Aging*, 33(6), 1023-1033.

Carlson, N., Buskist, W., Heth, C.D., Schmaltz, R. (2009). *Psychology: the science of behaviour*. 4th Canadian edn. Toronto: Pearson Education, Canada.

Carmona, S., Vilarroya, O., Bielsa, A., et al. (2005). Global and regional gray matter reductions in ADHD: a voxel-based morphometric study. *Neuroscience Lett*ers, 389(2), 88-93.

Caroli, A., Testa, C., Geroldi, C., et al. (2007). Cerebral perfusion correlates of conversion to Alzheimer's disease in amnestic mild cognitive impairment. *Journal of Neurology*, (12), 1698-1707.

Cascella, N.G., Fieldstone, S.C., Rao, V.A., et al. (2010). Gray-matter abnormalities in deficit schizophrenia. *Schizophrenia Research*, 120, 63-70.

Castro-Fornieles, J., Bargalló, N., Lázaro, L., et al. (2009). A cross-sectional and follow-up voxel-based morphometric MRI study in adolescent anorexia nervosa. *Journal of Psychiatry Research*, 43(3), 331-340.

Cauda, F., Costa, T., Nani, A., Fava, L., Palermo, S., Bianco, F., et al. (2017). Are schizophrenia, autistic, and obsessive spectrum disorders dissociable on the basis of neuroimaging morphological findings?. A voxel-based meta-analysis. *Autism Research*, 10, 1079-95.

Cauda, F., Costa, T., Torta, D.M., Sacco, K., D'Agata, F., Duca, S., et al. (2012a). Meta-analytic clustering of the insular cortex: characterizing the meta-analytic connectivity of the insula when involved in active tasks. *Neuroimage*, 62, 343-355.

Cauda, F., D'Agata, F., Sacco, K., Duca, S., Geminiani, G., & Vercelli, A. (2011). Functional connectivity of the insula in the resting brain. *Neuroimage*, 55(1), 8-23.

Cauda, F., Geminiani, G. C., Vercelli, A. (2014). Evolutionary appearance of von Economo's neurons in the mammalian cerebral cortex. *Frontiers in Human Neuroscience*, 8, 104. doi: 10.3389/fnhum.2014.00104.

Cauda, F., Nani, A., Costa, T., Palermo, S., Tatu, K., Manuello, J., et al. (2018a). The morphometric co-atrophy networking of schizophrenia, autistic and obsessive spectrum disorders. *Human Brain Mapping*, 39, 1898-928.

Cauda, F., Nani, A., Manuello, J., Liloia, D., Tatu, K., Vercelli, U., et al. (2019). The alteration landscape of the cerebral cortex. *Neuroimage*, 184, 359-371.

Cauda, F., Nani, A., Manuello, J., Premi, E., Palermo, S., Tatu, K., Duca, S., Fox, P.T., Costa, T. (2018b). Brain structural alterations are distributed following functional, anatomical and genetic connectivity. *Brain*, 141, 3211-3232.

Cauda, F., Torta, D. E., Sacco, K., D'Agata, F., Geda, E., Duca, S., et al. (2013). Functional anatomy of cortical areas characterized by Von Economo neurons. *Brain Structure & Function*, 218(1), 1-20. doi: 10.1007/s00429-012-0382-9.

Cauda, F., Torta, D.M., Sacco, K., Geda, E., D'Agata, F., Costa, T., et al. (2012b). Shared "core" areas between the pain and other task-related networks. *PLoS One*, 7, e41929.

Cauda, F., Vercelli, A. (2013). How many clusters in the insular cortex? *Cerebral Cortex*, 23(11), 2779-2780.

Ceccarelli, A., Rocca, M.A., Pagani, E., et al. (2008). A voxel-based morphometry study of grey matter loss in MS patients with different clinical phenotypes. *Neuroimage*, 42(1), 315-322.

Ceccarelli, A., Rocca, M.A., Valsasina, P., et al. (2009). A multiparametric evaluation of regional brain damage in patients with primary progressive multiple sclerosis. *Human Brain Mapping*, 30, 3009-3019.

Celle, S., Roche, F., Peyron, R., et al. (2010). Lack of specific gray matter alterations in restless legs syndrome in elderly subjects. *Journal of Neurology*, 257(3), 344-348.

Cerasa, A., Valentino, P., Chiriaco, C., et al. (2013). MR imaging and cognitive correlates of relapsing-remitting multiple sclerosis patients with cerebellar symptoms. *Journal of Neurology*, 260(5), 1358-1366.

Chan, C.H., Briellmann, R.S., Pell, G.S., et al. (2006). Thalamic Atrophy in Childhood Absence Epilepsy. *Epilepsia*, 47, 399-405.

Chaney, A., Carballedo, A., Amico, F., et al. (2014). Effect of childhood maltreatment on brain structure in adult patients with major depressive disorder and healthy participants. *Journal of psychiatry & neuroscience*, 39(1), 50-59.

Chang, C.C., Chang, Y.Y., Chang, W.N., et al. (2009). Cognitive deficits in multiple system atrophy correlate with frontal atrophy and disease duration. *European Journal of Neurology*, 16, 1144-1150.

Chang, J.L., Lomen-Hoerth, C., Murphy, J., et al. (2005). A voxel-based morphometry study of patterns of brain atrophy in ALS and ALS/FTLD. *Neurology*, 65(1), 75-80.

Chang, L.J., Yarkoni, T., Khaw, M.W., & Sanfey, A.G. (2013). Decoding the role of the insula in human cognition: functional parcellation and large-scale reverse inference. *Cerebral Cortex*, 23(3), 739-749.

Chanraud, S., Martelli, C., Delain, F., et al. (2007). Brain morphometry and cognitive performance in detoxified alcohol-dependents with preserved psychosocial functioning. *Neuropsychopharmacology*, 32(2), 429-438.

Chao, L.L., Lenoci, M., Neylan, T.C. (2012). Effects of post-traumatic stress disorder on occipital lobe function and structure. *Neuroreport*, 23(7), 412-419.

Chen, A.C., Oathes, D.J., Chang, C., Bradley, T., Zhou, Z.W., Williams, L.M., et al. (2013). Causal interactions between fronto-parietal central executive and default-mode networks in humans. *Proceedings of the National Academy of Sciences USA*, 110(49), 19944-19949.

Chen, S., Li, L., Xu, B., Liu, J. (2009). Insular cortex involvement in declarative memory deficits in patients with post-traumatic stress disorder. *BMC psychiatry*, 9, 39, doi:10.1186/1471-244X-9-39.

Chen, S., Xia, W., Li, L., et al. (2006). Gray matter density reduction in the insula in fire survivors with posttraumatic stress disorder: a voxel-based morphometric study. *Psychiatry Research*, 146(1), 65-72.

Chen, X., Wen, W., Malhi, G. S., et al. (2007). Regional Gray Matter Changes in Bipolar Disorder: A Voxel-Based Morphometric Study. *Australian & New Zealand Journal of Psychiatry*, 41(4), 327-336.

Chen, Y., Fu, K., Feng, C., et al. (2012). Different regional gray matter loss in recent onset PTSD and non PTSD after a single prolonged trauma exposure. *PloS one*, 7(11), e48298. doi:10.1371/journal.pone.0048298.

Cheng, B., Huang, X., Li, S., et al. (2015). Gray Matter Alterations in Post-Traumatic Stress Disorder, Obsessive-Compulsive Disorder, and Social Anxiety Disorder. *Frontiers in behavioral neuroscience*, 9, 219, doi:10.3389/fnbeh.2015.00219.

Cheng, Y., Chou, K.H., Fan, Y.T., Lin, C.P. (2011). ANS: aberrant neurodevelopment of the social cognition network in adolescents with autism spectrum disorders. *PloS one*, 6(4), e18905. doi:10.1371/journal.pone.0018905.

Cheng, Y.Q., Xu, J., Chai, P., et al. (2010). Brain volume alteration and the correlations with the clinical characteristics in drug-naïve first-episode MDD patients: a voxel-based morphometry study. *Neuroscience Letters*, 480(1), 30-34.

Chételat, G., Desgranges, B., De La Sayette, V., et al. (2002). Mapping gray matter loss with voxel-based morphometry in mild cognitive impairment. *Neuroreport*, 13(15), 1939-1943.

Chevalier-Larsen, E., Holzbaur, E.L. (2006). Axonal transport and neurodegenerative disease. *Biochimica et Biophysica Acta*, 1762, 1094-1108.

Chhatwal, J.P., Schultz, A.P., Johnson, K.A., Hedden, T., Jaimes, S., Benzinger, T.L.S. et al. (2018). Preferential degradation of cognitive networks differentiates Alzheimer's disease from ageing. *Brain*, 141, 1486-1500.

Chilton, J.K. (2006). Molecular mechanisms of axon guidance. *Developmental Biology*, 292, 13-24.

Chow, E.W., Ho, A., Wei, C., et al. (2011). Association of schizophrenia in 22q11.2 deletion syndrome and gray matter volumetric deficits in the superior temporal gyrus. *The American journal of psychiatry*, 168(5), 522-529.

Chua, S.E., Cheung, C., Cheung, V., et al. (2007). Cerebral grey, white matter and csf in never-medicated, first-episode schizophrenia. *Schizophrenia Research*, 89, 12-21.

Cioli, C., Abdi, H., Beaton, D., Burnod, Y., Mesmoudi, S. (2014). Differences in human cortical gene expression match the temporal properties of large-scale functional networks. *PLoS One*, 9: e115913.

Clavaguera, F., Grueninger, F., Tolnay, M. (2014). Intercellular transfer of tau aggregates and spreading of tau pathology: implications for therapeutic strategies. *Neuropharmacology*, 76(Pt A), 9-15.

Compta, Y., Ibarretxe-Bilbao, N., Pereira, J.B., et al. (2012). Grey matter volume correlates of cerebrospinal markers of Alzheimer-pathology in Parkinson's disease and related dementia. *Parkinsonism and Related Disorders*, 18(8), 941-947.

Cooke, M.A., Fannon, D., Kuipers, E., et al. (2008). Neurological basis of poor insight in psychosis: a voxel-based MRI study. *Schizophrenia research*, 103, 40-51.

Cope, T.E., Rittman, T., Borchert, R.J., Jones, P.S., Vatansever, D., Allinson, K., et al. (2018). Tau burden and the functional connectome in Alzheimer's disease and progressive supranuclear palsy. *Brain*, 141, 550-67.

Corbo, V., Clément, M.H., Armony, J.L., et al. (2005). Size versus shape differences: contrasting voxel-based and volumetric analyses of the anterior cingulate cortex in

individuals with acute posttraumatic stress disorder. *Biological Psychiatry*, 15, 58(2), 119-124.

Cordato, N.J., Duggins, A.J., Halliday, G.M., et al. (2005). Clinical deficits correlate with regional cerebral atrophy in progressive supranuclear palsy. *Brain*, 128, 1259-1266.

Cormack, F., Gadian, D.G., Vargha-Khadem, F., et al. (2005). Extra-hippocampal grey matter density abnormalities in paediatric mesial temporal sclerosis. *Neuroimage*, 27(3), 635-643.

Cosottini, M., Pesaresi, I., Piazza, S., et al. (2012). Structural and functional evaluation of cortical motor areas in Amyotrophic Lateral Sclerosis. *Experimental Neurology*, 234(1), 169-180.

Cowan, W.M. (1970). *Contemporary Research Methods in Neuroanatomy*. Springer, Berlin.

Craig, A.D. (2002). How do you feel? Interoception: the sense of the physiological condition of the body. *Nature Reviews Neuroscience*, 3(8), 655-666.

Craig, M., Zaman, S., Daly, E., et al. (2007). Women with autistic-spectrum disorder: Magnetic resonance imaging study of brain anatomy. *British Journal of Psychiatry*, 191(3), 224-228.

Critchley, H.D., Good, C.D., Ashburner, J., et al. (2003). Changes in cerebral morphology consequent to peripheral autonomic denervation. *Neuroimage*, 18(4), 908-916.

Crossley, N. A., Fox, P. T., & Bullmore, E. T. (2016a). Meta-connectomics: human brain network and connectivity meta-analyses. *Psychological Medicine*, 46(5), 897-907.

Crossley, N. A., Mechelli, A., Ginestet, C., Rubinov, M., Bullmore, E. T., & McGuire, P. (2016b). Altered Hub Functioning and Compensatory Activations in the Connectome: A Meta-Analysis of Functional Neuroimaging Studies in Schizophrenia. *Schizophrenia Bulletin*, 42(2), 434-442.

Crossley, N.A., Mechelli, A., Scott, J., Carletti, F., Fox, P.T., McGuire, P., Bullmore, E.T. (2014). The hubs of the human connectome are generally implicated in the anatomy of brain disorders. *Brain*, 137, 2382-95. doi:10.1093/brain/awu132.

Crossley, N.A., Scott, J., Ellison-Wright, I., Mechelli, A. (2015). Neuroimaging distinction between neurological and psychiatric disorders. *British Journal of Psychiatry*, 207, 429-434.

Cui, L., Li, M., Deng, W., et al. (2011). Overlapping clusters of gray matter deficits in paranoid schizophrenia and psychotic bipolar mania with family history. *Neuroscience Letters*, 489(2), 94-98.

Damasio, A. R., & Geschwind, N. (1984). The neural basis of language. *Annual Review of Neuroscience*, 7(1), 127-147.

de Araújo Filho, G.M., Jackowski, A.P., Lin, K., et al. (2009). Personality traits related to juvenile myoclonic epilepsy: MRI reveals prefrontal abnormalities through a voxel-based morphometry study. *Epilepsy Behavior*, 15(2), 202-207.

de Castro-Manglano, P., Mechelli, A., Soutullo, C., et al. (2011). Structural brain abnormalities in first-episode psychosis: differences between affective psychoses and schizophrenia and relationship to clinical outcome. *Bipolar Disorders*, 13, 545-555.

de Haan, W., Mott, K., van Straaten, E. C. W., Scheltens, P., Stam, C. J. (2012). Activity dependent degeneration explains hub vulnerability in Alzheimer's disease. *PLoS Computational Biology*, 8, e1002582.

de Oliveira-Souza, R., Hare, R.D., Bramati, I.E., et al. (2008). Psychopathy as a disorder of the moral brain: fronto-temporo-limbic grey matter reductions demonstrated by voxel-based morphometry. *Neuroimage*, 40(3), 1202-1213.

Delmaire, C., Vidailhet, M., Elbaz, A., et al. (2007). Structural abnormalities in the cerebellum and sensorimotor circuit in writer's cramp. *Neurology*, 69(4), 376-380.

Deng, M.Y., McAlonan, G.M., Cheung, C. et al. (2009). A naturalistic study of grey matter volume increase after early treatment in anti-psychotic naïve, newly diagnosed schizophrenia. *Psychopharmacology*, 206, 437-446.

Di Martino, A., Ross, K., Uddin, L. Q., Sklar, A. B., Castellanos, F. X., Milham, M. P. (2009). Functional brain correlates of social and nonsocial processes in autism spectrum disorders: an activation likelihood estimation meta-analysis. *Biological Psychiatry*, 65(1), 63-74.

Di Paola, M., Macaluso, E., Carlesimo, G.A. et al. (2007). *Journal of Neurology*, 254, 774-781.

Diamond, A., (2013). Executive functions. *Annual Review of Psychology*, 64, 135e168.

Dickstein, D.P., Milham, M.P., Nugent, A.C., et al. (2005). Frontotemporal alterations in pediatric bipolar disorder: results of a voxel-based morphometry study. *Archives of General Psychiatry*, 62(7), 734-741.

Doris, A., Belton, E., Ebmeier, K.P., et al. (2004). Reduction of cingulate gray matter density in poor outcome bipolar illness. *Psychiatry Research*, 130(2), 153-159.

Dosenbach, N. U., Fair, D. A., Miezin, F. M., Cohen, A. L., Wenger, K. K., Dosenbach, R. A., et al. (2007). Distinct brain networks for adaptive and stable task control in humans. *Proceedings of the National Academy of Sciences USA*, 104(26), 11073-11078.

Douaud, G., Groves, A.R., Tamnes, C.K., Westlye, L.T., Duff, E.P., Engvig, A., et al. (2014). A common brain network links development, aging, and vulnerability to disease. *Proceedings of the National Academy of Sciences USA*, 111, 17648-17653.

Douaud, G., Smith, S., Jenkinson, M., et al. (2007). Anatomically related grey and white matter

abnormalities in adolescent-onset schizophrenia. *Brain*, 130, 2375-2386.

Draganski, B., Thun-Hohenstein, C., Bogdahn, U., et al. (2003). "Motor circuit" gray matter changes in idiopathic cervical dystonia. *Neurology*, 61(9), 1228-1231.

Du, Y., Fryer, S.L., Fu, Z., Lin, D., Sui, J., Chen, J., et al. (2017). Dynamic functional connectivity impairments in early schizophrenia and clinical highrisk for psychosis. *Neuroimage*, 180(Pt B), 632-645.

Du, A. T., Schuff, N., Kramer, J. H., Rosen, H. J., Gorno-Tempini, M. L., Rankin, K., et al. (2007). Different regional patterns of cortical thinning in Alzheimer's disease and frontotemporal dementia. *Brain*, 130(Pt 4), 1159-1166.

Ebdrup, B.H., Glenthøj, B., Rasmussen, H., et al. (2010). Hippocampal and caudate volume reductions in antipsychotic-naive first-episode schizophrenia. *Journal of psychiatry & neuroscience*, 35(2), 95-104.

Eckart, C., Stoppel, C., Kaufmann, J., et al. (2011). Structural alterations in lateral prefrontal, parietal and posterior midline regions of men with chronic posttraumatic stress disorder. *Journal of psychiatry & neuroscience*, 36(3), 176-186.

Ecker, C., Rocha-Rego, V., Johnston, P., et al. (2010). Investigating the predictive value of whole-brain structural MR scans in autism: a pattern classification approach. *Neuroimage*, 49(1), 44-56.

Ecker, C., Suckling, J., Deoni, S.C., et al. (2012). Brain anatomy and its relationship to behavior in adults with autism spectrum disorder: a multicenter magnetic resonance imaging study. *Archives of General Psychiatry*, 69(2), 195-209.

Egger, K., Schocke, M., Weiss, E., et al. (2008). Pattern of brain atrophy in elderly patients with depression revealed by voxel-based morphometry. *Psychiatry Research*, 164(3), 237-244.

Eickhoff, S.B., Bzdok, D., Laird, A.R., Kurth, F., Fox, P.T. (2012). Activation likelihood estimation meta-analysis revisited. *Neuroimage*, 59, 2349-2361.

Eickhoff, S.B., Laird, A.R., Fox, P.M., Lancaster, J.L., Fox, P.T. (2017). Implementation errors in the GingerALE software: description and recommendations. *Human Brain Mapping*, 38, 7-11.

Eickhoff, S.B., Laird, A.R., Grefkes, C., Wang, L.E., Zilles, K., Fox, P.T. (2009). Coordinate-based activation likelihood estimation meta-analysis of neuroimaging data: a random-effects approach based on empirical estimates of spatial uncertainty. *Human Brain Mapping*, 30, 2907-2926.

Eickhoff, S.B., Nichols, T.E., Laird, A.R., Hoffstaedter, F., Amunts, K., Fox, P.T., et al. (2016). Behavior, sensitivity, and power of activation likelihood estimation characterized by massive empirical simulation. *Neuroimage*, 137, 70-85.

Ellis, C.M., Suckling, J., Amaro, E. Jr, et al. (2001). Volumetric analysis reveals corticospinal tract degeneration and extramotor involvement in ALS. *Neurology*, 57(9), 1571-1578.

Ellison-Wright, I., Bullmore, E. (2010). Anatomy of bipolar disorder and schizophrenia: a meta-analysis. *Schizophrenia Research*, 117, 1-12.

Etgen, T., Draganski, B., Ilg, C., et al. (2005). Bilateral thalamic gray matter changes in patients with restless legs syndrome. *Neuroimage*, 24(4), 1242-1247.

Etkin, A., Prater, K. E., Schatzberg, A. F., Menon, V., & Greicius, M. D. (2009). Disrupted amygdalar subregion functional connectivity and evidence of a compensatory network in generalized anxiety disorder. *Archives of General Psychiatry*, 66(12), 1361-1372.

Etkin, A., Wager, T.D. (2007). Functional neuroimaging of anxiety: a meta-analysis of emotional processing in PTSD, social anxiety disorder, and specific phobia. *American Journal of Psychiatry*, 164, 1476-1488.

Euler, M., Thoma, R.J., Gangestad, S.W., et al. (2009). The impact of developmental instability on Voxel-Based Morphometry analyses of neuroanatomical abnormalities in schizophrenia. *Schizophrenia research*, 115(1), 1-7.

Evans, A.C. (2013). Networks of anatomical covariance. *Neuroimage*, 80, 489-504.

Farrow, T.F., Whitford, T.J., Williams, L.M., et al. (2005). Diagnosis-related regional gray matter loss over two years in first episode schizophrenia and bipolar disorder. *Biological Psychiatry*, 58(9), 713-723.

Fedorenko, E., Duncan, J., Kanwisher, N. (2013). Broad domain generality in focal regions of frontal and parietal cortex. *Proceedings of the National Academy of Sciences USA*, 110, 16616e16621.

Feldmann, A., Trauninger, A., Toth, L., et al. (2008). Atrophy and decreased activation of fronto-parietal attention areas contribute to higher visual dysfunction in posterior cortical atrophy. *Psychiatry Research*, 178-184.

Filippi, M. (2009). *fMRI Techniques and Protocols*. Springer, Berlin.

Fjell, A. M., Amlien, I. K., Sneve, M. H., Grydeland, H., Tamnes, C. K., Chaplin, T. A., et al. (2015). The Roots of Alzheimer's Disease: Are High-Expanding Cortical Areas Preferentially Targeted? *Cerebral Cortex*, 25(9), 2556-2565.

Focke, N.K., Helms, G., Kaspar, S., et al. (2011). Multisite voxel-based morphometry—not quite there yet. *Neuroimage*, 56(3), 1164-1170.

Focke, N.K., Helms, G., Scheewe, S., et al. (2011). Individual voxel-based subtype prediction can differentiate progressive supranuclear palsy from idiopathic parkinson syndrome and healthy controls. *Human Brain Mapping*, 32, 1905-1915.

Focke, N.K., Thompson, P.J., Duncan, J.S. (2008a). Correlation of cognitive functions with voxel-based morphometry in patients with hippocampal sclerosis. *Epilepsy and Behavior*, 12(3), 472-476.

Focke, N.K., Symms, M.R., Burdett, J.L., Duncan, J.S. 2008b. Voxel-based analysis of whole brain FLAIR at 3T detects focal cortical dysplasia. *Epilepsia*, 49(5), 786–-793.

Fodor, J. A. (1983). *The modularity of mind.* MIT Press, New York.

Foland, L. C., Altshuler, L. L., Bookheimer, S. Y., Eisenberger, N., Townsend, J., Thompson, P. M. (2008). Evidence for deficient modulation of amygdala response by prefrontal cortex in bipolar mania. *Psychiatry Research*, 162(1), 27-37.

Foong, J., Symms, M.R., Barker, G.J., et al. (2001). Neuropathological abnormalities in schizophrenia: evidence from magnetization transfer imaging. *Brain*, 124, 882-892.

Fornito, A., Harrison, B. J., Zalesky, A., Simons, J. S. (2012). Competitive and cooperative dynamics of large-scale brain functional networks supporting recollection. *Proceedings of the National Academy of Sciences USA*, 109, 12788-12793.

Fornito, A., Zalesky, A., Breakspear, M. (2015). The connectomics of brain disorders. *Nature Reviews Neuroscience*, 16(3), 159-72.

Fox, M.D., Raichle, M.E. (2007). Spontaneous fluctuations in brain activity observed with functional magnetic resonance imaging. *Nature Reviews Neuroscience*, 8(9), 700-711.

Fox, M.D., Snyder, A.Z., Vincent, J.L., Corbetta, M., Van Essen, D.C., Raichle, M.E. (2005). The human brain is intrinsically organized into dynamic, anticorrelated functional networks. *Proceedings of the National Academy of Sciences USA*, 102(27), 9673-9678.

Fox, N.C, Ridgway, G.R., Schott, J.M. (2011). Algorithms, atrophy and Alzheimer's disease: Cautionary tales for clinical trials. *Neuroimage*, 57, 15-18.

Fox, P.T., Laird, A.R., Fox, S.P., Fox, P.M., Uecker, A.M., Crank, M., et al. (2005). BrainMap taxonomy of experimental design: description and evaluation. *Human Brain Mapping*, 25, 185-198.

Fox, P.T., Lancaster, J.L. (2002). Opinion: mapping context and content: the brainmap model. *Nature Reviews Neuroscience*, 3, 319-321.

Fox, P.T., Raichle, M.E., Mintun, M.A., Dence, C. (1988). Nonoxidative glucose consumption during focal physiologic neural activity. *Science*, 241, 462-464.

Fransson, P. (2005). Spontaneous low-frequency BOLD signal fluctuations: an fMRI investigation of the resting-state default mode of brain function hypothesis. *Human Brain Mapping*, 26(1), 15-29.

French, L., Pavlidis, P. (2011). Relationships between gene expression and brain wiring in the adult rodent brain. *PLoS Computational Biology*, 7, e1001049.

French, L., Tan, P.P., Pavlidis, P. (2011). Large-scale analysis of gene expression and connectivity in the rodent brain: insights through data integration. *Frontiers in Neuroinformatics*, 5: 12.

Friederich, H.C., Walther, S., Bendszus, M., et al. (2012). Grey matter abnormalities within cortico-limbic-striatal circuits in acute and weight-restored anorexia nervosa patients. *Neuroimage*, 59(2), 1106-1113.

Frisoni, G.B., Testa, C., Zorzan, A., et al. (2002). Detection of grey matter loss in mild Alzheimer's disease with voxel based morphometry. *Journal of neurology, neurosurgery and psychiatry*, 73(6), 657-664.

Friston, K.J. (1994). Functional and effective connectivity in neuroimaging: a synthesis. *Human Brain Mapping*, 2, 56-78.

Frodl, T.S., Koutsouleris, N., Bottlender, R., et al. (2008). Depression-related variation in brain morphology over 3 years: effects of stress? *Archives of General Psychiatry*, 65(10), 1156-1165.

Fusar-Poli, P., Broome, M.R., Woolley, J.B., et al. (2011). Altered brain function directly related to structural abnormalities in people at ultra high risk of psychosis: longitudinal VBM-fMRI study. *Journal of Psychiatric Research*, 45(2), 190-198.

Gale, S.D., Baxter, L., Roundy, N., Johnson, S.C. (2005). Traumatic brain injury and grey matter concentration: a preliminary voxel based morphometry study. *Journal of neurology, neurosurgery, and psychiatry*, 76(7), 984-988.

García-Martí, G., Aguilar, E.J., Lull, J.J., et al. (2008). Schizophrenia with auditory hallucinations: a voxel-based morphometry study. *Progress in Neuropsycho-pharmacology and Biological Psychiatry*, 32(1), 72-80.

Gardini, S., Venneri, A., Sambataro, F., Cuetos, F., Fasano, F., Marchi, M., et al. (2015). Increased functional connectivity in the default mode network in mild cognitive impairment: a maladaptive compensatory mechanism associated with poor semantic memory performance. *Journal of Alzheimer's Disease*, 45(2), 457-470.

Garrido, L., Furl, N., Draganski, B., et al. (2009). Voxel-based morphometry reveals reduced grey matter volume in the temporal cortex of developmental prosopagnosics. *Brain*, 132, 3443-3455.

Gascon, E., Vutskits, L., Kiss, J.Z. (2007). Polysialic acid-neural cell adhesion molecule in brain plasticity: from synapses to integration of new neurons. *Brain Research Reviews*, 56, 101-118.

Gaudio, S., Nocchi, F., Franchin, T., et al. (2011). Gray matter decrease distribution in the early stages of Anorexia Nervosa restrictive type in adolescents. *Psychiatry Research*, 191(1), 24-30.

Gavazzi, C., Nave, R.D., Petralli, R., et al. (2007). Combining functional and structural brain magnetic resonance imaging in Huntington disease. *Journal of Computer Assisted Tomography*, 31(4), 574-580.

Gejman, P.V., Sanders, A.R., Kendler, K.S. (2011). Genetics of schizophrenia: new findings and challenges. *Annual Review of Genomics and Human Genetics*, 12, 121-144.

Geschwind, D.H., Levitt, P. (2007). Autism spectrum disorders: developmental disconnection syndromes. *Current Opinion in Neurobiology*, 17, 103-111.

Ghosh, B.C., Calder, A.J., Peers, P.V., et al. (2012). Social cognitive deficits and their neural correlates in progressive supranuclear palsy. *Brain*, 135, 2089-2102.

Gilbert, A.R., Mataix-Cols, D., Almeida, J.R., et al. (2008). Brain structure and symptom dimension relationships in obsessive-compulsive disorder: a voxel-based morphometry study. *Journal of Affective Disorders*. 109, 117-126.

Giordano, A., Tessitore, A., Corbo, D., et al. (2013). Clinical and cognitive correlations of regional gray matter atrophy in progressive supranuclear palsy. *Parkinsonism and Related Disorders*, 19(6), 590-594.

Giuliani, N.R., Calhoun, V.D., Pearlson, G.D., et al. (2005). Voxel-based morphometry versus region of interest: a comparison of two methods for analyzing gray matter differences in schizophrenia. *Schizophrenia Research*, 74, 135-147.

Glasser, M.F., Sotiropoulos, S.N., Wilson, J.A., Coalson, T.S., Fischl, B., Andersson, J.L., et al. (2013). The minimal preprocessing pipelines for the Human Connectome Project. *Neuroimage*, 80, 105-124.

Gobbi, C., Rocca, M.A., Riccitelli, G., et al. (2014). Influence of the topography of brain damage on depression and fatigue in patients with multiple sclerosis. *Multiple Sclerosis*, 20(2), 192-201.

Goedert, M., Clavaguera, F., Tolnay, M. (2010). The propagation of prion-like protein inclusions in neurodegenerative diseases. *Trends in Neuroscience*, 33, 317-325.

Goel, P., Kuceyeski, A., LoCastro, E., Raj, A. (2014). Spatial patterns of genomewide expression profiles reflect anatomic and fiber connectivity architecture of healthy human brain. *Human Brain Mapping*, 35, 4204-4218.

Gong, Q., Wu, Q., Scarpazza, C., et al. (2011). Prognostic prediction of therapeutic response in depression using high-field MR imaging. *Neuroimage*, 55(4),1497-1503.

Gong, X., Lu, W., Kendrick, K.M., Pu, W., Wang, C., Jin, L., et al. (2014). A brain-wide association study of DISC1 genetic variants reveals a relationship with the structure and functional connectivity of the precuneus in schizophrenia. *Human brain mapping*, 35(11), 5414-5430.

Goodkind, M., Eickhoff, S.B., Oathes, D.J., Jiang, Y., Chang, A., Jones-Hagata, L.B., et al. (2015). Identification of a common neurobiological substrate for mental illness. *JAMA Psychiatry*, 72, 305-315.

Goulden, N., Khusnulina, A., Davis, N. J., Bracewell, R. M., Bokde, A. L., McNulty, J. P., et al. (2014). The salience network is responsible for switching between the default mode network and the central executive network: replication from DCM. *Neuroimage*, 99, 180-190.

Granert, O., Peller, M., Jabusch, H., et al. (2011). Sensorimotor skills and focal dystonia are linked to putaminal grey-matter volume in pianists. *Journal of Neurology, Neurosurgery & Psychiatry*, 82, 1225-1231.

Gregory, S., ffytche, D., Simmons, A., et al. (2012). The antisocial brain: psychopathy matters. *Archives of General Psychiatry*, 69(9), 962-972.

Grieve, S.M., Korgaonkar, M.S., Koslow, S.H., et al. (2013). Widespread reductions in gray matter volume in depression. *NeuroImage. Clinical*, 3, 332-339.

Gross, R.G., Ash, S., McMillan, C.T., et al. (2010). Impaired information integration contributes to communication difficulty in corticobasal syndrome. *Cognitive and behavioral neurology*, 23(1), 1-7.

Grosskreutz, J., Kaufmann, J., Frädrich, J., et al. (2006). Widespread sensorimotor and frontal cortical atrophy in Amyotrophic Lateral Sclerosis. *BMC neurology*, 6, 17, doi:10.1186/1471-2377-6-17.

Guedj, E., Barbeau, E.J., Didic, M. et al. (2009). Effects of medial temporal lobe degeneration on brain perfusion in amnestic MCI of AD type: deafferentation and functional compensation? *European Journal of Nuclear Medicine and Molecular Imaging*, 36, 1101-1112.

Guest, W.C., Silverman, J.M., Pokrishevsky, E., O'Neill, M.A., Grad, L.I., Cashman, N.R. (2011). Generalization of the prion hypothesis to other neurodegenerative diseases: an imperfect fit. *Journal of toxicology and environmental health. Part A*, 74, 1433-1459.

Guimera, R., Nunes Amaral, L. A. /2005). Functional cartography of complex metabolic networks. *Nature*, 433, 895-900.

Guo, W., Liu, F., Yu, M., et al. (2014). Functional and anatomical brain deficits in drug-naive major depressive disorder. *Progress in Neuropsychopharmacology and Biological Psychiatry*, 54, 1-6.

Guo, X., Wang, Z., Li, K., et al. (2010). Voxel-based assessment of gray and white matter volumes in Alzheimer's disease. *Neuroscience letters*, 468(2), 146-150.

Gupta, C.N., Calhoun, V.D., Rachakonda, S., Chen, J., Patel, V., Liu, J., et al. (2015). Patterns of gray matter abnormalities in schizophrenia based on an international mega-analysis. *Schizophrenia Bulletin*, 41, 1133-1142.

Ha, T.H., Ha, K., Kim, J.H., Choi, J.E. (2009). Regional brain gray matter abnormalities in patients with bipolar II disorder: a comparison study with bipolar I patients and healthy controls. *Neuroscience Letters*, 456(1), 44-48.

Ha, T.H., Youn, T., Ha, K.S., et al. (2004). Gray matter abnormalities in paranoid schizophrenia and their clinical correlations. *Psychiatry Research*, 132(3), 251-260.

Hagmann, P., Jonasson, L., Maeder, P., Thiran, J.P., Wedeen, V.J., Meuli, R. (2006). Understanding diffusion MR imaging techniques: from scalar diffusion-weighted imaging to diffusion tensor imaging and beyond. *Radiographics*, 26 Suppl 1, S205-223.

Hakamata, Y., Matsuoka, Y., Inagaki, M., et al. (2007). Structure of orbitofrontal cortex and its longitudinal course in cancer-related post-traumatic stress disorder. *Neuroscience Research*, 59(4), 383-389.

Haldane, M., Cunningham, G., Androutsos, C., Frangou, S. (2008). Structural brain correlates of response inhibition in Bipolar Disorder I. *Journal of Psychopharmacology*, 22(2), 138-143.

Hall, A.M., Moore, R.Y., Lopez, O.L., et al. (2008). Basal forebrain atrophy is a presymptomatic marker for Alzheimer's disease. *Alzheimer's & dementia*, 4(4), 271-279.

Haller, S., Xekardaki, A., Delaloye, C., et al. (2011). Combined analysis of grey matter voxel-based morphometry and white matter tract-based spatial statistics in late-life bipolar disorder. *Journal of psychiatry & neuroscience*, 36(6), 391-401.

Hämäläinen, A., Pihlajamäki, M., Tanila, H., et al. (2007). Increased fMRI responses during encoding in mild cognitive impairment. *Neurobiology of Aging*, 28(12), 1889-903.

Hamilton, J.P., Etkin, A., Furman, D.J., Lemus, M.G., Johnson, R.F., Gotlib, I.H. (2012). Functional neuroimaging of major depressive disorder: a meta-analysis and new integration of base line activation and neural response data. *American Journal of Psychiatry*, 169, 693-703.

Hardy, J., Revesz, T. (2012). The spread of Neurodegenerative disease. *New England Journal of Medidine*, 366, 2126-2128.

Harriger, L., van den Heuvel, M. P. & Sporns, O. (2012). Rich club organization of macaque cerebral cortex and its role in network communication. *PLoS ONE*, 7, e46497.

Hawrylycz, M.J., Lein, E.S., Guillozet-Bongaarts, A.L., Shen, E.H., Ng, L., Miller, J.A., et al. (2012). An anatomically comprehensive atlas of the adult human brain transcriptome. *Nature*, 489, 391-399.

Hebb, D.O. (1949). *The organization of behavior: a neuropsychological theory*. New York: Wiley.

Heck, A., Fastenrath, M., Ackermann, S., Auschra, B., Bickel, H., Coynel, D., Gschwind, L., Jessen, F., Kaduszkiewicz, H., Maier, W., Milnik, A., Pentzek, M., Riedel-Heller, S.G., Ripke, S., Spalek, K., Sullivan, P., Vogler, C., Wagner, M., Weyerer, S., Wolfsgruber, S., de Quervain, D.J., Papassotiropoulos, A. (2014). Converging genetic and functional brain imaging evidence links neuronal excitability to working memory, psychiatric disease, and brain activity. *Neuron*, 81(5), 1203-1213.

Henley, S.M., Wild, E.J., Hobbs, N.Z., et al. (2009). Relationship between CAG repeat length and brain volume in premanifest and early Huntington's disease. *Journal of Neurology*, 256(2), 203-212.

Herold, R., Feldmann, Á., Simon, M., et al. (2009). Regional gray matter reduction and theory of mind deficit in the early phase of schizophrenia: a voxel-based morphometric study. *Acta Psychiatrica Scandinavica*, 119: 199-208.

Herringa, R., Phillips, M., Almeida, J., et al. (2012). Post-traumatic stress symptoms correlate with smaller subgenual cingulate, caudate, and insula volumes in unmedicated combat veterans. *Psychiatry research*, 203, 139-145.

Hilgetag, C.C., Goulas, A. (2016). Is the brain really a small-world network? *Brain Structure & Function*, 221, 2361-2366, doi 10.1007/s00429-015-1035-6.

Hirao, K., Miyata, J., Fujiwara, H., et al. (2008). Theory of mind and frontal lobe pathology in schizophrenia: a voxel-based morphometry study. *Schizophrenia Research*, 105, 165-174.

Hirao, K,, Ohnishi, T., Matsuda, H., et al. (2006). Functional interactions between entorhinal cortex and posterior cingulate cortex at the very early stage of Alzheimer's disease using brain perfusion single-photon emission computed tomography. *Nuclear Medicine Communications*, 27(2), 151-156.

Hirokawa, N., Niwa, S. & Tanaka, Y. (2010). Molecular motors in neurons: transport mechanisms and roles in brain function, development, and disease. *Neuron*, 68, 610-638.

Hobert, O. (2003). Behavioral plasticity in C. elegans: Paradigms, circuits, genes. *Journal of Neurobiology*, 54, 203-223.

Hoeft, F., Lightbody, A.A., Hazlett, H.C., et al. (2008). Morphometric spatial patterns differentiating boys with fragile X syndrome, typically developing boys, and developmentally delayed boys aged 1 to 3 years. *Archives of general psychiatry*, 65(9), 1087-1097.

Hoeft, F., Meyler, A., Hernandez, A., et al. (2007). Functional and morphometric brain dissociation between dyslexia and reading ability. *Proceedings of the National Academy of Sciences of the United States of America*, 104(10), 4234-4239.

Honea, R.A., Meyer-Lindenberg, A., Hobbs, K.B., et al. (2008). Is gray matter volume an intermediate phenotype for schizophrenia? A voxel-based morphometry study of patients with schizophrenia and their healthy siblings. *Biological psychiatry*, 63(5), 465-474.

Honea, R.A., Thomas, G.P., Harsha, A., et al. (2009). Cardiorespiratory fitness and preserved medial temporal lobe volume in Alzheimer disease. *Alzheimer disease and associated disorders*, 23(3), 188-197.

Honey, C. J., Sporns, O. (2008). Dynamical consequences of lesions in cortical networks. *Human Brain Mapping*, 29, 802-809 (2008).

Honey, C. J., Sporns, O., Cammoun, L., Gigandet, X., Thiran, J. P., Meuli, R., et al. (2009). Predicting human resting-state functional connectivity from structural connectivity. *Procedings of the National Academy of Sciences USA*, 106, 2035-2040.

Horn, H., Federspiel, A., Wirth, M., et al. (2009). Structural and metabolic changes in language areas linked to formal thought disorder. *British Journal of Psychiatry*, 194(2), 130-138.

Horn, H., Federspiel, A., Wirth, M., et al. (2010). Gray matter volume differences specific to formal thought disorder in schizophrenia. *Psychiatry Research*, 182(2), 183-186.

Huang, H., Ding, M. (2016). Linking Functional Connectivity and Structural Connectivity Quantitatively: A Comparison of Methods. *Brain connectivity*, 6(2), 99-108.

Huber, A.B., Kolodkin, A.L., Ginty, D.D., Cloutier, J.F. (2003). Signaling at the growth cone: Ligand-Receptor Complexes and the Control of Axon Growth and Guidance. *Annual Review of Neuroscience*, 26, 509-563.

Huey, E.D., Pardini, M., Cavanagh, A., et al. (2009). Association of ideomotor apraxia with frontal gray matter volume loss in corticobasal syndrome. *Archives of neurology*, 66(10), 1274-1280.

Hulshoff Pol, H.E., Schnack, H.G., Mandl, R.C., et al. (2001). Focal gray matter density changes in schizophrenia. *Archives of General Psychiatry*, 58(12), 1118-1125.

Hulshoff Pol, H.E., Schnack, H.G., Mandl, R.C., et al. (2004). Focal white matter density changes in schizophrenia: reduced inter-hemispheric connectivity. *Neuroimage*, 21(1), 27-35.

Hulshoff Pol, H.E., Schnack, H.G., Mandl, R.C., et al. (2006). Gray and white matter density changes in monozygotic and same-sex dizygotic twins discordant for schizophrenia using voxel-based morphometry. *Neuroimage*, 31(2), 482-488.

Hyde, K.L., Samson, F., Evans, A.C., Mottron, L. (2010). Neuroanatomical differences in brain areas implicated in perceptual and other core features of autism revealed by cortical thickness analysis and voxel-based morphometry. *Human Brain Mapping*, 31, 556-566.

Ille, R., Schäfer, A., Scharmüller, W., et al. (2011). Emotion recognition and experience in Huntington disease: a voxel-based morphometry study. *Journal of psychiatry & neuroscience*, 36(6), 383-390.

Inkster, B., Rao, A.W., Ridler, K., et al. (2011). Structural Brain Changes in Patients with Recurrent Major Depressive Disorder Presenting with Anxiety Symptoms. *Journal of Neuroimaging*, 21, 375-382.

Ishii, K., Sasaki, H., Kono, A.K., et al. (2005). Comparison of gray matter and metabolic reduction in mild Alzheimer's disease using FDG-PET and voxel-based morphometric MR studies. *European Journal of Nuclear Medicine and Molecular Imaging*, 32(8), 959-963.

Iturria-Medina, Y., Evans, A.C. (2015). On the central role of brain connectivity in neurodegenerative disease progression. *Frontiers in Aging Neuroscience*, 7, 90.

Iturria-Medina, Y., Sotero, R.C., Toussaint, P.J., Evans, A.C. (2014). Epidemic spreading model to characterize misfolded proteins propagation in aging and associated neurodegenerative disorders. *PLoS Computational Biology*, 10, e1003956.

Ivo, R., Nicklas, A., Dargel, J., et al. (2013). Brain structural and psychometric alterations in chronic low back pain. *European spine journal*, 22(9), 1958-1964.

Jagust, W. (2013). Vulnerable neural systems and the borderland of brain aging and neurodegeneration. *Neuron*, 77, 219-234.

Jang, D.P., Namkoong, K., Kim, J.J., et al. (2007). The relationship between brain morphometry and neuropsychological performance in alcohol dependence. *Neuroscience Letters*, 428(1), 21-26.

Janssen, J., Reig, S., Parellada, M., et al. (2008). Regional gray matter volume deficits in adolescents with first-episode psychosis. *Journal of American Academy of Child and Adolescent Psychiatry*, 47(11), 1311-1320.

Jayakumar, P.N., Venkatasubramanian, G., Gangadhar, B.N., et al. (2005). Optimized voxel-based morphometry of gray matter volume in first-episode, antipsychotic-naive schizophrenia. *Progress in Neuropsychopharmacology and Biological Psychiatry*, 29(4), 587-591.

Jones, D. T., Knopman, D. S., Gunter, J. L., Graff-Radford, J., Vemuri, P., Boeve, B. F., et al. (2016). Cascading network failure across the Alzheimer's disease spectrum. *Brain*, 139(Pt 2), 547-562.

Joos, A., Klöppel, S., Hartmann, A., et al. (2010). Voxel-based morphometry in eating disorders: correlation of psychopathology with grey matter volume. *Psychiatry Research*, 182(2), 146-151.

Jucker, M., Walker, L.C. (2011). Pathogenic protein seeding in Alzheimer disease and other neurodegenerative disorders. *Annuals in Neurology*, 70, 532-540.

Kanda, T., Ishii, K., Uemura, T., et al. (2008). Comparison of grey matter and metabolic reductions in frontotemporal dementia using FDG-PET and voxel-based morphometric MR studies. *European Journal of Nuclear Medicine and Molecular Imaging*, 35(12), 2227-2234.

Kania, A., Johnson, R.L., Jessell, T.M. (2000). Coordinate Roles for LIM Homeobox Genes in Directing the Dorsoventral Trajectory of Motor Axons in the Vertebrate Limb. *Cell*, 102, 161-173.

Kapur, S. (2003). Psychosis as a state of aberrant salience: a framework linking biology, phenomenology, and pharmacology in schizophrenia. *American Journal of Psychiatry*, 160(1), 13-23.

Kasai, K., Yamasue, H., Gilbertson, M.W., et al. (2008). Evidence for acquired pregenual anterior cingulate gray matter loss from a twin study of combat-related posttraumatic stress disorder. *Biological psychiatry*, 63(6), 550-556.

Kasparek, T., Marecek, R., Schwarz, D., Prikryl, R., Vanicek, J., Mikl, M., et al. (2010). Source-based morphometry of gray matter volume in men with first-episode schizophrenia. *Human Brain Mapping*, 31, 300-310.

Kaspárek, T., Prikryl, R., Mikl, M., et al. (2007). Prefrontal but not temporal grey matter changes in males with first-episode schizophrenia. *Progress in Neuropsycho-pharmacology and Biological Psychiatry*, 31(1), 151-157.

Kassubek, J., Juengling, F.D., Ecker, D., Landwehrmeyer, G.B., et al. (2005). Thalamic atrophy in Huntington's disease co-varies with cognitive performance: a morphometric MRI analysis. *Cerebral Cortex*, 15(6), 846-853.

Kassubek, J., Juengling, F.D., Kioschies, T., et al. (2004). Topography of cerebral atrophy in early Huntington's disease: a voxel based morphometric MRI study. *Journal of neurology, neurosurgery, and psychiatry*, 75(2), 213-220.

Kassubek, J., Juengling, F.D., Sperfeld, A.D. (2007). Widespread white matter changes in Kennedy disease: a voxel based morphometry study. *Journal of neurology, neurosurgery, and psychiatry*, 78(11), 1209-1212.

Kato, S., Watanabe, H., Senda, J., et al. (2012). Widespread cortical and subcortical brain atrophy in Parkinson's disease with excessive daytime sleepiness. *Journal of Neurology*, 259(2), 318-326.

Kaufmann, C., Schuld, A., Pollmächer, T., Auer, D.P. (2002). Reduced cortical gray matter in narcolepsy: preliminary findings with voxel-based morphometry. *Neurology*, 58(12), 1852-1855.

Kawachi, T., Ishii, K., Sakamoto, S., et al. (2006). Comparison of the diagnostic performance of FDG-PET and VBM-MRI in very mild Alzheimer's disease. *European Journal of Nuclear Medicine and Molecular Imaging*, 33(7), 801-809.

Kawada, R,, Yoshizumi, M., Hirao, K., et al. (2009). Brain volume and dysexecutive behavior in schizophrenia. *Progress in Neuropsychopharmacology and Biological Psychiatry*, 33(7), 1255-1260.

Kawasaki, Y., Suzuki, M., Kherif, F., et al. (2007). Multivariate voxel-based morphometry successfully differentiates schizophrenia patients from healthy controls. *Neuroimage*, 34(1), 235-242.

Kawasaki, Y., Suzuki, M., Nohara, S., et al. (2004). Structural brain differences in patients with schizophrenia and schizotypal disorder demonstrated by voxel-based morphometry. *European Archives of Psychiatry and Clinical Neuroscience*, 254(6), 406-414.

Ke, X., Hong, S., Tang, T., et al. (2008). Voxel-based morphometry study on brain structure in children with high-functioning autism. *Neuroreport*, 19(9), 921-925.

Keller, S.S., Cresswell, P., Denby, C., et al. (2007). Persistent seizures following left temporal lobe surgery are associated with posterior and bilateral structural and functional brain abnormalities. *Epilepsy Research*, 74, 131-139.

Keller, S.S., Roberts, N. (2008). Voxel-based morphometry of temporal lobe epilepsy: an introduction and review of the literature. *Epilepsia*, 49(5), 741-757.

Keller, S.S., Wieshmann, U.C., Mackay, C.E., et al. (2002). Voxel based morphometry of grey matter abnormalities in patients with medically intractable temporal lobe epilepsy: effects of side of seizure onset and epilepsy duration. *Journal of neurology, neurosurgery, and psychiatry*, 73(6), 648-655.

Kelly, C., Toro, R., Di Martino, A., Cox, C. L., Bellec, P., Castellanos, F. X., et al. (2012). A convergent functional architecture of the insula emerges across imaging modalities. *Neuroimage*, 61(4), 1129-1142.

Kesler, S.R., Reiss, A.L., Vohr, B., et al. (2008). Brain volume reductions within multiple cognitive systems in male preterm children at age twelve. *The Journal of pediatrics*, 152(4), 513-520.

Khaleeli, Z., Cercignani, M., Audoin, B., et al. (2007). Localized grey matter damage in early primary progressive multiple sclerosis contributes to disability. *Neuroimage*, 37(1), 253-261.

Kim, D., Cho, H.B., Dager, S.R., et al. (2013). Posterior cerebellar vermal deficits in bipolar disorder. *Journal of affective disorders*, 150(2), 499-506.

Kim, E.J., Rabinovici, G.D., Seeley, W.W., et al. (2007). Patterns of MRI atrophy in tau positive and ubiquitin positive frontotemporal lobar degeneration. *Journal of neurology, neurosurgery, and psychiatry*, 78(12), 1375-1378.

Kim, J.H., Lee, J.K., Koh, S.B., et al. (2007). Regional grey matter abnormalities in juvenile myoclonic epilepsy: a voxel-based morphometry study. *Neuroimage*, 37(4), 1132-1137.

Kim, M.J., Hamilton, J.P., Gotlib, I.H. (2008). Reduced caudate gray matter volume in women with major depressive disorder. *Psychiatry research*, 164(2), 114-122.

Kim, S., Youn, Y.C., Hsiung, G.Y., et al. (2011). Voxel-based morphometric study of brain volume changes in patients with Alzheimer's disease assessed according to the Clinical Dementia Rating score. *Journal of Clinical Neuroscience*, 18(7), 916-921.

Kim, S.J., Lyoo, I.K., Lee, Y.S., et al. (2009), Gray matter deficits in young adults with narcolepsy. *Acta Neurologica Scandinavica*, 119, 61-67.

Kiryushko, D., Berezin, V., Bock, E. (2004). Regulators of neurite outgrowth: role of cell adhesion molecules. *Annals of the New York Academy of Sciences*, 1014, 140-154.

Kitsak, M., Gallos, L. K., Havlin, S., Liljeros, F., Muchnik, L. (2010). Identification of influential spreaders in complex networks. *Nature Physics*, 6, 888-893.

Klein, T. A., Ullsperger, M., Danielmeier, C. (2013). Error awareness and the insula: links to neurological and psychiatric diseases. *Frontiers in Human Neuroscience*, 7, 14.

Klin, A., Jones, W., Schultz, R., & Volkmar, F. (2003). The enactive mind, or from actions to cognition: lessons from autism. *Philosophical Transactions of the Royal Society London B Biological Sciences*, 358(1430), 345-360.

Klupp, E., et al. (2014). In Alzheimer's disease, hypometabolism in low-amyloid brain regions may be a functional consequence of pathologies in connected brain regions. *Brain Connectivity*, 4, 371-383.

Kobel, M., Bechtel, N., Specht, K., et al. (2010). Structural and functional imaging approaches in attention deficit/hyperactivity disorder: does the temporal lobe play a key role? *Psychiatry Research*, 183(3), 230-236.

Kohn, N., Eickhoff, S.B., Scheller, M., Laird, A.R., Fox, P.T., Habel, U. (2014). Neural network of cognitive emotion regulationean ALE meta-analysis and MACM analysis. *Neuroimage*, 87, 345e355.

Kondor, R.I., Lafferty, J. (2002). Diffusion kernels on graphs and other discrete input spaces. In: Proceedings of the nineteenth international conference on machine learning (ICML). Morgan Kaufmann Publishers Inc., pp. 315-322.

Koprivová, J., Horácek, J., Tintera, J., et al. (2009). Medial frontal and dorsal cortical morphometric abnormalities are related to obsessive-compulsive disorder. *Neuroscience Letters*, 464(1), 62-66.

Korth, C. (2012). Aggregated proteins in schizophrenia and other chronic mental diseases: DISC1opathies. *Prion*, 6, 134-141.

Kosaka, H., Omori, M., Munesue, T., et al. (2010). Smaller insula and inferior frontal volumes in young adults with pervasive developmental disorders. *Neuroimage*, 50(4), 1357-1363.

Koskenkorva, P., Khyuppenen, J., Niskanen, E., et al. (2009). Motor cortex and thalamic atrophy in Unverricht-Lundborg disease: voxel-based morphometric study. *Neurology*, 73(8), 606-611.

Kotz, S., Balakrishnan, N., Johnson, N.L. (2000). *Continuous Multivariate Distributions*. Wiley, New York.

Koutsouleris, N., Gaser, C., Jäger, M., et al. (2008). Structural correlates of psychopathological symptom dimensions in schizophrenia: a voxel-based morphometric study. *Neuroimage*, 39(4), 1600-1612.

Kraus, A., Groveman, B.R., Caughey, B. (2013). Prions and the potential transmissibility of protein misfolding diseases. *Annual Review of Microbiology*, 67, 543-564.

Kubicki, M., Shenton, M.E., Salisbury, D.F., et al. (2002). Voxel-based morphometric analysis of gray matter in first episode schizophrenia. *Neuroimage*, 17(4), 1711-1719.

Kuchinad, A., Schweinhardt, P., Seminowicz, D.A., et al. (2007). Accelerated brain gray matter loss in fibromyalgia patients: premature aging of the brain? *The Journal of neuroscience*, 27(15), 4004-4007.

Kurth, F., Narr, K.L., Woods, R.P., et al. (2011). Diminished gray matter within the hypothalamus in autism disorder: a potential link to hormonal effects? *Biological psychiatry*, 70(3), 278-282.

Kwon, H., Ow, A.W., Pedatella, K.E., et al. (2004). Voxel-based morphometry elucidates structural neuroanatomy of high-functioning autism and Asperger syndrome. *Developmental Medicine & Child Neurology*, 46: 760-764.

Labate, A., Cerasa, A., Aguglia, U., et al. (2010), Voxel-based morphometry of sporadic epileptic patients with mesiotemporal sclerosis. *Epilepsia*, 51, 506-510.

Ladouceur, C.D., Almeida, J., Birmaher, B., et al. (2008). Subcortical gray matter volume abnormalities in healthy bipolar offspring: potential neuroanatomical risk marker for bipolar disorder? *Journal of the American Academy of Child and Adolescent Psychiatry*, 47(5), 532-539.

Lagarde, J., Valabrègue, R., Corvol, J.C., et al. (2013). Are frontal cognitive and atrophy patterns different in PSP and bvFTD? A comparative neuropsychological and VBM study. *PloS one*, 8(11), e80353. doi:10.1371/journal.pone.0080353.

Lagarias, J.C., Reeds, J.A., Wright, M.H., Wright, P.E. (1998). Convergence properties of the nelder–mead simplex method in low dimensions. *SIAM Journal on Optimization*, 9, 112-147.

Lahiri, D.K., Maloney, B. (2010). The "LEARn" (Latent Early-life Associated Regulation) model integrates environmental risk factors and the developmental basis of Alzheimer's disease, and proposes remedial steps. *Experimental Gerontology*, 45, 291-296.

Lai, C.H., Wu, Y.T. (2012). Fronto-temporo-insula gray matter alterations of first-episode, drug-naïve and very late-onset panic disorder patients. *Journal of Affective Disorders*, 140(3), 285-291.

Laird, A.R., Fox, P.M., Price, C.J., Glahn, D.C., Uecker, A.M., Lancaster, J.L., et al. (2005a). ALE meta-analysis: controlling the false discovery rate and performing statistical contrasts. *Hum Brain Mapping*, 25, 155-164.

Laird, A.R., Lancaster, J.L., Fox, P.T. (2005b). BrainMap: the social evolution of a human brain mapping database. *Neuroinformatics*, 3, 65-78.

Lancaster, J. L., Laird, A. R., Eickhoff, S. B., Martinez, M. J., Fox, P. M., Fox, P. T. (2012). Automated regional behavioral analysis for human brain images. *Frontiers in Neuroinformatics*, 6, 23.

Lancaster, J. L., Woldorff, M. G., Parsons, L. M., Liotti, M., Freitas, C. S., Rainey, L., et al. (2000). Automated Talairach atlas labels for functional brain mapping. *Human Brain Mapping*, 10(3), 120-131.

Le Bihan, D., Mangin, J.F., Poupon, C., Clark, C.A., Pappata, S., Molko, N., Chabriat, H. (2001). Diffusion tensor imaging: concepts and applications. *Journal of Magnetic Resonance Imaging*, 13, 534-546.

Lee, H., Heller, A.S., van Reekum, C.M., Nelson, B., Davidson, R.J. (2012). Amygdala-prefrontal coupling underlies individual differences in emotion regulation. *Neuroimage*, 62(3), 1575-1581.

Lee, H.Y., Tae, W.S., Yoon, H.K., et al. (2011). Demonstration of decreased gray matter concentration in the midbrain encompassing the dorsal raphe nucleus and the limbic subcortical regions in major depressive disorder: an optimized voxel-based morphometry study. *Journal of Affective Disorders*, 133(1-2), 128-136.

Lee, J.E., Cho, K.H., Song, S.K., et al. (2014). Exploratory analysis of neuropsychological and neuroanatomical correlates of progressive mild cognitive impairment in Parkinson's disease. *Journal of Neurology, Neurosurgery and Psychiatry*, 85(1), 7-16.

Leung, K.K., Lee, T.M., Wong, M.M., et al. (2009). Neural correlates of attention biases of people with major depressive disorder: a voxel-based morphometric study. *Psychological Medicine*, 39(7), 1097-106.

Li, H., Chan, R.C., McAlonan, G.M., Gong, Q.Y. (2010). Facial emotion processing in schizophrenia: a meta-analysis of functional neuroimaging data. *Schizophrenia Bulletin*, 36(5), 1029-1039.

Li, C.T., Lin, C.P., Chou, K.H., et al. (2010). Structural and cognitive deficits in remitting and non-remitting recurrent depression: a voxel-based morphometric study. *Neuroimage*, 50(1), 347-356.

Li, L., Chen, S., Liu, J., et al. (2006). Magnetic resonance imaging and magnetic resonance spectroscopy study of deficits in hippocampal structure in fire victims with recent-onset posttraumatic stress disorder. *Canadian Journal of Psychiatry*, 51(7), 431-437.

Li, M., Cui, L., Deng, W., et al. (2011). Voxel-based morphometric analysis on the volume of gray matter in bipolar I disorder. *Psychiatry Research*, 191(2), 92-97.

Liang, X., Zou, Q., He, Y., Yang, Y. (2013). Coupling of functional connectivity and regional cerebral blood flow reveals a physiological basis for network hubs of the human brain. *Proceedings of the National Academy of Sciences USA*, 1929-1934.

Libon, D.J., McMillan, C., Gunawardena, D., et al. (2009). Neurocognitive contributions to verbal fluency deficits in frontotemporal lobar degeneration. *Neurology*, 73(7), 535-542.

Lichtman, J.W., Sanes, J.R. (2008). Ome sweet ome: what can the genome tell us about the connectome? *Current Opinion in Neurobiology*, 18(3), 346-353.
doi: 10.1016/j.conb.2008.08.010.

Lin, A., Chen, F., Liu, F., et al. (2013). Regional gray matter atrophy and neuropsychologcal problems in relapsing-remitting multiple sclerosis. *Neural regeneration research*, 8(21), 1958-1965.

Lin, C.H., Chen, C.M., Lu, M.K., Tsai, C.H., Chiou, J.C., Liao, J.R., et al. (2013). VBM reveals brain volume differences between Parkinson's disease and essential tremor patients. *Frontiers in Human Neuroscience*, 7: 247. doi:10.3389/fnhum.2013.00247.

Lin, K., Jackowski, A.P., Carrete, H. Jr, et al. (2009). Voxel-based morphometry evaluation of patients with photosensitive juvenile myoclonic epilepsy. *Epilepsy Research*, 86, 138-145.

Liu, C.H., Jing, B., Ma, X., et al. (2014). Voxel-based morphometry study of the insular cortex in female patients with current and remitted depression. *Neuroscience*, 262, 190-199.

Liu, M., Concha, L., Beaulieu, C., Gross, D.W. (2011). Distinct white matter abnormalities in different idiopathic generalized epilepsy syndromes. *Epilepsia*, 52, 2267-2275.

Lochhead, R.A., Parsey, R.V., Oquendo, M.A., Mann, J.J. (2004). Regional brain gray matter volume differences in patients with bipolar disorder as assessed by optimized voxel-based morphometry. *Biological Psychiatry*, 55(12), 1154-1162.

Löwel, S., Singer, W. (1992). Selection of Intrinsic Horizontal Connections in the Visual Cortex by Correlated Neuronal Activity. *Science*, 255(5041), 209-212. doi: 10.1126/science.1372754.

Lu, C., Peng, D., Chen, C., et al. (2010). Altered effective connectivity and anomalous anatomy in the basal ganglia-thalamocortical circuit of stuttering speakers. *Cortex*, 46(1), 49-67.

Ludolph, A.G., Juengling, F.D., Libal, G., et al. (2006). Grey-matter abnormalities in boys with Tourette syndrome: magnetic resonance imaging study using optimised voxel-based morphometry. *British Journal of Psychiatry*, 188, 484-485.

Lui, S., Deng, W., Huang, X., et al. (2009). Association of cerebral deficits with clinical symptoms in antipsychotic-naive first-episode schizophrenia: an optimized voxel-based morphometry and resting state functional connectivity study. *American Journal of Psychiatry*, 166(2), 196-205.

Lyoo, I.K., Kim, M.J., Stoll, A.L., et al. (2004). Frontal lobe gray matter density decreases in bipolar I disorder. *Biological Psychiatry*, 55(6), 648-651.

Mainz, V., Schulte-Rüther, M., Fink, G.R., et al. (2012). Structural brain abnormalities in adolescent anorexia nervosa before and after weight recovery and associated hormonal changes. *Psychosomatic Medicine*, 74(6), 574-582.

Mak, A.K., Wong, M.M., Han, S.H., Lee, T.M. (2009). Gray matter reduction associated with emotion regulation in female outpatients with major depressive disorder: a voxel-based morphometry study. *Progress in Neuropsychopharmacology and Biological Psychiatry*, 33(7), 1184-1190.

Mak, E., Zhou, J., Tan, L.C.S., et al. (2014). Cognitive deficits in mild Parkinson's disease are associated with distinct areas of grey matter atrophy. *Journal of Neurology, Neurosurgery & Psychiatry*, 85, 576-580.

Mañeru, C., Serra-Grabulosa, J.M., Junqué, C., et al. (2003). Residual Hippocampal Atrophy in Asphyxiated Term Neonates. *Journal of Neuroimaging*, 13: 68-74.

Mantel, N. (1967). The detection of disease clustering and a generalized regression approach. *Cancer Research*, 27, 209-220.

Manuello, J., Nani, A., Premi, E., Borroni, B., Costa, T., Tatu, K., et al. (2018). The pathoconnectivity profile of alzheimer's disease: a morphometric coalteration network analysis. *Frontiers in Neurology*, 8, 739.

Marcelis, M., Suckling, J., Woodruff, P., et al. (2003). Searching for a structural endophenotype in psychosis using computational morphometry. *Psychiatry Research*, 122(3), 153-167.

Markus, A., Patel, T.D., Snider, W.D. (2002). Neurotrophic factors and axonal growth. *Current Opinion in Neurobiology*, 12, 523-531.

Martí-Bonmatí, L., Lull, J.J., García-Martí, G., et al. (2007). Chronic auditory hallucinations in schizophrenic patients: MR analysis of the coincidence between functional and morphologic abnormalities. *Radiology*, 244(2), 549-556.

Massana, G., Serra-Grabulosa, J.M., Salgado-Pineda, P., (2003). Parahippocampal gray matter density in panic disorder: a voxel-based morphometric study. *American Journal of Psychiatry*, 160(3), 566-568.

Matsuda, H., Kitayama, N., Ohnishi, T., et al. (2002). Longitudinal evaluation of both morphologic and functional changes in the same individuals with Alzheimer's disease. *Journal of Nuclear Medicine*, 43(3), 304-311.

Matsumoto, R., Ito, H., Takahashi, H., et al. (2010). Reduced gray matter volume of dorsal cingulate cortex in patients with obsessive–compulsive disorder: A voxel-based morphometric study. *Psychiatry and Clinical Neurosciences*, 64, 541-547.

Matsunari, I., Samuraki, M., Chen, W.P., et al. (2007). Comparison of 18F-FDG PET and optimized voxel-based morphometry for detection of Alzheimer's disease: aging effect on diagnostic performance. *Journal of Nuclear Medicine*, 48(12), 1961-1970.

Mazère, J., Prunier, C., Barret, O., et al. (2008). In vivo SPECT imaging of vesicular acetylcholine transporter using [(123)I]-IBVM in early Alzheimer's disease. *Neuroimage*, 40(1), 280-288.

McAlonan, G.M., Cheung, V., Cheung, C., et al. (2005). Mapping the brain in autism. A voxel-based MRI study of volumetric differences and intercorrelations in autism. *Brain*, 128, 268-276.

McAlonan, G.M., Cheung, V., Cheung, C., et al. (2007). Mapping brain structure in attention deficit-hyperactivity disorder: a voxel-based MRI study of regional grey and white matter volume. *Psychiatry Research*, 154(2), 171-180.

McAlonan, G.M., Daly, E., Kumari, V., et al. (2002). Brain anatomy and sensorimotor gating in Asperger's syndrome. *Brain*, 125(Pt 7), 1594-1606.

McAlonan, G.M., Suckling, J., Wong, N., et al. (2008). Distinct patterns of grey matter abnormality in high-functioning autism and Asperger's syndrome. *Journal of Child Psychology and Psychiatry*, 49, 1287-1295.

McIntosh, A.M., Job, D.E., Moorhead, T.W., et al. (2004). Voxel-based morphometry of patients with schizophrenia or bipolar disorder and their unaffected relatives. *Biological Psychiatry*, 56(8), 544-552.

McKenna, M.C., Gruetter, R., Sonnewald, U., Waagepetersen, H.S., Schousboe, A. (2006). "Energy metabolism of the brain". In Siegel GJ, Wayne Albers R, Brady ST, Price DL (eds.) *Basic Neurochemistry: Molecular, Cellular, and Medical Aspects*, 7th ed., Academic Press, 531-558.

McIntosh, A.R. (1998). Understanding neural interactions in learning and memory using functional neuroimaging. *Annals of the New York Academy of Sciences*, 855, 556-571.

McIntosh, A.R. (1999). Mapping cognition to the brain through neural interactions. *Memory*, 7, 523-548.

McIntosh, A.R. (2004). Contexts and catalysts: a resolution of the localization and integration of function in the brain. *Neuroinformatics*, 2, 175-182.

McIntosh, A.R., Gonzalez-Lima, F. (1994). Structural equation modeling and its application to network analysis in functional brain imaging. *Human Brain Mapping*, 2, 2-22.

McIntosh, A.R., Fitzpatrick, S.M., Friston, K.J. (2001). On the marriage of cognition and neuroscience. *Neuroimage*, 14, 1231-1237.

McMillan, A.B., Hermann, B.P., Johnson, S.C., et al. (2004). Voxel-based morphometry of unilateral temporal lobe epilepsy reveals abnormalities in cerebral white matter. *Neuroimage*, 23(1), 167-174.

McTeague, L.M., Goodkind, M.S., Etkin, A. (2016). Transdiagnostic impairment of cognitive control in mental illness. *Journal of Psychiatry Research*, 83, 37-46.

Mechelli, A., Friston, K.J., Frackowiak, R.S., Price, C.J. (2005). Structural covariance in the human cortex. *Journal of Neuroscience*, 25(36), 8303-8310.

Meda, S.A., Giuliani, N.R., Calhoun, V.D., et al. (2008). A large scale (N=400) investigation of gray matter differences in schizophrenia using optimized voxel-based morphometry. *Schizophrenia research*, 101, 95-105.

Medford, N., Critchley, H. D. (2010). Conjoint activity of anterior insular and anterior cingulate cortex: awareness and response. *Brain Structure and Function*, 214(5-6), 535-549.

Meisenzahl, E.M., Koutsouleris, N., Bottlender, R., et al. (2008). Structural brain alterations at

different stages of schizophrenia: a voxel-based morphometric study. *Schizophrenia Research*, 104, 44-60.

Mengotti, P., D'Agostini, S., Terlevic, R., et al. (2011). Altered white matter integrity and development in children with autism: a combined voxel-based morphometry and diffusion imaging study. *Brain Research Bulletin*, 84(2), 189-195.

Menon, V. (2011). Large-scale brain networks and psychopathology: a unifying triple network model. *Trends in Cognitive Sciences*, 15(10), 483-506.
doi: 10.1016/j.tics.2011.08.003.

Menon, V. (2013). Developmental pathways to functional brain networks: emerging principles. *Trends in Cognitive Sciences*, 17, 627-640.

Meppelink, A.M., de Jong, B.M., Teune, L.K. van Laar, T. (2011). Regional cortical grey matter loss in Parkinson's disease without dementia is independent from visual hallucinations. *Movement Disorders*, 26, 142-147.

Mesaros, S., Rocca, M.A., Absinta, M., et al. (2008). Evidence of thalamic gray matter loss in pediatric multiple sclerosis. *Neurology*, 70, 1107-1112.

Mesulam, M. M., Mufson, E. J. (1982). Insula of the old world monkey. III: Efferent cortical output and comments on function. *Journal of Comparative Neurology*, 212(1), 38-52.

Mezzapesa, D.M., Ceccarelli, A., Dicuonzo, F., et al. (2007). Whole-brain and regional brain atrophy in amyotrophic lateral sclerosis. *American Journal of Neuroradiology*, 28(2), 255-259.

Miettinen, P.S., Pihlajamäki, M., Jauhiainen, A.M., et al. (2011). Structure and function of medial temporal and posteromedial cortices in early Alzheimer's disease. *European Journal of Neuroscience*, 34, 320-330.

Milham, M.P., Nugent, A.C., Drevets, W.C., et al. (2005). Selective reduction in amygdala volume in pediatric anxiety disorders: a voxel-based morphometry investigation. *Biological Psychiatry*, 57(9), 961-966.

Minnerop, M., Specht, K., Ruhlmann, J., et al. (2007). Voxel-based morphometry and voxel-based relaxometry in multiple system atrophy-a comparison between clinical subtypes and correlations with clinical parameters. *Neuroimage*, 36(4), 1086-1095.

Misic, B., Betzel, R. F., de Reus, M. A., van den Heuvel, M. P., Berman, M. G., McIntosh. A. R., et al. (2016). Network-level structure-function relationships in human neocortex. *Cerebral Cortex*, 26. 3285-3296.

Molina, V., Galindo, G., Cortés, B., et al. (2011). Different gray matter patterns in chronic schizophrenia and chronic bipolar disorder patients identified using voxel-based morphometry. *European Archives of Psychiatry and Clinical Neuroscience*, 261(5), 313-322.

Molina, V., Sanz, J., Villa, R., et al. (2010). Voxel-based morphometry comparison between first episodes of psychosis with and without evolution to schizophrenia. *Psychiatry Research*, 181(3), 204-210.

Moorhead, T.W., Job, D.E., Spencer, M.D., et al. (2005). Empirical comparison of maximal voxel and non-isotropic adjusted cluster extent results in a voxel-based morphometry study of comorbid learning disability with schizophrenia. *Neuroimage*, 28(3), 544-552.

Morgen, K., Sammer, G., Courtney, S.M., et al. (2006). Evidence for a direct association between cortical atrophy and cognitive impairment in relapsing-remitting MS. *Neuroimage*, 30(3), 891-898.

Mori, S., Zhang, J. (2006). Principles of diffusion tensor imaging and its applications to basic neuroscience research. *Neuron*, 51, 527-539.

Mueller, S.G., Laxer, K.D., Cashdollar, N., et al. (2006). Voxel-based optimized morphometry (VBM) of gray and white matter in temporal lobe epilepsy (TLE) with and without mesial temporal sclerosis. *Epilepsia*, 47(5), 900-907.

Mühlau, M., Buck, D., Förschler, A., et al. (2013). White-matter lesions drive deep gray-matter atrophy in early multiple sclerosis: support from structural MRI. *Multiple Sclerosis*, 19(11), 1485-1492.

Mühlau, M., Weindl, A., Wohlschläger, A.M., et al. (2007). Voxel-based morphometry indicates relative preservation of the limbic prefrontal cortex in early Huntington disease. *Journal of Neural Transmission*, 114(3), 367-372.

Müller, V.I., Langner, R., Cieslik, E.C., Rottschy, C., Eickhoff, S.B. (2015). Interindividual differences in cognitive flexibility: influence of gray matter volume, functional connectivity and trait impulsivity. *Brain Structure and Function*, 220(4), 2401e2414.

Müller-Vahl, K.R., Kaufmann, J., Grosskreutz, J., et al. (2009). Prefrontal and anterior cingulate cortex abnormalities in Tourette Syndrome: evidence from voxel-based morphometry and magnetization transfer imaging. *BMC neuroscience*, 10, 47, doi:10.1186/1471-2202-10-47.

Murray, K.D., Choudary, P.V., Jones, E.G. (2007) Nucleus- and cell-specific gene expression in monkey thalamus. *Proceedings of the National Academy of Sciences USA*, 104, 1989-1994.

Myers, N., et al. (2014). Within-patient correspondence of amyloid-β and intrinsic network connectivity in Alzheimer's disease. *Brain*, 137, 2052-2064.

Nagano-Saito, A., Washimi, Y., Arahata, Y., et al. (2005). Cerebral atrophy and its relation to cognitive impairment in Parkinson disease. *Neurology*, 64(2), 224-229.

Nardo, D., Högberg, G., Lanius, R.A., et al. (2013). Gray matter volume alterations related to trait dissociation in PTSD and traumatized controls. *Acta Psychiatrica Scandinavica*, 128(3), 222-233.

Narita, K., Suda. M., Takei. Y., et al. (2011). Volume reduction of ventromedial prefrontal cortex in bipolar II patients with rapid cycling: a voxel-based morphometric study. *Progress in Neuropsychopharmacology and Biological Psychiatry*, 35(2), 439-445.

Nestor, P.J., Graham, N.L., Fryer, T.D., et al. (2003). Progressive non-fluent aphasia is associated with hypometabolism centred on the left anterior insula. *Brain*, 126, 2406-2418.

Niedtfeld, I., Schulze, L., Krause-Utz, A., et al. (2013). Voxel-based morphometry in women with borderline personality disorder with and without comorbid posttraumatic stress disorder. *PloS one*, 8(6), e65824. doi:10.1371/journal.pone.0065824.

Nieuwenhuys, R. (2012). The insular cortex: a review. *Progress in Brain Research*, 195, 123-163.

Nishio, Y., Hirayama, K., Takeda, A., et al. (2010). Corticolimbic gray matter loss in Parkinson's disease without dementia. *European Journal of Neurology*, 17, 1090-1097.

Northoff, G., Duncan, N.W. (2016). How do abnormalities in the brain's spontaneous activity translate into symptoms in schizophrenia? From an overview of resting state activity findings to a proposed spatiotemporal psychopathology. *Progress in Neurobiology*, 145-6, 26-45.

Nugent, A.C., Milham, M.P., Bain, E.E., et al. (2006). Cortical abnormalities in bipolar disorder investigated with MRI and voxel-based morphometry. *Neuroimage*, 30(2), 485-497.

Nunnally, J.C., Bernstein, I.H. (1994). *Psychometric theory*, 3rd ed. New York: McGraw-Hill.

O'Daly, O.G., Frangou, S., Chitnis, X., Shergill, S.S. (2007). Brain structural changes in schizophrenia patients with persistent hallucinations. *Psychiatry Research*, 156(1), 15-21.

O'Muircheartaigh, J., Vollmar, C., Barker, G.J., et al. (2011). Focal structural changes and cognitive dysfunction in juvenile myoclonic epilepsy. *Neurology*, 76(1), 34-40.

Obermann, M., Rodriguez-Raecke, R., Naegel, S., et al. (2013). Gray matter volume reduction reflects chronic pain in trigeminal neuralgia. *Neuroimage*, 74, 352-358.

Obermann, M., Yaldizli, O., De Greiff, A., et al. (2007). Morphometric changes of sensorimotor structures in focal dystonia. *Movement Disorders*, 22, 1117-1123.

Ohnishi, T., Hashimoto, R., Mori, T., et al. (2006). The association between the Val158Met polymorphism of the catechol-O-methyl transferase gene and morphological abnormalities of the brain in chronic schizophrenia. *Brain*, 129, 399-410.

Ohnishi, T., Matsuda, H., Tabira, T., et al. (2001). Changes in brain morphology in Alzheimer disease and normal aging: is Alzheimer disease an exaggerated aging process? *American Journal of Neuroradiology*, 22(9), 1680-1685.

Ortiz-Gil, J., Pomarol-Clotet, E., Salvador, R., et al. (2011). Neural correlates of cognitive impairment in schizophrenia. *British Journal of Psychiatry*, 199(3), 202-210.

Overmeyer, S., Bullmore, E.T., Suckling, J., et al. (2001). Distributed grey and white matter deficits in hyperkinetic disorder: MRI evidence for anatomical abnormality in an attentional network. *Psychological Medicine*, 31(8), 1425-1435.

Oxtoby, N.P., Garbarino, S., Firth, N.C., Warren, J.D., Schott, J.M., Alexander, D.C. (2017). Data-driven sequence of changes to anatomical brain connectivity in sporadic Alzheimer's disease. *Frontiers in Neurology*, 8. 580.

Padovani, A., Borroni, B., Brambati, S.M., et al. (2006). Diffusion tensor imaging and voxel based morphometry study in early progressive supranuclear palsy. *Journal of neurology, neurosurgery, and psychiatry*, 77(4), 457-463.

Pail, M., Brázdil, M., Mareček, R., Mikl, M. (2010). An optimized voxel-based morphometric study of gray matter changes in patients with left-sided and right-sided mesial temporal lobe epilepsy and hippocampal sclerosis (MTLE/HS). *Epilepsia*, 51, 511-518.

Paillère-Martinot, M., Caclin, A., Artiges, E., et al. (2001). Cerebral gray and white matter reductions and clinical correlates in patients with early onset schizophrenia. *Schizophrenia Research*, 50(1-2), 19-26.

Palaniyappan, L., Liddle, P. F. (2012). Does the salience network play a cardinal role in psychosis? An emerging hypothesis of insular dysfunction. *Journal of Psychiatry and Neuroscience*, 37(1), 17-27.

Pandya, S., Mezias, C., Raj, A. (2017). Predictive model of spread of progressive supranuclear palsy using directional network diffusion. *Frontiers in Neurology*, 8, 692.

Pantano, P., Totaro, P., Fabbrini, G., et al. (2011). A transverse and longitudinal MR imaging voxel-based morphometry study in patients with primary cervical dystonia. *American Journal of Neuroradiology*, 32(1), 81-84.

Pardini, M., Huey, E.D., Cavanagh, A.L., Grafman, J. (2009). Olfactory function in corticobasal syndrome and frontotemporal dementia. *Archives of neurology*, 66(1), 92-96.

Parisi, L., Rocca, M.A., Mattioli, F., et al. (2014). Patterns of regional gray matter and white matter atrophy in cortical multiple sclerosis. *Journal of Neurology*, 261(9), 1715-1725.

Pardoe, H., Pell, G.S., Abbott, D.F., et al. (2008). Multi-site voxel-based morphometry: methods and a feasibility demonstration with childhood absence epilepsy. *Neuroimage*, 42(2), 611-616.

Patel, R. S., Bowman, F. D., Rilling, J. K. (2006). A Bayesian approach to determining connectivity of the human brain. *Human Brain Mapping*, 27(3), 267-276.

Pearson, R.C., Esiri, M.M., Hiorns, R.W., Wilcock, G.K., Powell, T.P. (1985). Anatomical correlates of the distribution of the pathological changes in the neocortex in Alzheimer disease. *Procedings of the National Academy of Sciences USA*, 82, 4531-4534.

Peinemann, A., Schuller, S., Pohl, C., et al. (2005). Executive dysfunction in early stages of Huntington's disease is associated with striatal and insular atrophy: a neuropsychological and voxel-based morphometric study. *Journal of the Neurological Sciences*, 239(1), 11-19.

Pell, G.S., Briellmann, R.S., Pardoe, H., et al. (2008). Composite voxel-based analysis of volume and T2 relaxometry in temporal lobe epilepsy. *Neuroimage*, 39(3), 1151-1161.

Peng, J., Liu, J., Nie, B., et al. (2011). Cerebral and cerebellar gray matter reduction in first-episode patients with major depressive disorder: a voxel-based morphometry study. *European Journal of Radiology*, 80(2), 395-399.

Pennanen, C., Testa, C., Laakso, M.P., et al. (2005). A voxel based morphometry study on mild cognitive impairment. *Journal of neurology, neurosurgery, and psychiatry*, 76(1), 11-14.

Pereira, J.B., Junqué, C., Martí, M.J., et al. (2009). Structural brain correlates of verbal fluency in Parkinson's disease. *Neuroreport*, 20(8), 741-744.

Pereira, J. M., Williams, G.B., Acosta-Cabronero, J., et al. (2009). Atrophy patterns in histologic vs clinical groupings of frontotemporal lobar degeneration. *Neurology*, 72(19), 1653-1660.

Perlson, E., Maday, S., Fu, M.M., Moughamian, A.J. and Holzbaur, E.L.F. (2010). Retrograde axonal transport: pathways to cell death? *Trends in Neuroscience*, 33, 335-344.

Petrie, E.C., Cross, D.J., Yarnykh, V.L., et al. (2014). Neuroimaging, behavioral, and psychological sequelae of repetitive combined blast/impact mild traumatic brain injury in Iraq and Afghanistan war veterans. *Journal of neurotrauma*, 31(5), 425-436.

Polleux, F., Ince-Dunn, G., Ghosh, A. (2007). Transcriptional regulation of vertebrate axon guidance and synapse formation. *Nature Reviews Neuroscience*, 8, 331-340.

Pomarol-Clotet, E., Canales-Rodríguez, E.J., Salvador, R., et al. (2010). Medial prefrontal cortex pathology in schizophrenia as revealed by convergent findings from multimodal imaging. *Molecular psychiatry*, 15(8), 823-830.

Power, J.D., Schlaggar, B.L., Lessov-Schlaggar, C.N., Petersen, S. E. (2013). Evidence for hubs in human functional brain networks. *Neuron*, 79, 798-813.

Prakash, R.S., Snook, E.M., Motl, R.W., Kramer, A.F. (2010). Aerobic fitness is associated with gray matter volume and white matter integrity in multiple sclerosis. *Brain research*, 1341, 41-51.

Premi, E., Cauda, F., Costa, T., Diano, M., Gazzina, S., Gualeni, V., et al. (2016). Looking for neuroimaging markers in frontotemporal lobar degeneration clinical trials: a multi-voxel pattern analysis study in granulin disease. *Journal of Alzheimer's Disease*, 51, 249-262.

Premi, E., Cauda, F., Gasparotti, R,, Diano, M., Archetti, S., Padovani, A., et al. (2014). Multimodal FMRI resting-state functional connectivity ingranulin mutations: the case of fronto-parietal dementia. *PLoS On*e, 9: e106500.

Preziosa, P., Rocca, M.A., Pagani, E., et al. (2016). Structural MRI correlates of cognitive impairment in patients with multiple sclerosis. *Human Brain Mapping*, 37, 1627-1644.

Price, G., Cercignani, M., Chu, E.M., et al. (2010). Brain pathology in first-episode psychosis: magnetization transfer imaging provides additional information to MRI measurements of volume loss. *Neuroimage*, 49(1), 185-192.

Prieto, C., Risueño, A., Fontanillo, C., De Las Rivas, J. (2008). Human Gene Coexpression Landscape: Confident Network Derived from Tissue Transcriptomic Profiles. *PLoS ONE*, 3(12), e3911. doi: 10.1371/journal.pone.0003911.

Prinster, A., Quarantelli, M., Lanzillo, R., et al. (2010). A voxel-based morphometry study of disease severity correlates in relapsing – remitting multiple sclerosis. *Multiple sclerosis*, 16(1), 45-54.

Prinster, A., Quarantelli, M., Orefice, G., et al. (2006). Grey matter loss in relapsing-remitting multiple sclerosis: a voxel-based morphometry study. *Neuroimage*, 29(3), 859-867.

Pujol, J., Soriano-Mas, C., Alonso, P., et al. (2004). Mapping structural brain alterations in obsessive-compulsive disorder. *Archives of General Psychiatry*, 61(7), 720-730.

Qiu, L., Tian, L., Pan, C., et al. (2011). Neuroanatomical circuitry associated with exploratory eye movement in schizophrenia: a voxel-based morphometric study. *PloS one*, 6(10), e25805. doi:10.1371/journal.pone.0025805.

Quarantelli, M., Lanzillo, R., Del Vecchio, W., et al. (2006). Modifications of brain tissue volumes in facioscapulohumeral dystrophy. *Neuroimage*, 32(3), 1237-1242.

Quattrone, A., Cerasa, A., Messina, D., et al. (2008). Essential head tremor is associated with cerebellar vermis atrophy: a volumetric and voxel-based morphometry MR imaging study. *American Journal of Neuroradiology*, 29(9), 1692-1697.

Quiroz, Y.T., Schultz, A.P., Chen, K., Protas, H.D., Brickhouse, M., Fleisher, A.S., et al. (2015). Brain imaging and blood biomarker abnormalities in children with autosomal dominant Alzheimer disease: a cross-sectional study. *JAMA Neurology*, 72, 912-919.

Rabinovici, G.D., Seeley, W.W., Kim, E.J., et al. (2007). Distinct MRI atrophy patterns in autopsy-proven Alzheimer's disease and frontotemporal lobar degeneration. *American journal of Alzheimer's disease and other dementias*, 22(6), 474-488.

Raichle, M.E., Gusnard, D.A. (2002). Appraising the brain's energy budget. *Proceedings of the National Academy of Science USA*, 99(16), 10237-10239.

Raichle, M.E., Mintun, M.A. (2006). Brian work and brain imaging. *Annual Review Neuroscience*, 29, 449-476.

Raichle, M.E., Snyder, A.Z. (2007). A default mode of brain function: a brief history of an evolving idea. *Neuroimage*, 37(4), 1083-1090.

Raj, A., Kuceyeski, A., Weiner, M. (2012). A network diffusion model of disease progression in dementia. *Neuron*, 73(6), 1204-1215.

Rami, L., Gómez-Anson, B., Monte, G.Cet al. (2009). Voxel based morphometry features and follow-up of amnestic patients at high risk for Alzheimer's disease conversion. *International Journal of Geriatric Psychiatry*, 24, 875-884.

Ramírez-Ruiz, B., Martí, M.-J., Tolosa, E., et al. (2007). Cerebral atrophy in Parkinson's disease patients with visual hallucinations. *European Journal of Neurology*, 14, 750-756.

Ranjeva, J.P., Audoin, B., Au Duong, M,V., et al. (2005). Local tissue damage assessed with statistical mapping analysis of brain magnetization transfer ratio: relationship with functional status of patients in the earliest stage of multiple sclerosis. American Journal of Neuroradiology, 26(1), 119-127.

Ravits, J. (2014). Focality, stochasticity and neuroanatomic propagation in ALS pathogenesis. *Experimental Neurology*, 262, 121-126.

Redlich, R., Almeida, J.J., Grotegerd, D., et al. (2014). Brain morphometric biomarkers distinguishing unipolar and bipolar depression. A voxel-based morphometry-pattern classification approach. *JAMA psychiatry*, 71(11), 1222-1230.

Rémy, F., Mirrashed, F., Campbell, B., Richter, W. (2005). Verbal episodic memory impairment in Alzheimer's disease: a combined structural and functional MRI study. *Neuroimage*, 25(1), 253-266.

Reuter, M., Rosas, H.D., Fischl, B. (2010). Highly accurate inverse consistent registration: a robust approach. *Neuroimage*, 53, 1181-1196.

Riccitelli, G., Rocca, M.A., Pagani, E., et al. (2012). Mapping regional grey and white matter atrophy in relapsing-remitting multiple sclerosis. *Multiple Sclerosis*, 18(7), 1027-1037.

Richiardi, J., Altmann, A., Milazzo, A. C., Chang, C., Chakravarty, M. M., Banaschewski, T., et al. (2015). Brain networks. correlated gene expression supports synchronous activity in brain networks. *Science*, 348, 1241-1244.

Riederer, F., Lanzenberger, R., Kaya, M., et al. (2008). Network atrophy in temporal lobe epilepsy: a voxel-based morphometry study. *Neurology*, 71(6), 419-425.

Riederer, F., Marti, M., Luechinger, R., et al. (2012). Grey matter changes associated with medication-overuse headache: correlations with disease related disability and anxiety. *The World Journal of Biological Psychiatry*, 13(7), 517-525.

Ries, M.L., Wichmann, A., Bendlin, B.B., Johnson, S.C. (2009). Posterior Cingulate and Lateral Parietal Gray Matter Volume in Older Adults with Depressive Symptoms. *Brain imaging and behavior*, 3(3), 233-239.

Riva, D., Bulgheroni, S., Aquino, D., Di Salle, F., et al. (2011). Basal forebrain involvement in low-functioning autistic children: a voxel-based morphometry study. *American Journal of Neuroradiology*, 32(8), 1430-1435.

Robinson, P.A. (2012). Interrelating anatomical, effective, and functional brain connectivity using propagators and neural field theory. *Physical review. E, Statistical, nonlinear, and soft matter*, 85(1 Pt 1), 011912.

Robinson, J. L., Laird, A. R., Glahn, D. C., Lovallo, W. R., Fox, P. T. (2010). Meta-analytic connectivity modeling: delineating the functional connectivity of the human amygdala. *Human Brain Mapping*, 31(2), 173-184.

Rocca, M.A., Ceccarelli, A., Falini, A., et al. (2006). Brain gray matter changes in migraine patients with T2-visible lesions: a 3-T MRI study. *Stroke*, 37(7), 1765-1770.

Rocca, M.A., Parisi, L., Pagani, E., et al. (2014). Regional but not global brain damage contributes to fatigue in multiple sclerosis. *Radiology*, 273(2), 511-520.

Rocha-Rego, V., Pereira, M.G., Oliveira, L., et al. (2012). Decreased premotor cortex volume in victims of urban violence with posttraumatic stress disorder. *PloS one*, 7(8), e42560. doi:10.1371/journal.pone.0042560.

Rohrer, J.D., Nicholas, J.M., Cash, D.M., et al. (2015). Presymptomatic cognitive and neuroanatomical changes in genetic frontotemporal dementia in the genetic frontotemporal dementia initiative (GENFI) study: a cross-sectional analysis. *Lancet Neurology*, 14, 253-262.

Rossi, R., Boccardi, M., Sabattoli, F., et al. (2006). Topographic correspondence between white matter hyperintensities and brain atrophy. *Journal of Neurology*, 253(7), 919-927.

Rossi, R., Pievani, M., Lorenzi, M., et al. (2013). Structural brain features of borderline personality and bipolar disorders. *Psychiatry Research*, 213(2), 83-91.

Rowan, A., Vargha-Khadem, F., Calamante, F., et al. (2007). Cortical abnormalities and language function in young patients with basal ganglia stroke. *Neuroimage*, 36(2), 431-440.

Rüsch, N., Tebartz van Elst, L., Baeumer, D., et al. (2004). Absence of cortical gray matter abnormalities in psychosis of epilepsy: a voxel-based MRI study in patients with temporal lobe epilepsy. *Journal of Neuropsychiatry and Clinical Neuroscience*, 16(2), 148-155.

Salehi, A., Delcroix, J.-D., Belichenko, P.V., Zhan, K., Wu, C., Valletta, J.S., Takimoto-Kimura, R., Kleschevnikov, A.M., Sambamurti, K., Chung, P.P., Xia, W., Villar, A., Campbell, W.A., Kulnane, L.S., Nixon, R.A., Lamb, B.T., Epstein, C.J., Stokin, G.B., Goldstein, L.S.B., Mobley, W.C., (2006), Increased App expression in a mouse model of Down's syndrome disrupts NGF transport and causes cholinergic neuron degeneration, *Neuron*, 51, 1, 29-42.

Salgado-Pineda, P., Baeza, I., Pérez-Gómez, M., et al. (2003). Sustained attention impairment correlates to gray matter decreases in first episode neuroleptic-naive schizophrenic patients. *Neuroimage*, 19, 365-375.

Salgado-Pineda, P., Fakra, E., Delaveau, P., et al. (2011). Correlated structural and functional brain abnormalities in the default mode network in schizophrenia patients. *Schizophrenia Research*, 125, 101-109.

Salgado-Pineda, P., Junqué, C., Vendrell, P., et al. (2004). Decreased cerebral activation during CPT performance: structural and functional deficits in schizophrenic patients. *Neuroimage*, 21(3), 840-847.

Salmond, C.H., Vargha-Khadem, F., Gadian, D.G., et al. (2007). Heterogeneity in the patterns of neural abnormality in autistic spectrum disorders: evidence from ERP and MRI. *Cortex*, 43(6), 686-699.

Salvadore, G., Nugent, A.C., Lemaitre, H., et al. (2011). Prefrontal cortical abnormalities in currently depressed versus currently remitted patients with major depressive disorder. *Neuroimage*, 54(4), 2643-2651.

Salvador, R., Suckling, J., Coleman, M.R., Pickard, J.D., Menon, D., Bullmore, E. (2005). Neurophysiological architecture of functional magnetic resonance images of human brain. *Cerebral Cortex*, 15(9), 1332-1342.

Sanchis-Segura, C., Cruz-Gómez, A.J., Belenguer, A., et al. (2016). Increased regional gray matter atrophy and enhanced functional connectivity in male multiple sclerosis patients. *Neuroscience Letters*, 630, 154-157.

Santana, M.T., Jackowski, A.P., da Silva, H.H., et al. (2010). Auras and clinical features in temporal lobe epilepsy: a new approach on the basis of voxel-based morphometry. *Epilepsy Research*, 89, 327-338.

Saper, C.B., Wainer, B.H., German, D.C. (1987). Axonal and transneuronal transport in the transmission of neurological disease: potential role in system degenerations, including Alzheimer's disease. *Neuroscience*, 23, 389-398.

Sarıçiçek, A., Yalın, N., Hıdıroğlu, C., et al. (2015). Neuroanatomical correlates of genetic risk for bipolar disorder: A voxel-based morphometry study in bipolar type I patients and healthy first degree relatives. *Journal of Affective Disorders*, 186, 110-118.

Sasayama, D., Hayashida, A., Yamasue, H., et al. (2010). Neuroanatomical correlates of attention-deficit–hyperactivity disorder accounting for comorbid oppositional defiant disorder and conduct disorder. *Psychiatry and Clinical Neurosciences*, 64, 394-402.

Saxena, S., Caroni, P. (2011). Selective neuronal vulnerability in neurodegenerative diseases: from stressor thresholds to degeneration. *Neuron*, 71. 35-48.

Saykin, A.J., Wishart, H.A., Rabin, L.A., et al. (2006). Older adults with cognitive complaints show brain atrophy similar to that of amnestic MCI. *Neurology*, 67(5), 834-842.

Scheuerecker, J., Meisenzahl, E.M., Koutsouleris, N., et al. (2010). Orbitofrontal volume reductions during emotion recognition in patients with major depression. *Journal of psychiatry & neuroscience*, 35(5), 311-320.

Schiffer, B., Leygraf, N., Müller, B.W., et al. (2013). Structural brain alterations associated with schizophrenia preceded by conduct disorder: a common and distinct subtype of schizophrenia? *Schizophrenia bulletin*, 39(5), 1115-1128.

Schiffer, B., Peschel, T., Paul, T., et al. (2007). Structural brain abnormalities in the frontostriatal system and cerebellum in pedophilia. *Journal of Psychiatric Research*, 41(9), 753-762.

Schmidt-Wilcke, T., Gänssbauer, S., Neuner, T., et al. (2008). Subtle grey matter changes between migraine patients and healthy controls. *Cephalalgia*, 28(1), 1-4.

Schmidt-Wilcke, T., Hierlmeier, S. Leinisch, E. (2010). Altered Regional Brain Morphology in Patients With Chronic Facial Pain. *Headache*, 50, 1278-1285.

Schmidt-Wilcke, T., Leinisch, E., Straube, A., et al. (2005). Gray matter decrease in patients with chronic tension type headache. *Neurology*, 65(9), 1483-1486.

Schmidt-Wilcke, T., Poljansky, S., Hierlmeier, S., et al. (2009). Memory performance correlates with gray matter density in the ento-/perirhinal cortex and posterior hippocampus in patients with mild cognitive impairment and healthy controls – A voxel based morphometry study. *Neuroimage*, 47(4), 1914-1920.

Schroeter, M. L., Raczka, K., Neumann, J., von Cramon, D. Y. (2008). Neural networks in frontotemporal dementia – A meta-analysis. *Neurobiology of Aging*, 29(3), 418-426.

Schuster, C., Schuller, A.M., Paulos, C., et al. (2012). Gray matter volume decreases in elderly patients with schizophrenia: a voxel-based morphometry study. *Schizophrenia bulletin*, 38(4), 796-802.

Schwartz, D.L., Mitchell, A.D., Lahna, D.L., et al. (2010). Global and local morphometric differences in recently abstinent methamphetamine-dependent individuals. *Neuroimage*, 50(4), 1392-1401.

Seeley, W.W., Carlin, D.A., Allman, J.M., Macedo, M.N., Bush, C., Miller, B.L., et al. (2006). Early frontotemporal dementia targets neurons unique to apes and humans. *Annals of Neurology*, 60: 660-667.

Seeley, W.W., Crawford, R., Rascovsky, K., et al. (2008). Frontal paralimbic network atrophy in very mild behavioral variant frontotemporal dementia. *Archives of neurology*, 65(2), 249-255.

Seeley, W.W., Crawford, R.K., Zhou, J., Miller, B.L., Greicius, M.D. (2009). Neurodegenerative diseases target large-scale human brain networks. *Neuron*, 62, 42-52.

Seeley, W. W., Menon, V., Schatzberg, A. F., Keller, J., Glover, G. H., Kenna, H., et al. (2007). Dissociable intrinsic connectivity networks for salience processing and executive control. *Journal of Neuroscience*, 27(9), 2349-2356.

Seeley, W. W., Zhou, J., Kim, E. J. (2012). Frontotemporal dementia: what can the behavioral variant teach us about human brain organization? *The Neuroscientist*, 18(4), 373-385.

Senda, J., Kato, S., Kaga, T., et al. (2011). Progressive and widespread brain damage in ALS: MRI voxel-based morphometry and diffusion tensor imaging study. *Amyotrophic Lateral Sclerosis*, 12(1), 59-69.

Senjem, M.L., Gunter, J.L., Shiung, M.M. et al. (2005). Comparison of different methodological implementations of voxel-based morphometry in neurodegenerative disease. *Neuroimage*, 26, 600-608.

Sepulcre, J., Sastre-Garriga, J., Cercignani, M., et al. (2006). Regional gray matter atrophy in early primary progressive multiple sclerosis: a voxel-based morphometry study. *Archives of Neurology*, 63(8), 1175-1180.

Serra-Blasco, M., Portella, M.J., Gómez-Ansón, B., et al. (2013). Effects of illness duration and treatment resistance on grey matter abnormalities in major depression. *British Journal of Psychiatry*, 202, 434-440.

Shad, M.U., Muddasani, S., Rao, U. (2012). Gray matter differences between healthy and depressed adolescents: a voxel-based morphometry study. *Journal of child and adolescent psychopharmacology*, 22(3), 190-197.

Shapleske, J., Rossell, S.L., Chitnis, X.A., et al. (2002). A computational morphometric MRI study of schizophrenia: effects of hallucinations. *Cerebral Cortex*, 12(12), 1331-1341.

Shiino, A., Watanabe, T., Maeda, K., et al. (2006). Four subgroups of Alzheimer's disease based on patterns of atrophy using VBM and a unique pattern for early onset disease. *Neuroimage*, 33(1), 17-26.

Shin, S., Lee, J.E., Hong, J.Y., et al. (2012). Neuroanatomical substrates of visual hallucinations in patients with non-demented Parkinson's disease. *Journal of Neurology, Neurosurgery, and Psychiatry*, 83(12), 1155-1161.

Shulman, R.G. (2001). Functional imaging studies: linking mind and basic neuroscience. *American Journal of Psychiatry*, 158, 11-20.

Sigmundsson, T., Suckling, J., Maier, M., et al. (2001). Structural abnormalities in frontal, temporal, and limbic regions and interconnecting white matter tracts in schizophrenic patients with prominent negative symptoms. *American Journal of Psychiatry*, 158(2), 234-243.

Simons, L. E., Elman, I., Borsook, D. (2014). Psychological processing in chronic pain: a neural systems approach. *Neuroscience and Biobehavioral Reviews*, 39, 61-78.

Singh, M.K., Chang, K.D., Chen, M.C., et al. (2012). Volumetric reductions in the subgenual anterior cingulate cortex in adolescents with bipolar I disorder. *Bipolar disorders*, 14(6), 585-596.

Skudlarski, P., Jagannathan, K., Calhoun, V. D., Hampson, M., Skudlarska, B. A., Pearlson, G. (2008). Measuring brain connectivity: diffusion tensor imaging validates resting state temporal correlations. *Neuroimage*, 43, 554-561.

Smesny, S., Milleit, B., Nenadic, I., et al. (2010). Phospholipase A2 activity is associated with structural brain changes in schizophrenia. *Neuroimage*, 52(4), 1314-1327.

Smith, S.M., Nichols, T.E. (2009). Threshold-free cluster enhancement: addressing problems of smoothing, threshold dependence and localisation in cluster inference. *Neuroimage*, 44, 83-88.

Smith, S.M., Zhang, Y., Jenkinson, M., et al. (2002). Accurate, robust, and automated longitudinal and cross-sectional brain change analysis. *Neuroimage*, 17, 479-489.

Sobanski, T., Wagner, G., Peikert, G., et al. (2010). Temporal and right frontal lobe alterations in panic disorder: a quantitative volumetric and voxel-based morphometric MRI study. *Psychological Medicine*, 40(11), 1879-1886.

Soriano-Mas, C., Hernández-Ribas, R., Pujol, J., et al. (2011). Cross-sectional and longitudinal assessment of structural brain alterations in melancholic depression. *Biological Psychiatry*, 69(4), 318-325.

Soto, C., Estrada, L.D. (2008). Protein misfolding and neurodegeneration. *Archives of Neurology*, 65, 184-189.

Sowell, E.R., Thompson, P.M., Mattson, S.N., et al. (2001). Voxel-based morphometric analyses of the brain in children and adolescents prenatally exposed to alcohol. *Neuroreport*, 12(3), 515-523.

Spanò, B., Cercignani, M., Basile, B., et al. (2010). Multiparametric MR investigation of the motor pyramidal system in patients with 'truly benign' multiple sclerosis. *Multiple Sclerosis*, 16(2), 178-188.

Specht, K., Minnerop, M., Abele, M., et al. (2003). In vivo voxel-based morphometry in multiple system atrophy of the cerebellar type. *Archives of Neurology*, 60(10), 1431-1435.

Specht, K., Minnerop, M., Müller-Hübenthal, J., Klockgether, T. (2005). Voxel-based analysis of multiple-system atrophy of cerebellar type: complementary results by combining voxel-based morphometry and voxel-based relaxometry. *Neuroimage*, 25(1), 287-293.

Spencer, M.D., Moorhead, T.W., Lymer, G.K., et al. (2006). Structural correlates of intellectual impairment and autistic features in adolescents. *Neuroimage*, 33(4), 1136-1144.

Sporns, O. (2010). *Networks of the Brain.* MIT Press.

Sporns, O., Tononi, G., and Kötter, R. (2005). The human connectome: A structural description of the human brain. *PLoS Computational Biology*, 1, e42.

Sprooten, E., Rasgon, A., Goodman, M., Carlin, A., Leibu, E., Lee, W.H., et al. (2017). Addressing reverse inference in psychiatric neuroimaging: meta-analyses of task-related brain activation in common mental disorders. *Human Brain Mapping*, 38: 1846-1864.

Sridharan, D., Levitin, D. J., Menon, V. (2008). A critical role for the right fronto-insular cortex in switching between central-executive and default-mode networks. *Proceedings of the National Academy of Sciences USA*, 105(34), 12569-12574.

Stanfield, A.C., Moorhead, T.W.J., Job, D.E., et al. (2009), Structural abnormalities of ventrolateral and orbitofrontal cortex in patients with familial bipolar disorder. *Bipolar Disorders*, 11, 135-144.

Stanley, J. (1971). Educational measurement Washington, DC: American Council on Education.

Stephani, C., Fernandez-Baca Vaca, G., Maciunas, R., Koubeissi, M., Luders, H. O. (2011). Functional neuroanatomy of the insular lobe. *Brain Structure and Function*, 216(2), 137-149.

Sternberg, S. (2011). Modular processes in mind and brain. Cognitive neuropsychology, 28(3-4), 156-208.

Stonnington, C.M., Tan, G., Klöppel, S., et al. (2008). Interpreting scan data acquired from multiple scanners: a study with Alzheimer's disease. *Neuroimage*, 39(3), 1180-1185.

Stratmann, M., Konrad, C., Kugel, H., et al. (2014). Insular and hippocampal gray matter volume reductions in patients with major depressive disorder. *PloS one*, 9(7), e102692. doi:10.1371/journal.pone.0102692.

Stuart, J.M., Segal, E., Koller, D., Kim, S.K. (2003). A gene-coexpression network for global discovery of conserved genetic modules. *Science*, 302, 249-255.

Suchan, B., Busch, M., Schulte, D., et al. (2010). Reduction of gray matter density in the extrastriate body area in women with anorexia nervosa. *Behavioral Brain Research*, 206(1), 63-67.

Summerfield, C., Junqué, C., Tolosa, E., et al. (2005). Structural brain changes in Parkinson disease with dementia: a voxel-based morphometry study. *Archives of Neurology*, 62(2), 281-285.

Supekar, K., Menon, V. (2012). Developmental maturation of dynamic causal control signals in higher-order cognition: a neurocognitive network model. *PLoS Computational Biology*, 8(2), e1002374.

Suzuki, M., Nohara, S., Hagino, H., et al. (2002). Regional changes in brain gray and white matter in patients with schizophrenia demonstrated with voxel-based analysis of MRI. *Schizophrenia Research*, 55, 41-54.

Sydykova, D., Stahl, R., Dietrich, O., et al. (2007). Fiber connections between the cerebral cortex and the corpus callosum in Alzheimer's disease: a diffusion tensor imaging and voxel-based morphometry study. *Cerebral Cortex*, 17(10), 2276-2282.

Szeszko, P.R., Christian, C., Macmaster, F., et al. (2008). Gray matter structural alterations in psychotropic drug-naive pediatric obsessive-compulsive disorder: an optimized voxel-based morphometry study. *American Journal of Psychiatry*, 165(10), 1299-1307.

Tae, W.S., Hong, S.B., Joo, E.Y., et al. (2006). Structural brain abnormalities in juvenile myoclonic epilepsy patients: volumetry and voxel-based morphometry. *Korean journal of radiology*, 7(3), 162-172.

Tae, W.S., Joo, E.Y., Kim, S.T., Hong, S.B. (2010). Gray, white matter concentration changes and their correlation with heterotopic neurons in temporal lobe epilepsy. *Korean journal of radiology*, 11(1), 25-36.

Takahashi, R., Ishii, K., Kakigi, T., et al. (2011). Brain alterations and mini-mental state examination in patients with progressive supranuclear palsy: voxel-based investigations using f-fluorodeoxyglucose positron emission tomography and magnetic resonance imaging. *Dementia and geriatric cognitive disorders extra*, 1(1), 381-392.

Takahashi, R,, Ishii, K., Miyamoto, N., et al. (2010). Measurement of gray and white matter atrophy in dementia with Lewy bodies using diffeomorphic anatomic registration through exponentiated lie algebra: A comparison with conventional voxel-based morphometry. *American Journal of Neuroradiology*, 31(10), 1873-1878.

Taki, Y., Kinomura, S., Awata, S., et al. (2005). Male elderly subthreshold depression patients have smaller volume of medial part of prefrontal cortex and precentral gyrus compared with age-matched normal subjects: a voxel-based morphometry. *Journal of Affective Disorders*, 88(3), 313-320.

Tang, L.R., Liu, C.H., Jing, B., et al. (2014). Voxel-based morphometry study of the insular cortex in bipolar depression. *Psychiatry Research*, 224(2), 89-95.

Tatu, K., Costa, T., Nani, A., et al. (2018). How do morphological alterations caused by chronic pain distribute across the brain? A meta-analytic co-alteration study. *Neuroimage*, 18, 15-30.

Tavanti, M., Battaglini, M., Borgogni, F., et al. (2012). Evidence of diffuse damage in frontal and occipital cortex in the brain of patients with post-traumatic stress disorder. *Neurological Sciences*, 33(1), 59-68.

Tavazzi, E., Laganà, M.M., Bergsland, N., et al. (2015). Grey matter damage in progressive multiple sclerosis versus amyotrophic lateral sclerosis: a voxel-based morphometry MRI study. *Neurological Sciences*, 36(3), 371-377.

Taylor, K.S., Seminowicz, D.A., Davis, K.D. (2009). Two systems of resting state connectivity between the insula and cingulate cortex. *Human Brain Mapping*, 30(9), 2731-2745.

Telesford, Q.K., Joyce, K.E., Hayasaka, S., et al. (2011). The ubiquity of small-world networks. *Brain connectivity*, 1(5), 367-375.doi:10.1089/brain.2011.0038.

Tessier, M.L., Goodman, C.S. (1996). The Molecular Biology of Axon Guidance. *Science*, 274, 1123-1133.

Tessitore, A., Amboni, M., Cirillo, G., et al. (2012). Regional gray matter atrophy in patients with Parkinson disease and freezing of gait. *American Journal of Neuroradiology* 33(9), 1804-1809.

Théberge, J., Williamson, K.E., Aoyama, N., et al. (2007). Longitudinal grey-matter and glutamatergic losses in first-episode schizophrenia. *British Journal of Psychiatry*, 191, 325-334.

Thivard, L., Pradat, P.F., Lehéricy, S., et al. (2007). Diffusion tensor imaging and voxel based morphometry study in amyotrophic lateral sclerosis: relationships with motor disability. *Journal of neurology, neurosurgery, and psychiatry*, 78(8), 889-892.

Thomaes, K., Dorrepaal, E., Draijer, N., et al. (2010). Reduced anterior cingulate and orbitofrontal volumes in child abuse-related complex PTSD. *Journal of Clinical Psychiatry*, 71(12), 1636-1644.

Tian, L., Meng, C., Yan, H., et al. (2011). Convergent evidence from multimodal imaging reveals amygdala abnormalities in schizophrenic patients and their first-degree relatives. *PloS one*, 6(12), e28794. doi:10.1371/journal.pone.0028794.

Tiihonen, J., Rossi, R., Laakso, M.P., et al. (2008). Brain anatomy of persistent violent offenders: more rather than less. *Psychiatry Research*, 163(3), 201-212.

Tir, M., Delmaire, C., le Thuc, V., et al. (2009). Motor-related circuit dysfunction in MSA-P: Usefulness of combined whole-brain imaging analysis. *Movement Disorders*, 24, 863-870.

Toal, F., Daly, E.M., Page, L., et al. (2010). *Psychological Medicine*, 40(7), 1171-1181.

Togao, O., Yoshiura, T., Nakao, T., et al. (2010). Regional gray and white matter volume abnormalities in obsessive-compulsive disorder: a voxel-based morphometry study. *Psychiatry Research*, 184(1), 29-37.

Tomasi, D., Wang, G.J., Volkow, N.D. (2013). Energetic cost of brain functional connectivity. *Proceedings of the National Academy of Sciences USA*, 110, 13642-13647.

Tomelleri, L., Jogia, J., Perlini, C., et al. (2009). Brain structural changes associated with chronicity and antipsychotic treatment in schizophrenia. *European Journal of Neuropsychopharmacology*, 19(12), 835-840.

Toro, R., Fox, P.T., Paus, T. (2008). Functional coactivation map of the human brain. *Cerebral Cortex*, 18, 2553-2559.

Tost, H., Ruf, M., Schmäl, C., et al. (2010). Prefrontal-temporal gray matter deficits in bipolar disorder patients with persecutory delusions. *Journal of Affective Disorders*, 120, 54-61.

Tregellas, J.R., Shatti, S., Tanabe, J.L., et al. (2007). Gray matter volume differences and the effects of smoking on gray matter in schizophrenia. *Schizophrenia Research*, 97, 242-249.

Tuch, D.S., Reese, T.G., Wiegell, M.R., Wedeen, V.J. (2003). Diffusion MRI of complex neural architecture. *Neuron*, 40, 885-895.

Turkeltaub, P.E., Eickhoff, S.B., Laird, A.R., et al. (2012). Minimizing within-experiment and within-group effects in activation likelihood estimation meta-analyses. *Human Brain Mapping*, 33, 1-13.

Tzarouchi, L.C., Astrakas, L.G., Konitsiotis, S., et al. (2010). Voxel-Based Morphometry and Voxel-Based Relaxometry in Parkinsonian Variant of Multiple System Atrophy. *Journal of Neuroimaging*, 20, 260-266.

Uchida, R.R., Del-Ben, C.M., Busatto, G.F., et al. (2008). Regional gray matter abnormalities in panic disorder: a voxel-based morphometry study. *Psychiatry Research*, 163(1), 21-29.

Uddin, L. Q. (2015). Salience processing and insular cortical function and dysfunction. *Nature Reviews Neuroscience*, 16(1), 55-61.

Uddin, L. Q., Supekar, K., Lynch, C. J., Khouzam, A., Phillips, J., Feinstein, C., et al. (2013). Salience network-based classification and prediction of symptom severity in children with autism. *JAMA Psychiatry*, 70(8), 869-879.

Uddin, L. Q., Supekar, K. S., Ryali, S., Menon, V. (2011). Dynamic reconfiguration of structural and functional connectivity across core neurocognitive brain networks with development. *Journal of Neuroscience*, 31(50), 18578-18589.

Valente, A.A. Jr, Miguel, E.C., Castro, C.C., et al. (2005). Regional gray matter abnormalities in obsessive-compulsive disorder: a voxel-based morphometry study. *Biological Psychiatry*, 58(6), 479-487.

van de Pavert, S.H., Muhlert, N., Sethi, V., et al. (2016). DIR-visible grey matter lesions and atrophy in multiple sclerosis: partners in crime? *Journal of neurology, neurosurgery, and psychiatry*, 87(5), 461-467.

van de Ven, V.G., Formisano, E., Prvulovic, D., Roeder, C.H., Linden, D.E. (2004). Functional connectivity as revealed by spatial independent component analysis of fMRI measurements during rest. *Human Brain Mapping*, 22(3), 165-178.

van den Heuvel, M.P., Kahn, R.S., Goni, J., Sporns, O. (2012). High-cost, high-capacity backbone for global brain communication. *Proceedings of the National Academy of Sciences USA*, 109, 11372-11377.

van den Heuvel, M.P., Mandl, R.C., Hulshoff Pol, H.E. (2008). Normalized cut group clustering of resting-state fMRI data. *PLoS ONE*, 3(4), e2001.

van den Heuvel, M.P., Mandl, R.C., Kahn, R.S., Hulshoff Pol, H.E. (2009). Functionally linked resting-state networks reflect the underlying structural connectivity architecture of the human brain. *Human Brain Mapping*, 30, 3127-3141.

van den Heuvel, M.P., Sporns, O. (2011). Rich-club organization of the human connectome. *Journal of Neuroscience*, 31, 15775-15786.

van den Heuvel, O.A., Remijnse, P.L., Mataix-Cols, D., et al. (2009). The major symptom dimensions of obsessive-compulsive disorder are mediated by partially distinct neural systems. *Brain*, 132, 853-868.

van Eijndhoven, P., van Wingen, G., Katzenbauer, M., et al. (2013). Paralimbic cortical thickness in first-episode depression: evidence for trait-related differences in mood regulation. *American Journal of Psychiatry*, 170(12), 1477-1486.

van Essen, D.C., Ugurbil, K., Auerbach, E., Barch, D., Behrens, T.E., Bucholz, R., et al. (2012). The human connectome project: a data acquisition perspective. *Neuroimage*, 62, 2222-2231.

van Tol, M.J., Li, M., Metzger, C.D., et al. (2014). Local cortical thinning links to resting-state disconnectivity in major depressive disorder. *Psychological Medicine*, 44(10), 2053-2065.

van Tol, M.J., van der Wee, N.J., van den Heuvel, O.A., et al. (2010). Regional brain volume in depression and anxiety disorders. *Archives of General Psychiatry*, 67(10), 1002-1011.

Vanasse, T.J., Fox, P.M., Barron, D.S., Robertson, M., Eickhoff, S.B., Lancaster, J.L., et al. (2018). BrainMap VBM: an environment for structural meta-analysis. *Human Brain Mapping*, 39, 3308-3325.

Venkatasubramanian, G., Jayakumar, P.N., Gangadhar, B.N., Keshavan, M.S. (2008). Neuroanatomical correlates of neurological soft signs in antipsychotic-naive schizophrenia. *Psychiatry Research*, 164(3), 215-222.

Vercelli, U., Diano, M., Costa, T., Nani, A., Duca, S., Geminiani, G., et al. (2016). Node Detection Using High-Dimensional Fuzzy Parcellation Applied to the Insular Cortex. *Neural Plasticity*, 2016, 1938292. doi: 10.1155/2016/1938292.

Verstraete, E., Veldink, J. H., van den Berg, L. H., van den Heuvel, M. P. (2013). Structural brain network imaging shows expanding disconnection of the motor system in amyotrophic lateral sclerosis. *Human Brain Mapping*, 35, 1351-1361.

Voets, N.L., Hough, M.G., Douaud, G., et al. (2008). Evidence for abnormalities of cortical development in adolescent-onset schizophrenia. *Neuroimage*, 43(4), 665-675.

Voytek, B., Knight, R. T. (2015). Dynamic network communication as a unifying neural basis for cognition, development, aging, and disease. *Biological Psychiatry*, 77(12), 1089-1097.

Wagner, G., Koch, K., Schachtzabel, C., et al. (2008). Enhanced rostral anterior cingulate cortex activation during cognitive control is related to orbitofrontal volume reduction in unipolar depression. *Journal of psychiatry & neuroscience*, 33(3), 199-208.

Wagner, G., Koch, K., Schachtzabel C., et al. (2011). Structural brain alterations in patients with major depressive disorder and high risk for suicide: evidence for a distinct neurobiological entity? *Neuroimage*, 54(2), 1607-1614.

Walker, L.C., Diamond, M.I., Duff, K.E., Hyman, B.T. (2013). Mechanisms of protein seeding in neurodegenerative diseases. *JAMA Neurology*, 70, 304-310.

Wang, F., Kalmar, J.H., Womer, F.Y., et al. (2011). Olfactocentric paralimbic cortex morphology in adolescents with bipolar disorder. *Brain*, 134, 2005-2012.

Wang, W.Y., Yu, J.T., Liu, Y., et al. (2015). Voxelbased meta-analysis of grey matter changes in Alzheimer's disease. *Translational Neurodegeneration*, 4: 6.

Wang, Y., Chen, K., Yao, L., et al. (2013). Structural interactions within the default mode network identified by bayesian network analysis in Alzheimer's disease. *PLoS One*, 8: e74070. doi: 10.1371/journal.pone.0074070.

Waragai, M., Okamura, N., Furukawa, K., et al. (2009). Comparison study of amyloid PET and voxel-based morphometry analysis in mild cognitive impairment and Alzheimer's disease. *Journal of Neurological Sciences*, 285(1-2), 100-108.

Warren, D.E., et al. (2014). Network measures predict neuropsychological outcome after brain injury. *Proceedings of the National Academy of Sciences USA*, 111, 14247-14252.

Warren, J.D., Rohrer, J.D., Schott, J.M., et al. (2013). Molecular nexopathies: a new paradigm of neurodegenerative disease. *Trends in Neuroscience*, 36, 561-569.

Watkins, K.E., Vargha-Khadem, F., Ashburner, J., et al. (2002). MRI analysis of an inherited speech and language disorder: structural brain abnormalities. *Brain*, 125, 465-478.

Watson, D.R., Anderson, J.M., Bai, F., et al. (2012). A voxel based morphometry study investigating brain structural changes in first episode psychosis. *Behavioral Brain Research*, 227(1), 91-99.

Wei, W., Zhang, Z., Xu, Q., et al. (2016). More Severe Extratemporal Damages in Mesial Temporal Lobe Epilepsy With Hippocampal Sclerosis Than That With Other Lesions: A Multimodality MRI Study. *Medicine*, 95(10), e3020. doi:10.1097/MD.0000000000003020.

Weintraub, S., Mesulam, M.M. (1996). 'From neuronal networks to dementia: four clinical profiles'. In: *La Demence: Pourquoi?* Paris: Foundation Nationale de Gerontologie.

Whitford, T.J., Grieve, S.M., Farrow, T.F., et al. (2006). Progressive grey matter atrophy over the first 2-3 years of illness in first-episode schizophrenia: a tensor-based morphometry study. *Neuroimage*, 32(2), 511-519.

Whitwell, J.L., Duffy, J.R., Strand, E.A., et al. (2013). Neuroimaging comparison of primary progressive apraxia of speech and progressive supranuclear palsy. *European journal of neurology*, 20(4), 629-637.

Whitwell, J.L., Jack, C.R., Jr, Kantarci, K., et al. (2007). Imaging correlates of posterior cortical atrophy. *Neurobiology of aging*, 28(7), 1051-1061.

Whitwell, J.L., Sampson, E.L., Loy, C.T., et al. (2007). VBM signatures of abnormal eating behaviours in frontotemporal lobar degeneration. *Neuroimage*, 35(1), 207-213.

Wilke, M., Kaufmann, C., Grabner, A., et al. (2001). Gray matter-changes and correlates of disease severity in schizophrenia: a statistical parametric mapping study. *Neuroimage*, 13(5), 814-824.

Wilson, S.M., Henry, M.L., Besbris, M., et al. (2010). Connected speech production in three variants of primary progressive aphasia. *Brain*, 133, 2069-2088.

Winkler, A.M., Ridgway, G.R., Webster, M.A., et al. (2014). Permutation inference for the general linear model. *Neuroimage*, 92, 381-397.

Woermann, F.G., Free, S.L., Koepp, M.J., et al. (1999). Voxel-by-voxel comparison of automatically segmented cerebral gray matter—a rater-independent comparison of structural MRI in patients with epilepsy. *Neuroimage*, 10(4), 373-384.

Woermann, F.G., van Elst, L.T., Koepp, M.J., et al. (2000). Reduction of frontal neocortical grey matter associated with affective aggression in patients with temporal lobe epilepsy: an objective voxel by voxel analysis of automatically segmented MRI. *Journal of neurology, neurosurgery, and psychiatry*, 68(2), 162-169.

Wolf, L., Goldberg, C., Manor, N., et al. (2011). Gene expression in the rodent brain is associated with its regional connectivity. *PLoS Computational Biology*, 7(5), e1002040. doi: 10.1371/journal.pcbi.1002040.

Wolf, R.C., Höse, A., Frasch, K., et al. (2008). Volumetric abnormalities associated with cognitive deficits in patients with schizophrenia. *European Psychiatry*, 23(8), 541-548.

Wolf, R.C., Vasic, N., Schönfeldt-Lecuona, C., et al. (2009). Cortical dysfunction in patients with Huntington's disease during working memory performance. *Human Brain Mapping*, 30, 327-339.

Wright, I.C., McGuire, P.K., Poline, J.B., et al. (1995). A voxel-based method for the statistical analysis of gray and white matter density applied to schizophrenia. *Neuroimage*, 2(4), 244-252. doi:10.1006/nimg.1995.1032.

Wylie, K.P., Tregellas, J.R. (2010). The role of the insula in schizophrenia. *Schizophrenia Research*, 123(2-3), 93-104.

Xie, S., Xiao, J.X., Gong, G.L., et al. (2006). Voxel-based detection of white matter abnormalities in mild Alzheimer disease. *Neurology*, 66(12), 1845-1849.

Xu, L., Groth, K.M., Pearlson, G., et al. (2009). Source-based morphometry: the use of independent component analysis to identify gray matter differences with application to schizophrenia. *Human brain mapping*, 30(3), 711-724.

Yamada, M., Hirao, K., Namiki, C., et al. (2007). Social cognition and frontal lobe pathology in schizophrenia: a voxel-based morphometric study. *Neuroimage*, 35(1), 292-298.

Yang, F.C., Chou, K.H., Fuh, JL., et al. (2013). Altered gray matter volume in the frontal pain modulation network in patients with cluster headache. *Pain*, 154(6), 801-807.

Yasuda, C.L., Morita, M.E., Alessio, A., et al. (2010). Relationship between environmental factors and gray matter atrophy in refractory MTLE. *Neurology*, 74(13), 1062-1068.

Yasuda, C.L., Valise, C., Saúde, A.V., et al. (2010). Dynamic changes in white and gray matter volume are associated with outcome of surgical treatment in temporal lobe epilepsy. *Neuroimage*, 49(1), 71-79.

Yates, D. (2012). Neurodegenerative networking. *Nature Reviews Neuroscience*, 13, 288.

Yeh, F.C., Badre, D., Verstynen, T. (2016). Connectometry: a statistical approach harnessing the analytical potential of the local connectome. *Neuroimage*, 125, 162-171.

Yeh, F.C., Tseng, W.Y. (2011). NTU-90: a high angular resolution brain atlas constructed by q-space diffeomorphic reconstruction. *Neuroimage*, 58, 91-99.

Yeh, F.C., Verstynen, T.D., Wang, Y., Fernandez-Miranda, J.C., Tseng, W.Y. (2013). Deterministic diffusion fiber tracking improved by quantitative anisotropy. *PLoS One*, 8, e80713.

Yeh, F.C., Wedeen, V.J., Tseng, W.Y. (2010). Generalized q-sampling imaging. *IEEE Transanctions of Medical Imaging*, 29, 1626-1635.

Yoneyama, E., Matsui, M., Kawasaki, Y., et al. (2003). Gray matter features of schizotypal disorder patients exhibiting the schizophrenia-related code types of the Minnesota Multiphasic Personality Inventory. *Acta Psychiatrica Scandinavica*, 108, 333-340.

Yoo, H.K., Kim, M.J., Kim, S.J., et al. (2005). Putaminal gray matter volume decrease in panic disorder: an optimized voxel-based morphometry study. *European Journal of Neuroscience*, 22, 2089-2094.

Yoo, S.Y., Roh, M.S., Choi, J.S., et al. (2008). Voxel-based morphometry study of gray matter abnormalities in obsessive-compulsive disorder. *Journal of Korean medical science*, 23(1), 24-30.

Yoshihara, Y., Sugihara, G., Matsumoto, H., et al. (2008). Voxel-based structural magnetic resonance imaging (MRI) study of patients with early onset schizophrenia. *Annals of general psychiatry*, 7, 25. doi:10.1186/1744-859X-7-25.

Yuan, B., Fang, Y., Han, Z., et al. (2017). Brain hubs in lesion models: predicting functional network topology with lesion patterns in patients. *Scientific Reports*, 7, 17908.

Yushkevich, P.A., Avants, B.B., Das, S.R., et al. (2010). Bias in estimation of hippocampal atrophy using deformation-based morphometry arises from asymmetric global normalization: an illustration in ADNI 3T MRI data. *Neuroimage*, 50, 434-445.

Yuste, R. (2015). From the neuron doctrine to neural networks. *Nature Reviews Neuroscience*, 16, 487-497.

Zahn, R., Buechert, M., Overmans, J., et al. (2005). Mapping of temporal and parietal cortex in progressive nonfluent aphasia and Alzheimer's disease using chemical shift imaging, voxel-based morphometry and positron emission tomography. *Psychiatry Research*, 140(2), 115-131.

Zalesky, A., Fornito, A., Harding, I.H., et al. (2010). Whole-brain anatomical networks: does the choice of nodes matter? *Neuroimage*, 50, 970-983.

Zamboni, G., Huey, E.D., Krueger, F., et al. (2008). Apathy and disinhibition in frontotemporal dementia: Insights into their neural correlates. *Neurology*, 71(10), 736-742.

Zamora-López, G. (2010). Cortical hubs form a module for multisensory integration on top of the hierarchy of cortical networks. *Frontiers in Neuroinformation*, 19, 4.

Zamora-López, G., Zhou, C., Kurths, J. (2011). Exploring brain function from anatomical connectivity. *Frontiers in neuroscience*, 5, 83. doi:10.3389/fnins.2011.00083.

Zapala, M.A., Hovatta, I., Ellison, J.A., et al. (2005). Adult mouse brain gene expression patterns bear an embryologic imprint. *Proceedings of the National Academy of Sciences USA*, 102, 10357-10362.

Zawia, N.H., Basha, M.R. (2005). Environmental risk factors and the developmental basis for Alzheimer's disease. *Reviews in the Neurosciences*, 16, 325-337.

Zhang, J., Tan, Q., Yin, H., et al. (2011). Decreased gray matter volume in the left hippocampus and bilateral calcarine cortex in coal mine flood disaster survivors with recent onset PTSD. *Psychiatry Research*, 192(2), 84-90.

Zhang, T.J., Wu, Q.Z., Huang, X.Q., et al. (2009). Magnetization transfer imaging reveals the brain deficit in patients with treatment-refractory depression. *Journal of Affective Disorders*, 117(3), 157-161.

Zhang, X., Yao, S., Zhu, X., et al. (2012). Gray matter volume abnormalities in individuals with cognitive vulnerability to depression: a voxel-based morphometry study. *Journal of Affective Disorders*, 136(3), 443-452.

Zhang, X., Zhang, F., Huang, D., et al. (2016). Contribution of Gray and White Matter Abnormalities to Cognitive Impairment in Multiple Sclerosis. *International journal of molecular sciences*, 18(1), 46. doi:10.3390/ijms18010046.

Zhang, Y., Brady, M., Smith, S. (2001). Segmentation of brain MR images through a hidden Markov random field model and the expectation-maximization algorithm. *IEEE Transactions in Medical Imaging*, 20(1), 45-57.

Zhou, J., Gennatas, E.D., Kramer, J.H., et al. (2012). Predicting regional neurodegeneration from the healthy brain functional connectome. *Neuron*, 73(6), 1216-1227. doi:10.1016/j.neuron.2012.03.004.

Zhou, J., Greicius, M.D., Gennatas, E.D., et al. (2010). Divergent network connectivity changes in behavioural variant frontotemporal dementia and Alzheimer's disease. *Brain*, 133, 1352-1367.

Zou, K., Deng, W., Li, T., et al. (2010). Changes of brain morphometry in first-episode, drug-naïve, non-late-life adult patients with major depression: an optimized voxel-based morphometry study. *Biological Psychiatry*, 67(2), 186-188.